Investigating the Regulation of Host Tissue Colonisation by The Rice Blast Fungus *Magnaporthe oryzae*

Submitted by Wasin Sakulkoo

to the University of Exeter as a thesis for the degree of
Doctoral of Philosophy in Biological Sciences
September 2016

Wasin Sakulkoo

Abstract

The filamentous fungus *Magnaporthe oryzae* is a devastating pathogen of cultivated rice. *M. oryzae* elaborates a pressurized dome-shaped infection structure, called the appressorium, which physically ruptures the cuticle and gains entry into host tissue. Intracellular invasive hyphae invade neighbouring host cells through plasmodesmata. The Pmk1 MAPK cascade is well known for its roles in regulating the formation and function of the appressorium. Interestingly, Δ*pmk1* mutants cannot infect host plant tissue through wounds, suggesting a role in invasive growth. Here, I define biological functions of the Pmk1 MAPK at various stages of the life cycle, by using a controllable version of Pmk1 that is specifically inhibited by a cell-permeable compound without disturbing other wild-type kinases. The Pmk1 MAPK signalling regulates morphogenesis of narrow invasive hyphae traversing the host cell wall, and modulates production of several putative secreted effectors, providing a direct link between the signalling cascade and effector-driven host immune suppression. These results indicate that the Pmk1 pathway is a central regulator of infection-related development necessary for many stages of plant infection including appressorium development, plant penetration, and importantly tissue colonisation. I also report the role of cell cycle progression in the development of plant infection structure. By using two novel conditional mutants that arrest in S and G2 phases, I defined that S-phase progression is crucial for appressorium-mediated plant penetration.

Table of Contents

Appendix 1

Osés-Ruiz, M., Sakulkoo, W. and Talbot, N. J. (2016) 4 Septation and Cytokinesis in Pathogenic Fungi. In: *Growth, Differentiation and Sexuality.* (Wendland, J., ed.). Cham: Springer International Publishing, pp. 67-79

Appendix 2

Osés-Ruiz, M., Sakulkoo, W., Littlejohn G. R., Martin-Urdiroz M. and Talbot, N. J. Two independent S-phase checkpoints regulate appressorium-mediated plant infection by the rice blast fungus *Magnaporthe oryzae.* Under revision.

List of Figures

List of Tables

Abbreviations

ATP	adenosine triphosphate
AS	analogue sensitive
bp	base pair
cDNA	complementary DNA
CM	complete medium
cAMP	cyclic adenosine monophosphate
CDK	cyclin-dependent kinase
°C	degrees Celsius
DNA	deoxyribonucleic acid
DIC	differential interference contrast
ER	endoplasmic reticulum
EDTA	ethylenediaminetetraacetic acid
EIHM	extra-invasive hyphal membrane
FCW	fungal cell wall
FPM	fungal plasma membrane
g	grams
g L^{-1}	grams per litre
GFP	green fluorescence protein
CTAB	hexadecyltrimethylammonium bromide
hpi	hour post-inoculation
hpi	hour post inoculation
HU	hydroxyurea
IH	invasive hyphae or invasive hypha
kb	kilobase
L	litre
MAPK	mitogen-activated protein kinase
MAPKK	MAPK kinase
MAPKKK	MAPKK kinase
µg	micrograms

µL	microlitre
µM	micromolar
mg	miligrams
mg L^{-1}	miligrams per litre
mL	mililitre
mM	milimolar
min	minute
M	molar
NOX	NADPH oxidase
nM	nanomolar
NADPH	nicotinamide adenine dinucleotide phosphate
ORF	open reading frame
%	percentage
% v/v	percentage volume by volume
% w/v	percentage weight by volume
PD	plasmodesmata
PCR	polymerase chain reaction
PKA	protein kinase A
PKC	protein kinase C
ROS	reactive oxygen species
RFP	red fluorescence protein
rpm	revolutions per minute
RNA	ribonucleic acid
RCW	rice cell wall
RPM	rice plasma membrane
RNA-seq	RNA sequencing
sec	second
TS	temperature sensitive
TEM	transmission electron microscopy
WT	wild type

Acknowledgements

I would like to express my sincere gratitude to my supervisor Nick Talbot for his continuous support for my study, for his patience, motivation, immense knowledge, and for being a role model in science. I would like to thank Les and Claire Halpin, the generous sponsors of Halpin Trust, for supporting my studentship, research funding, and so much more needed to train the next generation of molecular plant pathologists.

I thank George Littlejohn for helping with confocal microscopy. I thank Darren Soanes for helping with bioinformatics. I thank Christian Hacker at the Bio-imaging Suite for helping with electron microscopy, Andrey Farbos and Karen Moore at the Exeter Sequencing Service. I would like to thank Stephen Osmani (Ohio State University) for providing unpublished information about cell cycle mutants of *Aspergillus nidulans*, and Steve James (Gettysburg College) for providing these *A. nidulans* strains. I thank Satoko Yoshida (RIKEN Centre for Sustainable Resource Science, Japan) for providing NahG rice line. Special thanks for both present and past members of the Halpin Lab, who are great colleagues including Mick, Lauren, Miriam, Magdalena, Yasin, Yogesh, Xia, David, Vincent, Clara, Bozeng, Tina and Andy, for making our lab a wonderful place.

I would like to thank my previous supervisors David Arnot (Biological Sciences, The University of Edinburgh), Pataradawn Pinyopich and Pongchai Harnyuttanakorn (Department of Biology, Chulalongkorn University, Thailand) and Chantragan Phiphobmongkol (Chulabhorn Research Institute, Thailand) for supporting me during my masters and undergrad.

A million thanks for my friends, Prachya Boonkwan (Arm), Phunpiti Bhovichitra (Pat), Woranop Sukparangsi (Yoon), Wanaruk Chaimayo (Bong), Chadtip Rodtassana (Toey), Chidchanok Thepsoonthorn (Cheeze), Sittikorn Assavanives (Pepe), Pawinee Boonserm (Pop), Maslin Buaban (Lin), Kritchasorn Jarupasin (Pol), Paveena Chamchoy (Joyce), and other Thai students in Exeter for the great friendship. I am everything I am because of you guys!

Lastly, I would like to thank my loving family, my parents, Piroj and Pojchanart Sakulkoo, and my sisters, Kamonchanok, Phantira and Nanticha Sakulkoo, for supporting me, for giving me faith.

Dedicated to Les Halpin 1957-2013,

for his generosity providing opportunities to students from rice growing developing countries and funding research into rice blast disease that each year kills enough rice to feed 60 million people.

Rice fields in Chiang Mai, Thailand (Photo by Chatrawee Wiratgasem, shutterstock)**.**

"I always hope that my research will, somehow, help farmers including ones in my home country, Thailand."

Wasin Sakulkoo

Chapter 1 General Introduction

1.1 The future of food security needs better understanding of plant-microbe interactions

The global human population is predicted to reach 9.2 billion by 2050, and 86% of people live in underdeveloped countries. The world therefore faces a huge challenge in ensuring global food security. Changes in climatic and environmental conditions, farmland availability, and the emergence of new diseases caused by rapidly evolving pathogens, however, made this challenge even more difficult. It has long been recognised that fungi and fungi-like organisms constitute a serious threat to plants (Fisher *et al.*, 2012). Food security depends on achieving sustainable agricultural yields, novel disease control strategies, such as the development of resistance traits, agrochemicals and crop rotation, are therefore vital to reduce crop losses and alleviate food shortage. Identification and exploitation of natural sources of durable resistance, assisted by genomic data of crops and pathogens, will accelerate the development of such disease control (Lo Iacono *et al.*, 2013). Moreover, many microbial organisms, such as mycorrhizal fungi, are well known for their roles in promoting plant growth and protect plant from infections by pathogens (Gosling *et al.*, 2016). To achieve this, we need better understanding of the biology of plant-microbe interactions which can be translated into development of robust pathogen surveillance systems and novel strategies for crop disease control, which will ultimately ensure global food security (Skamnioti & Gurr, 2009).

1.2 Rice immunity against fungal pathogens

Cultivated rice *Oryza sativa* is a major staple food crop that feed more than 50% of the world's population (Sasaki & Burr, 2000). However, rice is susceptible to a range of microbial infections, leading to significant yield losses. Rice blast caused by the filamentous fungus *Magnaporthe oryzae* (synonym: *Pyricularia oryzae*) is among the most serious threats to rice production (Zhang *et al.*, 2016a, Wilson & Talbot, 2009). Without protections, the rice blast can cause harvest losses, accounting for food crops sufficient to feed more than 60 million people in one year. The rice blast affected rice production in at least 85 countries (Liu *et al.*, 2014, Skamnioti & Gurr, 2009, Talbot, 2003). Due to scientific and economic importance of this pathosystem, great efforts have been made over the past two decades to understand cellular and molecular basis of rice blast disease and resistance (Ebbole, 2007, Liu *et al*., 2014, Sasaki & Burr, 2000, Talbot, 2003, Wilson & Talbot, 2009).

Plant innate immunity depends on two layers of pathogen sensing systems. Cell surface-localised pattern recognition receptors (PRRs) sense pathogen-associated molecular patterns (PAMPs) and activate PAMP-triggered immunity (PTI). Adapted pathogens are able to circumvent PTI to colonise host plants by delivering effectors into plant cells. Resistant plants have evolved to detect effectors directly, or indirectly, by intracellular resistance (R) proteins which activate effector-triggered immunity (ETI), which can be accompanied by a hypersensitive response (HR) of infected cells. PTI and ETI transmit signals to initiate a number of downstream responses (Cui *et al.*, 2015). Although PTI and ETI are activated by different mechanisms, the resulting gene expression

signatures of such activations are extensively overlapping (Jones & Dangl, 2006, Dangl & Jones, 2001, Dodds & Rathjen, 2010). The wealth of knowledge of plant immunity in Arabidopsis has been leading the way, but studies in rice plant are gathering pace (Liu *et al*., 2014, Couto & Zipfel, 2016, Chen & Ronald, 2011, Yang *et al.*, 2013, Liu *et al.*, 2013) . The rice genome encodes a number of conserved PRRs that sense classical PAMPs (Liu *et al*., 2014). Chitin oligosaccharides, important elements of fungal cell walls, are recognised as PAMPs by several rice PRRs. The chitin elicitor-binding protein (CEBiP) is a receptor-like transmembrane protein with two extracellular LysM domains which lacks an intracellular kinase domain (Kouzai *et al.*, 2014b). Transduction of chitin-triggered signals involves recruitment of a receptor-like kinase chitin elicitor receptor kinase 1 (OsCERK1) to CEBiP, forming a sandwich-type receptor system (Shimizu *et al.*, 2010). Two additional LysM motif containing-proteins, LYP4 and LYP6, also bind to chitin (Liu *et al.*, 2012). However, *M. oryzae* secretes in turn a LysM domain containing-protein effector, Slp1, to sequester free chitin released from invasive hyphae (Mentlak *et al.*, 2012). This appears to be a common strategy found in diverse fungal pathogens to evade PAMP recognition (de Jonge *et al.*, 2010, Sanchez-Vallet *et al.*, 2013). Upon ligand binding and activation of PRR complex, signals are rapidly transmitted through a branched signalling cascade to activate local and systemic defence responses (Couto & Zipfel, 2016). These include a rapid calcium ion flux, a burst of reactive oxygen species (ROS), activation of MAPK cascades, rewiring of global gene expression, callose deposition at sites of penetration attempts and at plasmodesmata, and the initiation of localised cell death (Dangl & Jones, 2001, Jones & Dangl, 2006). In rice, chitin-triggered ROS generation

depends on activation of a small GTPase OsRAC1 by a cognate guanine nucleotide exchange factor OsRacGEF1. OsCERK1 directly phosphorylates OsRacGEF1 which in turn activates the OsRAC1. Active OsRAC1 interacts and triggers a ROS generating NADPH oxidase, OsRBOH. This pathway represents a direct link between PRR complex and downstream signalling (Shinya *et al.*, 2015, Akamatsu *et al.*, 2013, Couto & Zipfel, 2016).

ETI is the second layer of pathogen recognition system in plants which relies on intracellular receptors containing nucleotide binding (NB) domains and leucine rich repeats (LRR). NB-LRR proteins detect pathogens effectors by either direct binding, or indirectly, through an accessory protein incorporated in an NB-LRR complex. Direct recognition can be predicted by yeast-two-hybrid (Y2H) assays or by an *in vitro* protein interaction assay, such as co-immunoprecipitation, but *in vivo* immunoprecipitation is necessary to infer a biologically relevant interaction. R proteins and effectors display strong diversifying selection and high degree of sequence polymorphism amongst host and pathogen populations, respectively (Dodds & Rathjen, 2010).

Approximately 100 rice NB-LRRs have been shown to confer resistance against the rice blast fungus *M. oryzae*, and 23 of these have been cloned to date (Liu *et al*., 2014). For instance, the rice NB-LRR protein Pi-ta directly binds to *M. oryzae* secreted metalloprotease effector AVR-Pita, showing a direct gene-for-gene relationship (Jia *et al.*, 2000). However, virulence functions of the AVR-Pita effector are unknown (Orbach *et al.*, 2000). In some cases, gene-for-gene resistance requires two NB-LRR proteins acting together. For example, a pair of rice NB-LRRs, RGA4 and RGA5, co-ordinately mediates recognition of AVR-Pia

and AVR1-CO39. RGA4 triggers HR, whereas RGA5 acts as a repressor of RGA4 and serves as an AVR receptor (Cesari *et al.*, 2013). Intriguingly, recognition of AVR-Pik by the rice NB-LRR pair, Pik-1/Pik-2, occurs at a heavy-metal associated (HMA) domain integrated in the middle part of the Pik-1 NB-LRR (Maqbool *et al.*, 2015, Yoshida *et al.*, 2009). The integrated HMA domain is likely to have evolved from endogenous rice protein families that contain an HMA domain which may be an effector target for suppression of PTI (Wu *et al.*, 2015). It has been proposed that the integrated atypical domains in NB-LRR immune receptors may act as decoys to detect pathogen effectors, and these integrated decoy domains have proven to be widespread (Kroj *et al.*, 2016, Sarris *et al.*, 2015).

1.3 Mitogen-activated protein kinase signalling in plant pathogenic fungi

To initiate plant infection, fungal pathogens must perceive the presence of a compatible host using activation of pathogen's intracellular signalling pathways, leading to differentiation of infection structures that are used to gain entry into host tissue (Hamel *et al.*, 2012). Mitogen-activated protein kinase (MAPK) cascades are evolutionarily conserved signal transduction pathways present in all eukaryotes. These contain three-tiered protein kinases that operate sequentially: a MAP kinase kinase kinase (MAPKKK or MEKK), a MAP kinase kinase (MAPKK or MEK) and a MAPK. Recognition of stimuli results in activation of the MEKK which phosphorylates the MEK, which in turn phosphorylates the MAPK (Dhillon *et al.*, 2007). The activated MAPK then phosphorylates several substrates, such as transcription factors, which modulate transcription of specific target genes. During plant–microbe interactions, plant MAPKs have been implicated in immune

signalling that promotes defence mechanisms, whereas fungal MAPKs regulate mechanical and enzymatic penetration of host tissues (Hamel *et al*., 2012). In this way, the fungal MAPK pathways transmit plant-derived signals to the nucleus, leading to initiation of virulence program (Hamel *et al*., 2012, Li *et al.*, 2012, Zhao *et al.*, 2007). In the budding yeast *Saccharomyces cerevisiae*, Fus3 and Kss1 MAPKs mediate pheromone response and filamentous invasive growth (Fig. 1.1) (Chen & Thorner, 2007). Interestingly, homologues of Fus3/Kss1 MAPKs are implicated in regulating plant infection process in biologically and taxonomically diverse pathogenic fungi (Hamel *et al*., 2012, Li *et al*., 2012, Perez-Nadales *et al.*, 2014, Rispail *et al.*, 2009, Zhao *et al*., 2007).

The dimorphic fungus, *Ustilago maydis,* causes smut disease in maize (*Zea mays*) which is characterised by formation of galls, tumour-like structures on plant tissues (Brefort *et al.*, 2009, Kahmann & Kämper, 2004). Away from host plants, *U. maydis* grows as a saprobic, haploid, unicellular yeast. Once contact with the host plant is made, two compatible haploid cells mate and initiate dikaryotic filamentous growth, followed by appressorium formation, plant penetration and invasive growth (Brefort *et al*., 2009). The Fus3/Kss1-type MAPK and the cyclic AMP (cAMP) response pathways are activated by pheromone and host signals to mediate the mating process. *U. maydis* possesses two Fus3/Kss1-type MAPKs, Kpp2 (also known as Ubc3) and Kpp6. Deletion of *KPP2* partially attenuates mating and formation of filamentous dikaryotic hyphae and virulence (Mayorga & Gold, 1999), while disruption of *KPP6* only affected plant penetration (Brachmann *et al.*, 2003). Mutants lacking both *KPP2* and *KPP6* completely fail to mate and become non-

pathogenic (Brachmann *et al*., 2003), and phenocopied mutants lacking Fuz7, a *U. maydis* homologue of Ste7 of *S. cerevisiae* (Banuett & Herskowitz, 1994).

Homologues of Fus3/Kss1 MAPK pathway are essential for virulence of many plant pathogenic fungi that form appressoria, such as *M. oryzae* (Xu & Hamer, 1996), *Cochliobolus heterostrophus* (Lev *et al.*, 1999), *Colletotrichum orbiculare* (formerly known as *C. lagenarium* (Takano *et al.*, 2000), *C. gloeosporioides* (Kim *et al.*, 2000) and *Pyrenophora teres* (Ruiz-Roldan *et al.*, 2001). Deletion mutants of *FUS3/KSS1* homologues in these fungi are unable to form appressoria. Interestingly, the Fus3/Kss1-type MAPKs of *M. oryzae, P. teres* and *C. lagenarium* are all required for invasive growth (Zhao *et al*., 2007). Plant infection by other fungi that do not form appressoria also however requires activation of the Fus3/Kss1-type MAPK cascade (Hamel *et al*., 2012). These include wheat pathogens *Mycospaerella graminicola* (Cousin *et al.*, 2006) and *Stagonospora nodorum* (Solomon *et al.*, 2005). *M. graminicola* mutants lacking MgFus3 are unable to penetrate host plants through stromata and fail to undergo asexual fructification (Cousin *et al*., 2006).

The Fus3/Kss1-type MAPKs are required for virulence of many pathogens that bring about vascular wilt disease in several crop plants. *Fusarium oxysporum* mutants lacking the MAPK gene *FMK1* fails to differentiate penetration hyphae (Di Pietro *et al.*, 2001). Fmk1 and a downstream transcription factor Ste12 regulate a number of virulence-related processes including hyphal adhesion, hyphal fusion, production of plant cell wall degrading enzymes and chemotropic sensing of host signals (Rispail & Di Pietro, 2009). In *Verticillium dahliae,* deletion of *VMK1* also affects virulence against many host plants (Rauyaree *et al.*, 2005). Similarly,

deletion of the MAPK gene *MAP1/Gpmk1* in *Fusarium graminearum* results in loss of pathogenicity, which is associated with decreased production extracellular enzymes involving in plant cell wall degradation (Urban *et al.*, 2003, Jenczmionka & Schäfer, 2005). Taken together, it seems likely that the Fus3/Kss1-type MAPKs control a range of pathogenicity factors critical for virulence in a wide variety of plant pathogens. Although most of core components of Fus3/Kss1 MAPK cascades are widely conserved in the fungal kingdom, different inputs and outputs of these pathways allow them to regulate gene expression associated with the diverse life styles of these fungi, (Hamel *et al*., 2012, Turra *et al.*, 2014), summarised in Fig. 1.2.

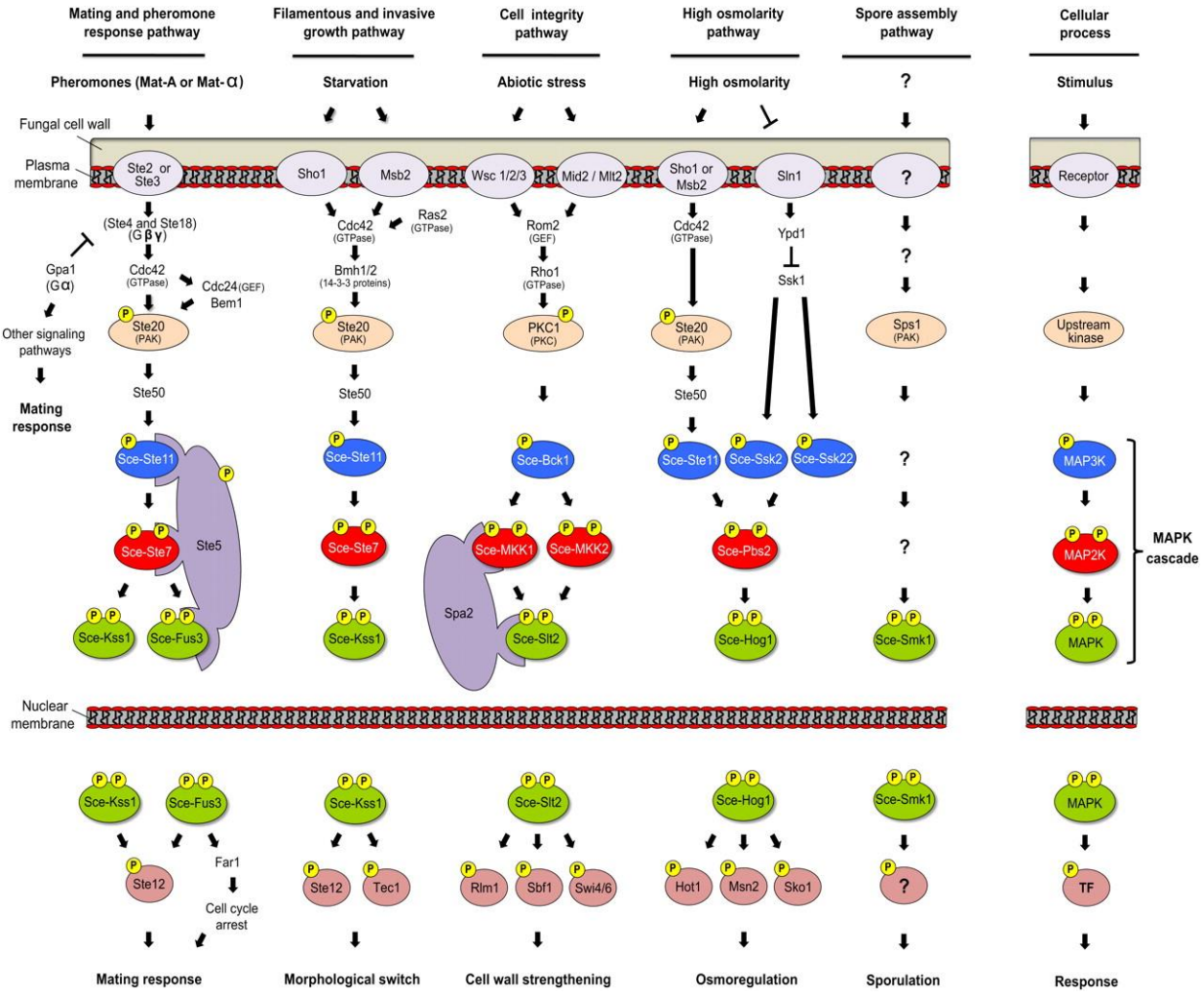

Figure 1.1 MAPK Pathways in *S. cerevisiae* (Hamel *et al*., 2012).

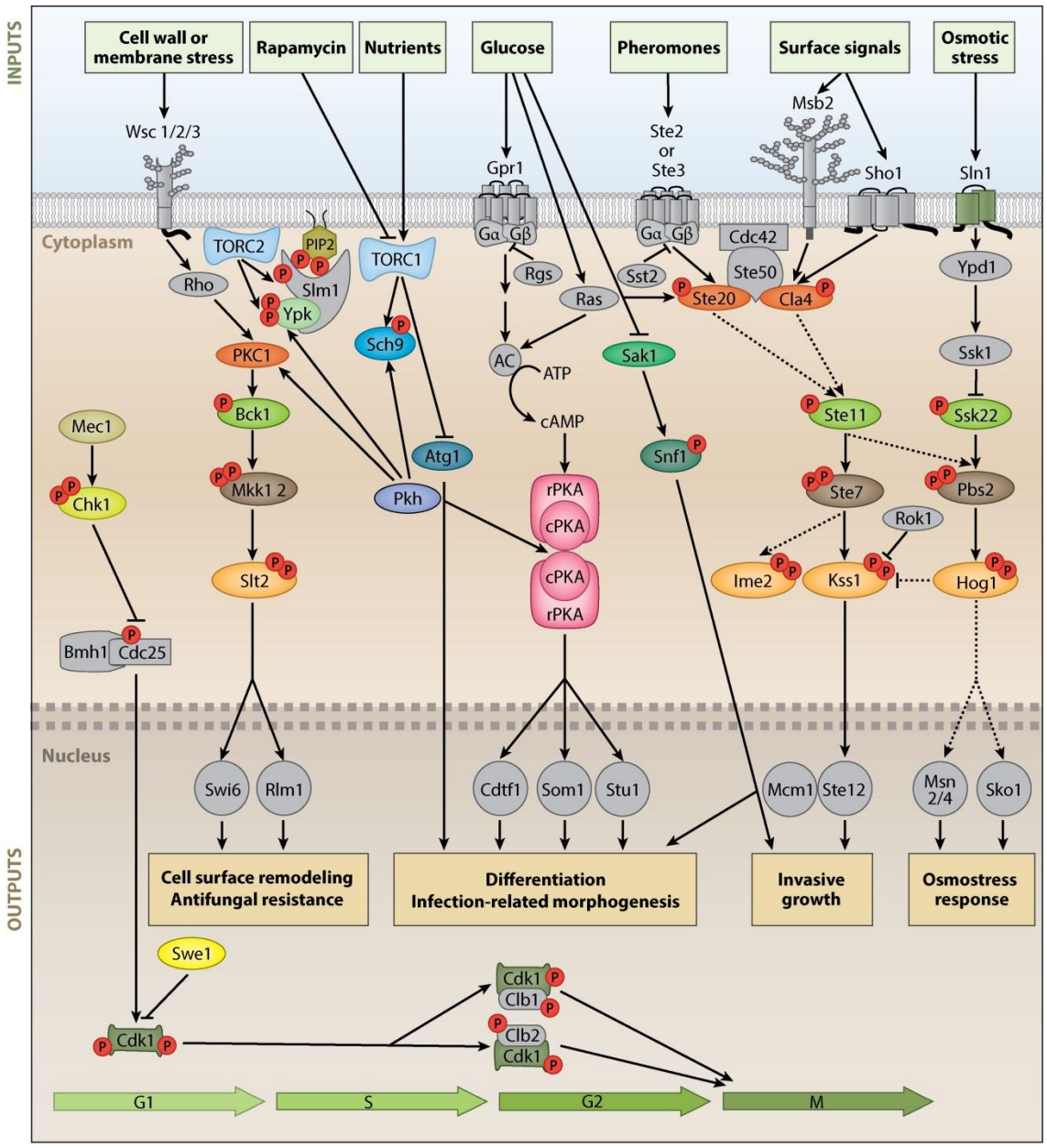

Figure 1.2 Protein kinase pathways in plant-pathogenic fungi (Turra *et al*., 2014).

1.4 The filamentous fungus *Magnaporthe oryzae* as a model for plant-fungal pathogen interaction

The filamentous fungus *M. oryzae* (synonym of *Pyricularia oryzae*) is a causal agent of blast disease in rice, wheat, and other grasses (Wilson & Talbot, 2009, Zhang *et al*., 2016a). Based on phylogenetic analysis and mating experiments, *M. oryzae* was defined as a new species separate from the morphologically indistinguishable crabgrass-infecting *Magnaporthe grisea* (Couch & Kohn, 2002). *M. oryzae* is also capable to infect a wide range of other grass species, including economically important cereals, such as wheat, barley and finger millet (Talbot, 2003). Rice blast disease has spread throughout sub-Sahara, Africa, where the demand of rice in many countries has been dramatically increasing in the last few years, though yields remain low (Kihoro *et al.*, 2013). A distinct lineage of *M. oryzae* that infects wheat was discovered in Brazil in 1985, and emerged as one of the most serious threats to wheat production due to a lack of resistance and suitable fungicides (Igarashi *et al.*, 1986). Wheat blast disease has spread to Bangladesh, the first report in Asia, posing a serious threat to wheat production in this continent (Islam *et al.*, 2016, Malaker *et al.*, 2016).

M. oryzae has also emerged as a model organism for investigating host-pathogen interaction, due to its economic importance, and experimental tractability (Ebbole, 2007, Wilson & Talbot, 2009). Published genome sequences of the rice blast fungus *M. oryzae* and its host rice plant *O. sativa* allow straightforward gene identification, and transcriptomic and proteomic analyses of the rice blast interaction (Sequencing Project International Rice, 2005, Dean *et al.*, 2005). The genetic toolbox of *M. oryzae* has been greatly expanded in recent decades. High

throughput insertional mutagenesis using Agrobacterium-mediated transformation allowed large scale-functional analysis of more than 200 novel genes required for virulence (Jeon *et al.*, 2007). Using Δ*ku70* and Δ*ku80* mutants defective in non-homologous-end joining DNA repair have enhanced the efficacy of targeted-gene disruption (Kershaw & Talbot, 2009, Villalba *et al.*, 2008). In addition, gene replacement technique can also generate conditional alleles, such as temperature-sensitive (TS) alleles, which greatly extend the range of reverse genetic studies (Saunders *et al.*, 2010a, Veneault-Fourrey *et al.*, 2006). Recently, CRISPR/Cas9 technology has been developed for *M. oryzae* providing higher efficiency in gene targeting (Arazoe *et al.*, 2015). Live-cell imaging using expression of fluorescently-labelled fungal and plant proteins has also been fundamental for understanding host-pathogen interactions (Giraldo & Valent, 2013). The *M. oryzae*-rice interaction therefore provides a useful genetic system that helps us to gain more insight into the molecular basis of fungal cell differentiation and pathogenesis (Wilson & Talbot, 2009). Importantly, *M. oryzae* shares several features of its infection strategy with other significant plant pathogens, such as appressorium formation and tissue invasion (Perez-Nadales *et al*., 2014). These highlight the possibility of defining common disease determinants, which can be targeted for broad-spectrum disease control.

1.5 The infection cycle of *M. oryzae*

To complete its life cycle, the rice blast fungus has to undergo cellular differentiation to match its environment both outside and inside its host plant (Fig. 1.3 and 1.4). Outside the host, the key challenge that the fungus encounters is to

gain entry into host tissue by direct penetration of the host cuticle, which is a formidable, hard, impermeable barrier (Howard *et al.*, 1991). This step represents a remarkably sophisticated achievement of fungal evolution. The disease cycle is initiated when a three-celled asexual spore, known as a conidium, lands on the waxy rice surface and sticks firmly by the secretion of an adhesive substance released from the spore tip, called spore tip mucilage (Hamer *et al.*, 1988). As soon as spore germination occurs, two hydrophobin proteins, Mpg1 and Mph1, are implicated in fungal spore adhesion, surface perception, and direct the action of cutinases, leading to successful plant penetration (Pham *et al.*, 2016, Talbot *et al.*, 1993, Giraldo *et al.*, 2013). A germ tube rapidly emerges from the tapering end of the conidium, and the germ tube tip subsequently flattens against its substratum and swells slightly. This process is called hooking, and is thought to be a signature of surface recognition prior to development of an infection cell, at which the first morphogenetic transition occurs (Mitchell & Dean, 1995). At this stage, growth of the germ tube switches from polarized to isotropic mode, leading to formation of a dome-shaped infection cell called, the appressorium. The appressorium develops a melanin layer and accumulates compatible solutes, such as glycerol, allowing turgor pressure to build up and to be translated into mechanical force pushing a penetration peg through the rice surface (de Jong *et al.*, 1997, Howard *et al*., 1991). The emergence of penetration peg at the base of appressorium is the second morphogenetic transition involving re-polarisation of cell growth towards the appressorium pore (Bourett & Howard, 1990). Invasive hyphae proliferate inside living plant cells in a symptomless, biotrophic manner for a prolonged period (Kankanala *et al.*, 2007). During this stage, the fungus encounters a robust, multi-

layered plant immune system. The fungus in turn employs various strategies to evade and suppress host immunity to facilitate its growth and reproduction (Mosquera *et al.*, 2009). After 72 hour of infection, disease lesions become apparent on the leaf surface when to the fungus undergoes necrotic growth by which host cells are killed. *M. oryzae* is classified as a hemibiotrophic pathogen which is characterised by a parasitic growth in living host tissue for some time and then starting to kill host tissue (Kankanala *et al.*, 2007). Asexual spores are produced from the lesions and spread rapidly to adjacent plants by wind and dewdrop splash (Shi *et al.*, 1998).

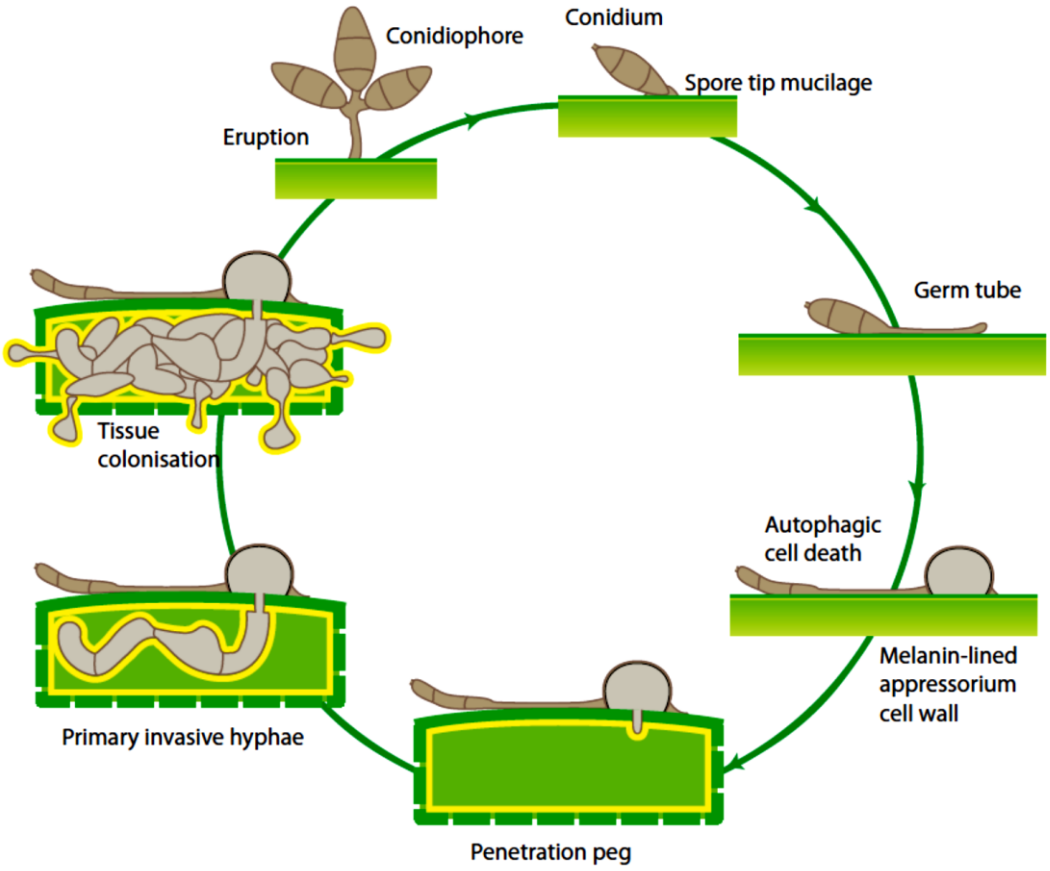

Figure 1.3 Life cycle of *M. oryzae.* This image was prepared by Dr George Littlejohn, Bioscience, University of Exeter.

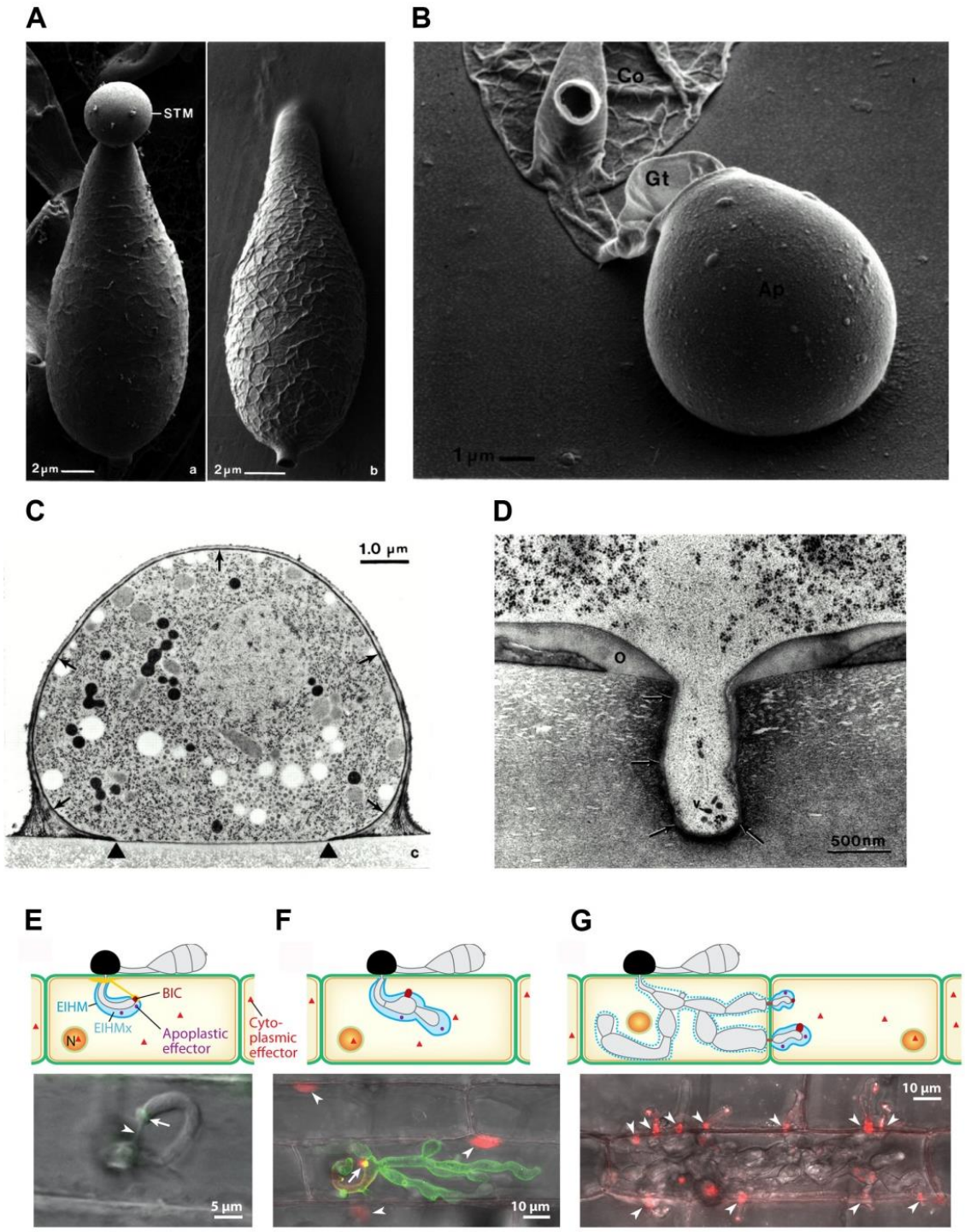

Figure 1.4 Micrographs and schematic diagram showing infection-related development of *M. oryzae*. (A, left panel) Cryo scanning electron micrograph (SEM) of **a** conidium attached on conidiophore with spore tip mucilage (STM). **(A, right panel)** A conidium landed on hard hydrophobic surface. **(B)** Mature appressorium with a collapsed conidium. **(C)** Transmission electron micrograph

(TEM) to show a mature appressorium. Arrows, melanin layer. Appressorium pore, between arrowheads. (D) Nascent penetration peg. **(E)** A primary hypha with a biotrophic interfacial complex (BIC) at the tip. **(F)** Bulbous invasive hyphal cells. **(G)** Invasive hyphae invaded neighbouring host cells. **(A)** to **(D)** were taken from (Howard & Valent, 1996). **(E)** to **(G)** were taken from (Yi & Valent, 2013).

1.6 Regulation of appressorium morphogenesis

The first morphogenetic transition during infection-related development by *M. oryzae* is a switch from polarised to isotropic growth of the germ tube tip leading to the formation of a dome-shaped appressorium (Veneault-Fourrey *et al*., 2006). This switch depends on the perception of hardness, hydrophobicity, and plant derived compounds, such as waxes and cutin monomers present on leaf surfaces. Two intracellular signalling pathways are implicated in development of plant infection structures and pathogenicity (Li *et al*., 2012). The cyclic AMP-protein kinase A (cAMP-PKA) regulates recognition of plant surface, early development of appressoria and turgor generation (Choi & Dean, 1997). The Pmk1 mitogen-activated protein kinase (MAPK) pathway controls development of the appressorium (Xu & Hamer, 1996). Recognition of extracellular signals is mediated by G-protein coupled receptors (GPCRs) (Liu & Dean, 1997). The *M. oryzae* genome contains a very large set of GPCRs (Dean *et al*., 2005). Of these, Pth11 is a GPCR with a conserved fungal-specific extracellular membrane-spanning domain (a CFEM domain), and operates upstream of the cAMP-PKA pathway (DeZwaan *et al.*, 1999). Immediately after conidial germination, the G-protein coupled receptor Pth11 potentially triggers dissociation of the heteromeric G-proteins, MagA and MagB, which then activate intracellular production of cAMP (DeZwaan *et al*., 1999). Rgs1 is also involved in regulation of G-protein signalling

during the perception of inductive surfaces (Ramanujam *et al.*, 2012, Liu *et al.*, 2007). The G-beta subunit Mgb1 plays important roles in both cAMP signaling and Pmk1 MAPK pathways, and is necessary for regulating multiple steps of infection-related morphogenesis by *M. oryzae* (Nishimura *et al.*, 2003). Mgb1 also physically interacts with Mst50, an adaptor protein that provides a direct link between G-protein signalling and the Pmk1 MAPK pathway (Park *et al.*, 2006). Null mutants of *MGB1* were defective in appressorium development. Exogenous cAMP rescued appressorium formation in the Δ*mgb1* mutants, but these appressoria were aberrant in shape and non-functional, suggesting that additional stimuli might be involved in proper formation and function of the appressorium (Nishimura *et al*., 2003). Surface proteins, such as MoMsb2, MoSho and MoCbp1, play overlapping functions in appressorium formation upstream of the Pmk1 pathway (Liu *et al.*, 2011, Wang *et al.*, 2015). Although the cytoplasmic domain of MoMsb2 is dispensable for appressorium formation on either artificial hydrophobic or plant surfaces, it has important roles in appressorium penetration and invasive growth (Liu *et al*., 2011). The mutants lacking whole cytoplasmic region of MoMsb1 were able to form appressorium at the frequency near the wild type, but their appressoria rarely penetrated plant surface (Wang *et al*., 2015). Primary hyphae that emerged from those appressoria finally failed to differentiate branched invasive hyphae (Liu *et al*., 2011, Wang *et al*., 2015). How multiple signals are integrated into a cohesive response during plant infection by the rice blast fungus is an important biological question that remains unclear.

Exogenous cAMP can rescue appressorium differentiation during conidial germination on non-inductive surfaces, suggesting a role for cAMP-dependent

signalling in this process (Lee & Dean, 1993). Upon surface perception, adenylate cyclase Mac1 produced intracellular cAMP. Deletion mutant of *MAC1* cannot form appressorium or infect rice plants (Choi & Dean, 1997). A cyclase-associated protein, Cap1, is required for Mac1 activation (Zhou *et al.*, 2012). Increased levels of cAMP induce dissociation of the regulatory subunit of PKA from the catalytic subunit CpkA, leading to initiation of appressorium morphogenesis (Adachi & Hamer, 1998, Lee & Dean, 1993). Null mutants of PKA subunits produce non-functional appressoria and cannot infect plants (Mitchell & Dean, 1995). The constitutively active regulatory subunit of PKA, Sum1, can override the requirement of cAMP signalling and re-mediates phenotype of the *Δmac1* mutant (Adachi & Hamer, 1998). Operating downstream of the cAMP-PKA pathway, three transcription factors Mstu1, Som1 and Cdtf1 have been identified and are necessary for normal sporulation and appressorium differentiation (Yan *et al.*, 2011).

The *M. oryzae* genome encodes elements of three canonical MAPK pathways, the Pmk1, Mps1 and Osm1 pathway, which serve different roles in infection-related development and fungal adaptation to environmental stress. These conserved MAPK pathways also play important roles in pathogenicity of various fungal pathogens (Li *et al*., 2012, Rispail *et al*., 2009). The Pmk1 MAPK is a functional homologue of yeast Fus3 and Kss1 MAPKs, responsible for appressorium morphogenesis and invasive growth (Xu & Hamer, 1996). Δ*pmk1* mutants fail to develop appressoria on any inductive conditions, but still respond to exogenous cAMP, by producing a terminal swelling of the germ tube tip, called a hooking (Xu & Hamer, 1996). Interestingly, Δ*pmk1* mutants are unable to cause

disease through wound inoculation, which bypasses appressorium formation and penetration step, indicating that Pmk1 also controls infectious growth of the fungus (Xu & Hamer, 1996). GFP-tagged Pmk1 is poorly detectable in vegetative hyphae, conidiophores, conidia, and germ tubes, whereas a stronger GFP signal can be observed in developing conidia and appressoria (GFP for green fluorescence protein) (Bruno *et al.*, 2004). During appressorium formation and maturation, GFP-Pmk1 is localised to the cytoplasm and appressorium nucleus, consistent with observations in various organisms that MAPKs are translocated into the nucleus in response to appropriate stimuli (Bruno *et al*., 2004). The Pmk1 MAPK is activated by the upstream kinases Mst7 and Mst11, constituting a three-tied MAPK module, Mst11-Mst7-Pmk1 (Zhao *et al.*, 2005). Expression of the $MST7^{S212D\ T216E}$ allele rescued the defect in appressorium formation, but not plant infection, in *mst7* or *mst11* deletion mutants (Zhao *et al*., 2005). Hyper-activation of Pmk1 by expression of a constitutively active *MST7* allele blocked appressorium penetration, possibly by interfering with the normal fluctuation of *PMK1* activity during plant infection (Zhao *et al*., 2005). Mst50 is also essential for activation of the Pmk1 MAPK cascade by serving as an adaptor protein to stabilize the Mst11-Mst7 interaction, and also interacting with upstream components, such as Ras1, Ras2, Mgb2, and Cdc42 to activate the MAPK cascade (Park *et al*., 2006). Ras2 operates upstream of both the Pmk1 MAPK and cAMP-PKA pathways (Zhou *et al.*, 2014). Although *RAS2* appears to be an essential gene, preventing straightforward gene functional analysis, expression of a dominant-active allele of *RAS2* bypasses requirements for spore attachment and recognition to hard hydrophobic surfaces in appressorium development. The dominant active mutant of *RAS2* forms

appressoria-like structure on non-inductive surfaces due to improper activation of the cAMP-PKA and Pmk1 pathways (Zhou *et al*., 2014). Ras2 physically interacts with the cytoplasmic tail of Msb2 and with the MAPKKK Mst11, representing a link between a surface sensor and intracellular signal transduction (Qi *et al.*, 2015, Wang *et al*., 2015). Therefore, the Pmk1 MAPK and cAMP-dependent pathways are clearly core signalling pathways of appressorium morphogenesis and plant infection by *M. oryzae* (Li *et al*., 2012).

Activated Pmk1 MAPK phosphorylates several downstream effectors and transcriptional regulators to alter global gene expression required for appressorium development and plant infection (Li *et al*., 2012). Two Pmk1-interacting clones (PICs), for example, were identified and shown to have roles in conidiation and appressorium differentiation (Zhang *et al.*, 2011). Protein microarrays and co-immunoprecipitation analyses identified a transcription factor, Sfl1, as a direct substrate of the Pmk1 MAPK (Li *et al.*, 2011). Deletion of *SFL1* resulted in defect in a heat tolerance and a significant reduction in virulence on rice or barley. The Δ*sfl1* mutant can form appressoria, but its invasive hyphae appear to be confined to the first infected rice cells (Li *et al*., 2011). Comparative transcriptome analysis using super serial analysis of gene expression (SuperSAGE) showed that during germination of the Δ*pmk1* mutant, 481 genes were down regulated which might be regulated by Pmk1 (Soanes *et al.*, 2012). Some of these genes were already known to be virulence factors, such as *GAS1, GAS2, HOX7*, and *PTH11* (Soanes *et al*., 2012). A homeobox transcription factor MoHox7 and a C2/H2 Zn finger-domain transcription factor Znf1 potentially operate downstream of the Pmk1

pathway, and are required for appressorium development (Yue *et al.*, 2016, Kim *et al.*, 2009).

Generation of reactive oxygen species (ROS) and activation of the small GTPase Rac1 are implicated in fungal cell differentiation, such as appressorium development (Chen *et al.*, 2008, Egan *et al.*, 2007). ROS are detected in germinating conidia, growing hyphal tips and in developing appressoria. Scavenging ROS strongly reduces appressorium development and affects appressorium morphology (Egan *et al*., 2007). Deletion of *MgRAC1* resulted in a mutant defective in appressorium formation and conidiation (Chen *et al*., 2008). MgRac1 physically interacts with Chm1 and the NADPH oxidases Nox1 and Nox2 (Chen *et al*., 2008). Chm1 is a homologue of the p21-activated kinase (PAK) Cla4 (Li *et al.*, 2004). *M. oryzae* mutants lacking *CHM1* are defective in appressorium formation, penetration and plant infection (Li *et al*., 2004). In *S. cerevisiae,* Cla4 PAK is an effector of the small Rho GTPase Cdc42, and is primarily responsible for phosphorylation of septins to induce septin ring assembly at the bud neck during cell division (Weiss *et al.*, 2000, Versele & Thorner, 2004). Inactivation of Cla4 kinase activity results in a Swe1-dependent cell cycle arrest in G2, and gives rise to highly elongated buds in which actin and septins are concentrated to bud tips (Weiss *et al*., 2000). It is likely that Δ*chm1* mutants are unable to efficiently form appressoria, due to the defects in septin collar formation at the neck of appressoria, leading to activation of the morphogenesis checkpoint and cell cycle arrest (Li *et al*., 2004). The Rac1-Chm1 pathway is therefore required for conidiation, regulation of ROS generation, appressorium formation and pathogenicity (Chen *et al*., 2008). Recently, two thioredoxins, Trx1 and Trx2, were

shown to regulate activation of the Pmk1 MAPK pathway, providing a possible link between the MAPK cascade and ROS signalling. Trx2 physically interacts with, and is required for proper folding of the Mst7 protein (Zhang *et al.*, 2016b). Interrelationships between different signalling pathways, such as Rac1-Chm1-Nox, Ras2-cAMP-PKA, Pmk1 MAPK and cell cycle control, during appressorium development and plant penetration remain to be elucidated.

Faithful cell cycle regulation is important for cellular morphogenesis which is required for establishment of plant infection in many fungal pathogens (Perez-Martin *et al.*, 2016). In the cucumber anthracnose fungus *Colletotrichum orbiculare*, for example, S-phase entry is controlled by two component GAP and Tem1 GTPase signalling, and is required for plant penetration (Fukada & Kubo, 2015). In corn smut fungus *U. maydis*, cell cycle arrest in G2, mediated by elements of DNA damage checkpoint and the Hsl1 kinase, is important for generation of filamentous infectious hyphae (Castanheira *et al.*, 2014). Appressorium development by the rice blast fungus however involves a distinct cell division program. The initiation of appressorium formation requires cell cycle progression through S-phase, whereas maturation of the appressorium depends on entry into mitosis. Inhibition of DNA replication by using hydroxyurea (HU) or by using temperature-sensitive mutants of the regulatory subunit of the Dbf4-Cdc7 complex, *nim1*^{I327E}, prevents appressorium formation (Veneault-Fourrey *et al*., 2006, Saunders *et al*., 2010a). Blocking the cell cycle in mitosis, by using a conditional mutant of *BIM1* or by expression of stablised versions of B-type cyclins did not block appressorium differentiation, but instead prevented appressorial re-polarisation required for plant penetration (Saunders *et al*., 2010a).

Asymmetric cell division accompanies migration of a daughter nucleus into a daughter cell, and is specifically associated with infection-related morphogenesis in *M. oryzae* (Jones *et al.*, 2016a, Osés-Ruiz *et al.*, 2016, Saunders *et al.*, 2010b). In hyphae of *M. oryzae*, contractile actomyosin rings consistently form at the position of the pre-mitotic nucleus and the medial position of the mitotic spindle (Saunders *et al*., 2010b). A similar pattern also occurs during both hyphal branching and subapical nuclear division within growing hyphae (Saunders *et al*., 2010b). By contrast, during appressorium formation, the germ tube nucleus divides close to the site of germ tube emergence followed by a long distance migration of one daughter nucleus into the incipient appressorium (Saunders *et al*., 2010b). Interestingly, the appressorium septation site is defined by septin ring formation at the neck of the appressorium, which precedes mitosis in the germ tube (Saunders *et al*., 2010b). This pattern might be comparable to budding in *S. cerevisiae*. In late G1 of the yeast cell cycle, the septin complex assembles into a ring at the future bud site before expanding into an hourglass-shape structure delimiting the neck of the forming bud during S and M phases (Cid *et al.*, 2001).

1.7 Regulation of appressorium-mediated plant penetration

To gain entry into host tissues, the single-celled appressorium of the rice blast fungus generates enormous turgor pressure, which is then translated into mechanical force sufficient to breach the plant cuticle (Howard and Valent, 1996; Ryder and Talbot, 2015). Deposition of melanin layer on the inner side of fungal cell wall of the appressorium represents a final and functionally significant stage of appressorium differentiation (Chumley & Valent, 1990, Howard *et al*., 1991,

Howard & Valent, 1996). However, the melanin layer is absent from the region in contact with the substratum, the so called appressorium pore (Howard & Valent, 1996). Initially the fungal cell wall is also extremely thin at this site, according to transmission electron microscopy (TEM) analysis (Bourett & Howard, 1990). The pore ring is a ring of material at the plane of contact surrounding the perimeter of the appressorium pore that seals the pore to the substratum (Howard & Valent, 1996).

Cellular turgor is generated by influx of water into the appressorium, due to accumulation of glycerol as a compatible solute and the presence of melanin layer on the inner side of appressorium cell wall (de Jong *et al*., 1997). The melanin layer blocks efflux of glycerol but allows diffusion of surrounding water, leading to increased internal turgor of up to 8.0 MPa (Howard *et al*., 1991). Disruption of melanin biosynthesis using tricyclazole treatment, or mutations in genes encoding melanin biosynthetic enzymes results in non-melanised appressoria, that are unable to accumulate sufficient turgor pressure and fail to penetrate rice surface (Chumley & Valent, 1990, de Jong *et al*., 1997). *M. oryzae* spore does not contain glycerol and appressorium formation occurs in a nutrient-free environment. Therefore, storage compounds in the spore, such as mannitol, glycogen, lipids and trehalose, must be mobilised and converted into glycerol in the mature appressorium (Talbot, 2003; Wilson and Talbot, 2009). Lipid bodies are translocated from the spore and taken up into appressorial vacuoles where they are hydrolysed by triacylglycerol lipases (Weber *et al.*, 2001). This process is controlled by the Pmk1 MAPK and the cAMP-PKA pathways (Thines *et al.*, 2000). The activity of lipases liberates glycerol from the fatty acids moiety via β-oxidation,

and lipid catabolism to yield acetyl-CoA. Acetyl-CoA can be used to produce glucose, via gluconeogenesis or melanin biosynthesis via secondary metabolic pathways (Wang *et al.*, 2003). Peroxisomal lipid catabolism likely contributes to metabolism during appressorium development, whereas mitochondrial lipid metabolism primarily serves for maintenance of redox state during invasive growth (Patkar *et al.*, 2012). The rapid increase of glycerol levels during appressorium formation coincides with autophagic cell death of conidial cells (Veneault-Fourrey *et al*., 2006). Mutants in components of the non-selective macro-autophagy pathway still form appressoria but they are non-functional leading to loss of pathogenicity (Kershaw & Talbot, 2009, Veneault-Fourrey *et al*., 2006). Interestingly, completion of mitosis in the germ tube is required for degeneration of the conidial nuclei and collapse of the conidium, suggesting a link between the cell cycle control and autophagy (Kershaw & Talbot, 2009, Veneault-Fourrey *et al*., 2006). Turgor levels of the appressorium are modulated by a two-component histidine kinase, MoSln1 (Zhang *et al.*, 2010). Deletion of *MoSLN1* gene resulted in hypersensitivity to osmotic stress, defects in maintenance of cell wall integrity, reduced ROS production, and loss of pathogenicity (Zhang *et al*., 2010). Appressoria of the Δ*MoSLN1* mutant generate abnormally high turgor but fail to penetrate plant surface, suggesting that Sln1 involved in a negative feedback loop controlling turgor, possibly via reducing glycerol production, and an appropriate turgor level is required of the emergence of penetration peg (Zhang *et al*., 2010, Dixon *et al.*, 1999, Jacob *et al.*, 2014). It has been proposed that appressorium-mediated penetration is initiated when cellular turgor reaches a critical threshold level (Ryder & Talbot, 2015).

Emergence of a narrow penetration peg is considered as the second morphogenetic transition during infection-related development, involving re-establishment of cell polarity and secretion towards the base of the appressorium (Dagdas *et al.*, 2012, Gupta *et al.*, 2015, Howard *et al*., 1991, Howard & Valent, 1996). There are numerous vesicles at the appressorium-cuticle interface suggesting that the appressorium pore is a site for active fungal secretion, consistent with the localisation of exocyst components at this site (Gupta *et al*., 2015, Yi & Valent, 2013). Septins form a ring-shaped hetero-oligomeric complex around the appressorium pore, which acts as a lateral diffusion barrier restricting polarity determinants, endocytic proteins, and actin regulators (Dagdas *et al*., 2012). Septins also scaffold the F-actin network to provide cortical rigidity necessary for stablising cellular protrusion of the penetration peg which breaches the leaf surface (Dagdas *et al*., 2012). Septins are necessary for recruitment of the octomeric exocyst complex which directs the polarised protein secretion at the appressorium pore (Gupta *et al*., 2015). The organisation of F-actin and polarity determinants at the appressorium pore is regulated by ROS signalling, involving the action of the Chm1 kinase, the NADPH oxidase (NOX) complex, as well as the Pmk1 and Mps1 MAPK pathways. Mutants lacking Chm1, Nox2, NoxR, Mst12 or Mps1 are unable to organise F-actin and septins into a ring around appressorium pore and failed to penetrate the rice cuticle (Dagdas *et al*., 2012, Ryder *et al.*, 2013). Mst12, a homologue of *S. cerevisiae* Ste12, functions downstream of the Pmk1 MAPK pathway required for plant penetration (Park *et al.*, 2004, Park *et al.*, 2002). Mps1 is an orthologue of yeast Slt2 MAPK responsible for the maintenance of cell wall integrity (Xu *et al.*, 1998). In summary, appressorial penetration involves

complex integration of intracellular signals manifesting in re-organisation of cytoskeletons that directs secretion and cell growth towards the base of appressorium and brings about the emergence of a narrow penetration peg (Dagdas *et al*., 2012).

1.8 Cell biology of blast biotrophic growth

After successful rupture of the rice cuticle, a narrow penetration peg differentiates into a tubular primary hypha that enters lumen of the rice cell accompanied with invagination of the rice plasma membrane (Kankanala *et al*., 2007, Mentlak *et al*., 2012). The primary hypha then differentiates into bulbous invasive hyphae that morphologically resemble to pseudohyphae of a dimorphic fungus, *Candida albicans,* which have constrictions at septal junctions (Giraldo *et al*., 2013, Kankanala *et al*., 2007). This is considered the third morphological transition of the *M. oryzae* life cycle. Dye loading experiments using the endocytic tracker dye FM4-64 showed that the dye outlines invasive hyphae but is not internalised by invasive hyphae (Kankanala *et al.*, 2007). Live-cell imaging using a transgenic rice line expressing plasma membrane marker Lti6B-GFP confirmed that invasive hyphae are surrounded by invaginated rice plasma membrane (Giraldo *et al*., 2013, Mentlak *et al*., 2012, Mochizuki *et al.*, 2015). During plasmolysis, the rice plasma membrane is pulled away from the cell wall but stays around the invasive hyphae, suggesting that it is attached to the base of primary hypha (Kankanala *et al*., 2007). Fluorescently-labelled secreted apoplastic effectors are found to outline invasive hyphae, but not in other apoplastic compartments away from the invasive hyphae (Khang *et al.*, 2010, Mosquera *et al*.,

2009). These individual lines of evidence indicate that bulbous invasive hyphae are enclosed within a plant-derived membrane, called the extra invasive hyphal membrane (EIHM). The EIHM is sealed by a neckband-like structure near an entry point of the primary hypha to produce a separate apoplastic compartment around invasive hyphae (Jones *et al.*, 2016b, Kankanala *et al*., 2007, Khang *et al*., 2010, Mentlak *et al*., 2012, Mosquera *et al*., 2009). Interestingly, a plasma membrane-localised immune receptor OsCERK1 appears to be excluded from the EIHM (Kouzai *et al.*, 2014a). Recently, the rice cytosol was shown to accumulate near the fungal penetration site beneath the appressorium and the invasive hyphae are surrounded by rice vacuolar membrane (Mochizuki *et al*., 2015). How the EIHM is built, the composition of this membrane, and its specialised physiology to accommodate the pathogen, remain important questions that are unanswered.

To suppress plant defense responses and promote biotrophic fungal growth, *M. oryzae* secretes a battery of effectors to different locations in plant cells (Giraldo & Valent, 2013, Lo Presti *et al.*, 2015). These effector proteins possess classical signal peptides required for delivery into the ER and secretion from the fungal cells (Khang *et al*., 2010, Mosquera *et al*., 2009). The ER chaperone Lhs1 and the aminophopholipid translocases Pde1 and Apt2 are implicated in effector secretion during tissue colonisation (Balhadère & Talbot, 2001, Gilbert *et al.*, 2006, Yi *et al.*, 2009). Initial evidence for translocation of secreted fungal proteins across EIHM into rice cytoplasm is derived from a study of the AVR-Pita gene product, which is recognised by an intracellular immune NLR receptor Pi-ta, suggesting that AVR-Pita performs its function inside host cells (Jia *et al*., 2000, Orbach *et al*., 2000). In oomycete pathogens, the presence of well-conserved translocation motifs (RXLR

and EER) following the classical signal peptide in cytoplasmic effectors allows bioinformatic prediction (Whisson *et al.*, 2007). In the maize smut fungus *U. maydis,* some *in planta* specific-secreted effector genes are found in genome clusters and also provide clues to which genes encode delivered effectors (Kamper *et al.*, 2006). However, none of these strategies can be applied for *M. oryzae* effectors (Mosquera *et al*., 2009). Identification of putative fungal effector genes has largely been based on association genetics and transcriptome analysis of genes encoding secreted proteins that are specifically expressed during *in planta* growth (Mosquera *et al*., 2009, Yoshida *et al*., 2009). Although most fungal effectors lack significant homology to other known proteins, recent structural analysis of effector proteins from *M. oryzae* and other pathogenic fungi has revealed a family of structurally conserved effectors, so called MAX effectors (de Guillen *et al.*, 2015). The study suggests that this structural conservation of fungal effectors might therefore play roles in suppression of host immunity, while also allowing high diversification of amino acid sequences among effector proteins (de Guillen *et al*., 2015).

Live-cell imaging of *M. oryzae* invasive hyphae expressing fluorescently-labelled effector proteins shows distinct patterns of accumulation at the plant-pathogen interface (Khang *et al*., 2010, Mosquera *et al*., 2009). Apoplastic effectors, such as Bas4 and Slp1, outline the entire invasive hyphae. Several avirulence (AVR) and Bas1 effectors preferentially accumulate in the biotrophic interfacial complex (BIC). These effectors, so called cytoplasmic effectors, are translocated across the EIHM into host cytoplasm (Khang *et al*., 2010, Mosquera *et al*., 2009). Initially, BICs were identified as membranous caps located at the tips of

primary hyphae, and the filamentous hyphae that newly invade adjacent cells (Kankanala *et al.*, 2007). Once the primary hypha differentiates into a bulbous invasive hypha, the BIC remains beside the first bulbous invasive hyphal cell as other invasive hyphal cells continue to grow by budding (Khang *et al.,* 2010). The BIC is a plant-derived interfacial structure located outside the fungal cell wall in a region rich in plant plasma membrane, cytosol and ER (Mentlak *et al.*, 2012; Giraldo *et al.,* 2013; Mochizuki *et al.,* 2015). The host central vacuolar membrane surrounds the BIC but does not intermingle with the EIHM (Mochizuki *et al.,* 2015). High resolution visualisation of BICs reveals that Pwl2-mCherry accumulates in BICs as dynamic puncta, and that these puncta are encircled by rice plasma membrane, suggesting that this cytoplasmic effector is packed in vesicles after entering host cells. It has been proposed that rice cells uptake fungal effectors via the endocytic pathway, and that the BICs are composed of aggregated effector-containing vesicles that are then sorted to other cellular domains (Nishizawa *et al.*, 2016); Barbara Valent and Ely Oliveira Garcia, personal communication). Interestingly, some cytoplasmic effectors, for example Bas1 and Pwl2, move ahead into many layers of surrounding plant cells before the arrival of invasive hyphae, implying that these effectors may prepare host cells before invasion and the plasmodesmata remain open to allow diffusion of effectors at this time (Khang *et al.*, 2010).

Cytoplasmic and apoplastic effectors appear to be delivered by two distinct secretion mechanisms: the conventional ER-to-Golgi secretion pathway for apoplastic effectors, and an unconventional secretion pathway requiring exocyst components for cytoplasmic effectors (Giraldo *et al*., 2013). Inhibition of the

conventional ER-to-Golgi secretion using Brefeldin A (BFA) treatment resulted in retention of apoplastic effectors, such as Bas4 and Slp1, within ER-like compartments of invasive hyphae, but secretion of cytoplasmic effectors, for example Pwl2 and Bas1, was unaffected (Giraldo *et al*., 2013). The BIC-associated hyphal cell contains several important components of the secretory machinery, consistent with focal delivery of cytoplasmic effectors to this site. Effector secretion to the BIC appears to involve exocyst components, Exo70 and Sec5 (Giraldo *et al.,* 2013). How a subset of secretory machineries is retained in BIC-associated invasive hyphal cells, while other invasive hyphal cells continue growing, is still unclear (Giraldo *et al.,* 2013).

Only a very small subset of blast effectors have known virulence functions. The LysM protein Slp1 is one of the best characterised secreted effectors in *M. oryzae* (Mentlak *et al.,* 2012). Slp1 can bind to chitin and accumulates at the apoplastic compartment between the fungal cell wall and the rice plasma membrane, similar to Bas4 protein. Slp1 is able suppress chitin-induced plant defence responses by sequestering free chitin oligosaccharises so that they do not bind to CEBiP, a chitin sensor of rice cells. Slp1 is required for full virulence of the rice blast disease (Mentlak *et al.,* 2012). Slp1 and Bas4 effectors have been shown to undergo *N*-glycosylation by α-1,3-mannosyltransferase Alg3, which is important for function and stability of several effector proteins (Chen *et al*., 2012). Screen for suppressors of cell death (SPD) identified 11 SPD effectors. These include, for example, SPD5, a paralogue of apoplastic effector Bas4 which outlines the invasive hyphae during the biotrophic phase, and SPD6 which is also known as Bas3 localises to BICs and cell wall crossing sites (Sharpee *et al.,* 2016; Mosquera

et al., 2009). SPD5 and SPD6 are able to inhibit host cell death caused when they are co-expressed with necrosis inducing factors, such as Nep1 and BAX, in *Nicotiana benthamiana* (Sharpee *et al.*, 2016). The AvrPiz-t secreted effector suppresses rice innate immunity, thereby targeting the ubiquitin 26S proteasome degradation system (UPS) which mediates PTI signalling (Li *et al.*, 2009, Park *et al.*, 2016, Park *et al.*, 2012). The AvrPiz-t effector is translocated into rice cytoplasm, in a BIC-dependent manner, where it interacts with rice RING finger ubiquitin ligase E3, APIP6 (Park *et al*., 2012). Silencing of APIP6 in rice reduces several defence response makers, such as PAMP-induced ROS production and defence-related gene expression, and finally enhances susceptibility to *M. oryzae* (Park *et al*., 2012). Moreover, the AvrPiz-t interacts with another three UPS proteins, suggesting that the fungal effector interferes with many components of host proteolysis (Park *et al*., 2012). Importantly, AvrPiz-t can be recognised by its cognate R gene product Piz-t NB-LRR (Zhou *et al.*, 2006). AVR-Pii also has several binding partners that play different functions in host immunity (Fujisaki *et al.*, 2015). Using gel filtration chromatography and co-immunoprecipitation assays, the effector AVR-Pii was found to interact with two rice Exo70 proteins, potentially involved in exocytosis (Fujisaki *et al*., 2015). However, simultaneous silencing of two rice *EXO70* genes completely disrupts Pii-dependent resistance, suggesting a function of rice Exo70 proteins as decoys or helpers in Pii and AVR-Pii interactions (Fujisaki *et al*., 2015). Recently, Y2H screening of AVR-Pii interactors has additionally identified rice NADP-malic enzyme (Os-NADP-ME2) required for innate immunity against rice blast fungus (Singh *et al.*, 2016). The AVR-Pii effector

inhibits enzymatic activity of Os-NADP-ME2, which in turn suppresses ROS burst and promote fungal infection (Singh *et al*., 2016).

How expression of different sets of fungal effectors is regulated in order to match their invasion stages is an interesting topic in plant-microbe interactions. Most fungal effectors, including those of *M. oryzae,* are specifically expressed during interaction with host plants (Mosquera *et al.*, 2009; Mentlak *et al*., 2012; Yi and Valent, 2013; Kleemann *et al.*, 2012). In an ascomycete pathogen causing anthracnose disease *Colletotrichum higginsianum,* most of its secreted effector genes are expressed in consecutive waves associated with four different pathogenic transitions: (1) pre-penetrated appressoria; (2) penetrated appressoria with initial biotrophic hyphae; (3) biotrophic-to-necrotrophic switch; (4) late necrotrophy (Kleemann *et al*., 2012). These sets of fungal effectors appear to be associated with functions in promoting cell viability or cell death, according to the timing of their gene expression. This study indicates that distinct effector sets are deployed at each invasion stage (Kleemann *et al*., 2012). Homologues of WOPR transcription factors serve several roles in fungal development, including morphological transitions and modulation of effector gene expression, in various pathogenic fungi (Cain *et al.*, 2012). A recent study showed that *U. maydis* WOPR transcription factor, Ros1, controls gene expression of at least 60% (194 genes) of putative secreted effectors in the late biotrophic stage of plant infection (Tollot *et al.*, 2016). The *M. oryzae* WOPR transcription factor, MoGTI1, is required for formation of penetration peg, differentiation of branched invasive hyphae, and expression of small set of fungal effectors (Li *et al.*, 2015, Chen *et al.*, 2014).

However, how transcription of a large set of *M. oryzae* effectors is regulated at different stages of infection-related development remains largely unknown.

To succeed in host tissue colonisation, *M. oryzae* not only use secreted effectors to disable host immunity, but also produces many plant hormones or hormone-like compounds to promote a favourable environment for its growth and reproduction. *M. oryzae* is capable of producing cytokinin (CK) (Chanclud *et al.*, 2016) and indole-3-acetic acid (IAA) auxin phytohormones (Tanaka *et al.*, 2011). Mutants of *CKS1*, defective in CK bio-synthesis, are unable to suppress host defence responses such as the ROS burst and expression of defence-related marker genes. Interestingly, sugar and amino acid contents around infection sites of the Δ*cks1* mutant are also altered (Chanclud *et al*., 2016). The roles of fungal-derived CK in maintenance of nutrient levels or modification of nutrient fluxes around infection sites are consistent with metabolomic analysis indicating that *M. oryzae* induces relocation of nutrients towards infection sites (Parker *et al.*, 2009). Immunolocalisation study reveals the distribution of IAA around invasive hyphae of *M. oryzae,* consistent with local expression of auxin-responding gene at infection sites (Tanaka *et al.*, 2011). The fungal-derived IAA may promote a positive feedback loop of rice IAA production. IAA induces expression of expansins, a family of proteins responsible for cell wall loosening, and makes rice plant more susceptible to fungal pathogens (Tanaka *et al.*, 2011). The rice *GH3-2* gene encoding an IAA-amido synthetase was found to mediate basal resistance by inactivating pathogen-inducing IAA production (Fu *et al.*, 2011). The pathogen can also interfere with jasmonic acid (JA) signalling involved in plant growth and immunity (Patkar *et al.*, 2015). *M. oryzae* secretes a fungal antibiotic biosynthesis

monooxygenase (Abm) during host penetration to evade host defences and facilitate tissue colonisation (Patkar *et al*., 2015). The Abm prevents accumulation of defence-inducing methyl JA by converting endogenous free JA into 12OH-JA which antagonises with the JA signalling (Patkar *et al*., 2015).

As the life cycle of *M. oryzae* involves multiple steps of development both outside and inside host cells, the metabolism of fungal cells must correctly adapt to changes in environment and nutrient availability (Fernandez & Wilson, 2014). Outside the host plant, the metabolism of developing appressoria involves fatty acid β-oxidation, the glyoxylate cycle, and translocation of acetyl-CoA from the peroxisome (Patkar *et al*., 2012, Wang *et al*., 2003). During *in planta* growth, the fungus appears to respond to the glucose-rich and nitrogen-poor environment by shifting to glucose-utilising metabolism involved in maintenance of redox homeostasis (Fernandez & Wilson, 2014). Comparative transcriptome analysis suggests that rice blast biotrophic growth is closely related to adaptation of nutrient-limited conditions rather than oxidative or temperature stresses (Mathioni *et al.*, 2013). Integration of carbon and nitrogen metabolism of *M. oryzae* is mediated by the sugar sensor trehalose-6-phosphate synthase 1 (Tps1) (Wilson *et al.*, 2007, Fernandez & Wilson, 2011, Foster *et al.*, 2003). Deletion of *TPS1* results in mutant strains that are able to develop appressoria, but fail to form necrotic lesions (Foster *et al*., 2003). Tps1 senses the levels of glucose 6-phosphate (G6P) to control the levels of NADPH, which in turn mediates adaptation to nutrient availability and redox states during invasive growth (Wilson *et al*., 2007). These lead to the initiation of carbon catabolite repression (CCR) in order to ensure the appropriate use of glucose over alternative carbon sources, and the activation of

nitrogen utilisation in the presence of G6P (Fernandez *et al.*, 2012). Importantly, the *Δtps1* mutants fail to repress expression of cell wall degrading enzymes that, in wild type, are not normally induced until necrotrophic phase of plant infection (Fernandez *et al*., 2012). Therefore, the Tps1-dependent pathway represses the use of cell wall polysaccharides in the early biotrophic invasion, when G6P appears to be abundant in host cells (Fernandez & Wilson, 2014, Wilson *et al*., 2007, Wilson *et al.*, 2010).

1.9 Cell-to-cell invasion during tissue colonisation by the rice blast fungus

Movement of *M. oryzae* invasive hyphae into neighbouring cells occurs through pit fields, where the invasive hyphae extremely constrict (Kankanala *et al*., 2007). Time-lapse and confocal scanning microscopy demonstrated that blast invasive hyphae seek out particular locations of plant cell walls before crossing, and shows the connection of the EIHM with primary pit fields. TEM analysis confirms that the invasive hyphae preferentially contact plant cell wall at the pit fields, and use pit fields for their cell wall crossing. Observations that invasive hyphae also fail to enter guard cells, which lack functional plasmodesmata further supported the hypothesis that invasive hyphae of *M. oryzae* co-opt plasmodesmata for cell-to-cell movement. *M. oryzae* invasive hyphae have diameters of larger than 5 µm, are constricted at least 10-fold to approximately 0.5 µm in diameter at cell wall crossing points. The initial invasive hyphae that have newly crossed the cell wall are filamentous and lack nuclei, morphologically similar to that of primary hypha growing from the penetration peg of appressorium (Kankanala *et al*., 2007).

Differentiation of the penetration invasive hyphae peg is considered as the fourth morphological transition of the life cycle. A nucleus dividing in the bulbous invasive hyphal cell in the first invaded side, and one daughter nucleus squeezes through the constricted region of the invasive hyphal cell (Jones *et al.,* 2016). A similar pattern of nuclear division and migration into the daughter cells has been previously found in spore germination of *C. albicans* (Thomson *et al.*, 2016). This phenomenon suggests the potential parallel between morphogenetic transformation of the fungal cells during external and internal cell wall penetration. The diameters of invasive hyphae crossing the cell wall are still larger than normal diameter of plasmodesma (30 to 50 nm). Therefore, penetration of invasive hyphae through the plasmodesmatal channels may require further constriction of the invasive hyphae at the initial penetration and may involve dilation of the channel for an invasive hyphal cell to fit in. *M. oryzae* may manipulate individual plasmodesmata, possibly using certain effectors, in order to move into the next plant cells. Fungal effectors may be involved in this process. Bas2 and Bas3, for example, secreted fungal effector proteins that accumulate at cell wall crossing points of invasive hyphae, in addition to their localisation at BICs, suggesting a putative role of fungal effectors in manipulating plasmodesmata (Mosquera *et al*., 2009). Studies regarding the nature of BICs, EIHM, the role of plasmodesmata, and response of plant cell during biotrophic growth all stemmed from the elegant cytological study by Kankanala *et al.* (2007).

Using various rice and fungal transformants expressing specifically localized fluorescent proteins, very interesting dynamics of subcellular components of rice cells during second cell invasion have been revealed (Mochizuki *et al.,* 2015).

When *M. oryzae* starts to invade neighbouring rice cells, the first invaded cells appear to collapse and thus may undergo cell death. This involves the loss of ability to be plasmolysed and disintegration of several plant organelles including plasma membrane, EIHM, endoplasmic reticulum (ER) and vacuole (Kankanala *et al.,* 2007; Mochizuki *et al*., 2015; Nishizawa *et al.*, 2016). Interestingly, during late host cell colonisation, the localisation pattern of the apoplastic effector Bas4 changes from smooth outlining the entire invasive hyphae to patchy distribution with some fractions of Bas4 spill into the host cytoplasm but not diffusing into adjacent cells. This observation suggests that the EIHM loses integrity and plasmodesmata are likely to be closed at this stage. Therefore, the first infected cells lose viability around the time that the pathogen prepares to invade neighbouring cells (Mochizuki *et al.,* 2015).

1.10 Introduction to the current study

This study set out to investigate how the rice blast fungus gains entry to rice cells and then proliferates within rice tissue. The study focuses on defining the role of the Pmk1 MAPK pathway, not only in appressorium development, but also later during growth of *M. oryzae* within plant cells. The investigation also sought to define further the role of cell cycle checkpoints in regulating morphogenesis and plant infection. Finally the manner in which cell cycle control and MAPK signalling might be integrated was studied.

A critical unresolved question relates to how fungal morphogenesis is regulated during intracellular biotrophic growth. The blast fungus exhibits dimorphism, involving switch between bulbous invasive hyphae and filamentous

invasive hyphae during intercellular passage (Kankanala *et al.,* 2007). Cuticle penetration by the appressorium involves re-polarisation of cell growth towards the base of the appressorium. This requires assembly of septin GTPases which scaffold F-actin, providing cortical rigidity and maintaining cellular constriction at penetration sites (Dagdas *et al*., 2012; Ryder *et al.,* 2013). Importantly, the Pmk1 MAPK pathway regulates such fungal morphogenesis, including appressorium formation. However, the role of Pmk1 MAPK during invasive growth remains poorly understood (Wilson & Talbot, 2009, Li *et al*., 2012). How signalling pathways, polarity determinants, cytoskeletal elements and effector secretion are coordinately regulated to achieve successful host tissue colonisation remains a fundamental challenge in understanding plant infection by fungi. This study aimed to understand how regulation of fungal morphogenesis occurs during plant infection. I set out to investigate the role of the Pmk1 MAPK and cell cycle control at different stages of pathogenic life cycle of the rice blast fungus. Two key research questions were addressed in the study:

1. How does cell cycle regulation drive morphogenesis of plant infection structure of *M. oryzae*?
2. How does the Pmk1 MAPK pathway regulate invasive growth of *M. oryzae*?

In Chapter 3, I present reverse genetic analysis that I carried out to create two temperature-sensitive mutants of a B-type cyclin gene to investigate the role of cell cycle control in regulation of fungal morphogenesis during host cell infection. In Chapter 4, I report how I established a chemical genetic system for targeted inactivation of the Pmk1 activity by generating an analogue-sensitive mutant of *PMK1* (*pmk1*^{AS}) which allow functional characterisation at any stages of plant

infection. This mutant was used to elucidate the long-standing unknown biological functions of Pmk1 MAPK during invasive growth, which is presented in Chapter 5. In Chapter 6, I discuss these findings and relate them together to provide new insight into the molecular control of plant infection by the rice blast fungus.

Extracts from this chapter contributed to the publication of a book chapter of the Mycota, “Septation and Cytokinesis in Pathogenic Fungi”. Parts of results gained from this study have contributed to a manuscript which is waiting for a revision by *Proceedings of the National Academy of Sciences of the USA.* I am a second author, was responsible for designing and performing the experiments using the B-type cyclin mutants of *M. oryzae*. I presented genetic evidence to define cell cycle phases associated with morphogenesis of plant infection structure by the rice blast fungus. A copy of these manuscripts can be found in Appendix 1 and 2.

Chapter 2 Materials and Methods

2.1 Growth and maintenance of fungal stocks

Magnaporthe oryzae strains used and generated in this study are stored in the laboratory of Nicholas J. Talbot at School of Biosciences, University of Exeter. Vegetative hyphae of *M. oryzae* were grown on solid complete medium (CM) and incubated at 24°C in a fungal growth room with a 12-hour light and dark cycle (Talbot *et al*., 1993). The CM contains 10 g L^{-1} glucose, 2 g L^{-1} peptone, 1 g L^{-1} yeast extract (BD Biosciences), 1 g L^{-1} casamino acids, 0.1 % (v/v) trace elements (22 mg L^{-1} zinc sulphate heptahydrate, 11 mg L^{-1} boric acid, 5 mg L^{-1} manganese (II) chloride tetrahydrate, 5 mg L^{-1} iron (II) sulphate heptahydrate, 1.7 mg L^{-1} cobalt (II) chloride hexahydrate, 1.6 mg L^{-1} copper (II) sulphate pentahydrate, 1.5 mg L^{-1} sodium molybdate dehydrate, 50 mg L^{-1} ethylenediaminetra-acetic acid), 0.1 % (v/v) vitamin supplement (0.001 g L^{-1} biotin, 0.001 g L^{-1} pyridoxine, 0.001 g L^{-1} thiamine, 0.001 g L^{-1} riboflavin, 0.001 g L^{-1}, 0.001 g L^{-1} nicotinic acid), 6 g L^{-1} $NaNO_3$, 0.5 g L^{-1} KCl, 0.5 g L^{-1} $MgSO_4$, 1.5 g L^{-1} KH_2PO_4, [adjust pH to 6.5 with NaOH]), and 15 g L^{-1} agar. When making liquid stocks, agar is omitted. For long-term storage of fungal strains, *M. oryza*e mycelia were left to grow over sterile filter paper discs (Whatman International) placed on CM agar plates. The paper discs were then desiccated and stored with desiccant at -20°C. All chemicals were obtained from Sigma-Aldrich unless otherwise stated.

2.2 Pathogenicity and infection-related development assays

2.2.1 Plant infection assays

Conidia of *M. oryzae* were harvested from 10-day-old cultures grown on CM plates. The plate was flooded with sterile water, and gently scraped with a sterile plastic spreader to release the conidia. The conidial suspension was filtered through a layer of sterile Miracloth (Calbiochem), and centrifuged at 5000 x *g* for 10 min at room temperature. Conidial suspension was prepared at 5 x 10^4 conidia mL^{-1} in 0.2% gelatine. For spray inoculation, the conidial suspension was sprayed onto three pots of 3-week-old rice plants of CO-39 cultivar using an artist's airbrush (Badger Airbrush, Franklin Park, Illinois USA). After spraying, plants were watered well and kept in polythene bags for 48 hours and then grown for further 5 days in a controlled environment chamber (Reftech, Holland) at 24°C with 12 hour light/dark cycle and 90% humidity, as described previously (Valent *et al.*, 1991). For leaf drop inoculation, 20 µL droplets of conidial suspension were placed onto detached rice leaves placed in a moist chamber. Disease lesions were recorded at 5 days post-inoculation.

2.2.2 Assays for conidial germination and appressorium development

Conidial germination and appressorium formation were carried out using a method adapted from Hamer *et al*, 1988. A conidial suspension of 10^5 conidia mL^{-1} was prepared in sterile water. A 50 µL drop of conidial suspension was inoculated onto a borosilicate glass coverslip (Fisher Scientific UK Ltd.) previously placed on wet paper towels in a moist chamber, and incubated at 24°C. At the appropriate time points the cover slip was mounted on a glass slide with small pieces of

petroleum gel placed at the edge of the cover slips to prevent drying of the sample. Conidial germination and appressorium development were monitored and recorded by light or epifluorescence microscopy. For chemical treatments during germination on coverslips, the water was removed and replaced with the desired chemical solution.

2.2.3 Leaf sheath inoculation assay for examining plant penetration and invasive growth

Leaf sheath inoculation assays were performed according to (Kankanala *et al*., 2007). Leaf sheaths were prepared from cut leaves of 3-4 week-old-rice plants of CO-39 cultivar and cut into approximate 5 cm lengths. Conidial suspensions were prepared at concentration of 10^5 conidia mL^{-1} in 0.2% gelatine solution, and then injected by pipetting into the hollow space enclosed by the sides of the leaf sheath. Inoculated sheaths were placed horizontally flat with the mid-vein faces downward in a moist chamber, so that the spores settled on the mid-vein region. The inoculated leaf sheaths were then incubated at 24°C, or as otherwise stated. For microscopic observations, the sheaths were hand-trimmed to remove the sides and expose the epidermis above the mid-vein. Lower mid-vein cells were cut to produce a thin section of three to four cell layers. The section was then mounted on a glass slide and examined by microscopy. For chemical treatments on appressoria or invasive hyphae in rice leaf sheaths, solution filled in the hollow space of the leaf sheath was removed by blotting with dry paper, and replaced with the desired chemical.

2.2.4 Tissue staining procedures

In situ hydrogen peroxide detection was performed as described (Chi *et al.*, 2009). An aqueous solution of 1 mg mL^{-1} of 3,3'-diaminobenzidine (DAB) in 10 mM Na_2HPO_4 was added from the edge of the cover glass to previously mounted leaf sheath tissue on the glass slide. After incubation for 4 h at room temperature, DAB is oxidized and forms an insoluble brown precipitant which can be observed by standard light microscopy.

For callose staining, methyl blue (0.1 mg mL^{-1}) in 150 mM KH_2PO_4 solution was added to pre-mounted tissue for up to 30 min before rinsing with water and imaging by confocal scan microscopy. The methyl blue fluorochrome was excited with a 405-nm laser and collected at 440–490-nm (Faulkner *et al.*, 2013).

2.3 Microscopy

Conventional epifluorescence and differential interference contrast (DIC) microscopy was performed on an IX81 motorized inverted microscope (Olympus, Hamburg, Germany). A Photometrics CoolSNAP HQ2 camera system (Roper Scientific, Germany) under the control of MetaMorph software package (MDS Analytical Technologies, Winnersh, UK) was used to capture images from the microscope. Confocal laser scanning fluorescence microscopy was performed on a Leica TCS SP8 microscope using a 40x oil immersion objective lens.

The TEM procedure was modified from previously described (Hacker *et al.*, 2014). Small pieces of infected rice leaf sheaths were fixed for 2 h at room temperature with 5% glutaraldehyde and 4% formaldehyde in 0.05 M sodium cacodylate buffer (pH 7.2). Initial 5 min of fixation was under mild vacuum.

Samples were then kept in fridge overnight. The samples were washed with the buffer 3 times for 5 min, post-fixed for 1 h and 30 min with 1% osmium tetroxide reduced with 1.5% potassium hexacyanoferrate in deionized water, and then washed with distilled water 3 times for 5 min. The samples were dehydrated through a graded ethanol series: 30%, 50%, 70%, 80%, 90%, 95% and 4 times with 100% ethanol – 10 min each step. The dehydrated tissues were incubated in 1:2 mix of resin and 100% ethanol (Spurr resin; TAAB, Aldermaston, UK) overnight, then in 1:1 mix of resin and 100% ethanol for 2 h, followed by 2h in 2:1 mix resin and ethanol, and finally in pure Spurr resin overnight. Tissue pieces were embedded in fresh resin in silicon moulds, and allowed to polymerise at 65°C for 24 h. Cured resin blocks were trimmed with a razor blade before cut into ultrathin sections of 80 nm and collected on pioloform-coated 100 mesh copper EM grids. Tissue sections were contrasted with Reynold's lead citrate for 10 min (Reynolds, 1963). Grids were imaged using a JEOl JEM 1400 transmission electron microscope operated at 120kV and an ES 100W CCD digital camera (Gatan).

2.4 DNA manipulation

2.4.1 Restriction digestion of genomic or plasmid DNA

Restriction endonucleases were obtained from either Promega UK ltd. (Southampton, UK) or from New England Biolabs (Hitchin, UK). DNA digestions of a final volume 50 µL were composed of 0.2-1 µg of DNA, 5-10 units of enzyme, and 5 µL of an appropriate buffer solution supplied by the manufacturer. The mixture was incubated at 37C for at least 1 h, and the fractionated in agarose gel.

2.4.2 Polymerase chain reaction

Polymerase chain reaction (PCR) was performed using Applied Biosystems GeneAmp ® PCR system 2400 cycler according to manufacturer's instructions. For routine PCR, GoTaq® G2 Green Master Mix and 50-100 ng of template DNA were used for a 50 µL PCR reaction. PCR amplification using the GoTag® G2 Green Master Mix was carried out with the following conditions. Initial denaturation at 94°C for 5 min, 35 cycles of PCR cycling parameters: denaturation at 94°C for 30 sec, annealing at 56-60°C for 30 sec, and extension at 72°C for 1 min per 1 kb of expected product length, followed by a final extension at 72°C for 10 min and then held at 4 °C.

Phusion high-fidelity DNA polymerase (New England Biolabs, Thermo Scientific) was used when high-fidelity of the DNA amplicon was required. In 50 µL reaction, 10 µL of 5X Phusion HF buffer, 200 µM dNTPs, 0.5 µM of each primer, 100-200 ng of template DNA and 1 unit of Phusion DNA polymerase was combined in a PCR tube. PCR conditions were initial denaturation at 98°C for 30 sec, and 35 cycles of PCR cycling parameters: denaturation at 98°C for 10 sec, annealing at 58°C for 30 sec, and extension at 72°C for 30 sec per 1 kb of desired length of PCR product, then followed by a final extension at 72°C for 10 min and finally held at 4°C.

SapphireAmp Fast PCR Master Mix was used for colony PCR screening. In 50 µL reaction, 25 µL of 2X Premix SapphireAmp Fast PCR Master Mix, 0.2 µM of each primer, and template DNA of 100 pg to 10 ng were combined and made up to a final volume of 50 µL using sterile distilled water. The PCR conditions were an initial denaturation at 94°C for 5 min, and then 35 cycles of PCR cycling

parameters of: denaturation at 98°C for 5 sec, annealing at 55°C for 5 sec, and extension at 72°C for 10 sec per 1 kb of expected PCR product, then followed by a final extension at 72°C for 7 min and hold at 4°C.

2.4.3 DNA gel electrophoresis

DNA from restriction digestion or PCR amplification products were fractionated by gel electrophoresis experiments in 0.7-1.0% (w/v) agarose gel matrices in 1X Tris-borate EDTA (TBE) buffer (0.09 M Tris-borate, and 2 mM EDTA). The addition of ethidium bromide into molten agarose gel to a final concentration of 0.5 µg mL^{-1} was carried out for visualisation of DNA. The 1 kb plus size marker (Invitrogen) was also included in gel electrophoresis in order to estimate the size of DNA products. Fractionated DNA in the gel was visualised and recorded by using a UV transilluminator and gel documentation system (Image Master VDS with a Fujifilm Thermal Imaging system FTI-500, Pharmacia Biotech).

2.4.4 Gel purification of DNA fragments

Fractionated DNA was purified from pieces of agarose gel using a commercial kit (Wizard Plus SV Gel and PCR Clean-up System, Southampton, UK), according to the manufacturer's instructions. After gel electrophoresis, a piece of agarose gel containing the desired DNA fragment was excised using a razor blade, and placed in a pre-weighed vial. Membrane binding solution (4.5 M guanidine isothiocyanate and 0.5 M potassium acetate, pH 5.0) was added to the gel slice, at a ratio of 10 µL per 10 mg of gel slice. Samples were incubated at 65°C and mixed by regularly vortexing until the gel was completely dissolved. A

750 µL aliquot of dissolved gel mixture was transferred to a Wizard® SV Minicolumn placed in a 2 mL collection tube, and incubated at room temperature for 1 min. The samples were centrifuged at 13,000 x *g* for 1 min so that the DNA bound to the Wizard® SV Minicolumn. The flow-through was discarded. The column was washed twice with 500 µL Membrane Wash Solution, and centrifuged for 1 min to get rid of remaining liquid on the membrane. Finally, bound DNA was eluted by adding 30 µL of Nuclease-Free Water and centrifugation at 13,000 x *g* for 1 min. The DNA solution was stored at -20°C.

2.4.5 DNA cloning and bacterial transformation

For conventional cloning, 5´ phosphate groups of insert DNA and cut vector backbone were dephosphorylated with Antarctic Phosphatase (NEB) to prevent re-circularisation. The following reagents were combined: 1-5 µg DNA, 2 µL 10X Antarctic Phosphatase Reaction Buffer, 1 µL Antarctic Phosphatase, and sterile distilled water to a total volume of 20 µL. The mixture was incubated at 37°C for 15 min, and then inactivated at 65°C for 5 min. The digested DNA was gel purified. The ligation reaction was prepared as followed: insert DNA and vector at a 2:1 molar ratio, 1 µL 10X Ligation Buffer (Promega), 1 µL T4 Ligase (Promega), and sterile distilled water to a final volume of 10 µL. The ligation reaction was incubated at 4°C overnight, and 1-5 µL of the reaction was transformed into XL-10 Gold Ultra Competent Cells, according to the manufacturer's instructions.

The directional cloning of multiple DNA fragments was carried out by homologous recombination using the In-Fusion HD Cloning Kit (Clontech). Primers were designed to introduce 15 bp extensions which overlapped with adjacent

fragments allowing the ends to fuse during cloning. In-Fusion cloning reactions were set up as follows: 2 µL of 5X In-Fusion HD Enzyme Premix, 10-200 ng of each purified PCR fragment, 50-200 ng linearized vector, and deionized water to 10 µL total volume. The reaction was incubated for 15 min at 50°C, then placed on ice. A 2.5 µL aliquot of the reaction mixture was added to thawed 50 µL of Stellar Competent Cells in an ice-cold round-bottom plastic tube, mixed gently, and incubated on ice for 30 min. The bacterial cells were then heat-shocked at 42°C for exactly 45 sec, and then placed to ice for 2 min. Then 450 µL of pre-warmed SOC medium was added to the cells, and shaken gently at 37°C for 1 h. An aliquot of this bacterial culture was plated onto a Luria Broth (LB) agar plate containing appropriate antibiotic, and incubated overnight at 37°C. Positive clones were verified by colony PCR and restriction digestion.

2.4.6 Medium-scale preparation of plasmid DNA

High quality plasmid DNA for sequencing and for fungal transformation was prepared using a PureYield™ Plasmid Midiprep System, based on SDS cell lysis and silica-membrane column purification. A single bacterial colony was used to inoculate 50 mL LB media containing the appropriate antibiotic and grown overnight at 37°C with vigorous shaking (200 rpm). Bacterial cells were pelleted by centrifugation at 5,000 x *g* for 10 min. The pellet was re-suspended in 3 mL of Cell Resuspension Solution. The mixture was added with 3 mL of Cell Lysis Solution, mixed gently by inversion, and incubated at room temperature for 3 min. Then 5 mL of Neutralization Solution was added, mixed thoroughly and then centrifuged at 15,000 x *g* for 15 min. The supernatant was transferred to a PureYield^{TM} Clearing

Column which had been placed on top of a PureYield™ Binding Column which in turn was connected to a vacuum manifold. Vacuum was applied to draw the supernatant through the clearing membrane, allowing plasmid DNA to bind to the silica membrane in the PureYield™ Binding Column. The clearing column was removed. The binding column was washed sequentially with 5 mL of Endotoxin Removal Wash and 20 mL of Column Wash Solution using the vacuum to pull the solutions through the membrane in the column. Once the solutions had washed through, a vacuum was applied to the column for 1 min further to dry the membrane. To elute the DNA by centrifugation, the binding column was placed in a 50 mL Falcon tube. A 600 µL aliquot nuclease-free water was then added to the membrane, incubated for 1 min at room temperature, and then centrifuged in a swinging bucket rotor at 1,500-2,000 x *g* for 5 min. The eluted plasmid DNA was transferred to a 1.5 microcentrifuge tube and stored at -20°C.

2.4.7 Small-scale fungal genomic DNA preparation

Small mycelial plugs of *M. oryzae* were inoculated onto cellophane membrane discs (Lakeland) placed on CM agar and left to grow until they had covered the membrane surface. The cellophane membrane was peeled off and placed into mortar and ground into fine powder in liquid nitrogen. The powdered mycelium was transferred into 1.5 mL microcentrifuge tubes and stored at -80°C until needed. CTAB buffer composed of 2% (w/v) Hexadecyltrimethylammonium Bromide (CTAB), 100 mM Trisma base, 10 mM Ethylenediaminetraacetic acid (EDTA) and 0.7 M NaCl, was used for fungal genomic DNA isolation. An aliquot of 500 µL CTAB buffer, preheated to 65°C, was added to the mycelial powder in

microcentrifuge tubes, and incubated at 65°C for 30 min with regular shaking every 10 min. The samples were centrifuged at 17,000 x g for 10 min. Supernatants were transferred into new 1.5 mL microcentrifuge tubes, to which was added with an equal volume of chloroform:pentanol (24:1) solution, and were then mixed vigorously on a shaking platform. The chloroform:pentanol extraction was repeated once more after which the aqueous phase was transferred into fresh tubes before an equal volume of chilled isopropanol was added and incubated at -20°C for 10 min, and centrifuged at 17,000 x g for 10 min. The resulting pellets of nucleic acid were air-dried, resuspended in 500 µL of sterile water, and re-precipitated using two volumes of 100% ethanol and 1/10 volume of 3 M sodium acetate (pH 5.2) and. Samples were then centrifuged at 17,000 x g for 10 min, and washed with 500 µL of 70% (v/v) ethanol. Pellets of nucleic acid were air-dried for 10 min in vacuum rotary desiccator and dissolved in 30 µL of sterile water containing 4 µL of DNase-free RNase (20 µg mL^{-1}; Promega). Samples of genomic DNA were stored at -20°C.

2.4.8 Southern blotting

Southern blot analysis was performed according to Southern, (1975). Fungal genomic DNA (25 µg) was digested with the desired restriction enzyme overnight at 37°C, and fractionated by agarose gel electrophoresis. Resolved DNA in the gel was transferred onto a membrane by capillary transfer method. The DNA in the gel was depurinated by immersing the gel in 0.25 M HCl with gentle shaking for 15 min or until colour of loading buffer changes from blue to yellow. The gel was then neutralised in 0.4 M NaOH for 15 min or until colour of loading buffer changes

from yellow to blue. The gel was then placed onto a Whatmann paper sheet supported with a perspex sheet with two ends of the paper submerged in 0.4 m NaOH. Hybond-NX membrane (Amersham Biosciences) was carefully placed on the gel, followed by 2 layers of wet Whatmann Papers, 5 layers of dry Whatmann Papers, and high stack of paper towels. Finally a 500 g weight was placed on the stack. The blot was incubated at room temperature overnight for complete transfer of DNA onto the membrane. The blot was then exposed to UV in BLX crosslinker (Bio-Link) in order to immobilise the DNA.

2.4.9 Non-radioactive probe labelling

DIG Nonradioactive Nucleic Acid Labelling and Detection System was used to detect a specific sequence of DNA on the Hybond-NX membrane. The probe was generated by PCR amplification using Phusion DNA polymerase. Standard PCR reagents were used, with a dNTP mix replaced by a DIG DNA Labelling Mix (Roche). The PCR-labelled probe was evaluated by agarose gel electrophoresis, and then purified from the gel by using a Wizard Plus SV Gel and PCR Clean-up System as described above.

2.4.10 Hybridisation conditions

The Southern blot membrane was rolled and placed in a hybridisation bottle to which 30 mL Southern hybridisation buffer (0.5 M $NaPO_4$, 7% SDS, adjust to pH 7) was added. The hybridisation bottle was incubated in an oven at 62°C for at least 30 min. The probe was then mixed with fresh hybridisation buffer (to 25-50 ng mL^{-1}) in a 50 mL plastic Falcon tube, and boiled at 100°C for for 5 min and then put on ice for 2 min in order to denature the DNA. The hybridisation buffer in the bottle

was removed and replaced with the hybridisation buffer containing the probe, and the bottle incubated in the oven at 62°C for at least 6 h or overnight. Probe solution was transferred into a plastic tube and kept at -20°C for re-use. The blot was washed twice with a Southern wash buffer (0.1 M $NaPO_4$, 1% SDS, adjust to pH7) with incubation at 62°C for 15 min each time.

2.4.11 Chemiluminescent detection of DIG-labelled DNA

After hybridisation with the probe, the blot was removed from the hybridisation bottle to a plastic tray containing 20 mL DIG wash buffer (DIG Buffer 1 [0.1 M maleic acid, 0.15 M NaCl, 5 M NaOH adjust pH to 7.5], 0.3% Tween-20), and incubated at room temperature for 5 min on a rolling platform. The DIG wash buffer was replaced with 25 mL blocking solution (DIG Buffer1, 1% milk powder) and the membrane was then incubated for at least 30 min on a rolling platform. The blocking solution was removed and replaced with an antibody solution, consisting of 2 µL anti-DIG-alkaline phosphatase antibody in 20 mL of blocking solution, and the blot was incubated for a further 30 min. The membrane was then washed twice with DIG wash buffer for 15 min each time, and placed on a plastic sheet. CDP-Star solution (1 mL) was added to the membrane, and another plastic sheet was placed on top it so that the solution was well spread on the membrane without air bubbles. The stack was incubated at room temperature for 5 min after which the CDP-Star solution was drained off. The membrane and plastic sheets were attached to the inner side of a film cassette and incubated at 37°C for 15 min. X-ray film was exposed to the membrane in the cassette at room temperature, and was developed using Kodak chemicals.

2.5 Protoplast-mediated transformation of *M. oryzae*

The fungal transformation procedure was performed as previously described (Talbot *et al*., 1993). To prepare *M. oryzae* protoplasts, a piece of mycelium from the edge of a growing colony was sliced from a culture on a CM plate, blended in 150 mL of liquid CM medium, and incubated at 24°C with shaking at 125 rpm for 48 h. Mycelium was harvested by filtration through sterile Miracloth (Calbiochem) and rinsed with sterile distilled water. The mycelium was transferred to a sterile falcon tube (Becton Dickinson) containing OM buffer (1.2 M magnesium sulfate, 10 mM sodium sulfate, 5% Glucanex (Novo Industries, Copenhagen), pH 5.8), and incubated with gentle shaking at 75 rpm for 2-3 hours at 30°C. The mycelium in OM buffer was then transferred into sterile polycarbonate oakridge tubes (Nalgene), and overlaid with an equal volume of ice-cold ST buffer (0.6 M sucrose, 0.1 M Tris-HCl [pH 7.0]). Protoplasts were separated by centrifugation at 5000 x g for 15 min at 4 °C in a swinging bucket rotor (Beckman JS-13.3) in a Beckman J2.MC centrifuge. The protoplasts were recovered at the interface of OM and ST buffers, and transferred into a sterile Oakridge tube containing cold STC buffer (1.2 M sucrose, 10 mM Tris-HCl [pH 7.5]), 10 mM calcium chloride). The retrieved protoplasts were pelleted by centrifugation at 3000 x g for 10 min at 4°C, and after the supernatant was removed, the pellet was carefully resuspended in cold STC. This wash step was repeated a further two times after which the protoplasts were resuspended in 1 ml of cold STC and the final concentration was determined using a haemocytometer.

The transformation reaction was carried out in 1.5 microfuge tubes. An aliquot of protoplasts (10^7 cells mL^{-1}) was combined with 5-10 µg of DNA in a total volume of 150 µl STC buffer, and incubated at room temperature for 25 minutes. To this mixture 1 ml of PTC buffer (60% PEG 4000, 10 mM Tris-HCl (pH 7.5), 10 mM calcium chloride) was then added, mixed by gentle inversion, and incubated at room temperature for a further 15-20 minutes. The mixture was then added to 3 ml of TB3 buffer (20% sucrose, 0.3% yeast extract), and incubated at 24 °C with gentle shaking at 75 rpm for at least 16 hours. The mixture was added to molten 1.5% agar in osmotically stabilized CM (OCM) containing additional 0.8 M sucrose, mixed gently and poured into sterile Petri dishes (25 mL per plate).

For selection of hygromycin-resistant transformants, plate cultures were kept in the dark for at least 16 hours, and then overlaid with CM agar containing hygromycin B at 600 µg mL^{-1} to give a final concentration in the plate of 200 µg mL^{-1}. For selection of sulfonylurea (chlorimuron ethyl) or glufosinate ammonium (Basta) resistant transformants, BDCM (0.8 M sucrose, 1.7 g L^{-1} yeast nitrogen base without amino acids and ammonium sulphate (Difco), 2 g L^{-1} ammonium nitrate, 1 g L^{-1} asparagine, 10 g L^{-1} glucose [pH 6.0]) was used in place of OCM. BDCM omitting sucrose, but containing chlorimuron ethyl or glufosinate ammonium, both at final concentrations of 150 µg mL^{-1}, was used as the overlay. After incubation for at least 10 days in a dark chamber at 24°C, colonies emerged from the transformation plates were subcultured onto new BDCM plates supplemented with appropriate selection. Small sterile filter papers were placed next to the inoculum and collected once transformant mycelium had grown over it in order to keep the transformant as a long-term stock, as described in section 2.1.

2.6 RNA sequencing

2.6.1 RNA extraction from infected plant material

Total RNA was isolated from fresh infected plant tissue using a commercial kit (QIAGEN RNeasy Plant Mini Kit) according to then manufacturer's instructions. The procedure is based on guanidine-isothiocyanate lysis and silica-membrane purification to provide high-quality RNA with minimum contamination of DNA. Briefly, 100 mg of plant material was ground thoroughly in liquid nitrogen using a sterile mortar and pestle. The ground material was immediately transferred into a liquid-nitrogen-cooled 2 mL microcentrifuge tube, to which was added 450 µL buffer RLT previously mixed with 10 µL β-mercaptoethenol for every 1 mL of the RLT buffer, and vortexed vigorously. The lysate was transferred to a QIAshredder spin column placed in a 2 mL collection tube, and was centrifuged for 2 min at 13,000 rpm. Supernatant of the flow-through was transferred to a microcentrifuge tube, and mixed with 0.5 volumes of absolute ethanol by pipetting. The mixture was transferred to an RNeasy mini pin column placed in a 2 mL collection tube, and centrifuged at 13,000 rpm for 15 sec. The flow-through was discarded. 700 µL Buffer RW1 and 500 µL Buffer RPE were sequentially added to the RNeasy spin column with centrifugation at 13,000 rpm for 15 sec. Flow-through was removed between the steps. Next, a further 500 µL buffer RPE was added and centrifuged for 2 min at 13,000 rpm to dry the membrane. The RNeasy spin column was placed in a new 1.5 mL collection tube. RNA bound to the membrane of the RNeasy spin column was eluted in 30-50 µL RNase-free water, and stored at –80 °C. The concentration of resulting total RNA sample was estimated using a

NanoDrop spectrophotometer (Thermo Scientific). Aliquots of total RNA were further analysed on an Agilent 2100 Bioanalyzer using an RNA nano chip kit (Agilent). RNA samples with integrity number of at least 6 were used for library preparation.

2.6.2 Illumina sequencing

RNA-seq libraries were prepared using 5 µg of total RNA with TruSeq SBS Kit v3 from Illumina (Agilent) according to manufacturer's instructions. 100 base paired-end reads were sequenced from mRNA libraries on the Illumina HiSeq 2500 (Illumina, Inc.). Section was carried out by Exeter Sequencing Service (University of Exeter, UK).

2.6.3 Bioinformatic analysis

Initial bioinformatic analysis of raw data obtained from sequencing was carried out by Darren Soanes (University of Exeter, UK). Reads were filtered using the fastq-mcf program from the ea-utils package (http://code.google.com/p/ea-utils/) applying –x 0.01, –q 20, –p 10, and –u.

2.6.3.1 Alignment and differential gene expression *M. oryzae*

Filtered reads were mapped to the *M. oryzae* 70-15 reference genome version 8 (Dean *et al*., 2005) using the TopHat2 splice site-aware aligner (Kim *et al*., 2013). The Cufflinks suite of programs was used to estimate relative transcript abundance and to test for differential gene expression (Trapnell *et al.*, 2012).

2.6.3.2 Alignment and differential gene expression *Oryza sativa*

Filtered reads were mapped to the *O. sativa L. ssp. indica* genome (Yu *et al.*, 2002) using the TopHat2 splice site-aware aligner (Kim *et al.*, 2013). Counts of

reads mapping to each gene in the *O. sativa* genome were generated using the htseq-count function of the HTSeq package (Anders *et al.*, 2014). Relative gene expression was quantified and differentially expressed genes were identified using DESeq (Anders & Huber, 2010).

Chapter 3 Cell cycle-regulated Host Tissue Invasion by the Rice Blast Fungus *Magnaporthe oryzae*

3.1 Introduction

Eukaryotic cells undergo dramatic changes in morphology, mechanics and polarity as they progress through different stages of the cell division cycle (Berman, 2006, Howell & Lew, 2012). Cell cycle progression is driven by cyclin-dependent kinases (CDKs), which form complexes with various cyclins, constituting a primary layer of regulation (Bloom & Cross, 2007). Oscillation in levels of cyclins regulates the phosphorylation activity and substrate specificity of CDKs. In several fungal model organisms, a single Cdk1 governs cell cycle events. Expression levels of the cyclins are, in turn, controlled by both transcription and post-transcriptional ubiquitin-mediated proteolysis, in order to ensure orderly progression of the cell cycle. Anaphase-promoting complex (APC) is an E3 ubiquitin ligase that marks cell cycle proteins, including the cyclins, for degradation by 26S proteasome. The activity of CDK1 is modulated by inhibitory phosphorylation and by CDK-inhibitory proteins, reflecting the flexibility of the cell cycle in adaptation to various environmental conditions and development stages (Bloom & Cross, 2007). B-type cyclins are the major mitotic cyclins that were first identified in invertebrate embryos. All B-type cyclins contain degradation boxes that target these proteins for destruction by the APC. The fission yeast *Schizosaccharomyces pombe* possesses three B-type cyclins (Cig1, Cig2 and Cdc13), but only Cdc13 triggers periodic formation of CDK-cyclin complexes that control mitotic entry. Temperature-sensitive mutations in the *cdc13*+ gene prevent entry into mitosis. A

simple CDK-cyclin module, comprised of Cdc2 CDK and Cdc13 B-type cyclin, has been shown to autonomously drives the cell cycle through S and M phases (Coudreuse & Nurse, 2010).

To ensure the fidelity of cell division, transitions through cell cycle phases are precisely monitored by checkpoint systems that arrest the cell cycle when any errors are detected. The G1/S checkpoint, for example, controls entry into S phase, the G2/M checkpoint for entry into mitosis, and the spindle checkpoint for chromosomal segregation at anaphase (Furnari *et al.*, 1999, Rhind & Russell, 2000). In the presence of un-replicated DNA, elements of the DNA damage checkpoint, Cds1 and Chk1, inactivate the Cdc25 phosphatase and allow mitotic entry. During replication stress, *S. pombe* mutants lacking both Cds1 and Chk1 were unable to maintain cell cycle arrest and underwent aberrant mitosis (Sanchez *et al.*, 1999, Zeng *et al.*, 1998).

Cyclin-CDK1 complexes coordinate changes of cell shape with cell cycle progression (Lew & Reed, 1993). In *Saccharomyces cerevisiae,* the Cdc28 CDK is associated with the G1 cyclins Cln1/2 in late G1, and triggers progression through Start and establishment of the pre-bud site, whereas the Clb3-6 cyclins promote DNA replication and separation of spindle pole bodies (Lew & Reed, 1993). In late G1, cortical actin patches accumulate in a ring at the pre-bud site, followed by rearrangement of actin cables which direct delivery of secretory vesicles towards this site and promote polarised cell growth. This polarisation of cell growth is achieved by the small Rho GTPase Cdc42. Subsequently, the Cdc28 CDK associates with Clb1/2 cyclins, and induces mitotic events and isotropic bud growth. The G2 activity of the CDK promotes isotropic expansion of bud by

suppressing polarised cell growth (Lew & Reed, 1993). Therefore, the core cell cycle regulators co-ordinately control both nuclear and cytoplasmic events, leading to changes of cell shape through the cell cycle.

Pathogenic fungi exhibit distinct plasticity between the cell cycle and morphogenesis to match their infection strategies (Perez-Martin *et al*., 2016). Changes in the balance between polarised and isotropic growth modes, mediated by G1 or G2 activities of the CDKs, result in the variety of fungal cell shapes. Distinct cell cycle regulation becomes more evident during infection structure development and for successful host invasion by several animal and plant pathogenic fungi, such as *C. albicans* (Berman, 2006), *Ustilago maydis* (Pérez-Martín *et al.*, 2006), and *Colletotrichum orbiculare* (Fukada & Kubo, 2015). The rice blast fungus *Magnapothe oryzae* produces dome-shaped, melanised appressoria that generate turgor pressure to mechanically force penetration peg into host surface (Howard & Valent, 1996, Ebbole, 2007, Talbot, 2003, Wilson & Talbot, 2009). After germination of inductive surfaces, a polarized germ tube tip switches to isotropic cell expansion, leading to formation of a dome-shape appressorium. Morphogenesis of the appressorium is linked to cell cycle progression (Veneault-Fourrey *et al*., 2006, Saunders *et al*., 2010a). A conidial nucleus migrates into the germ tube where it undergoes division. One daughter nucleus moves back to the conidial cell, while another daughter nucleus travels to the developing appressorium. Inhibition of DNA replication prevents appressorium formation, while mitotic entry blocks maturation of the appressorium (Veneault-Fourrey *et al*., 2006, Saunders *et al*., 2010a). A cell cycle arrest after mitotic entry, by conditional inactivation of the Blocked-in-Mitosis 1 gene or expression of indestructible B-

cyclins, did not prevent appressorium differentiation but instead impaired the appressorium from invading host tissue (Saunders *et al.*, 2010a). These observations highlight the importance of cell cycle checkpoints operating during morphogenesis of plant infection structures by the rice blast fungus. It has been proposed that a subsequent round of nuclear division might be needed to initiate plant penetration (Saunders *et al.*, 2010a). Inhibition of DNA replication in the appressorium using HU resulted in mislocalisation of cytoskeletal markers associated with re-modeling of F-actin and re-polarisation of the appressorium, and prevented the emergence of penetration hyphae from the appressorium (Miriam Oses-Ruiz, PhD thesis, Biosciences, University of Exeter; Appendix 2). Visualisation of DNA replication using the LacO/LacI system confirmed that early germinating spores at 2 h were in G1 phase as shown by a single punctum of GFP-LacI-NLS signal. Between 2-3 h of germination, two closely spaced puncta were observed in the conidial nucleus, indicating a duplicated chromosome in S-phase occurs early during spore germination on inductive surface prior appressorium formation. Subsequently, appressorium progresses through S-phase around 24 h concomitant with plant penetration. These results suggested that the appressorial nucleus may need to progress through S phase to initiate plant penetration (Miriam Oses-Ruiz, unpublished data; Appendix 2).

In this Chapter, I set out to investigate how cyclin-CDK functions coordinate cell cycle progression during infection-related morphogenesis. Using a complementary genetic analysis of the B-type cyclin in *M. oryzae,* I defined that CDK-cyclin B activity is required for morphogenesis of the appressorium and also for appressorium-mediated plant infection.

3.2 Results

3.2.1 The DNA replication-associated checkpoint governs the initiation of appressorium formation in *M. oryzae*

To investigate the nature of the cell cycle checkpoint during appressorium formation, DNA replication of germinating conidia was chemically inhibited by hydroxyurea (HU). Exposure to HU prevented formation of dome-shaped appressoria, resulting in the development of undifferentiated germ tubes (Fig 3.1), confirming that S-phase progression of apical conidial nucleus is essential for appressorium formation (Veneault-Fourrey *et al.*, 2006; Saunders *et al.*, 2010a).

I hypothesised that the CDK1-cyclin complex might control morphogenesis of the appressorium and also be targeted by checkpoint systems during DNA replication stress induced by HU. In several model microorganisms, the DNA replication checkpoint targets the CDK-cyclin B complex that drives G2/M transition, resulting in G2 arrest (Rhind *et al.*, 1997, Sanchez *et al*., 1999). In the budding yeast *S. cerevisiae,* for instance, activation of B-type cyclins-Cdc28 complexes triggers depolarization of cortical actin and membrane growth in the bud necessary for the growth switch to isotropic expansion of the bud at the G2/M transition (Lew & Reed, 1993). I reasoned that morphogenetic regulation of appressorium development might be controlled by activation of the mitotic cyclin-CDK complex. I therefore decided to characterise the function of the *M. oyzae* B-type cyclin encoding gene.

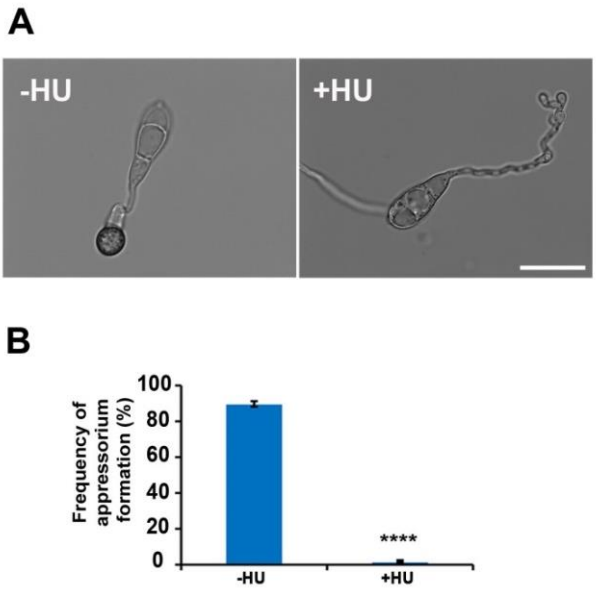

Figure 3.1 Inhibition of DNA replication in germinating conidia by HU. Representative micrographs **(A)** and bar chart **(B)** to show the effect of pharmacological inhibition of DNA replication, by adding 200 mM HU on appressorium formation in *M. oryzae* at 2 hpi. Conidia of Guy11 wild type were incubated on hydrophobic coverslips at 24°C for 24 h. The scale bar indicates 20 µm. The graph represents three biological replicate observations of 100 germinating conidia. ****$P < 0.0001$ using the *t*-test; error bars, standard errors.

3.2.2 Genetic analysis of cell cycle-regulated plant infection using temperature-sensitive (TS) mutants of *M. oryzae*

To investigate the relationship between cyclin B-directed cell cycle progression and appressorium development in *M. oryzae*, I set out to characterise a B-type cyclin gene, *CYC1. M. oryzae* Cyc1 was previously identified and showed typical sequence signatures of B-type cyclins, which is highly similar to *A. nidulans* NIME (Saunders *et al.,* 2010a). Expression of a stabilised version of Cyc1, in which the degradation box consensus sequence was removed, prevented mitotic exit (Saunders *et al.,* 2010a). Abundance of *CYC1* mRNA fluctuates during appressorium development corresponding with the timing of nuclear division in germ tubes at 4-6 h after germination (Fig 3.2). My initial attempts to generate null mutants of *CYC1* were unsuccessful, possibly due to its pivotal role in fungal growth, so I sought an alternative means to characterise *CYC1.* In the filamentous fungus *A. nidulans*, mutation of a B-type cyclin gene, *nimE6*, causes arrest in G2 phase, while another mutation in the same gene, called *nimE10* (originally identified as *nimG10*), caused an S-phase arrest (James *et al.*, 2014, O'Connell *et al.*, 1992, Bergen *et al.*, 1984a). Due to the functional conservation of cell cycle regulators among eukaryotic cells, I set out to generate the equivalent *nimE10* and *nimE6* mutants in *M. oryzae*. Unpublished data of the specific DNA sequence changes in the *A. nidulans nimE10* and *nimE6* mutants was provided by Stephen A. Osmani (Ohio State University). The *nimE10* allele carries a mutation at codon 369 in which serine (AGC) was changed to arginine (CGC). The *nimE6* allele contains a mutation in codon 445 which leucine codon (CTT) was altered to proline (CCT). To confirm these point mutations, the *NIME* locus of the *nimE10* (SWJ 019)

and *nimE6* (SWJ 1364) mutants, along with NIME from the isogenic wild-type strain (R153), was PCR amplified and sequenced (Fig 3.3 A). The *A. nidulans nimE10* and *nimE6* strains were kindly provided by Steven W. James (Gettysburg College, Gettysburg, PA). Due to sequence conservation between Cyc1 and NIME proteins, I decided to generate a $cyc1^{nimE10}$ allele carrying S389R amino acid substitutions, and a $cyc1^{nimE6}$ allele carrying F465P mutation, equivalent to the corresponding *A. nidulans nimE10* and *nimE6* mutations respectively (Fig 3.3 B).

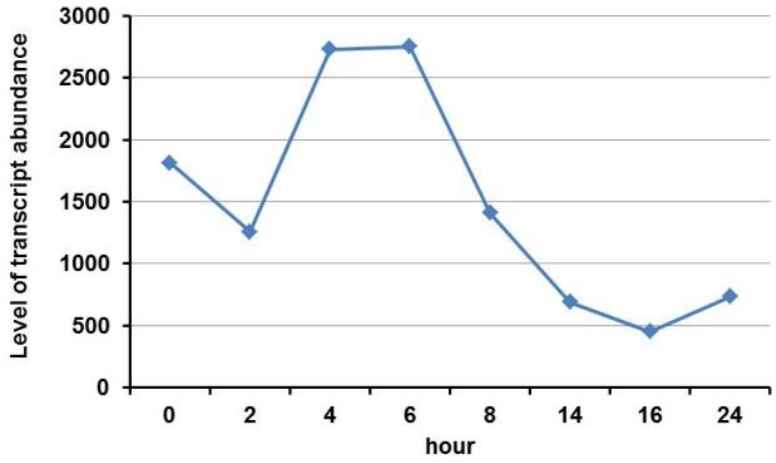

Figure 3.2 Fluctuation of the *CYC1* transcript (MGG_05646) during appressorium development by *M. oryzae.* Mean levels of relative transcript abundance of *CYC1* was obtained from RNA-seq analysis (Miriam Oses-Ruiz, unpublished data). Appressoria of the Guy11 strain were induced on hydrophobic glass cover slips. Mycelium transcriptome was used as a control. Total RNA was extracted at different time points, and used for cDNA library preparation for RNA-seq. Three biological replicates were undertaken for each time point.

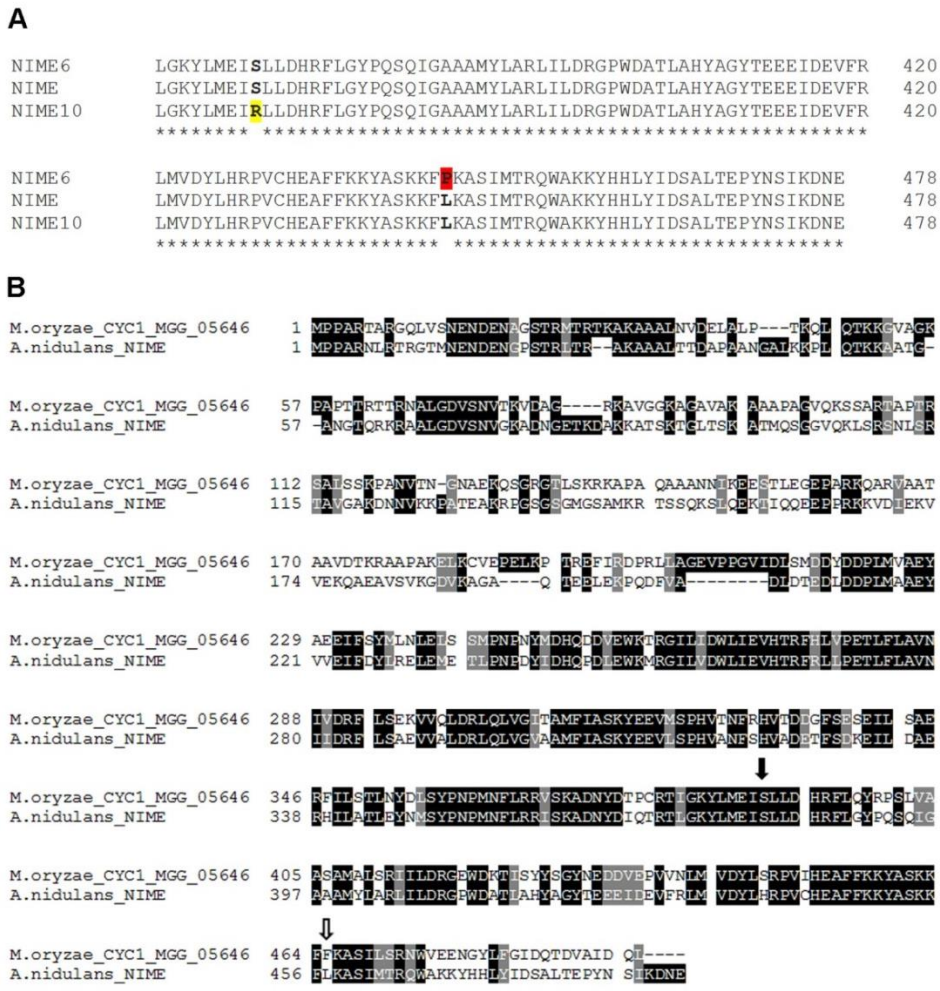

Figure 3.3 Identification of mutation sites conferring temperature sensitivity to *A. nidulans* B-type cyclin NIME and amino acid alignment with *M. oryzae* Cyc1 protein. (A) The partial amino acid sequence of *A. nidulans* NIME, NIME10, and NIME6 proteins were aligned using ClustalW2 and shaded using BoxShade version 3.21. *NIME* locus of *A. nidulans* wild type, *nimE*10 and *nimE*6 strains was PCR amplified using NIME-P1 and NIME-P2 primers. Amplicons were then subjected to DNA sequence analysis. The NIME10 protein contains S369R amino acid substitution (shaded in yellow background), while the NIME6 protein contains L445P substitution (shaded in red background). **(B)** Amino acid alignment of Cyc1 (MGG_05646) and NIME to show conserved amino acid residues. The black arrow indicates the S389 residue of Cyc1 equivalent to S369 of NIME. The white arrow indicates F465 of Cyc1, equivalent to NIME L445.

3.2.3 Generation the *cyc1*^{nimE10} and *cyc1*^{nimE6} gene replacement vectors

TS alleles of *CYC1* were generated using the In-fusion Cloning method (Clontech). The *cyc1*^{nimE10} allele contains S389R amino acid substitution, while the *cyc1*^{nimE6} carries F465P substitution. For the generation of the *cyc1*^{nimE10} allele, the CYC1 gene was amplified in two fragments (Fig 3.4). All primers used in this chapter are listed in Table 3.1. A 1.3 kb *CYC1-5'* fragment and a 0.5 kb *CYC1-3'* fragment were amplified using the V-BamHI-nimG10_P1/Mut-nimG10_P2 primer pair and Mut-nimG10_P3/Hyg-nimG10_P4 primer pair, respectively, amplifying either side of the region requiring the nucleotide substitution with 15 base pair overhangs complementary to the adjacent fragment. A substitution of codon 389 from a serine (AGC) to an arginine (CGC) codon was introduced to the 0.5 kb *CYC1* fragment using the Mut-nimG10_P3 primer. A 1.4 kb hygromycin resistance cassette *HPH* was amplified from pCB1004 (Carroll *et al*., 1994) using primers M13F and M13R. The 1.0 kb 3' untranslated region (3'-UTR) downstream of the *CYC1* locus was amplified (primers Hyg-nimG10-3UTR_P5, V-BamHI-nimG10-3UTR_P6) to provide a region of homology, 3' to the *HPH* cassette, in the gene replacement vector. Four inserts, including the 1.3 kb and 0.5 kb fragments of *CYC1* gene, the *HPH* cassette and the 3' UTR were cloned into a *Hin*dIII-digested *pNEB-Nat-Yeast* cloning vector.

To generate the *cyc1*^{nimE6} allele, A 1.6 kb *CYC1-5'* fragment (primers V-BamHI-nimG11_P1, Mut-nimE6_P2), and a 178 bp *CYC1-3'* fragment (primers Mut-nimE6_P3, Hyg-nimG10_P4) were amplified (Fig 3.5). Substitution of codon 465 from a phenylalanine (TTC) to proline (CCT) codon was introduced to the 178 bp *CYC1-3'* fragment using primer Mut-nimE6_P3. Four inserts including the 1.6 kb

and 178 bp fragments of *CYC1* gene, the *HPH* cassette and the 3'-UTR were cloned into the *Hin*dIII-digested *pNEB-Nat-Yeast* cloning vector. Finally, the *cyc*^{nimE10} and *cyc1*^{nimE6} gene replacement vectors were excised using *Bam*HI to generate the full length 4.2 kb vectors and were used to transform into the *M. oryzae* Guy11 strain using protoplast-mediated transformation (Talbot *et al*., 1993).

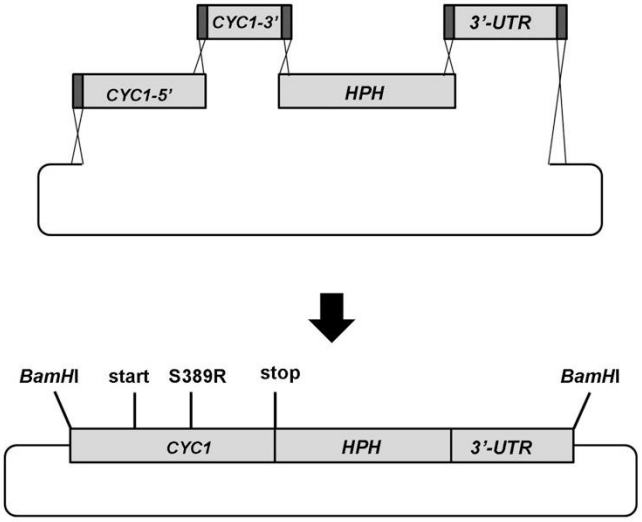

Figure 3.4 Schematic diagram illustrating the cloning strategy for generating the *cyc1*^{nimE10} vector. Recombination cloning was used to assemble DNA fragments into the *Hin*dIII-digested *pNEB-Nat-Yeast* cloning vector to generate the *cyc1*^{nimE10} construct in which a hygromycin resistance cassette *HPH* was inserted between stop codon and 3' UTR of the *CYC1.*

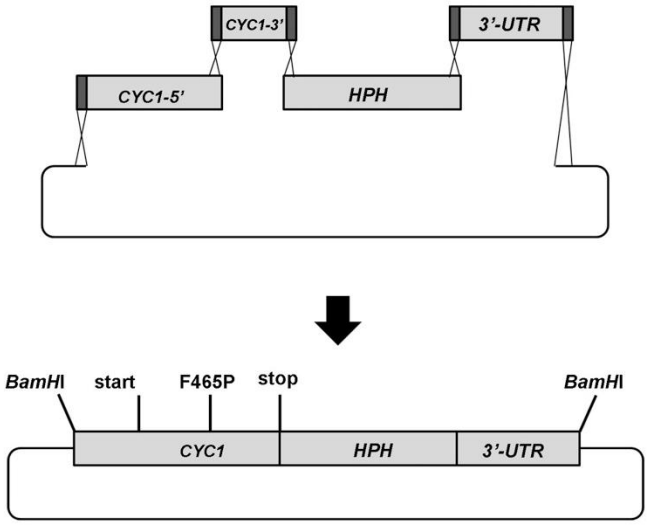

Figure 3.5 Schematic diagram illustrating the cloning strategy for generating the *cyc1*^{nimE6} vector. Recombination cloning was used to assemble DNA fragments into the *Hin*dIII-digested *pNEB-Nat-Yeast* cloning vector, to generate the *cyc1*^{nimE6} construct in which a hygromycin resistance cassette *HPH* was inserted between stop codon and 3' UTR of the *CYC1.*

Table 3.1 List of primers used in Chapter 3

Primer name	Sequence of oligo (5' to 3')
NIME-P1	TTGGTGTTGCTGCCATGTTT
NIME-P2	AGGCAAAGTATCCCGGAGAC
V-BamHI-nimG10_P1	GCAGGCATGCAAGCTGGATCCCACAGACTTGTACACCG GACAAGA
Mut-nimG10_P2	GCGGATTTCCATGAGATACTTGCC
Mut-nimG10_P3	TATCTCATGGAAATCCGCCTTCTCGATCATCGCTTCT
Hyg-nimG10_P4	GGGAAAACCCTGGCGTCTCCTACAGCTGGTCGATAGC
Hyg-nimG11-3UTR_P5	AAATTGTTATCCGCTTTTGGATGGGAAGTTTTGGACC
V-BamHI-nimG10-3UTR_P6	TGATTACGCCAAGCTGGATCCGGACGATCACGACAAGC ATAT
Mut-nimE6_P2	AGGGAATTTCTTGCTGGCATATTTCTT
Mut-nimE6_P3	AGCAAGAATTCCCTAAGGGTATGTTATCCGTCTCGT
M13F	CGCCAGGGTTTTCCCAGTCACGAC
M13R	AGCGGATAACAATTTCACACAGGA

3.2.4 Analysis of putative *cyc1*^{nimE10} and *cyc1*^{nimE6} transformants

Putative transformants of *cyc1*^{nimE10} or *cyc1*^{nimE6} were selected in the presence of hygromycin B (200 µg mL^{-1}) and grown at a permissive temperature of 24°C and at a restrictive temperature of 30°C. Six of 100 putative transformants selected displayed a hyphal growth defect at 30°C. Genomic DNA of these transformants was isolated, digested with *Sal*I restriction enzyme, fractionated by gel electrophoresis, and transferred onto HyBond-NX membrane (Amersham). Blots were probed with a restriction fragment, comprising the 3' UTR of *CYC1.* Successful allelic replacement of the *cyc1*^{nimE10}-T5 and *cyc1*^{nimE6}-T20 transformants was indicated by the presence of a 4.1 kb band, due to insertion of the 1.7 kb *HPH* cassette at the *CYC1* locus, in contrast to 2.4 kb wild-type fragments (Fig 3.6).

The *cyc1*^{nimE10}-T5 and *cyc1*^{nimE6}-T20 transformants displayed significant growth defects when incubated at a restrictive temperature of 30°C, which reverted by subsequent incubation at 24°C (Fig 3.7). These results suggest that the equivalent *nimE10* and *nimE6* mutations also confer temperature sensitivity to *M. oryzae,* and that *CYC1* is essential for growth of the fungus. These results are consistent with the unsuccessful attempts to generate null mutants of the *CYC1* using split-marker method, suggesting that *CYC1* is an essential gene in *M. oryzae*.

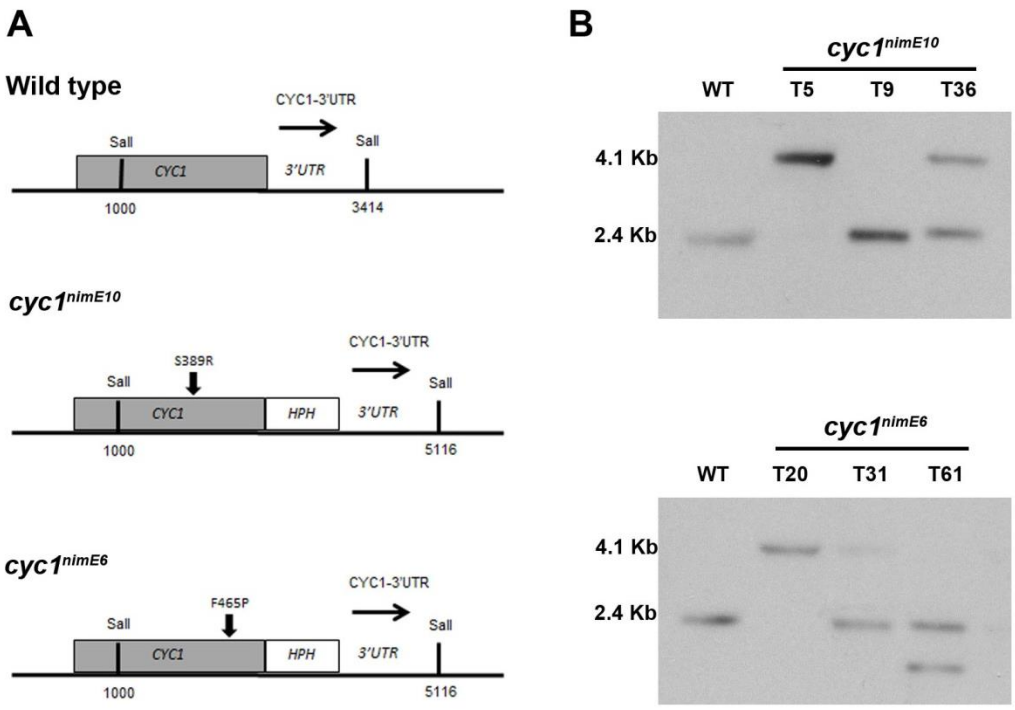

Figure 3.6 Southern blot analysis of the putative *cyc1*^{nimE10} and *cyc1*^{nimE6} mutants. (A) Gene replacement strategy of the *cyc1*^{nimE10} and *cyc1*^{nimE6} alleles to the *CYC1* locus. **(B)** Southern blot analysis to show successful replacement of TS alleles of *cyc1*^{nimE10} (upper panel) and *cyc1*^{nimE6} alleles (lower panel). The size difference in each blot is consistent with successful replacement of the gene construct containing the resistance cassette *HPH*. Genomic DNA of putative transformants and the wild type Guy11 were digested with *Sal*I. After fractionation by gel electrophoresis, blots were probed with a fragment comprising the 3' UTR of *CYC1.* The *CYC1* locus of the *cyc1*^{nimE10}-T5 and *cyc1*^{nimE6}-T20 transformants were confirmed to be successfully replaced with the corresponding TS alleles, as shown by band shifts from 2.4 kb to 4.1 kb consistent with the addition of 1.7 kb *HPH* cassette.

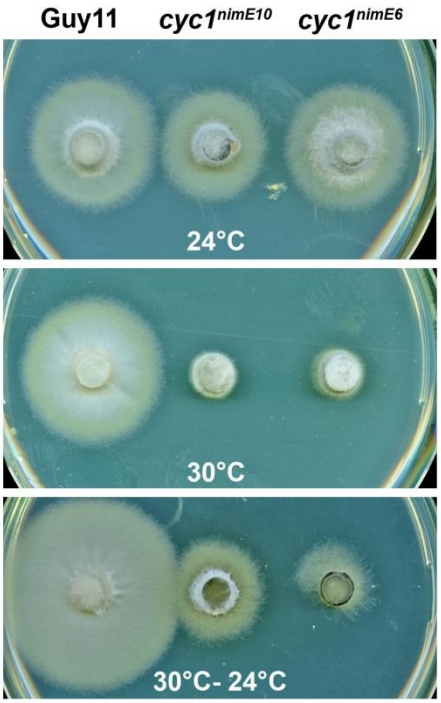

Figure 3.7 Growth defects of the *cyc1*^{nimE10} and *cyc1*^{nimE6} mutants. Mycelial plugs of 5 mm diameter were inoculated on complete medium agar plates and incubated at a permissive temperature of 24°C (top panel) or restrictive temperature of 30°C (middle panel) for 4 days. Growth of the transformants resumed when the plates were shifted to the permissive temperature and incubated for further 3 days (bottom panel).

3.2.5 The thermosensitive *cyc1*^{nimE10} and *cyc1*^{nimE6} mutants are impaired in appressorium formation

The ability of the *cyc1*^{nimE10} and *cyc1*^{nimE6} mutants to develop appressoria at the semi-restrictive temperature of 29°C was examined, along with previously generated cell cycle mutants (Saunders *et al*., 2010a). Conidia of *M. oryzae* strains were prepared in sterile distilled water, placed on hydrophobic coverslips, and incubated at the permissive temperature of 24°C, or the semi-restrictive temperature of 29°C for 24 h. Conidia of the *cyc1*^{nimE10} strain produced hyperpolarized germ tubes which subsequently failed to develop into appressoria, whereas the *cyc1*^{nimE6} mutant produced relatively thicker germ tubes that underwent flattening and hooking of the germ tube tip but were still unable to form dome-shape cells (Fig 3.8). The *nim1*^{I327E} mutant, which unable to initiate DNA synthesis and instead undergoes mitotic catastrophe, also failed to develop appressoria similar to the *cyc1*^{nimE10} mutant. By contrast the *bim1*^{F1763*} mutant was able to produce melanised appressoria (Fig 3.8; Saunders *et al.*, 2010a). Therefore, I conclude that appressorium morphogenesis requires discrete activities of B-type cyclin-CDK1 complex; the S-phase activity for hooking, and the G2 activity for isotropic expansion of the appressorium.

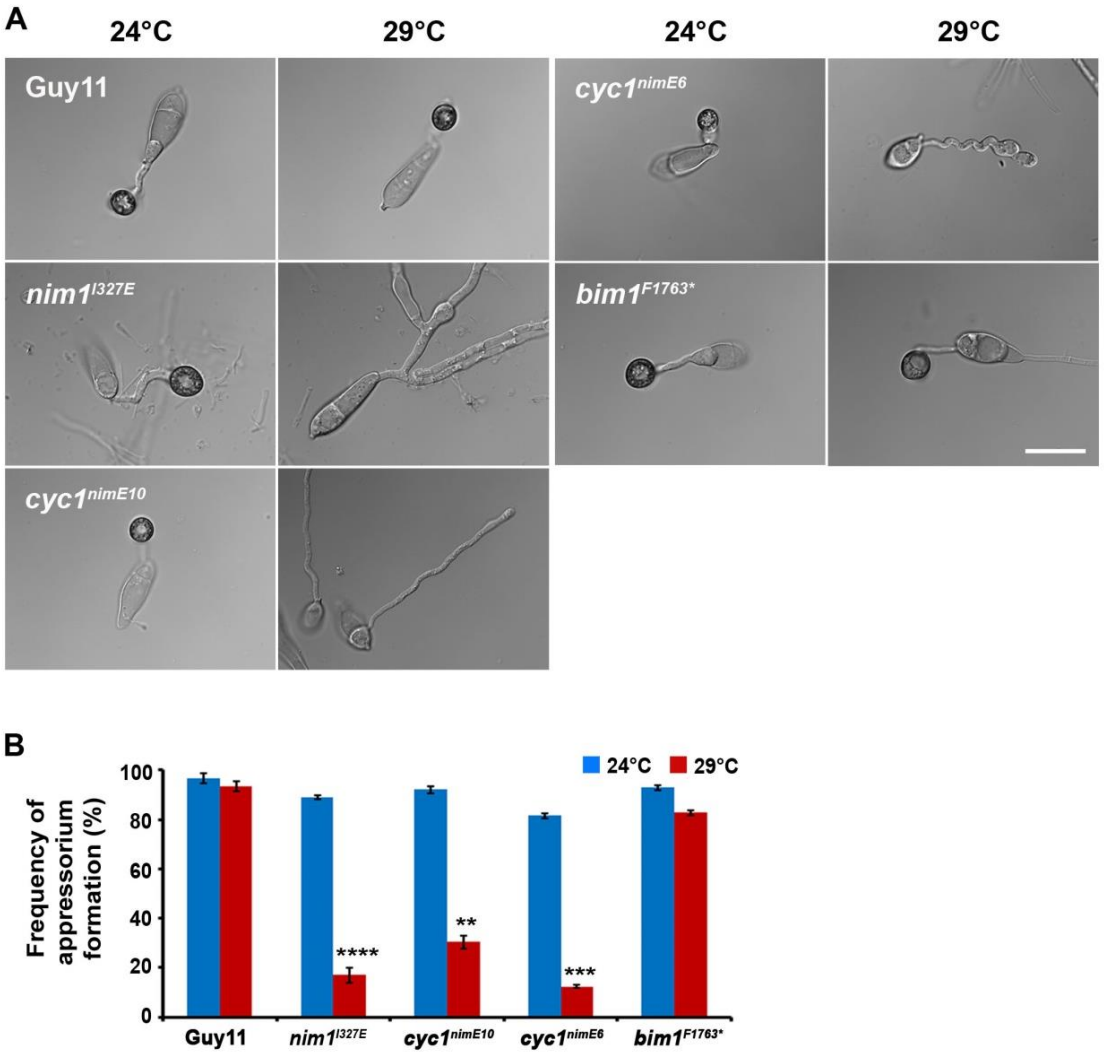

Figure 3.8 Appressorium morphogenesis requires S-phase progression. (A) Micrographs to show appressorium formation of Guy11 wild type, *nim1*^{I327E}, *cyc1*^{nimE10}, *cyc1*^{nimE6} and *bim1*^{F1673*} strains at 24°C and 29°C after 24 h. **(B)** Bar chart to show the frequency of appressorium formation of *M. oryzae* strains at 24°C and 29°C examine at 24 hpi. All scale bars indicate 20 µm. ***P* < 0.01; ****P* < 0.001; *****P* < 0.0001 using the *t*-test; error bars, standard errors.

3.3.6 Verification of cell cycle arrest in the *cyc1*^{nimE10} and *cyc1*^{nimE6} mutants

To determine whether the *cyc1*^{nimE10} and *cyc1*^{nimE6} mutations block in G1, S or G2 phase of the cell cycle, I continued phenotypic classification of the interphase mutants by using the reciprocal shift method (Bergen *et al.*, 1984b). Conidia of *M. oryzae* strains were germinated on hydrophobic cover slips either at the permissive temperature in the presence of DNA replication inhibitor HU or at the restrictive temperature in the absence of HU, for a period of time sufficient to allow most of the conidia to progress through the cell cycle and accumulate at the respective HU or TS block points. The conidia incubated at the permissive temperature in HU were then shifted to the restrictive temperature and released from HU block. Reciprocally the conidia germinated at restrictive temperature in the absence of HU were shifted to the permissive temperature in the presence of HU. By considering the effects of these reciprocal shifts on the ability of conidia to produce melanised appressoria as a marker for mitotic entry, the relationship between the arrest points of the mutations in relation to S phase of the mutants can be determined. This method is only applicable for a rapid and reversible cell cycle block, and I have shown that the *cyc1*^{nimE10} and *cyc1*^{nimE6} mutations were highly reversible (Fig 3.7).

There are theoretically three possible outcomes for this experiment.

1) If a given TS block is exerted in G1 (before S phase), then a TS block followed by HU will not allow completion of the cell cycle, but an HU block followed by a TS block will do.

2) If a given TS mutation causes S-phase arrest, then neither TS block followed by HU, nor a HU block followed by a TS block, will allow completion of the cell cycle.
3) If a given TS block is applied at G2 (after S phase), as TS block followed by HU will not inhibit nuclear division.

The results of the reciprocal shift analysis are shown in Table 3.2. The *cyc1*^{nimE10} mutant progressed poorly into mitosis, when it was incubated at 29°C, then shifted to 24°C in the presence of HU, and also failed to resume the cell cycle when germinated at 24°C in the presence of HU, then shifted to 29°C without HU. The result indicates that the *cyc1*^{nimE10} mutation causes an arrest in S phase. In contrast, the *cyc1*^{nimE16} and *nimA*^{E37G} mutants were able to produce melanised appressoria when they were incubated at 29°C then shifted to 24°C in the presence of HU, but were unable to progress in to mitosis after germination at 24°C, in the presence of HU, then shifted to 29°C without HU. Thus, I conclude that the *cyc1*^{nimE10} mutant arrests in S phase, whereas the *cyc1*^{nimE16} mutant arrests in G2 at the non-permissive condition. These observations are consistent with previous studies in *A. nidulans* using reciprocal shift assays and flow cytometric analysis of DNA content (Bergen *et al*., 1984; James *et al.*, 2014).

Table 3.2 Reciprocal shift experiments

strains	control	A	B	C	D	E	F	arrest point
Guy11	98.2	95.1	95.0	91.0	0.0	94.0	93.2	no arrest
cyc1^{nimE10}	90.0	10.0	50.0	0.0	0.0	87.0	10.3	S
cyc1^{nimE6}	82.0	28.3	40.3	43.8	0.0	78.0	6.0	G2
nimA^{E37G}	88.0	40.0	80.0	29.4	0.0	81.0	0.0	G2

The reciprocal shift method was used to establish the arrest points of the cell cycle mutants (Bergen *et al*., 1984). Conidia of the indicated strains were induced for appressorium development on cover slips and the percentages of conidia in which appressorium maturation had occurred was recorded indicating completion of mitosis. At least 200 conidia were counted for each determination. Two biological replications were undertaken. **Control**, 24 hours at 24°C; **A** 24 hours at 29°C; **B,** 8 hours at 29°C then 16 hours at 24°C; **C**, 8 hours at 29°C then 16 hours at 24°C with HU; **D**, 24 hours at 24°C with HU; **E,** 8 hours at 24°C with HU then 16 hours without HU; **F**, 8 hours at 24°C with HU, then 16 hours at 29°C without HU.

3.3.7 Cell cycle-dependent plant penetration by *M. oryzae* appressorium

In this study, I observed plant penetration using cell cycle mutants to provide complementary genetic evidence regarding cell cycle-dependent plant penetration by *M. oryzae*. Conidia of conditional mutants impaired at different cell cycle stages were inoculated onto rice leaf sheaths, and incubated at the permissive temperature of 24^{o}C for 10 h to allow completion of the first mitosis, then shifted to the restrictive temperature of 30^{o}C to block the cell cycle progression of the appressorial nucleus. Appressoria of the *cyc1*^{nimE10} mutant, which is arrested in S-phase, were unable to produce primary invasive hyphae or infect rice cells at 30^{o}C (Fig. 3.11). In contrast, the *cyc1*^{nimE6} mutant, which is arrested in G2 phase, were able to infect rice tissue and generate primary hyphae at 30^{o}C (Fig. 3.9). Previous observations found that appressoria of *nim1*^{I327E} mutant failed to penetrate rice cuticle, but the *bim1*^{F1763*} mutant, arrest in a pre-anaphase state, was able to invade rice cells at restrictive temperature (Miriam Oses-Ruiz, PhD thesis, Biosciences, University of Exeter). Primary invasive hyphae of *cyc1*^{nimE6} did not differentiate into bulbous invasive hyphae, suggesting that this morphogenetic transition may require a subsequent round of mitosis or arrival of a daughter nucleus in the differentiating invasive hyphae. Therefore, the emergence of the penetration peg is dependent on S-phase progression in the appressorium.

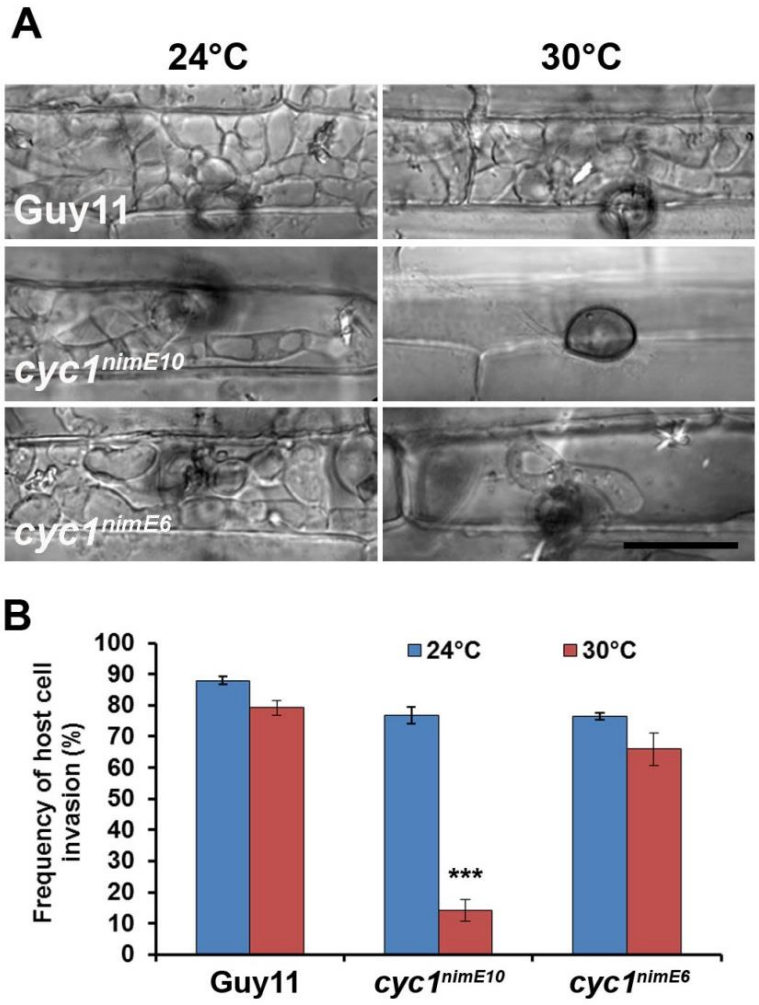

Figure 3.9 Inhibition of DNA replication impaired plant penetration. (A) Micrographs to show the effect of cell cycle arrest at different points on plant penetration assessed at 48 h. Rice leaf sheaths of cultivar CO-39 were inoculated with Guy11, *cyc1*^{nimE1} and *cyc1*^{nimE6} strains, incubated at 24°C for 10 h, then shifted to 30°C. Scale bar indicates 20 µm. **(B)** Bar chart to show the frequency of appressoria producing penetration hyphae. Penetration by the appressoria of the *cyc1*^{nimE10} mutant was significantly reduced, compared to the wild-type strain. ****P* < 0.001 using the *t*-test; error bars, standard errors.

3.4 Discussion

To initiate host infection, plant pathogenic fungi perceive a set of inductive cues and develop diverse infection structures to gain entry into host tissue. These range from entry through natural plant openings to various mechanisms of direct penetration through the outer leaf surface (Haueisen and Stukenbrock, 2016). The rice blast fungus *M. oryzae* produces a single-celled appressorium that directly breach the host cuticle (Howard and Valent, 1996). The appressorium generates enormous turgor pressure by accumulating molar concentrations of glycerol (de Jong *et al*., 1997). Previous studies demonstrated that a single round of mitosis in the germ tube is required for appressorium development of *M. oryzae*, and the next mitosis was speculated to be necessary for re-polarisation of the appressorium leading to plant penetration (Saunders *et al*., 2010a; Dagdas *et al*., 2012). In this chapter, I set out to elucidate how the conserved cell cycle machinery regulates plant infection by the rice blast fungus.

Here I demonstrated that the Cyc1 cyclin B directs S and G2 progressions of the *M. oryzae* cell cycle. The evidence to support this idea is based on analysis of the *nim1*^{I327E} and *cyc1*^{nimE10} mutants, impaired in S-phase progression, which were unable to form the terminal swelling of the germ tube tip, the hook, in response to hard hydrophobic surfaces. Swelling and bending at the germ tub apex is thought to be an early morphogenetic signature of host surface recognition that precedes appressorium development (Howard and Valent, 1996). These effects were similar to the chemical inhibition of DNA replication by HU which arrests the cell cycle in S phase (Veneault-Fourrey *et al.*, 2006; Saunders *et al.*, 2010a). These results demonstrate that the deformation of germ tube tips depends on S-

phase progression. This is also consistent with the timing of DNA replication during spore germination visualised by LacO/LacI chromosomal tagging system (Miriam Oses-Ruiz, unpublished observation; Appendix 2).

The cAMP-PKA pathway is well-known to mediate surface recognition controlling early stage of appressorium formation of *M. oryzae* (Lee & Dean, 1993). The phenotypes of *nim1*^{I327E} and *cyc1*^{nimE10} mutants were similar to *M. oryzae* wild type spores incubated on non-inductive surfaces, and to Δ*mac1* mutants, defective in production of cAMP and appressoria formation or undergoing hooking (Choi & Dean, 1997). In *S. cerevisiae*, the Ras/cAMP-dependent PKA phosphorylates Whi3, which is a cell cycle regulator controlling G1/S transition (Mizunuma *et al.*, 2013). The G1/S progression during the initiation of appressorium formation might be controlled by the Ras/cAMP-PKA pathway.

The second finding from this study is that activation of the CDK1-cyclin B complex in G2 phase is required for late stage of appressorium formation. The *cyc1*^{nimE6} mutant, which arrests in G2, was unable to form well-defined dome-shaped appressoria, but displayed an obvious terminal swelling of the germ tube tips. This suggests that isotropic expansion of the appressorial dome requires G2 activity of the CDK complex, consistent with the role of B-type cyclin in promoting bud growth at G2/M of the yeast cell cycle. In *S. cerevisiae*, the mitotic cyclin Clb2 promotes isotropic bud growth by inducing depolarisation of actin cytoskeleton in the bud (Lew and Reed, 1993). When the mitotic cyclin was depleted, the bud cannot expand isotropically and instead displays hyperpolarised growth. In *S. pombe*, when DNA replication is perturbed by HU treatment, the DNA damage checkpoint becomes active and inhibits the activity of the CDK1-cyclin B complex

at the G2/M transition (O'Connell *et al.*, 2000). When the cells encounter DNA replication stress and DNA damage, the conserved DDR pathway mediates inhibitory phosphorylation of CDK-cyclin B complexes which in turn arrests the cell cycle at G2, and prevents catastrophic mitosis (O'Connell *et al*., 2000). The current finding is consistent with the S-phase dependency of appressorium formation shown in the HU experiment. The same cell cycle target of the S-phase checkpoint may also regulate appressorium formation (Veneault-Fourrey *et al.*, 2006; Saunders *et al.*, 2010). Recent observations showed that *M. oryzae* mutants of DNA damage response pathway were able to form an appressorium-like structure in the presence of HU, suggesting that such a pathway coordinates the cyclin B-CDK activity with the successful S-phase progression during appressorium morphogenesis (Miriam Oses-Ruiz, PhD thesis, Biosciences, University of Exeter; Appendix 2).

The effects of G2 arrest by the *cyc1*^{nimE6} mutation rather resembles that of Δ*pmk1* mutants which also fail to develop an appressorium but still undergoes hooking (Xu & Hamer, 1996). The Pmk1 MAPK module consists of the Mst11, Mst7 and Pmk1 kinases which act sequentially to transmit environmental signals, and regulate infection-related development (Zhao *et al*., 2005). The *Δpmk1* mutant is unable to form appressoria, but still responds to exogenous cAMP by producing swollen tips of germ tubes (Xu and Hamer, 1996). Although the relationship between MAPK signalling and cell cycle control is well-established in *S. cerevisiae*, it is largely unknown how activation of *M. oryza*e MAPKs affects on the cell cycle progression which controls appressorium development. Yeast pheromone stimulation leads to cell cycle arrest in G1 via the action of a cyclin-CDK inhibitor

Far1 (Gartner *et al.*, 1998). However, germ tubes of Δ*pmk1* mutants underwent several rounds of mitosis but did not form a dome-shaped appressorium (Saunders *et al*., 2010b, Xu & Hamer, 1996). This suggests that Pmk1 MAPK activation does not lead to cell cycle arrest, as found in the yeast mating response. It is possible that the Pmk1 MAPK pathway modulates G2/M transition at the late stages of appressorium formation. In mammalian systems, ERK MAPK, an orthologue of *M. oryzae* Pmk1, is implicated in the regulation of the G2/M transition. One possible mechanism involves controlling nuclear localization of cyclin B1 (Chambard *et al.*, 2007). Nonetheless, attempts to localise Cyc1 in the *pmk1*^{AS} mutant in order to examine the effect of Pmk1 activation in cell cycle regulation have proven challenging. Fungal transformants expressing fluorescently-tagged Cyc1 were unstable and their fluorescence signals were quickly bleached following photoexcitation. Use of other version of fluorescence proteins, such as tandem repeat GFP or RFP may help resolve such problem. Taken together, S phase progression promotes terminal swelling of the germ tube tips, while G2 phase triggers isotropic expansion leading to the formation of the appressorial dome.

The third conclusion reaches in this study is that S-phase progression in the appressorium is necessary for plant penetration. Perturbations of S-phase, either by *nim1*^{I327E} and *cyc1*^{nimE10} mutations, prevented appressoria from elaborating penetration pegs that rupture plant cuticle. In contrast, cell cycle arrests at later stage by *cyc1*^{nimE6} (G2 arrest) and *bim1*^{F1763*} (post-mitotic arrest) mutations did not prevent plant infection (Fig 3.9; Miriam Oses-Ruiz, unpublished data; Appendix 2). However, the penetration hyphae of these mutants failed to differentiate into bulbous invasive hyphal cells, suggesting that the completion of cell cycle in the

appressorium or the arrival of daughter nuclear into the primary hyphae is needed for fungal cell morphogenesis. These observations are consistent with the effects of cell cycle arrest by the DNA replication inhibitor HU and by benomyl (Miriam Oses-Ruiz, PhD thesis, Biosciences, University of Exeter; Appendix 2). Time-lapse imaging showed that the development of the first bulbous invasive hyphal cell with subapical BIC is accompanied with the arrival of daughter nuclei into the primary hyphae (Miriam Oses-Ruiz and George Littlejohn, unpublished data; Appendix 2). In budding yeast, Cdc28 CDK1 controls the emergence and polarised growth of the bud during late G1 and S phases via activating the Cdc42 GTPase module (McCusker *et al.*, 2007). Cdc42 is responsible for polarisation of the actin cytoskeleton, septin assembly and secretion towards the bud (McCusker *et al*., 2007). However in the previous chapter, I have demonstrated that plant penetration of by Δ*cdc42* mutant was not completely abolished but only delayed. The Δ*cdc42* mutant also invaded neighbouring rice cell. These observations suggest that Cdc42 GTPase is not absolutely required for re-polarisation of *M. oryzae* appressoria or cell-to-cell movement. In the previous chapter, I have also reported that the Pmk1 activity is required for the rearrangement of cytoskeletons and subsequent plant penetration. Interestingly the strong interaction between Mst7 and Pmk1 was found later between 8 and 12 hours of appressorium development (Zhao & Xu, 2007), coinciding with septin ring assembly at the appressorium pore which marks the re-polarisation of the appressorium (Dagdas *et al.,* 2012). However, the activation of the Pmk1 pathway in appressorium may act in parallel with S-phase progression to trigger appressorial re-polarisation and penetration, because appressoria of the Δ*mst12* mutant defective in plant penetration were able

to progress into S-phase (Miriam Oses-Ruiz, unpublished data; Appendix 2). It has been shown that the build-up of turgor pressure in the appressorium is a positive signal required for S-phase entry, appressorium re-polarisation, and plant penetration (Miriam Oses-Ruiz and Wasin Sakulkoo, unpublished data; Appendix 2). How the increased turgor is sensed and integrated with downstream signalling cascades that trigger appressorium penetration remains to be explored.

In summary, this study has demonstrated the functional relationship between the core cell cycle machinery and appressorium-mediated plant infection. Cell cycle progression into S and G2 phases mediated by the CDK-cyclin B complex is critical for appressorium formation and function, and for the establishment of rice blast disease.

Chapter 4 Chemical genetic approach for functional characterisation of the Pmk1 MAPK in the rice blast fungus *Magnaporthe oryzae*

4.1 Introduction

Mitogen-activated protein kinase (MAPK) signalling pathways transmit environmental signals and govern cellular responses in eukaryotic cells (Widmann *et al.*, 1999). MAPK pathways are characterised by a cascade of three conserved protein kinases that function sequentially. MAPKs are activated by MAPK kinases (MAPKKs), which are activated in turn by MAPKK kinases (MAPKKKs). Scaffolds and adaptor proteins are also involved in controlling interactions among these components in order to achieve specificity of output, and to prevent inadvertent cross-talk between signal transduction pathways. Activation of MAPK cascades primarily results in transcriptional reprogramming (Widmann *et al*., 1999). In the budding yeast *Saccharomyces cerevisiae*, for example, different MAPK pathways regulate mating response, filamentous or invasive growth, cell well integrity, and the response to high osmolarity (Chen & Thorner, 2007). The mating response depends on the binding of mating pheromones to their cognate G-protein coupled receptors (GPCR), namely Ste2 and Ste3. This interaction results in the release of heteromeric G-protein subunits and transmits signals to the Cdc42 GTPase module, p21-activated kinase (PAK) Ste20, the Ste5 scaffold protein and the Fus3 MAPK cascade. The activated Fus3 MAPK triggers several cellular responses required for mating and cell-cell fusion. Primary targets of the pheromone response pathway are the cyclin-dependent kinase (CDK) inhibitor Far1, which mediates cell cycle arrest, and the transcription factor Ste12, which controls expression of mating

responsive genes (Herskowitz, 1995). Although components of the pheromone response pathway are shared with those that regulate filamentous growth, upstream components, such as pheromone receptors, heterotrimeric G proteins, and Ste5 scaffold protein are not required for activation of filamentation (Cullen & Sprague, 2012). Fus3 and Kss1 MAPKs serve partially overlapping functions in mating. Kss1 is essential for invasive growth, and can coordinate the mating response in the absence of *FUS3*. During nutrient starvation, activation of the Ste11-Ste7-Kss1 module instead, is mediated by two transmembrane proteins Sho1 and Msb2, and two small GTPases Ras2 and Cdc42. In addition to the Kss1 MAPK, appropriate filamentous growth requires two other classes of protein kinases: a 5'-AMP-dependent protein kinase (AMPK) Snf1 and a specific isoform of 3',5'-cyclic AMP-dependent protein kinase (PKA) called Tpk1 (Cullen & Sprague, 2012). However, the yeast mating response, filamentous growth and other cellular responses are obviously complex networks of interconnecting pathways, rather than a simple linear pathway (Chen & Thorner, 2007).

In the rice blast fungus *M. oryzae,* a Fus3/Kss1-type MAPK, called pathogenicity MAPK (Pmk1), was the first MAPK characterised in a fungal plant pathogen (Xu & Hamer, 1996). The Pmk1 regulates the late stages of appressorium morphogenesis and infectious growth. Null mutants of *PMK1* cannot form appressoria, but still respond to exogenous cAMP by producing swollen tips at the end of germ tubes (Xu & Hamer, 1996). The Mst11 MAPKKK, Mst7 MAPKK and Mst50 adaptor operate upstream of the Pmk1 MAPK, and are also required for appressorium formation (Zhao *et al*., 2005, Park *et al*., 2006). Conidial germination and appressorium formation of *M. oryzae* happen in the absence of exogenous

nutrients, so that cell growth and accumulation of compatible solutes, required for turgor pressure generation in the appressorium, rely instead on storage compounds in the conidium (Wilson & Talbot, 2009). Pmk1 signalling has been shown to control the mobilisation of lipids and glycogen from the conidium to the developing appressorium (Thines *et al*., 2000). The Pmk1 MAPK has been shown to activate Mst12, a homologue of the Ste12 transcription factor, that is required for appressorium-mediated penetration and infectious growth, but not for appressorium formation (Park *et al*., 2004, Park *et al*., 2002). The Δ*mst12* mutant was shown to be defective in re-organisation of the F-actin and septin cytoskeleton at the base of appressorium, consistent with a role in regulating re-polarisation of the appressorium (Dagdas *et al*., 2012). A Pmk1-interacting transcription factor, MoSfl1, involved in heat tolerance and virulence of *M. oryzae* has been identified using protein microarray analysis (Li *et al*., 2011). Significantly, orthologues of the Pmk1 MAPK have been shown to regulate infection-related development in various plant pathogenic fungi, such as *Colletotrichum lagenarium, Cochliobolus heterostrophus, Botrytis cinerea, Verticillium dahliae, U. maydis* and *Fusarium oxysporum* (Hamel *et al*., 2012, Zhao *et al*., 2007).

The Pmk1 MAPK pathway is likely to have roles that go beyond formation and function of appressoria (Xu & Hamer, 1996). The *Δpmk1* and *Δmst12* mutants failed to colonise wounded rice tissue, indicating a potential role in regulating invasive growth or survival in plant tissues (Park *et al*., 2002, Xu & Hamer, 1996). However, because both *Δpmk1* and *Δmst12* mutants are unable to penetrate the rice surface, the roles of Pmk1 MAPK signalling during later stages of the interaction between *M. oryzae* and its host plant could not be determined by a

traditional genetic approach. Thus, conditional mutants of the Pmk1 are needed for functional characterisation at any stages of plant infection. The generation of a temperature-sensitive (TS) allele of Pmk1 has also failed to date, because the mating process of *S. cerevisiae* is heat sensitive, meaning that TS mutants of Fus3 MAPK have not been isolated and it is not possible to predict which mutation confers temperature sensitivity (Bishop *et al.*, 2000a). Therefore in this project, I sought out to use an alternative approach for specific inhibition of Pmk1 MAPK function throughout plant infection.

A chemical genetic strategy can provide the means to specifically inhibit a selected enzyme in a dose-dependent and reversible manner (Bishop *et al*., 2000a). For protein kinases, this approach can be achieved by mutating a conserved gatekeeper residue within an ATP-binding pocket of a kinase to a smaller amino acid, rendering the kinase of interest susceptible to an ATP analogue, PP1 (Fleißner, 2013). This chemical genetic strategy has proven successful in kinases in a wide range of organisms including filamentous ascomycete fungi, *Neurosporra crassa* and *M. oryzae* (Fleissner *et al.*, 2009, Penn *et al.*, 2015). In this Chapter, I present evidence of how I have used a chemical genetic system for specific inhibition of the Pmk1 MAPK in order to examine its biological functions at different stages of plant infection. An analogue-sensitive mutants of *PMK1* (*pmk1*^{AS}) was then used to investigate the roles of Pmk1 MAPK after plant infection, which is described in Chapter 4. In this Chapter, I demonstrate that Pmk1 kinase activity is directly required for appressorium formation and for septin-dependent plant penetration.

4.2 Results

4.2.1 Chemical genetic approach for targeted inhibition of Pmk1 MAPK

To investigate biological functions of the Pmk1 MAPK at distinct stages of plant infection, I employed a chemical genetic approach by generating an analogue-sensitive mutant of Pmk1 (*pmk1*^{AS}) (Bishop *et al.*, 2000b). This system uses cell-permeable inhibitors that are highly selective to a modified kinase, therefore I reasoned that an ATP-analogue 1-(1,1-dimethylethyl)-3-(1-naphthalenyl)-1H-pyrazolo[3,4-d]pyrimidin-4-amine, in short 1NA-PP1, would specifically inhibit *pmk1*^{AS} protein and allow a straight-forward means to examine the Pmk1 function at different stages of plant infection. In the *S. cerevisiae* Fus3 MAPK, a point mutation at the gatekeeper residue, from glutamine 93 to glycine, which is located in the ATP-binding pocket, enhances sensitivity of the kinase to the ATP analogue 1NA-PP1 (Bishop *et al*., 2000b). I reasoned that because *M. oryzae PMK1* is homologous to *FUS3*, so introduction of an equivalent mutation to *PMK1* should similarly render the kinase susceptible to the inhibitor 1NA-PP1. The amino acid sequence of the Pmk1 protein was therefore aligned with the *S. cerevisiae* Fus3 to reveal a conserved region of the ATP-binding pocket where the gatekeeper residue is located (Fig. 4.1). I decided to mutate the gatekeeper residue of Pmk1 from glutamine at position 104 to glycine, in order to generate a putative *pmk1*^{AS} allele.

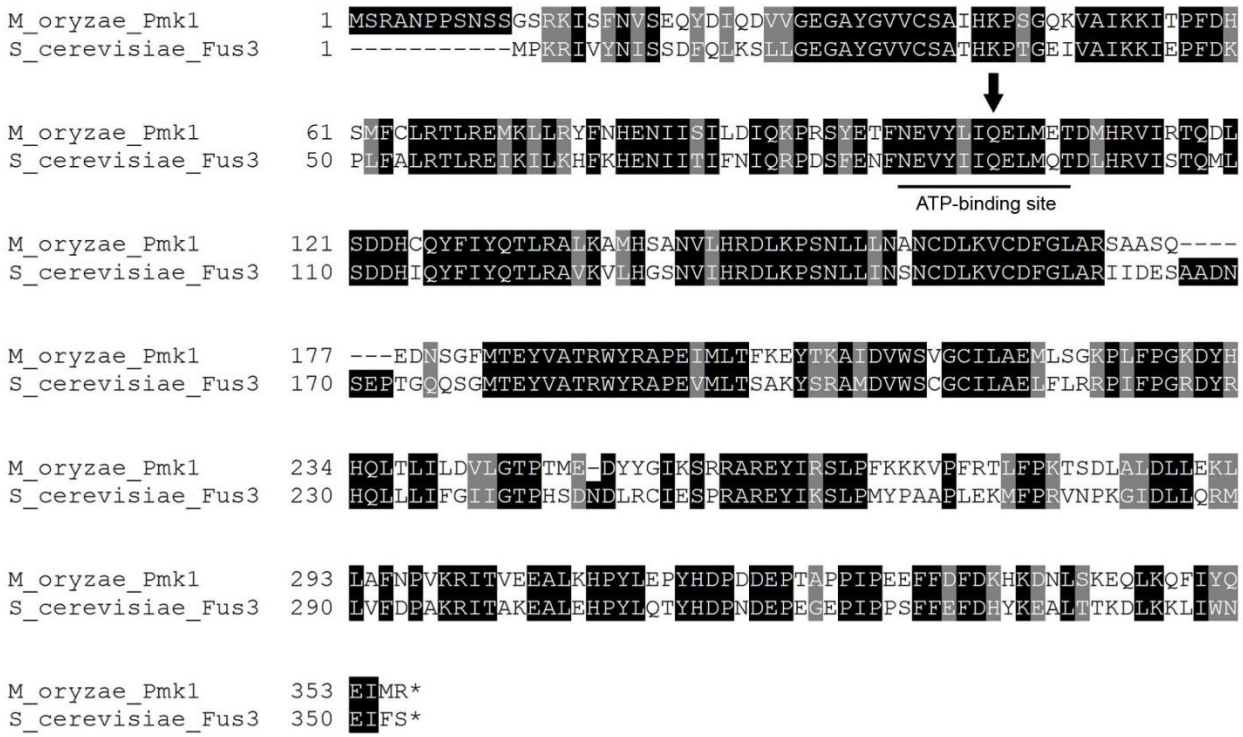

Figure 4.1 Amino acid alignment of predicted Pmk1 and Fus3 protein sequences showing the conserved gatekeeper residue in the catalytic pocket. The *M. oryzae* Pmk1 amino acid sequence was aligned with the *S. cerevisiae* Fus3 using Clustal Omega and shaded using BoxShade version 3.21. Numbers on the right indicate positions of amino acid residues. Residues shaded with black or grey are identical or partially similar among the two organisms respectively. Unshaded residues do not show any similarity. The black bar indicates the predicted ATP-binding site. The black arrow indicates the position of the gatekeeper residue glutamine (Q) to be mutated into glycine (G) to generate a putative *pmk1*^{AS} allele.

4.2.2 Generation and introduction of the analogue-sensitive allele of *PMK1*

A putative analogue-sensitive allele of *PMK1* (*pmk1*^{AS}) was generated using a fusion PCR method (Fig. 4.2). In the first round of PCR, a genomic fragment of *PMK1,* including a native promoter and 3' untranslated (3'-UTR) region, was amplified in two separated fragments using primers, Pmk1AS-1, -2, -3, and -4. *Eco*RI sites were introduced to primers Pmk1AS-1 and -4 (Table 3.1). The forward primer Pmk1-AS-3 contains nucleotide substitution of codon 104 from CAG to GGA and overlapping ends to complement with 3' end of a fragment amplified with Pmk1AS-1 and -2. The two fragments were then joined by fusion PCR, generating a 4.3 kb *pmk1*^{AS} allele. The *pmk1*^{AS} allele was excised by restriction digestion with *Eco*RI enzyme, and ligated into pCB1532 vector carrying a sulfonylurea resistant allele of *ILV1*. The nucleotide substitution in the *pmk1*^{AS} allele was confirmed by DNA sequencing. The resulting *pmk1*^{AS}*::ILV1* vector was then introduced into the Δ*pmk1* strain (Xu and Hamer, 1996) by protoplast transformation.

Putative fungal transformants expressing the *pmk1*^{AS} allele were pre-selected based on their ability to generate appressoria on a hydrophobic surface, indicating potential complementation of the Δ*pmk1* mutant by a functional *pmk1*^{AS} allele. Fungal transformants were then confirmed by Southern blot analysis for single copy insertion of the vector (Fig. 4.3). Genomic DNA of the wild-type strain Guy11, Δ*pmk1* mutant and putative *pmk1*^{AS} transformants were digested with *Eco*RV, which cuts only one site in the *pmk1*^{AS} vector, and subjected to Southern blot analysis used a probe specific to 188 bp region open reading frame (ORF) of the *PMK1* gene, amplified using primers Pmk1-ORF1 and Pmk1-ORF2. A single band was observed in Guy11 DNA (the positive control), whilst no band was

detected in the Δ*pmk1* mutant (the negative control). Transformants 101 and 103 contain a single copy insertion of the *pmk1*^{AS} construct, and were selected for further phenotypic analysis (Fig 4.3).

To test whether the *pmk1*^{AS} allele encodes a functional Pmk1 protein, the *pmk1*^{AS} transformants were used to infect susceptible CO-39 rice cultivar by spray inoculation assay of whole plants. The *pmk1*^{AS} transformants 101 and 103 were able to cause disease lesions on rice plants at similar levels to the Guy11 wild type, whereas the parental strain Δ*pmk1* was non-pathogenic (Fig. 4.4). Thus, the analogue-sensitive allele of *PMK1* encodes a functional Pmk1 protein that can complement the defects in pathogenicity of the Δ*pmk1* mutant in the absence of the ATP analogue.

Table 4.1 List of oligonucleotide primers used in Chapter 4

Primer	Sequence (5' to 3')
Pmk1AS-1	AGAATTCCAAGACCAACAAACAAAAAGAGTAGAAAA
Pmk1AS-2	CGGACTCCGATCAGGTACACCTCGTTGAA
Pmk1AS-3	CTACGAGACCTTCAACGAGGTGTACCTGATCGGAGTCCGTTGCTGCTGAACAC TCCT
Pmk1AS-4	TGTGTGTTGGTTGTCGTTTAATTTATTTGAATTCA
Pmk1-ORF1	AAGCTGCTCCGGTACTTCAA
Pmk1-ORF2	GCTCCTATACGGTGGTCGAA

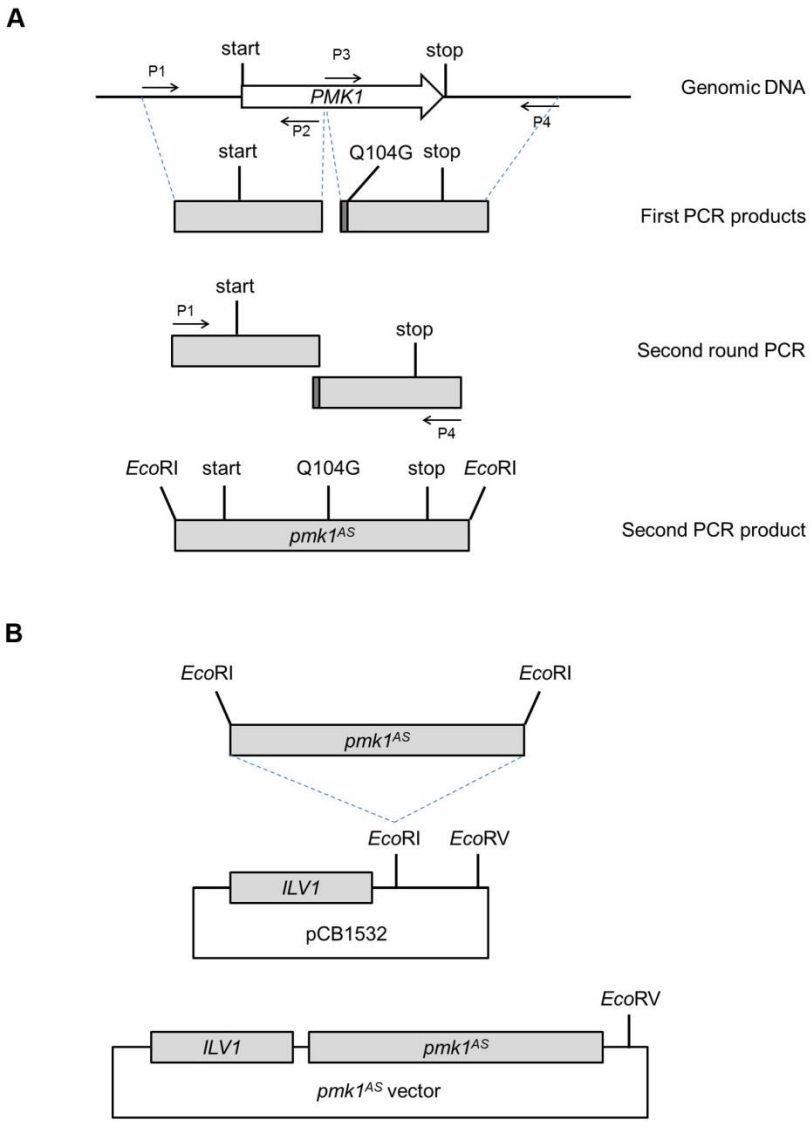

Figure 4.2 A schematic diagram depicting the cloning strategy for generating the *pmk1^{AS}* vector. (A) PCR amplification of two 2.2 kb *PMK1* gene fragments, a 5' region of the *PMK1* gene plus 2 kb promoter sequence and a 3' region of *PMK1* ORF plus 1.2 kb 3-UTR. The two resulting fragments were then joined by fusion PCR, generating a full length 4.3 kb *pmk1^{AS}* allele. The 4.3 kb fragment was excised with *Eco*RI to enable restriction site-mediated cloning. **(B)** Restriction site-mediated cloning strategy to generate *pmk1^{AS}* vector. The 4.3 kb *pmk1^{AS}* allele was ligated into the *Eco*RI site of pCB1532 carrying *ILV1*, a modified *M. oryzae* acetolactase gene conferring resistance to sulfonylurea. The *pmk1^{AS}::ILV1* vector contains a single *Eco*RV site.

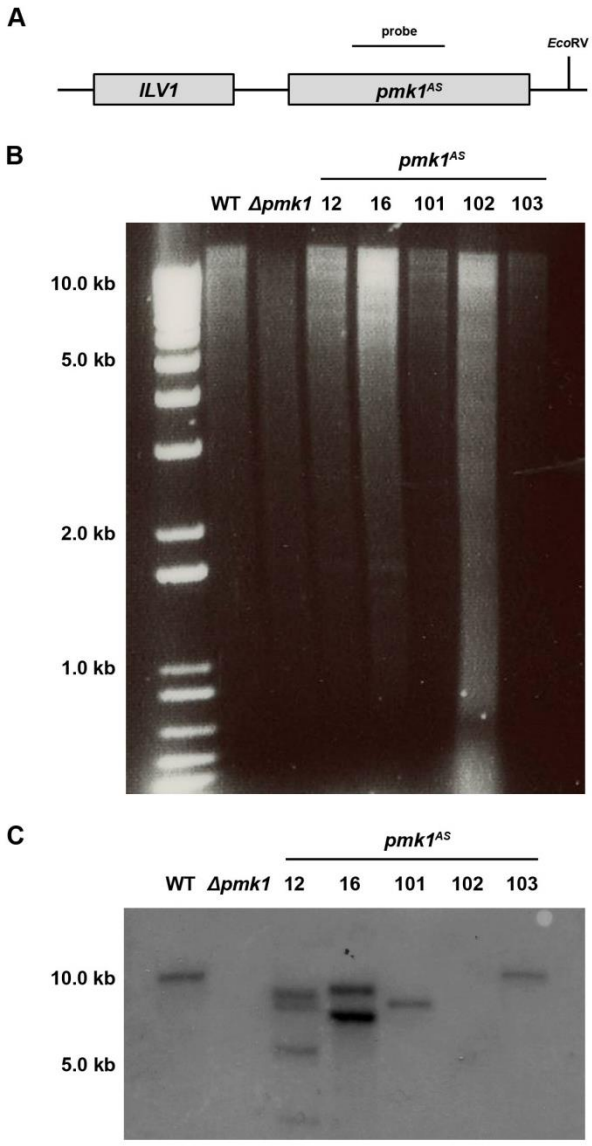

Figure 4.3 Southern blot analysis of putative *pmk1^{AS}* transformants. (A) Diagram to show the *pmk1^{AS}* vector containing a single *Eco*RV site. **(B)** Genomic DNA of the putative transformants were digested with *Eco*RV, gel fractionated, and transferred onto Hybond-NX. **(C)** The blot was probed with a 188 kb DNA fragment specific to the *PMK1* ORF, which hybridises and shows a single band in non-transformed Guy11 wild type and no bands in the Δ*pmk1* mutant. Transformants 101 and 103 of *pmk1^{AS}* were found to have single copy insertions and these transformants and were selected for further experiments.

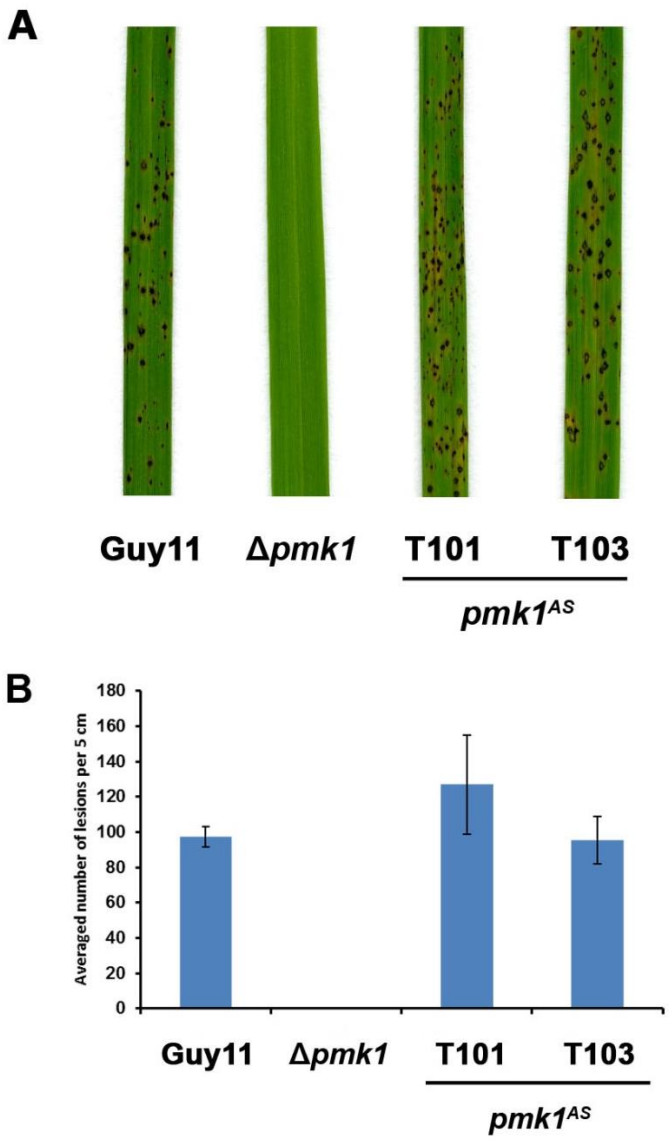

Figure 4.4 The analogue-sensitive *pmk1*^{AS} allele encodes a functional Pmk1 MAPK that fully restores the virulence of Δ*pmk1* mutant. (A) Conidial suspensions of equal concentration (5 x 10^4 spores mL^{-1}) from *M. oryzae* Guy11 wild type, Δ*pmk1,* and *pmk1*^{AS} strains were used to inoculate 21-day-old seedlings of a susceptible rice cultivar CO-39, and incubated for 5 days. Disease symptoms were fully restored on plants inoculated with *pmk1*^{AS} mutants. **(B)** Bar chart of mean lesion density of seedlings infected with Guy11 wild type, Δ*pmk1,* and *pmk1*^{AS} strains per 5 cm. Mean lesion density was not significantly different between Guy11 and *pmk1*^{AS} infections, as well as between T101 and T103 of *pmk1*^{AS} (unpaired, Student *t* test, P > 0.05). Error bars denote S.E. of the mean of three independent experiments.

4.2.3 *In vivo* determination of sensitivity towards the ATP analogue 1NA-PP1 in the *pmk1*^{AS} mutant

To determine the efficiency of chemical inhibition of the *pmk1*^{AS} mutant, different concentrations of 1NA-PP1 were applied to germinating conidia of the *pmk1*^{AS} strain. In the absence of 1NA-PP1, the *pmk1*^{AS}*-101* and *-103* transformants exhibited normal patterns of appressorium development, whereas upon 1NA-PP1 treatment (500 nM) appressorium formation was absent in both transformants (Fig. 4.5 A). To examine sensitivity of *pmk1*^{AS} mutant to the ATP analogue 1NA-PP1, different concentrations of 1NA-PP1 were added to germinating conidia of Guy11 and the *pmk1*^{AS} strains. Addition of 1NA-PP1 of 5 µM to 50 µM resulted in undifferentiated germ tubes with hooking similar to the phenotype of the Δ*pmk1* mutant (Fig. 4.5 B and C). Addition of high concentration of 1NA-PP1 (50 µM) did not affect appressorium formation by the wild-type Guy11 (Fig. 4.5 C). Thus, I chose to use 5 µM 1NA-PP1 as an optimal condition for Pmk1 inactivation. When the inhibitor was added after appressoria had formed at 4 or 6 hpi, germlings were able to differentiate into melanised appressoria, and the collapse of conidial cells occurred (Fig. 4.5 D). Targeted inhibition of the kinase activity of Pmk1 MAPK using the chemical genetic approach abrogates Pmk1 function during appressorium development. Therefore, Pmk1 kinase activity is required for appressorium formation, but if the inhibitor is added after the germ tube tip committed to differentiate into the appressorium, the process proceeds normally.

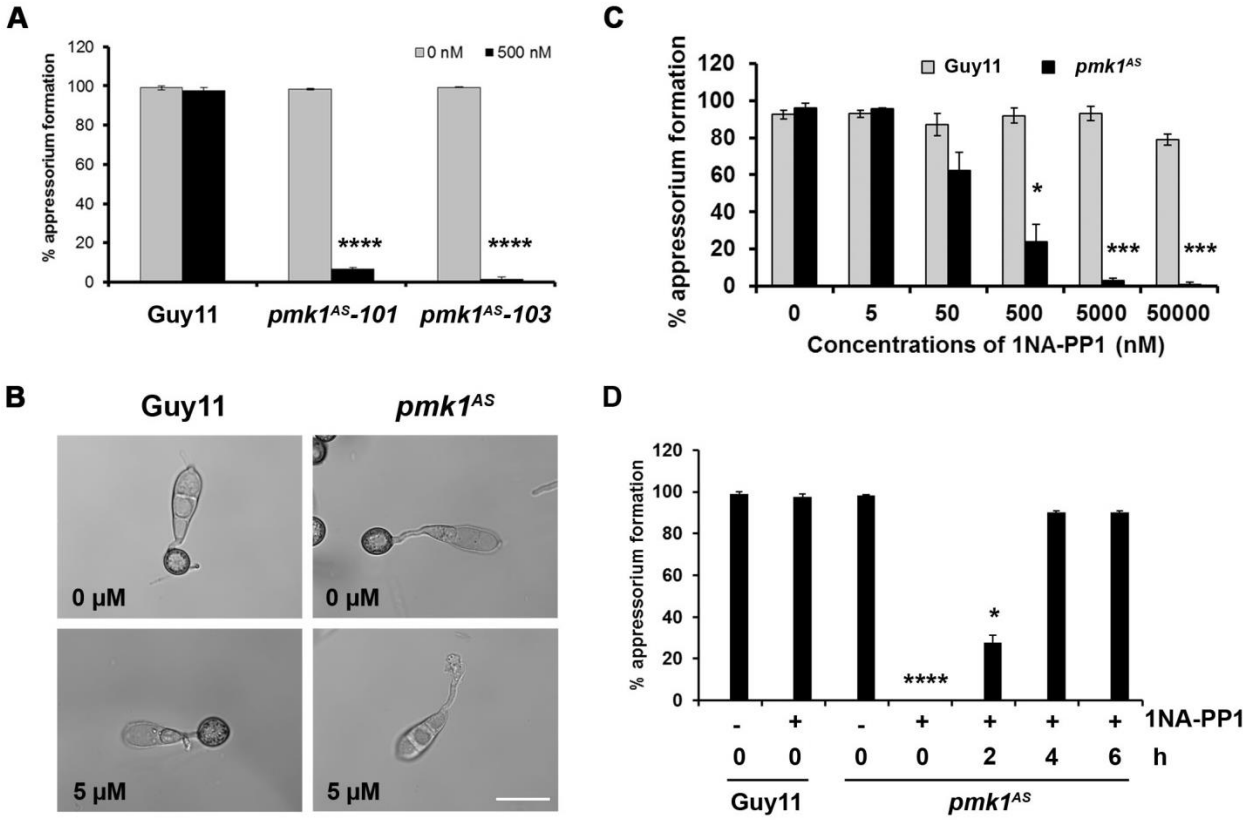

Figure 4.5 Effect of adding different concentrations of an ATP-analogue 1NA-PP1 on appressorium development in *M. oryzae*. (A) Bar chart to show sensitivity of the *pmk1*^{AS} mutants towards an ATP-analogue assessed at 24 hpi. Conidia were placed on cover slips, and incubated in a moist chamber, and added with 500 nM 1NA-PP1 at 2 hpi. Appressorium formation of the *pmk1*^{AS} mutants were significantly reduced compared to untreated control. **(B)** Appressorium formation of Guy11 and *pmk1*^{AS} (T101) exposed to 5 µM 1NA-PP1 at 2 hpi. Images were recorded at 24 hpi using an Olympus IX81 motorized inverted microscope. Scale bar represents 20 µm. **(C)** Bar chart to show the frequency of appressorium development of Guy11 and *pmk1*^{AS} mutant (T101) after addition of different concentration of 1NA-PP1, evaluated at 24 hpi. Aliquots of 0, 5, 50, 500, 5000, and 50000 nM of 1NA-PP1 were added to germinating conidia at 2 hpi. Appressorium formation of the *pmk1*^{AS} mutants were significantly reduced compared to the wild type treated with the same concentration of 1NA-PP1. **(D)** Bar chart of the frequency of appressorium development of Guy11 and *pmk1*^{AS} mutant at 24 hpi when 1NA-PP1 (5 µM) was added at different time points. Three technical and

three biological replicates were carried out with 100 conidia assessed for each technical replicate. *P < 0.05; ***P < 0.001; ****P < 0.0001 using unpaired two-tailed Student's *t*-test; error bars, standard errors.

4.2.4 Pmk1 kinase activity is required for septin-dependent plant penetration by appressoria

The Mst12 transcription factor is a downstream target of the Pmk1 MAPK pathway, regulating appressorium-mediated plant penetration and infectious growth by *M. oryzae.* Null mutants of *MST12* are unable to form a penetration peg or to grow invasively in rice tissue (Park *et al.,* 2002). I hypothesised that chemical inactivation of Pmk1 might provide a similar phenotype as that found in the Δ*mst12* mutants. To examine whether Pmk1 activity is required for appressorium-mediated penetration, appressoria of the *pmk1*^{AS} mutant was allowed to develop on the inner surface of rice leaf sheath and exposed to 5 µM 1NA-PP1 between 15 to 24 hpi. Exposure of appressoria to 1NA-PP1 at 15 h completely prevented generation of penetration hyphae, whereas increasing percentages of appressoria that could penetrate the plant surface were observed when treated with 1NA-PP1 at later time points (Fig. 4.6 A and B). Therefore, appressorium-mediated penetration requires time-dependent activation of Pmk1 MAPK around 18-24 h of appressorium development.

It has been shown that a large toroidal-shaped F-actin network and septin ring form around the appressorium pore prior plant surface penetration (Dagdas *et al*., 2012), Therefore, I asked whether re-organisation of the septin cytoskeleton at the appressorium pore is affected by Pmk1 inhibition. To do this, a fluorescently-labelled septin Sep5-GFP construct was introduced into the *pmk1*^{AS} mutant

background. In the absence of 1NA-PP1, a Sep5-GFP ring was observed around the appressorium pore similar to that seen in Guy11 (Dagdas *et al*., 2012). However, when 1NA-PP1 was added at 6 hpi the Sep5-GFP signal was mislocalised forming no distinctly organised shape within the appressoria (Fig. 4.6 C). Therefore, Pmk1 activity is required for septin assembly at the base of the appressorium.

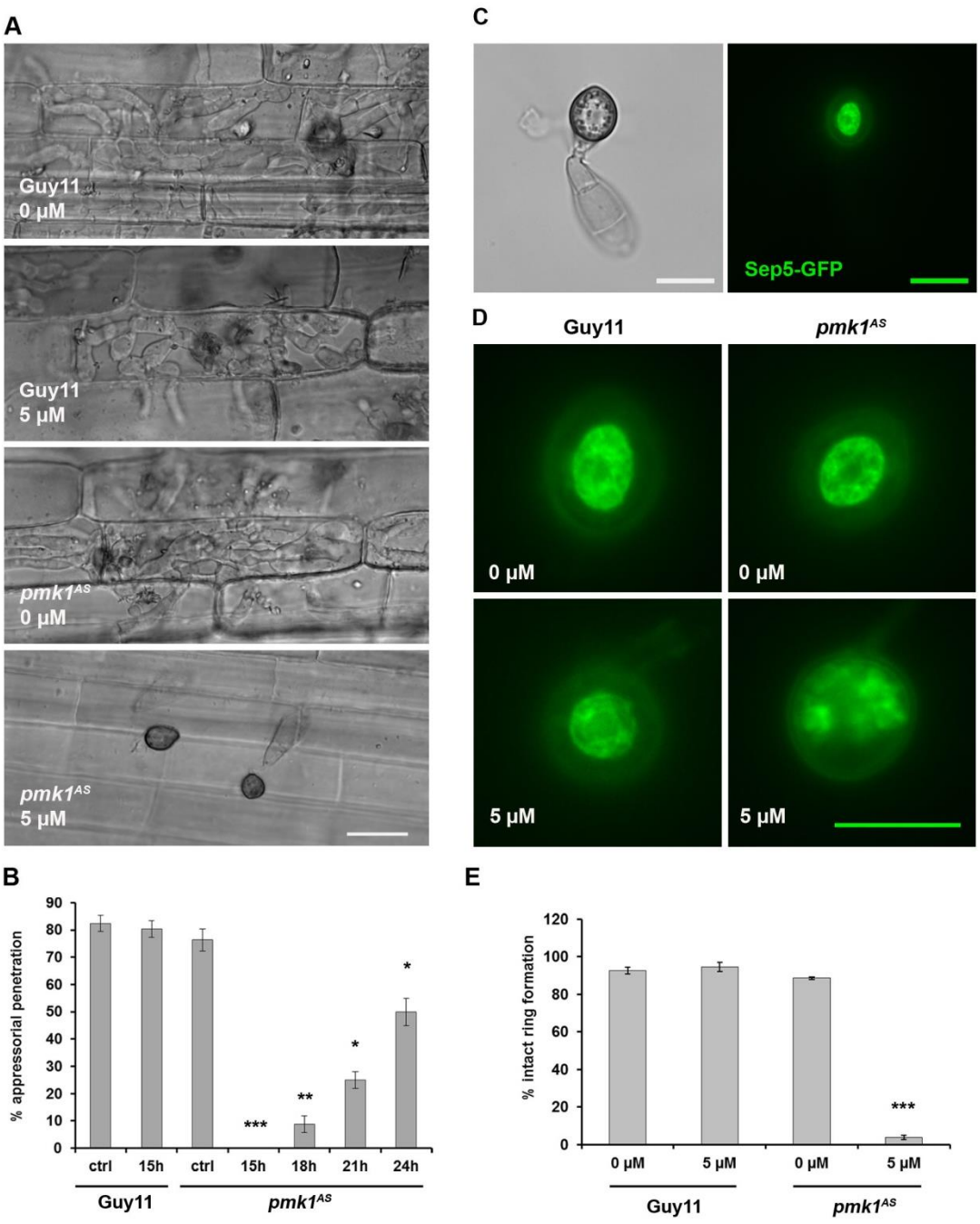

Figure 4.6 Pmk1 activity is necessary for septin-dependent plant penetration. **(A)** Micrographs to show the effect of Pmk1 kinase inactivation on plant penetration. Rice leaf sheaths of CO-39 cultivar were inoculated with the wild-type Guy11 and *pmk1*^{AS} spores, and were treated with 5 µM 1NA-PP1 at 15 hpi. Leaf sheaths were trimmed and checked for penetration at 42 hpi. Scale bar represents 20 µm. **(B)** Bar chart to show frequency of plant penetration when 1NA-PP1 was added to appressoria at different time points. **(C)** Localisation of Sep5-GFP in an

appressorium of Guy11 developed on a glass coverslip as visualised by epifluorescence microscope. Scale bar indicates 10 µM. **(D)** Representative images of localisation of Sep5-GFP in appressoria of Guy11 and *pmk1*^{AS} strains treated with 0 µM or 5 µM 1NA-PP1 at 6 hpi, and were recorded by at 24 hpi. **(E)** Bar chart to show percentage of appressoria showing intact septin ring assessed at 24 hpi. Three biological replicates were carried out with 50 appressoria assessed for each replicate. *P < 0.05; **P < 0.01; ***P < 0.001 using the *t*-test; error bars, standard errors.

4.2.6 Pmk1 kinase activity is essential for pathogenicity of *M. oryzae*

To examine the role of Pmk1 kinase activity in plant disease, seedlings of the susceptible rice cultivar CO-39, were inoculated with two independently generated *pmk1*^{AS} mutants, T101 and T103. Similar to the Guy11 wild type, the *pmk1*^{AS} mutants were able to cause disease lesions. Conidia were inoculated onto the susceptible rice cultivar CO-39. After 5 day of incubation, Guy11 wild type and *pmk1*^{AS} strains were able to cause obvious blast lesions, whereas the Δ*pmk1* mutant did not (Fig. 4.7). Spraying rice plants with *pmk1*^{AS} conidial suspension containing the 1NA-PP1 inhibitor gave inconsistent infection results, probably due to reduced ability of the inhibitor solution to stay on the leaf surface for the duration of the infection process. We therefore used leaf drop infection as the routine test for virulence of the *pmk1*^{AS} mutants.

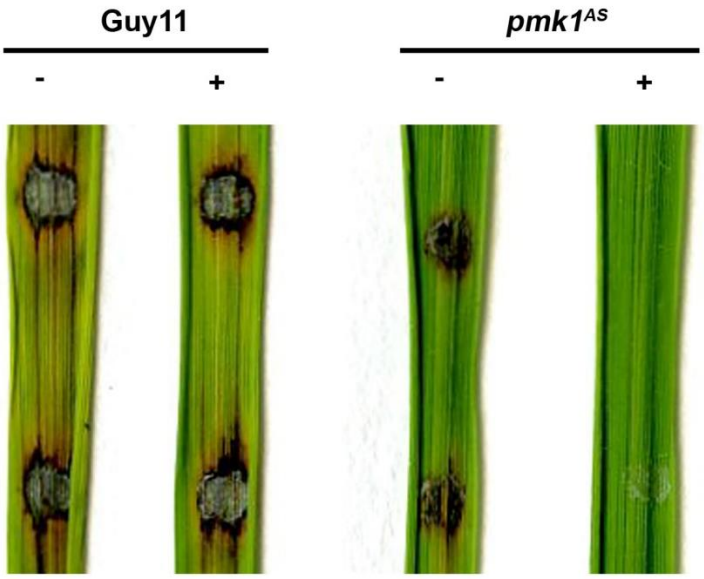

Figure 4.7 Pmk1 kinase activity is essential for pathogenicity of *M. oryzae.*
Macroscopic lesion formation by Guy11 and *pmk1*^{AS} conidia treated with an ATP-analogue 1NA-PP1. Conidial suspensions (5 x 10^4 spores mL^{-1}) were prepared in 0.2% gelatine solution with (+) or without (-) 5 µM 1NA-PP1. Drops of 20 µL conidial suspensions were placed on detached rice leaves. The leaves were incubated in moist chamber, and monitored after 5 days.

4.3 Discussion

Homologues of Kss1/Fus3-type MAPKs in fungi orchestrate a wide range of cellular responses including establishment of various infection strategies in several plant pathogenic fungi (Hamel *et al*., 2012, Zhao *et al*., 2007). Kss1/Fus3 homologues are also required for appressorium formation by *U. maydis* (Feldbrügge *et al.*, 2004), *Cochliobolus heterostrophus* (Lev *et al*., 1999), *Colletotrichum orbiculare* (formerly known as *C. lagenarium*; Takano *et al*., 2000), and *Pyrenophora teres* (Ruiz-Roldan *et al*., 2001). In other plant pathogenic fungi that do not develop appressoria, the Kss1/Fus3 MAPKs are also required for distinct strategies to invade host tissues. For example in *Mycosphaerella graminicola,* Fus3 MAPK is necessary for stomatal penetration (Cousin *et al*., 2006). In the soil-borne vascular wilt fungus *Fusarium oxysporum,* Fmk1 MAPK is associated with differentiation of penetration hyphae and with production of cell wall degrading enzyme required for host tissue invasion (Di Pietro *et al*., 2001). Thus the conserved Kss1/Fus3-type MAPK cascades coordinate a variety of cellular responses in order to achieve the growth and development of evolutionarily and biologically diverse fungi.

In this Chapter, I have described the establishment of the chemical genetic means of inhibiting the Pmk1 MAPK to enable functional characterisation at different development stages of plant infection by *M. oryzae*. Failure of Δ*pmk1* mutants to infect rice plants through wounds indicated that Pmk1 might have roles during invasive growth (Xu and Hamer, 1996; Thines *et al.*, 2000). However, defining the precise role of Pmk1 during post-penetration stages has been difficult, because the null mutant of *PMK1* cannot form an appressorium, the infection

structure required for plant penetration (Xu and Hamer, 1996). Cellular functions of Pmk1 during invasive growth therefore remained unclear. Chemical genetic approaches have previously been shown to be feasible for *M. oryzae* for specific inhibition of protein kinase C, Pkc1 (Penn *et al.*, 2015). Here, I generated the analogue-sensitive (AS) mutant of *PMK1*, called *pmk1*^{AS}, and showed that the AS kinase is specifically susceptible to a cell-permeable molecule 1NA-PP1. Inhibition of Pmk1 activity by 1NA-PP1 in germinating conidia abolished appressorium formation in a dose-dependent manner, and phenocopied the non-pathogenic Δ*pmk1* mutant. High concentrations of 1NA-PP1 meanwhile had no discernible effects on the wild-type strain, confirming that 1NA-PP1 is specific to the *pmk1*^{AS} protein. A previous study showed that a kinase-inactive mutant of *PMK1* were also unable to produce appressoria and failed to cause blast disease (Bruno *et al*., 2004). Here, I have showed that inhibition of Pmk1 activity after appressorium formation does not prevent melanisation of the appressorium or nuclear degeneration of the conidia. This observation suggests that there is period of Pmk1 activation after spore attachment after which the cell is committed to cellular reprograming that leads to complete appressorium differentiation, and this occurs independent of Pmk1.

Application of 1NA-PP1 to mature appressoria subsequently inhibited plant penetration, and also affected organisation of the septin cytoskeleton around the appressorium pore, suggesting a direct role of Pmk1 kinase activity in appressorium-mediated plant penetration. These defects were comparable to the phenotype of the null mutant of *MST12,* a gene encoding a transcription factor operating downstream of the Pmk1 MAPK pathway (Park *et al*, 2002). The defect

in plant penetration caused by chemical inhibition of Pmk1 implies that phosphorylation of the Mst12 transcription factor by Pmk1 MAPK may be required for repolarisation of the cytoskeleton and cell growth toward the base of the appressorium for initiation of plant penetration. A previous study using bimolecular fluorescence complementation (BiFC) assays demonstrated the interaction of an upstream Mst7 MAPKK and Pmk1 MAPK occurred only at late stages of appressorium development, but not in swollen germ tubes (Zhao & Xu, 2007). These observations indicate that the Pmk1 MAPK might not be activated during the early stage of appressorium formation known as hooking. This is consistent with the idea that Pmk1 is dispensable for surface recognition. The interaction between Mst7 and Pmk1 was detected after 8 h when germ tubes had formed appressoria. Interestingly, the interaction signal continued to increase until 24 hpi, coinciding with septin ring assembly around the appressorium pore that marks re-polarisation of the appressorium (Dagdas *et al.,* 2012). These observations support the importance of activation and function of the Pmk1 MAPK during plant penetration, as demonstrated here using a chemical genetic method. However, monitoring phosphorylation levels on the activation loop of the Pmk1 MAPK using a phospho-p44/42 MAPK antibody and on downstream targets of Pmk1 is still needed to provide direct evidence regarding the timing of Pmk1 activation during formation and differentiation of appressoria. The Pmk1 MAPK operates upstream of large transcriptional networks. RNA-seq has recently identified over 5,000 Pmk1-regulated genes during appressorium development, including up to 172 transcription factors including Mst12, Hox7, Swi6, and Stu1 (Miriam Oses-Ruiz, unpublished data). Phosphoproteomic analysis will be needed to identify novel

downstream components of the Pmk1 pathway. In conclusion, I have shown that Pmk1 kinase activity is essential for both formation and function of the appressorium and for pathogenicity.

The results in this Chapter highlight three advantages of the chemical genetic approach for protein kinase characterisation. Firstly, high *in vivo* selectivity of the ATP analogues to the modified kinase can be achieved, because the bulky size of ATP analogues used as inhibitors is sterically occluded from the catalytic site of wild type kinases. In theory, this structural feature might reduce the likelihood of off-target inhibition found in other kinase inhibitors. I have demonstrated here that even high concentrations of the ATP analogue did not cause noticeable effects on plant infection in wild-type *M. oryzae,* confirming the specificity of chemical inhibition by the analogue 1NA-PP1. Second, cell permeability of ATP analogues allows rapid inhibition of modified kinases to facilitate investigation of dynamic biological processes, such as appressorium development. Addition of the inhibitor 1NA-PP1 to germinating conidia of the *pmk1*^{AS} strain rapidly blocked appressorium formation, which occurs shortly after inoculation. Third, flexible timing of inhibition is useful for functional characterization of proteins in organisms with a complex life cycle such as plant pathogenic fungi. In *N. crassa,* an AS mutant of mak-2 MAPK was used to reveal the roles of the kinase in multiple steps of cell fusion (Fleissner *et al.,* 2009). Taken together, I have showed that a chemical genetic approach is feasible for characterisation of the kinase activity of the Pmk1 MAPK, confirming the importance of Pmk1 function in formation and function of the appressorium of *M.*

oryzae. Effects of Pmk1 inhibition at post-penetration stages will be discussed in Chapter 5.

Chapter 5 The Pmk1 MAP Kinase Regulates Invasive Cell-To-Cell Movement During Tissue Colonisation by the Rice Blast Fungus

5.1 Introduction

Filamentous pathogens employ a variety of distinct strategies to colonise host tissues and obtain nutrients for their growth and reproduction (Haueisen & Stukenbrock, 2016). The human pathogenic fungus *Candida albicans,* for example, can grow in yeast, hyphal and pseudohyphal forms, depending on external stimuli, such as temperature, pH, nutrient availability, and host-derived molecules, such as blood serum (Sudbery, 2011). The morphological plasticity of *C. albicans* is a key virulence determinant (Sudbery, 2011). In particular, the hyphal form of *C. albicans* plays a key role in penetration of host tissues, while the yeast phase is important in blood-borne infection and spread (Mayer *et al.*, 2013). In the plant pathogenic fungus *U. maydis*, the morphological transition from yeast to filamentous growth is explicitly linked to pathogenicity (Brefort *et al*., 2009). Budding haploid cells are saprophytic and non-pathogenic, whereas upon mating of compatible strains, the fungus switches to dikaryotic filamentous growth and initiates obligate parasitism (Brefort *et al*., 2009). The filamentous hyphae proliferate in the host plant, induce tumour formation and undergo additional cellular differentiation which results in production of melanised diploid teliospores (Brefort *et al*., 2009). Signalling through cAMP-PKA and MAPK cascades are implicated in transmitting different extracellular stimuli to promote morphological transition into hyphae by various fungal pathogens. These pathways culminate in a number of transcription factors inducing hyphal-specific gene expression (Turra *et al*., 2014).

The hemibiotrophic ascomycete fungus *Magnaporthe oryzae* grows within living rice cells and secretes a repertoire of effector molecules to subvert host immunity and thereby facilitate infection (Yi & Valent, 2013, Oliveira-Garcia & Valent, 2015, Khang *et al*., 2010, Kankanala *et al*., 2007, Giraldo & Valent, 2013, Giraldo *et al*., 2013). Invasive hyphae of *M. oyzae* are surrounded by plant-derived membrane (Kankanala *et al*., 2007, Mentlak *et al*., 2012, Mochizuki *et al*., 2015). *M. oryzae* effector proteins are delivered to the host–pathogen interface and inside host cells via Golgi-dependent and independent pathways, respectively (Giraldo *et al*., 2013). Slp1, for instance, is a LysM domain-containing effector that accumulates in apoplastic compartment and sequesters chitin oligosaccharides released from fungal cell wall to prevent recognition by host cell (Mentlak *et al.,* 2012). Cytoplasmic effectors which are translocated into host cells, preferentially accumulate in the biotrophic interfacial complex (BIC). The BIC is a plant-derived structure enriched for plasma membrane, ER and cytosol which initially forms adjacent to primary hyphal tips but is then left behind adjacent to the first-differentiated invasive hyphal cells. This structure is proposed to be a destination for effectors that are translocated across plant membrane into the cytosol (Kankanala *et al.,* 2007; Khang *et al.,* 2010; Giraldo *et al.,* 2013; Mochizuki *et al.*, 2015). *M. oryzae* delivers AvrPiz-t effector, via BIC-dependent mechanism, into host cells to target the rice RING E3 ubiquitin ligase, APIP6, to suppress PAMP-induced immunity (Li *et al.,* 2009). The blast fungus also produces hydroxylated jasmonic acid (12OH-JA) to interfere with host JA signalling and facilitate tissue colonisation (Patkar *et al.,* 2015).

The rice blast fungus appears to exploit plasmodesmata for movement into neighbouring host cells, and to deliver secreted effectors into adjacent plant cells ahead of the infection front (Kankanala *et al.,* 2007; Khang *et al.,* 2010). For subsequent entry into new rice cells, a thin filamentous invasive hypha, traverses the internal rice cell wall before switching to pseudohyphal growth (Kankanala *et al.,* 2007; Khang *et al*., 2010). Although cell-to-cell spread of plant pathogens has instead been extensively studied in viruses, the mechanisms by which fungal pathogens spread through plasmodesmata remained poorly understood (Lucas, 2006). Upon viral infection, resistant plants close PD channels and block intercellular spread of viral particles. Adapted viruses actively suppress accumulation of callose at plasmodesmata by taking advantage of host callose-hydrolysing enzymes (Lucas, 2006). *F. graminearum* secretes lipase FGL1 to inhibit callose formation and thereby facilitate spread between wheat spikelets (Blümke *et al.*, 2014, Nguyen *et al.*, 2010, Salomon *et al.*, 2012, Voigt *et al.*, 2005). Plasmodesmata are intercellular channels which establish a symplastic communication network between neighbouring plant cells (Burch-Smith & Zambryski, 2012). Plasmodesmata are lined by the plasma membrane and ER, called desmotubules, forming concentric tubules along the channels (Tilsner *et al.*, 2016). The ER strand is connected to the plasma membrane lining inside the plasmodesmata by spoke-like elements. The gap between the plasma membrane and desmotubule is called cytoplasmic sleeve, defining the space available for cell-to-cell trafficking (Tilsner *et al.*, 2016). Deposition of callose at neck region of plasmodesmatal channels is a primary mechanism to control permeability of plasmodesmata (Oparka *et al.*, 1997, Burch-Smith & Zambryski, 2012, Knox &

Benitez-Alfonso, 2014, De Storme & Geelen, 2014). Homeostasis of callose at plasmodesmata is maintained by antagonistic action of β-1,3-glucanases and callose synthases (De Storme & Geelen, 2014). Increasing evidence indicates that plasmodesmatal regulation is an essential part of innate immunity of plants (Lee, 2015). It has been, for instance, shown that different callose synthases operate downstream of plant defence pathways, including ROS signalling, in order to reduce plasmodesmatal conductivity (Cui & Lee, 2016). A number of membrane-bound signalling proteins have for example been identified from plasmodesmatal proteome (Fernandez-Calvino *et al.*, 2011). Two immune receptors of *A. thaliana*, a flagellin-sensing receptor FLS2 and a chitin-sensing LYM2 are localised to plasmodesmata, and are required to restrict plasmodesmatal permeability by increasing callose deposition upon pathogen recognition (Faulkner *et al*., 2013). A member of plasmodesmata-located protein (PDLP) family, PDLP5, has been shown to be a link between SA signalling and plasmodesmatal control in response to invading pathogens (Lee *et al.*, 2011, Wang *et al.*, 2013a, Carella *et al.*, 2015).

In this Chapter, I applied chemical genetics, live-cell imaging, ultrastructure analysis and transcriptome study to investigate the role of the Pmk1 MAPK in post-penetration spread of *M. oryzae* in plant tissue. I report that the Pmk1 MAPK signalling is essential for cell-to-cell movement and host defence suppression during tissue colonisation by the rice blast fungus. These results highlight the diverse roles of fungal MAPK signalling in cell fate determination and adaptation to different host micro-environments.

5.2 Results

5.2.1 Pmk1 activity is required for cell-to-cell movement of blast invasive hyphae

To elucidate the biological functions of Pmk1 MAPK during invasive growth, Pmk1 activity was chemically inhibited by adding 1NA-PP1 to rice leaf sheaths that were infected with the *pmk1*^{AS} mutant at 26 h. At this time point, the fungus had entered rice cells by appressorial penetration, and invasive hyphae had not yet spread into adjacent rice cells. Addition of 1NA-PP1 resulted in entrapment of invasive hyphae in the first-invaded cells observed at 48 hpi. Interestingly, the *pmk1*^{AS} mutant continued growing until plant cells were completely filled. In contrast, untreated *pmk1*^{AS} mutant or Guy11 wild type were able to spread into neighbouring cells (Fig. 5.1 A, B). In the presence of 1NA-PP1, the *pmk1*^{AS} mutant still produced normal-appearing, bulbous invasive hyphae with BICs (Fig. 5.1 C). Primary BICs can be recognised, by their obvious size and predictable position beside the first-differentiated bulbous invasive hyphal cell (Khang *et al.,* 2010). Addition of 1NA-PP1 at earlier time points did not affect differentiation of bulbous invasive hyphal cells but blocked appressorial penetration as previously described in Chapter 3, suggesting that differentiation of bulbous invasive hyphae does not require Pmk1 activity. Interestingly, the invasive hyphae of *pmk1*^{AS} blocked in the first-invaded rice cells were able to differentiate into appressorium-like structures that pressed against rice cell wall, as early morphogenetic signature of attempted cell wall crossing (Kankanala *et al.,* 2007). These invasive hyphae repeatedly attempted to penetrate as they grew along the cell wall (Fig. 5.1 D). I conclude that the Pmk1 MAPK activity is required for cell-to-cell movement of invasive hyphae

within host tissue, but not for pseudohyphal growth of fungal hyphae or recognition of potential crossing sites at the plant cell wall.

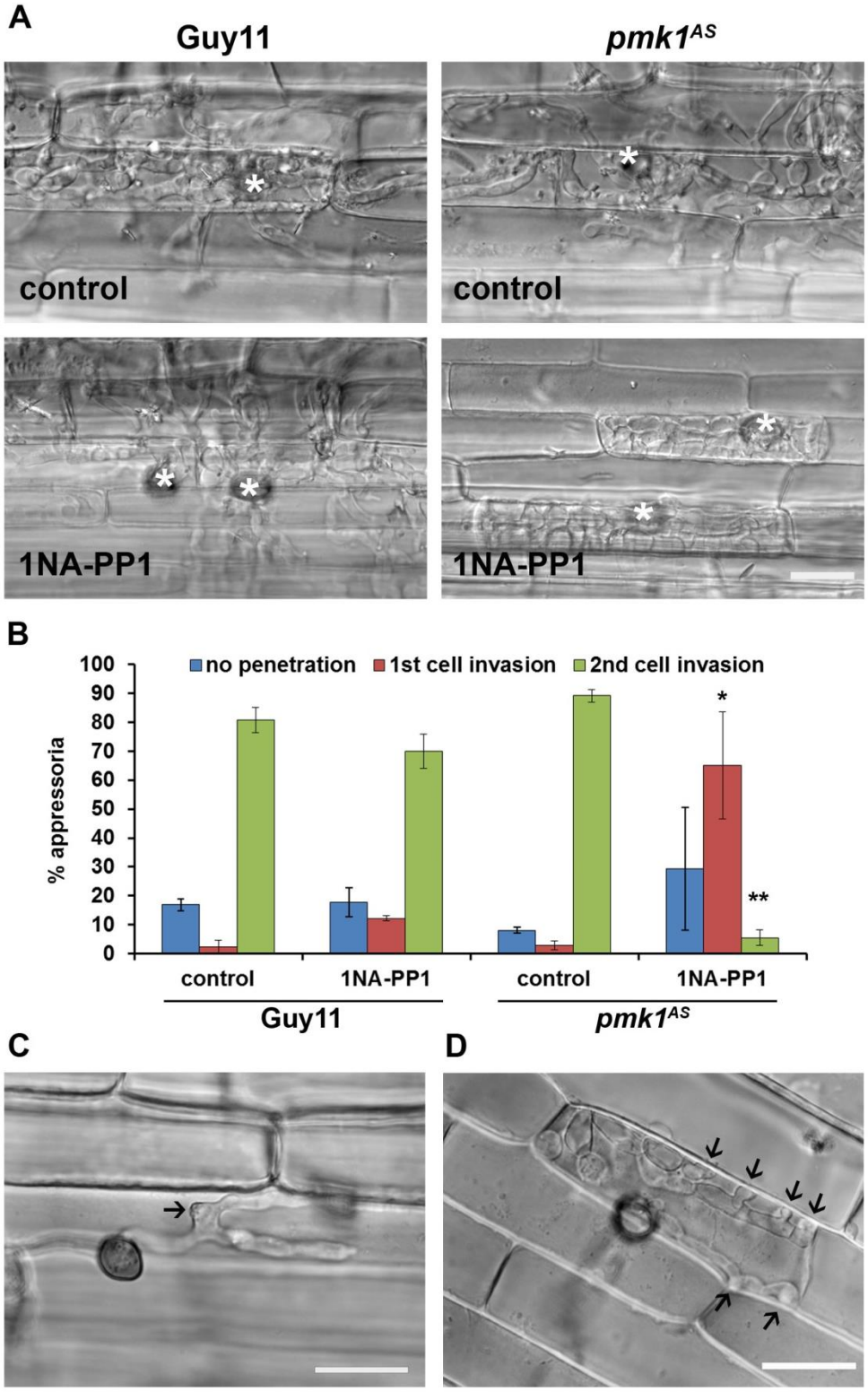

Figure 5.1 Pmk1 inhibition prevents second cell invasion by *M. oryzae*. Micrographs **(A)** and bar chart **(B)** to show the effect of Pmk1 inactivation in post-penetration proliferation of the fungus. Rice leaf sheaths were inoculated with conidia of Guy11 or *pmk1*^{AS} strains. 1NA-PP1 (5 µM) was added to infected tissue at 26 hpi, and infection progress was assessed at 48 hpi. Asterisks indicate sites of appressorial penetration. Second cell invasion by invasive hyphae of the *pmk1*^{AS} mutant was significantly decreased due to 1NA-PP1 treatment. *P < 0.05, **P < 0.01 using the *t*-test; error bars, standard errors. **(C)** Formation of the BIC and bulbous invasive hyphae of the *pmk1*^{AS} mutant treated with 1NA-PP1 and observed at 30 hpi. Arrow indicates a primary BIC. **(D)** Penetration attempts by the 1NA-PP1 treated *pmk1*^{AS} mutant were observed at 40 hpi. Arrows indicate swollen invasive hyphal cells pressed against the cell wall. All scale bars represent 20 µm.

5.2.2 Pmk1 regulates the ability of *M. oryzae* to inhibit the oxidative burst

Upon recognition of pathogens by PRR complexes, a branched signalling cascade is initiated to launch local and systemic defence responses in plants (Couto and Zipfel, 2016). Production of reactive oxygen species (ROS) is among the earlier outputs after pathogen recognition (Baxter *et al.*, 2013, Torres *et al.*, 2006). ROS are key molecules of plant immunity that act as direct toxic agents to pathogens and serve as signalling messengers that trigger other downstream responses (Dietz *et al.*, 2016). ROS also directly promote strengthening of plant cell walls via cross-linking of cell wall structural proteins (Bradley *et al.*, 1992). Because biotrophic and hemibiotrophic pathogens must actively suppress host defence responses during host tissue colonisation, I set out to investigate whether Pmk1 MAPK function is involved in suppression of host defence responses. I first examined the effect of Pmk1 inhibition on host ROS production. *In situ* accumulation of hydrogen peroxide (H_2O_2) in infected rice tissue can be detected

by 3,3′-diaminobenzidine (DAB) staining (Chi *et al*., 2009). Oxidization of DAB results in a brown precipitate. DAB precipitation was rarely detected in infection sites of wild-type Guy11 or those of the untreated *pmk1*^{AS} mutant (Fig. 5.2). In contrast, after adding 1NA-PP1, intense DAB precipitation was detected around invasive hyphae of the *pmk1*^{AS} mutant and periphery of infected plant cells (Fig. 5.2). It is important to note that H_2O_2 was not detected in adjacent host cells, suggesting that these infected rice cells might be symplastically isolated as a typical defence response (De Storme & Geelen, 2014). The induction of ROS was not simply a result of penetration attempts, because ROS production was also detected as early as 30 hpi, a time point when invasive hyphae had not attempted to cross the cell wall (Fig 5.2 B). These results suggest that Pmk1 activation enables *M. oryzae* to suppress host oxidative burst during biotrophic growth.

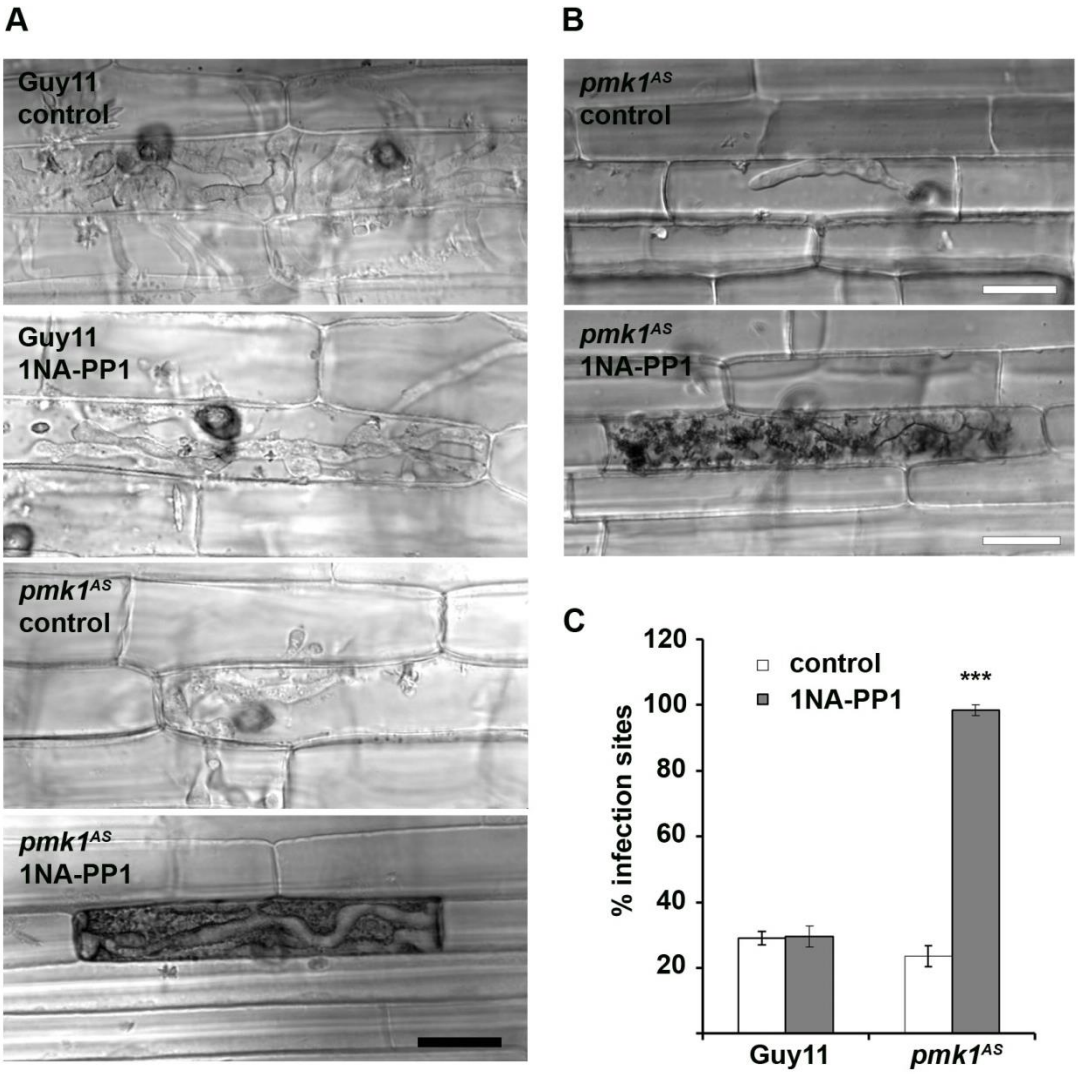

Figure 5.2 Pmk1 inhibition causes strong induction of ROS in rice cells. Representative images of *in situ* detection of H_2O_2 at Guy11 or *pmk1*^{AS} infection sites in the presence or absence of 1NA-PP1, recorded at 48 hpi **(A)** and at 30 hpi **(B)** Scale bars represent 20 µm. **(C)** Bar chart to show relative abundance of infection sites showing DAB precipitation assessed at 48 hpi. ****P* < 0.001 using the *t*-test; error bars, standard errors.

5.2.3 Pmk1 function is required for suppression of callose deposition at plant cell wall junctions

To understand the nature of the host cell response during biotrophic invasion by *M. oryzae*, I studied the temporal dynamics of callose deposition of blast invasion using aniline blue staining (Bougourd *et al.*, 2000). Callose deposition was almost absent in uninfected rice epidermal cells (Fig. 5.3). When invasive hyphae entered plant cells (27 hpi), a low level of PD callose deposition was initially detected. PD callose deposition increased as the fungus grew in the first rice cells at later stages (30 and 34 hpi). Prominent aniline blue-stained bodies, known as papillae, were found underneath most appressorial penetration sites. Interestingly, strong PD callose deposition was detected as a callose collar at the base of narrow invasive hypha that had traversed plant cell wall (Fig. 5.3 B). This structure resembles the callose collar seen at the neck of oomycete haustoria (Mims *et al.*, 2004). These observations suggest that *M. oryzae* can overcome callose-associated host responses during cell-to-cell movement. In rice cells invaded by the *pmk1*^{AS} mutant in the presence of 1NA-PP1, callose deposition was strongly induced, as shown by an increased number of callose puncta at the plant cell wall junction, presumably plasmodesmatal callose deposition, and by occurrence of large callose bodies located in uninvaded rice cells adjacent to infected cells (Fig 5.4). These results indicate that inactivation of Pmk1 MAPK triggers hyper-accumulation of callose deposition beyond PD, and Pmk1 function is also required for suppression of cell wall-based host defence (Malinovsky *et al.*, 2014).

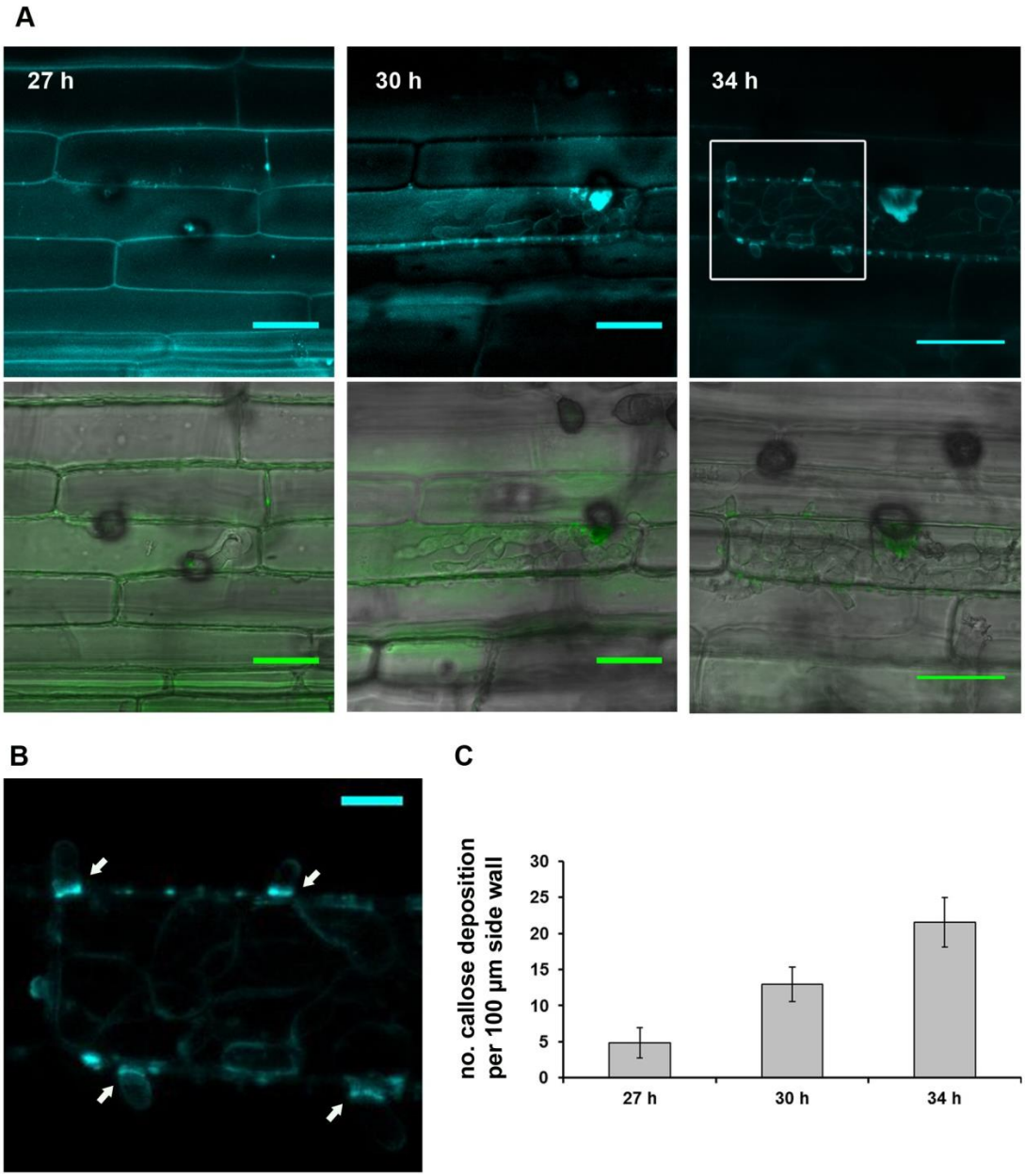

Figure 5.3 Callose deposition at host cell wall junctions visualised by aniline blue staining. (A) Confocal micrographs to show dynamics of callose deposition in infected rice cells at 27, 30 and 34 hpi. Rice leaf sheaths were infected with fully pathogenic wild type strain, Guy11. Top panels, aniline blue staining; bottom panels, Merged images of DIC and callose staining (Yellow). Scale bars represent 20 µm, **(B)** High magnification of an area marked in rectangular. Arrows indicate callose collars at crossing points. Scale bar represents 5 µm. **(C)** Quantification of callose deposition per 100 µm length of side wall of infected cells assessed each time point. Error bars indicate SE of the mean.

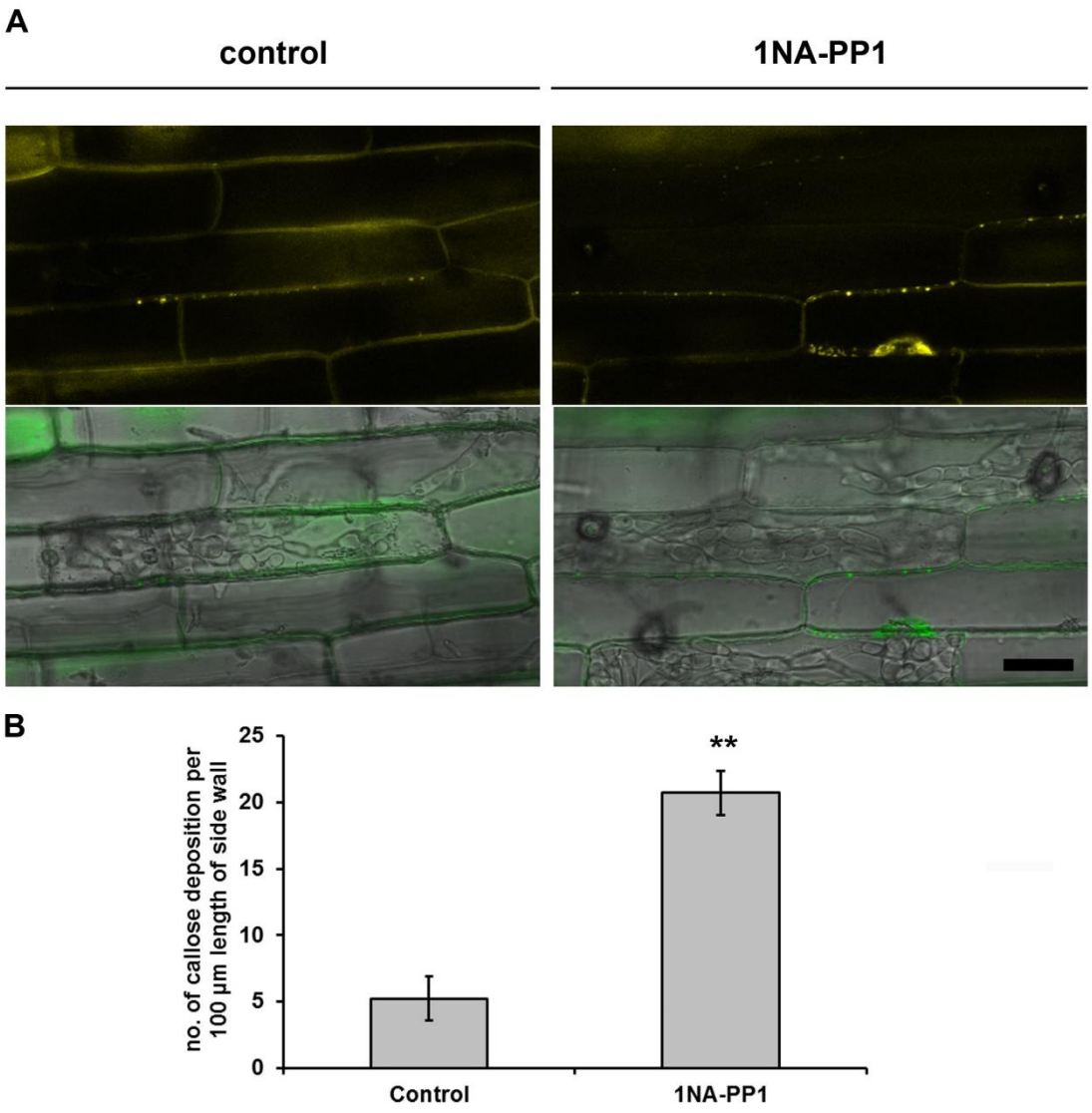

Figure 5.4 Increased callose deposition caused by Pmk1 inactivation.

(A) Confocal micrographs to show callose deposition shown by aniline blue staining, in *pmk1*^{AS}-infected rice cells treated or untreated with 5 µM 1NA-PP1 at 26 hpi and observed at 42 hpi. Upper panels, aniline blue staining; lower panels, merged DIC and aniline blue signal. Bar represents 20 µm. **(B)** Bar chart to show quantification of the number of callose puncta per 100 µm length of side wall of infected rice cells. Ten infected rice cells were assessed each treatment with three biological replicates. $^{**}P < 0.001$ using the *t*-test; error bars, SE of the mean.

5.2.4 Pmk1 MAPK-mediated transcriptome during tissue colonisation by *M. oryzae*

To understand a comprehensive picture of Pmk1-regulated tissue colonisation by *M. oryzae* at the global cell level, dual transcriptome analysis using RNA sequencing (RNA-seq) was performed in which gene expression changes in both the pathogen and rice host were analysed simultaneously. RNA-seq is fundamentally a massive parallel sequencing of RNA, in the form of corresponding cDNA, based on next-generation sequencing platform (Wang *et al.*, 2009). Rice tissues were infected with the *pmk1*^{AS} strain in the presence or absence of 1NA-PP1 inhibitor. Infected tissues were prepared, as previously described by Mosquera *et al* (2009). Detached rice leaf sheaths were inoculated with conidia of the *pmk1*^{AS} strain and treated with 1NA-PP1 after infection at 26 hpi. Control samples were untreated infected leaf sheaths. RNA was extracted from sheath tissues at 32 hpi representing early tissue colonisation stage (Fig. 5.5). With three biological replicates undertaken, pieces of infected leaf sheath were manually trimmed and immediately scanned for infection site density. Heavily infected tissues were frozen in liquid nitrogen, stored at -80°C, and total RNA was extracted. One microgram of total RNA was used for each RNA-seq library preparation. One hundred base paired-end reads were sequenced from mRNA libraries on the Illumina HiSeq 2500 (Exeter sequencing service, Bioscience, University of Exeter). Subsequently, sequencing reads were filtered using the fastq-mcf program from the ea-utils package (http://code.google.com/p/ea-utils/).

The Illumina sequencing generated about 25 to 50 million reads per samples (Table 5.1). Base calling accuracy (Q score) of all samples was between

94.1 and 94.7, indicating high sequencing accuracy. Approximately 1.7 to 3.2% of reads were mapped to the fungal genome reflecting the relatively low amount of fungal biomass in infected tissue samples (Table 5.1). To assess the overall similarity of rice and fungal transcriptomes between treated and untreated infections, Euclidean distance-based transcript abundance values for all genes were calculated between each sample, and illustrated by generation of a heatmap. Surprisingly, expression patterns of rice transcripts of control and 1NA-PP1 treated groups were not distinctly separated (Fig 5.6). In contrast, fungal gene expression pattern was very similar among biological replicates of each treatment, but very distinct between treated and untreated infections (Fig 5.7). These results indicate dramatic changes of fungal gene expression caused by Pmk1 inactivation.

Using an adjusted P-value of ≤ 0.05 for differential expression, no rice genes showed significantly altered expression. In contrast, up to 1,457 fungal genes showed differential expression levels during Pmk1 inhibition, accounting for 11.5 % of total protein encoding genes in the *M. oryzae* genome. Of these, 715 fungal genes were up-regulated in 1NA-PP1-treated samples, indicating that they are negatively regulated by the Pmk1 pathway. 742 fungal genes showed significantly down-regulated, suggesting that they are positively regulated. Gene ontology (GO) assignments were made using Blast2GO (Conesa & Götz, 2008). Here, I focus on five gene categories encoding proteins relevant to pathogenicity: secondary metabolism enzymes, candidate secreted effector proteins, transporters and carbohydrate-active enzymes. A total of 46 of *M. oryzae* genes encoding putative secondary metabolism enzymes were identified (Soanes *et al*., 2012), but no genes from this class showed differential expression in response to Pmk1

inhibition in the present data set. A search for sugar transporters based on the presence of Pfam motif PF0083 identified 69 *M. oryzae* genes (Soanes *et al.*, 2012), of which were 14 sugar transporter encoding genes that were induced, while the other 30 were repressed by Pmk1 inactivation (Fig 5.8).

In the current RNA-seq analysis, 212 fungal genes with a putative signal peptide were down-regulated after Pmk1 inhibition. In addition, 84 of 95 fungal genes most strongly down-regulated (zero reads detected) during Pmk1 inactivation represent putative secreted proteins without predicted functions. Previous RNA-seq analysis of *in planta* growth of *M. oryzae* identified 91 putative blast effectors that are co-regulated with *BAS1, BAS2, BAS3, BAS4, SLP1* and *AVR-PITA* genes (Xia Yan and Darren Soanes, unpublished data; Mosquera *et al*., 2009). A total of 59 of 91 BAS co-regulated genes were repressed during Pmk1 inhibition. Importantly, several known effector encoding genes were down-regulated in Pmk1-inactivated infections (Fig 5.9) These include *BAS2* (MGG_09693), *BAS3* (MGG_11610), *BAS4* (MGG_10914), *AVR-Pita* (MGG_15370), *AVR-Pik* (MGG_15972), *SLP1* (MGG_10097) and *MoHEG13/BAS52* (MGG_09378). Bas2 and Bas3 are putative *M. oryzae* effectors that localise to BICs and to cell wall crossing sites (Mosquera *et al*, 2009). The Slp1 effector is a secreted chitin-binding protein required for fungal evasion of chitin-triggered immunity (Mentlak *et al*, 2012). Mep1 (MGG_16353) is a novel apoplastic effector that appears to be associated with chloroplasts, and is necessary for full virulence (Xia Yan, unpublished data). However, virulence functions of other effectors remained poorly understood (Mosquera *et al*., 2009). A screen for suppressors of plant cell death (SPD) from *M. oryzae* identified 11

putative effectors (Sharpee *et al*., 2016). These include SPD3 (previously identified as MoHEG13/Bas52), SPD6 (previously identified as Bas3), and SPD5, a paralogue of Bas4. These *M. oryzae* effectors were able to reduce host cell death reaction triggered by necrosis and ethylene-inducing-protein-1 (Nep1) and mammalian BAX in tobacco leaves (Mogga *et al.,* 2016; Sharpee *et al.,* 2016). Therefore, the repressed expression of several putative fungal effectors in this study, including some with known virulence functions and some with host immune suppressing activities, may explain the wider consequences of Pmk1 inactivation in allowing elicitation of host defence responses.

Inactivation of Pmk1 activity also caused misregulation of cell wall-degrading enzyme-encoding genes. Fourteen hydrolase genes and nine secreted protease genes were repressed following Pmk1 inhibition (Fig 5.8). These include a serine protease encoding gene *SPM1* which was initially identified as a nitrogen-starvation responding gene, and is required for virulence (Donofrio *et al*., 2006). Several virulence-associated genes were found to be regulated by the Pmk1 pathway. These include those down-regulated (mod_lfc < -1) by Pmk1 inactivation: Mas3 (MGG_00703), an NADPH oxidase 1 gene (*NOX1*; MGG_00750), chitin binding protein gene (MGG_00245), sterigmatocystin biosynthesis peroxidase (MGG_07574), cutinases (MGG_03792; MGG_15185), secreted cellulase (MGG_07556). Interestingly, *CHM1* (MGG_06320), a *M. oryzae* homologue of Cla4 PAK essential for pathogenicity, were also repressed following Pmk1 inhibition. This pattern is similar to the expression of *CHM1* gene during appressorium development in which *CHM1* is down-regulated 3-fold in the *Δpmk1* mutant compared to the wild type at 14 hpi (Miriam Oses-Ruiz, PhD thesis,

Biosciences, University of Exeter). These results suggest a potential link between the Pmk1 pathway MAPK and fungal morphogenesis (Li *et al*., 2004). Taken together, the present RNA-sea data suggest that the Pmk1 pathway reprograms global gene expression of *M. oryzae* IH, by inducing expression of several putative secreted effectors and many virulence-associated genes, and by modulating production of cell wall degrading-enzymes during biotrophic growth of the rice blast fungus.

Despite the strong induction of host defence responses, including ROS generation and callose deposition, no rice genes showed differential expression after Pmk1 inactivation. These results contrast to the expression of fungal genes which was dramatically different between control and inhibitor-treated infections, because Pmk1 inactivation affected a larger set of fungal genes. However, removing outliners and repeating bioinformatic analysis identified only 15 down-regulated and 5 up-regulated rice genes upon 1NA-PP1 treatment. A homologue of the Arabidopsis MAPK, MKK7, implicated in activation of plant basal and systemic resistance, was up-regulated after 1NA-PP1 treatment. This is probably due to the low abundance of infected rice cells where Pmk1-dependent rice gene expression became diluted in the pool of total transcripts. A high degree of heterogeneity of the plant transcriptome across whole tissues, consisting of infected cells, cells adjacent to the infected cells, and heathy rice cells far away from the infection sites, may mask transcriptomic changes of rice genes caused by Pmk1 inactivation.

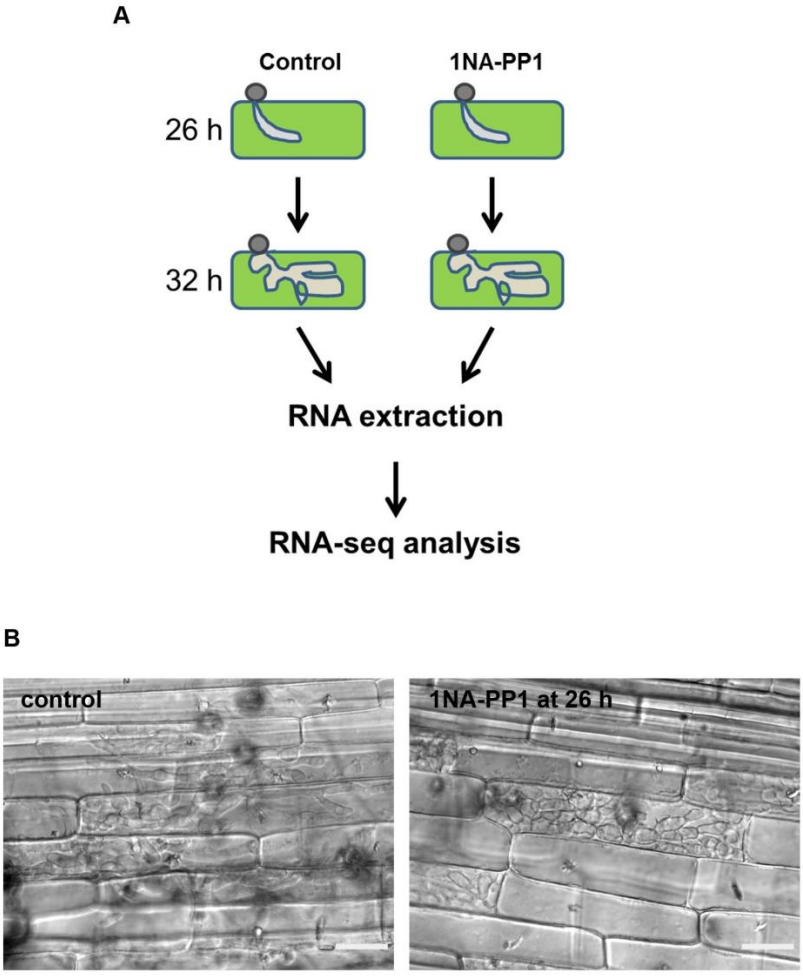

Figure 5.5 Sample preparations for RNA-seq analysis. (A) Flowchart to show experimental strategy. Conidia of the *pmk1*^{AS} strain (5 x 10^5 conidia mL^{-1}) were prepared in 0.25% gelatine solution and injected into the hollow space of rice leaf sheaths. *M. oryzae* conidia were allowed to develop appressoria and infect rice tissue. At 26 hpi, 1NA-PP1 (5 µM) was used to replace the liquid in infected tissues, while DMSO in an equivalent amount in water was used as a control solution. At 32 hpi, rice tissues were harvested, hand-trimmed for enrichment of infected rice cells, and total RNA was extracted. **(B**) Micrographs showing *pmk1*^{AS} mutant growing in rice cells of a susceptible cultivar CO-39 in the presence or absence of 1NA-PP1. Scale bars indicate 20 µm.

Table 5.1 Summary of RNA-seq read numbers and the abundance of fungal biomass in infected tissues (control as minus1-3, and 1NA-PP1 treated infections as plus1-3)

Sample ID	Total reads	Mapped reads of fungal genes	% fungal reads
minus1	49,282,546	979,544	1.99
minus2	53,925,954	1,713,533	3.18
minus3	48,935,968	996,697	2.04
plus1	100,290,176	1,712,053	1.71
plus2	55,106,338	1,142,440	2.07
plus3	55,596,410	1,801,465	3.24

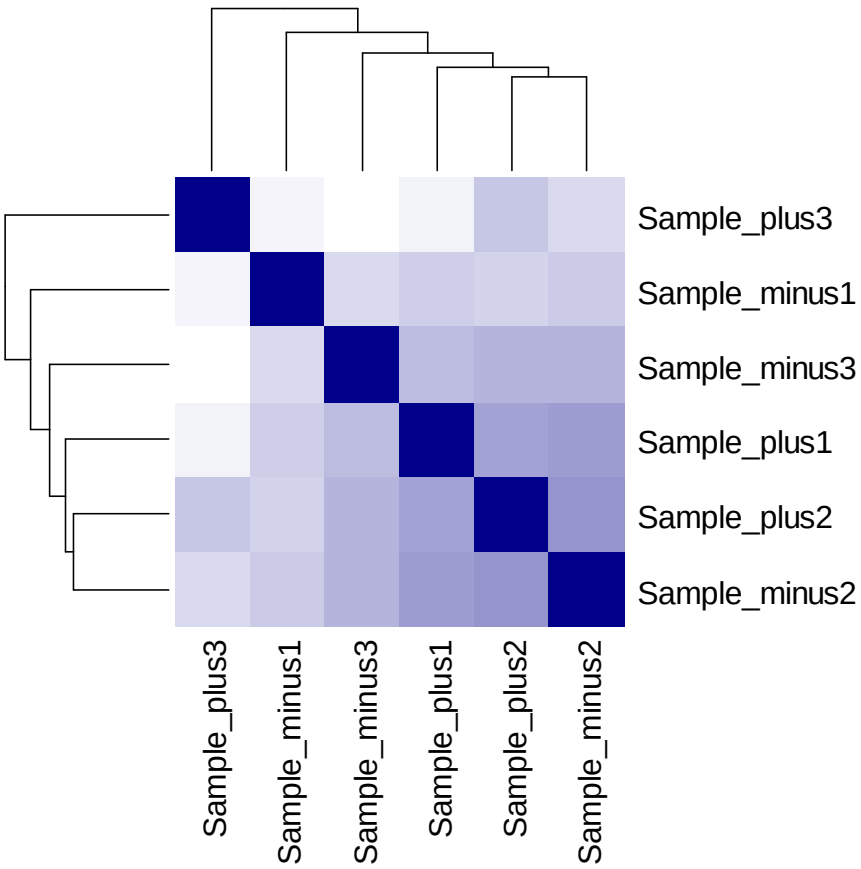

Figure 5.6 Heatmap to show Euclidean distance between rice gene expression patterns of 1NA-PP1-treated and untreated infections. The distance between each sample was calculated from a variance-stabilising transformation of the total count data (Soanes *et al*., 2012). The darker the colour, the closer the two datasets are together. Plus1-3 samples are three biological replicates of 1NA-PP1-treated infection. Minus1- 3 samples are untreated infection.

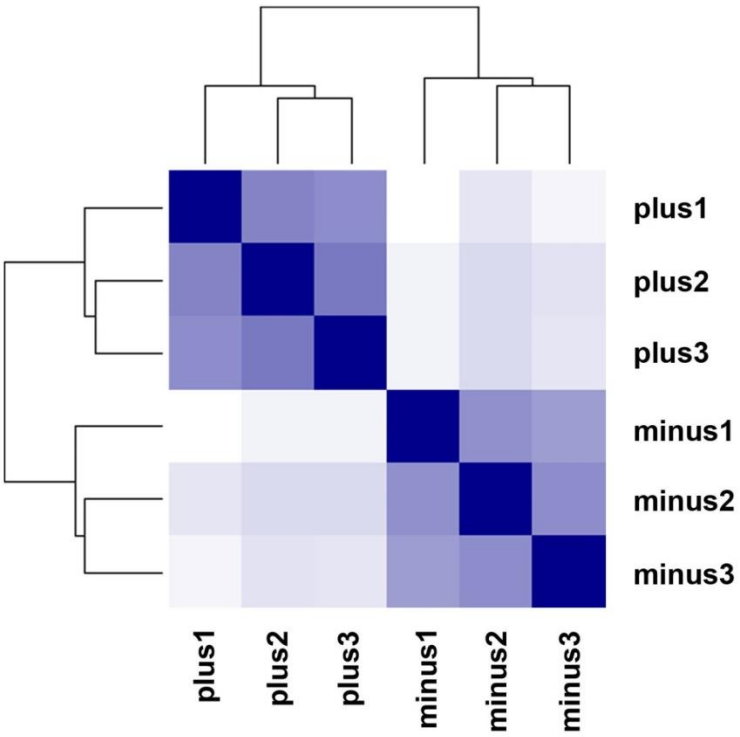

Figure 5.7 Heatmap to show Euclidean distance between fungal gene expression patterns of 1NA-PP1-treated and untreated infections. Same as figure 5.6.

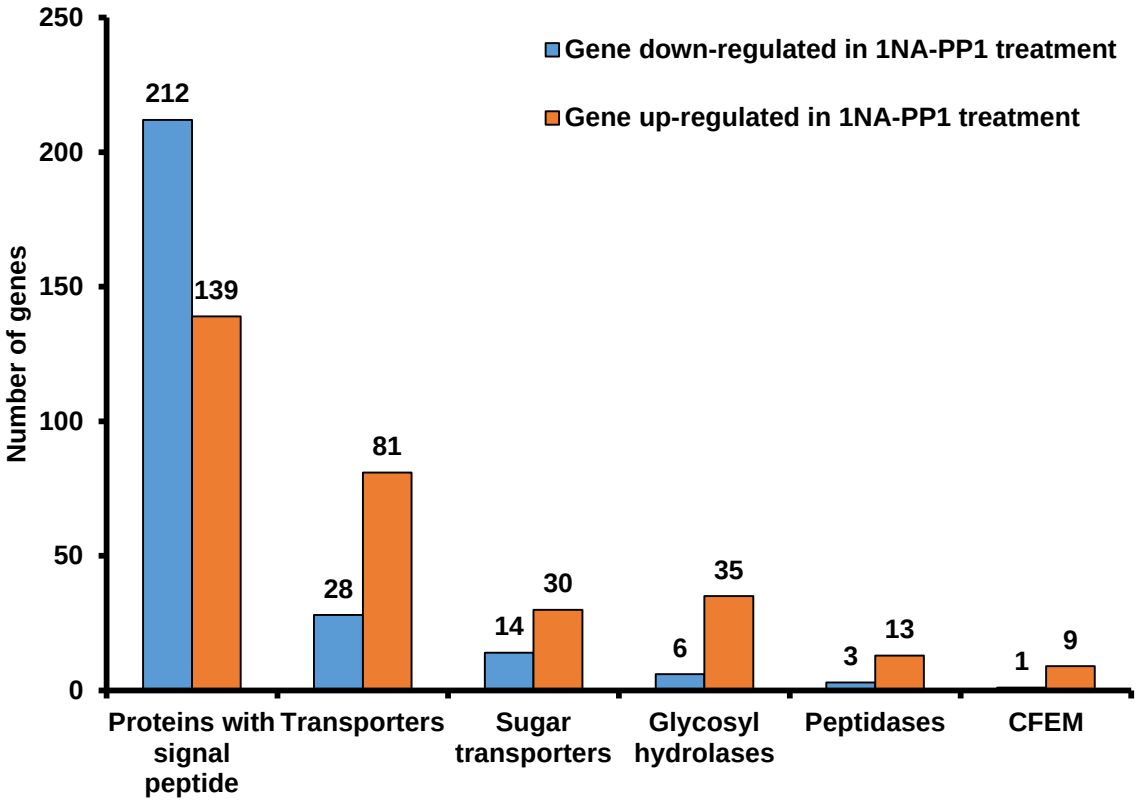

Figure 5.8 Classification of fungal genes that are differentially regulated upon Pmk1 inhibition during biotrophic growth of *M. oryzae* in rice tissue. Gene ontology was assigned using Blast2GO (Conesa & Götz, 2008).

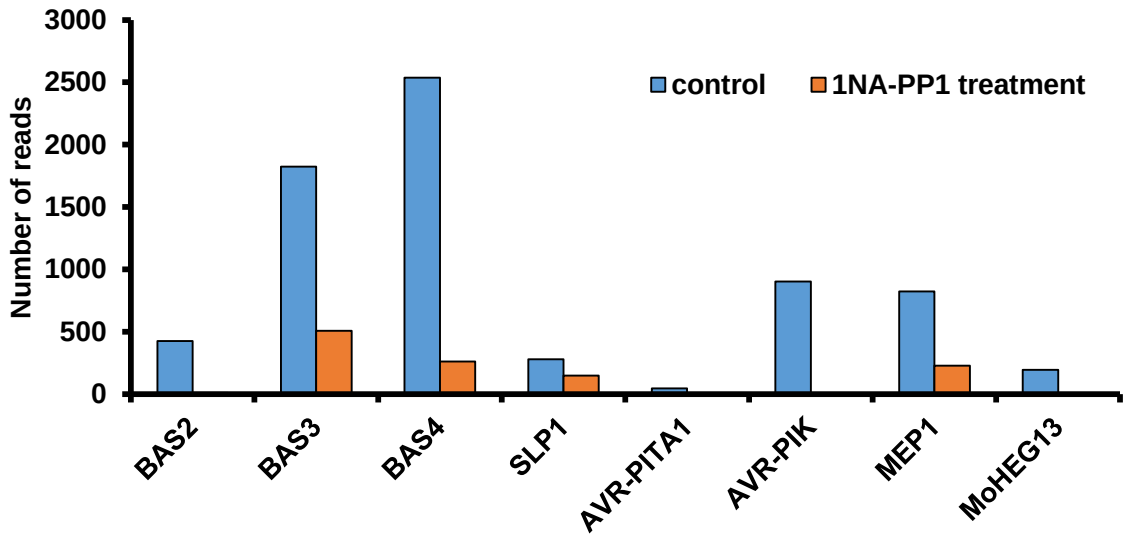

Figure 5.9 The Pmk1 MAPK pathway induces gene expression of several known effector-encoding genes. Bar chart comparing transcript abundance of known effectors that are significantly different ($P < 0.05$) between the control and 1NA-PP1 treated infections. Sequence data can be found in the GenBank/EMBL database under the following accession numbers: *BAS2* (MGG_09693), *BAS3* (MGG_11610), *BAS4* (MGG_10914), *SLP1* (MGG_10097), *AVR-Pita1* (MGG_15370), *AVR-Pik* (MGG_15972), *MEP1* (MGG_16353) and *MoHEG13* (MGG_09378).

5.2.5 Pmk1 MAPK is necessary for the production of effector proteins

RNA-seq analysis revealed several known fungal effectors potentially regulated by the Pmk1 MAPK pathway. These include two *M. oryzae* effectors, Bas2 and Bas3, previously shown to be localised at BICs and at cell wall crossing sites (Mosquera *et al.*, 2009). Although gene replacement analysis of *BAS2* and *BAS3* failed to detect discernible phenotypes in pathogenicity, their localization patterns are suggestive of functions in cell wall crossing (Mosquera *et al.,* 2009). Comparative transcriptome analysis of appressorium development showed that *BAS2* and *BAS3* effector genes were down-regulated after germination and germ tube development of Δ*pmk1* and Δ*mst12* mutants (Fig 5.10). These data confirm that expression of these effector genes is likely to be regulated by the Pmk1 MAPK pathway. Other known effector genes, including *BAS1, BAS4, SLP1,* and *PWL2,* were not significantly induced during *in vitro* appressorium development of Guy11 (Miriam Oses-Ruiz, unpublished data).

To test whether Pmk1 activation is associated with production of secreted effectors, C-terminal fusion constructs of known effectors, including Bas2 and Bas3, were generated and introduced into the *pmk1*^{AS} mutant. The cloning strategy for the *BAS2:GFP* construct is described in Figure 5.11, as an example of all other GFP fusion constructs made. Positive *M. oryzae* transformants of each GFP fusion were screened for fluorescence during biotrophic growth. In the absence of 1NA-PP1, localisation of these effectors in *pmk1*^{AS} was similar to those reported in the wild-type strain (Fig. 5.12 and 5.13; Mosquera *et al.,* 2009; Mentlak *et al.,* 2012). Pwl2 and Bas1 accumulated as puncta beside the first bulbous invasive hyphal cells, representing primary BICs, while Slp1 and Bas4 outlined the IH, representing

apoplastic compartment (Fig. 5.13). When 1NA-PP1 inhibitor was added to infected leaf sheaths after penetration, the fluorescence of Bas2-GFP and Bas3-GFP fusion proteins was lost from the BIC of bulbous invasive hyphae in initially invaded cells (Fig. 5.12). In contrast, fluorescence of other BIC-localised effectors, such as Bas1 and Pwl2, was unaffected after 1NA-PP1 treatment (Fig. 5.13). Although *BAS4* and *SLP1* genes were found to be regulated by the Pmk1 MAPK, based on RNA-seq analysis, I did not notice changes in their protein localisation and fluorescence level upon 1NA-PP1 treatment, using epifluorescence microscopy. I hypothesised that protein turnover rate of apoplastic effectors might be much lower than the cytoplasmic effectors, so that disruption of transcription may result in rapid disappearance of protein accumulation at BICs. I conclude that Pmk1 function is dispensable for establishment of the BICs or for maintaining the integrity of the EIHM, but is necessary for the production and localisation of a specific set of secreted effectors implicated in cell wall crossing.

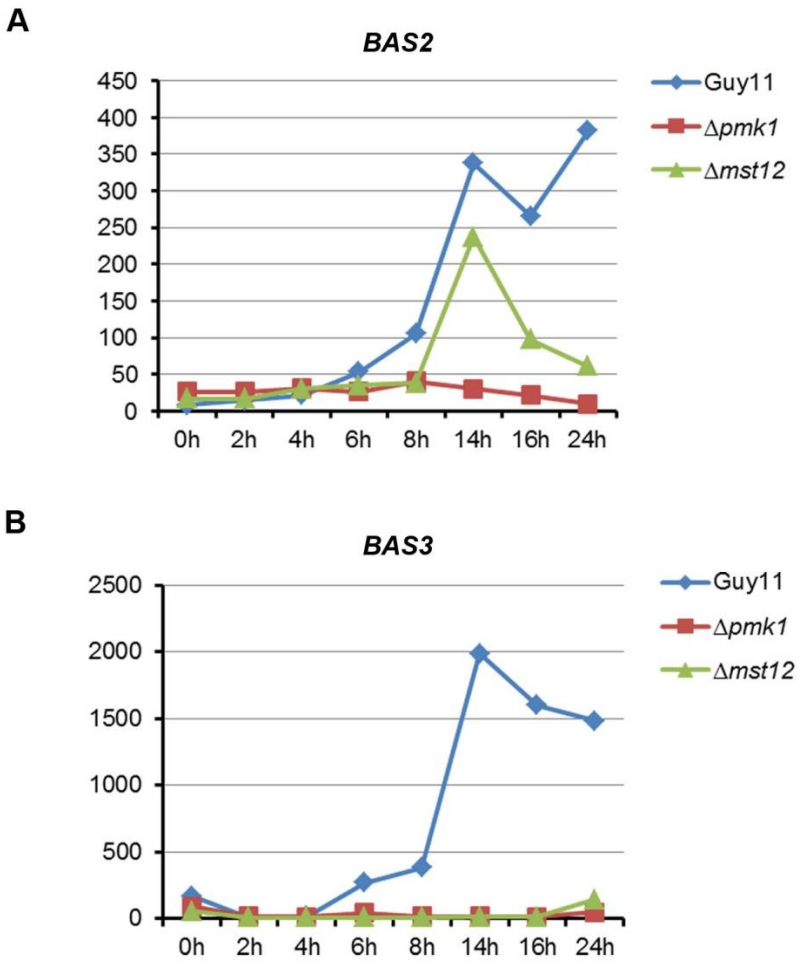

Figure 5.10 Transcription of *BAS2* and *BAS3* effector genes may be regulated by the Pmk1 MAPK cascade. Line graphs showing transcriptional levels of *BAS2* **(A)** and *BAS3* **(B)** during *in vitro* appressorium development by Guy11, Δ*pmk1* and Δ*mst12* mutants (Miriam Oses-Ruiz, unplublished data).

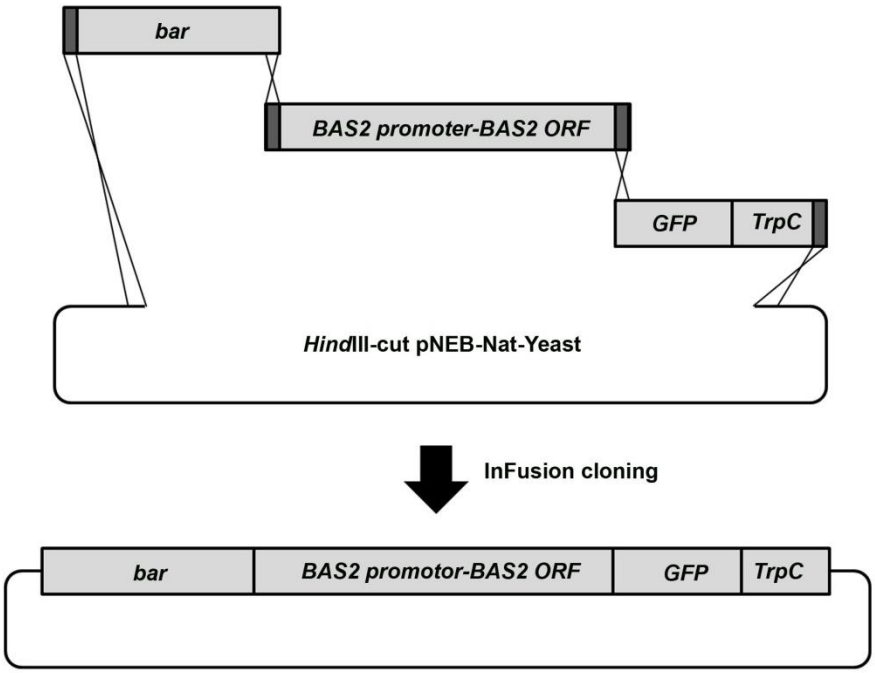

Figure 5.11 Schematic diagram showing cloning strategy used for the generation of the *BAS2:GFP* vector. The same cloning methods were used for the other effector genes or promoter analysis. The bialaphos resistance (*bar*) gene was amplified from pCB1530 plasmid using bar-P1 and bar-P2 primers. The bar-P1 primer contains a 15 bp overhang at 5' end homologous to vector end. A 2.0 kb native promoter and open reading frame (ORF) of *BAS2* was PCR amplified from genomic DNA of Guy11 strain of *M. oryzae* using Bas2-P1 and Bas2-P2 primers. Bas2-P1 primer contains a 15 bp extension at its 5' end homologous to the 3' end of the *bar* fragment, while that of Bas2-P2 primer is complementary to the 5' end of *GFP* fragment. The *GFP* coding fragment fused with *TrpC* terminator, derived from *Aspergillus nidulans,* were amplified from a plasmid carrying *SEP3:GFP as* a single fragment using GFP-F and trpC-R primers (Dagdas *et al*, 2012). The trpC-R carries an overhang to be linked with another vector end. In-Fusion cloning was used to join several fragments of DNA, based on homologous recombination of 15 bp overhangs (dark grey shaded regions).

Table 5.2 Primers used in Chapter 5

Primer name	Sequence of oligo (5' to 3')
Bas1-BARlink-P1	cgagatttaggtcgaCGTGAGGTCACGTGAGATC
Bas1-GFPlink-P2	gcccttgctcaccatCGGGTAATAATTCTCCACC
Bas2-Barlink-P1	gagatttaggtcgacCTTCGGCGACTTTGTCTTCCTC
Bas2-GFPlink-P2	gcccttgctcaccatGAAACCCTGCTTCTTGACCTGCTC
Bas3-Barlink P1	gagatttaggtcgacTTGAAAAAAGCCCCGTGG
Bas3-GFPlink P2	gcccttgctcaccatGTGGGCACTGTTGGCAGC
Bas3prom-GFP-P2	gcccttgctcaccatCTTGATGGTTGGGTTTTG
Bas4-Barlink P1	cgagatttaggtcgaGCTCCAAACTGCAATACTCGCT
Bas4-GFPlink P2	gcccttgctcaccatAGCAGGGGGGATAGACGAGCCA
Slp1-Barlink-P1	gagatttaggtcgacAGGAGGAAGATAGCCCAGC
Slp1-GFPlink-P2	gcccttgctcaccatGTTCTTGCAGATGGGGATG
Pwl2-BARlink-P1	cgagatttaggtcgaCGTCAGTGAACAAACCTGT
Pwl2-GFPlink-P2	gcccttgctcaccatCATAATATTGCAGCCCTCT
BASTA-P1	GCAGGCATGCAAGCTGTCGACAGAAGATGATATTGAAG
BASTA-P2	GTCGACCTAAATCTCGGTGAC
GFP-P1	ATGGTGAGCAAGGGCGAGGAGCTG
GFP-P2	CTTGTACAGCTCGTCCATGCCGTG

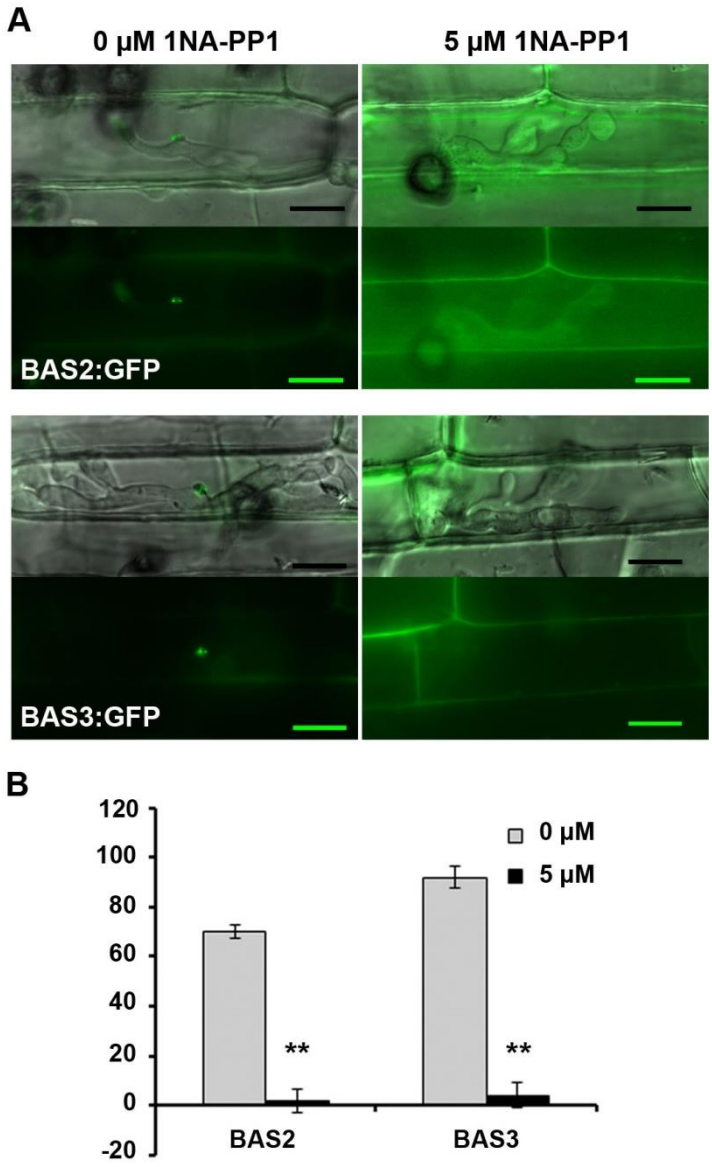

Figure 5.12 Production of fungal effectors associated with cell wall crossing sites is dependent on Pmk1 MAPK. (A) Conventional epifluorescence micrographs to show transformants of *pmk1*^{AS} expressing effector:GFP fusions growing in a susceptible CO-39 rice at 32 hpi. 1NA-PP1 was added to infected leaf sheaths at 26 hpi. Merged DIC and GFP images (top panels), and GFP fluorescence alone (lower panels) are shown. Scale bars represent 10 µm. **(B)** Bar chart to show the frequency of infection sites displaying GFP signal as puncta at primary BICs.

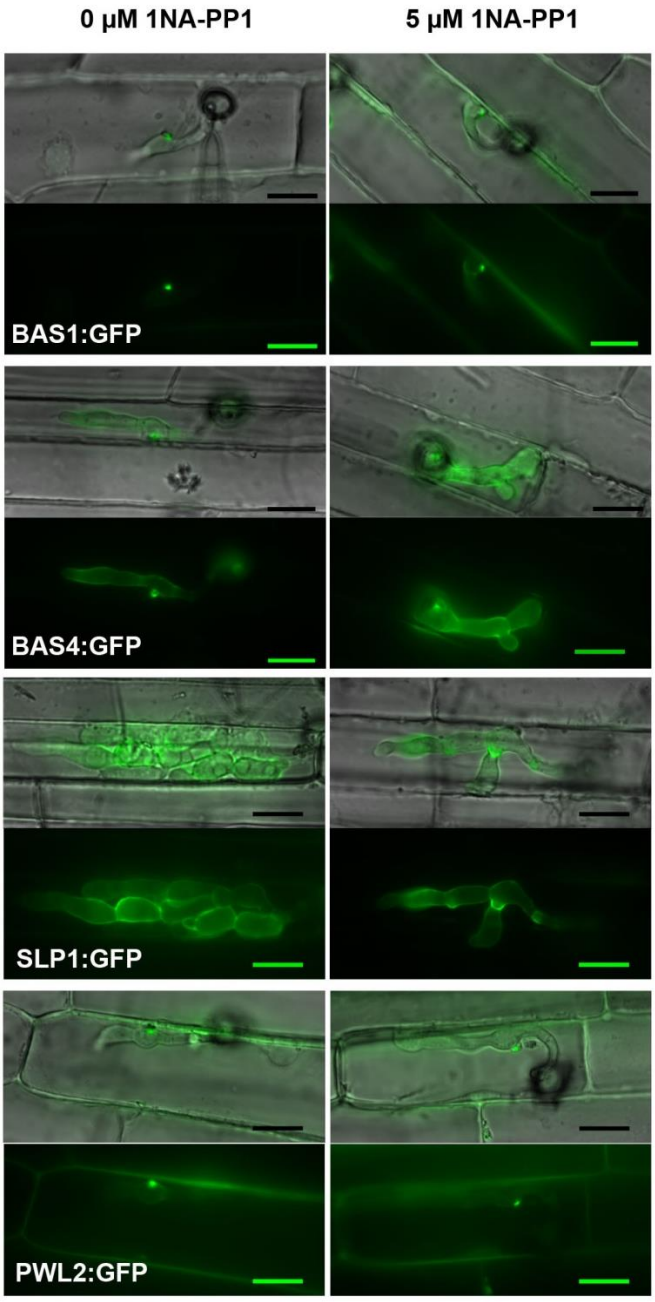

Figure 5.13 Pmk1 is dispensable for secretion and localisation of other fungal effectors. Conventional epifluorescence micrographs to show expression of effector:GFP fusions in the *pmk1*^{AS} mutant growing in susceptible rice tissue of cultivar CO-39 at 32 hpi. 1NA-PP1 was added to infected leaf sheaths at 26 hpi. Merged DIC and GFP images (top panels), and GFP fluorescence alone (lower panels) are shown. Scale bars represent 20 µm.

5.2.6 Assessing *BAS3* promoter activity using GFP as a reporter gene

To test whether Pmk1 activation induces expression of fungal effectors, *BAS3* was chosen, based on the relatively high expression level indicated by RNA-seq data. Cytoplasmic GFP was expressed under the control of 2.0 kb native *BAS3* promotor (*BAS3p:GFP*). The fluorescence pattern of *BAS3p:GFP* is based on microscopy visualisation of >50 appressoria or infection sites at each time point. The GFP signal in appressoria developed on glass cover slips was not significant, suggesting that *BAS3* gene was not highly induced on an artificial surface. Only autofluorescence of fungal cell walls was detected (Fig 5.14 A). By contrast, on rice sheath surfaces at 24 h, there was a mixture of appressoria that had, or had not, produced short penetration hyphae. Appressoria that had not produced penetration hyphae did not show significant fluorescence (less than 10 % of these appressoria showed a faint GFP signal; Fig 5.14 B). By contrast, approximately 70% of appressoria of the *pmk1*^{AS} mutant that had produced penetration hyphae showed obvious fluorescence signal of *BAS3p:GFP* (Fig 5.14 C). Appressoria of the *pmk1*^{AS} mutant treated with 1NA-PP1 did not show significant cytoplasmic GFP signal (less than 5% showed faint GFP signal; Fig 5.14 D). The *BAS3* promoter remained active during *in planta* growth as shown by expression of cytosolic GFP in invasive hyphae (Fig. 5.14 E). However, addition of 1NA-PP1 to disrupt Pmk1 activity did not abolish GFP signal in invasive hyphae, possibly due to the retention of GFP pool produced before addition of the inhibitor (Fig. 5.14 F). These results confirm that expression of the *BAS3* effector gene is dependent on Pmk1 activation and the presence of a living host plant where *BAS3* expression appeared to be induced around the time that the appressorium starts to penetrate.

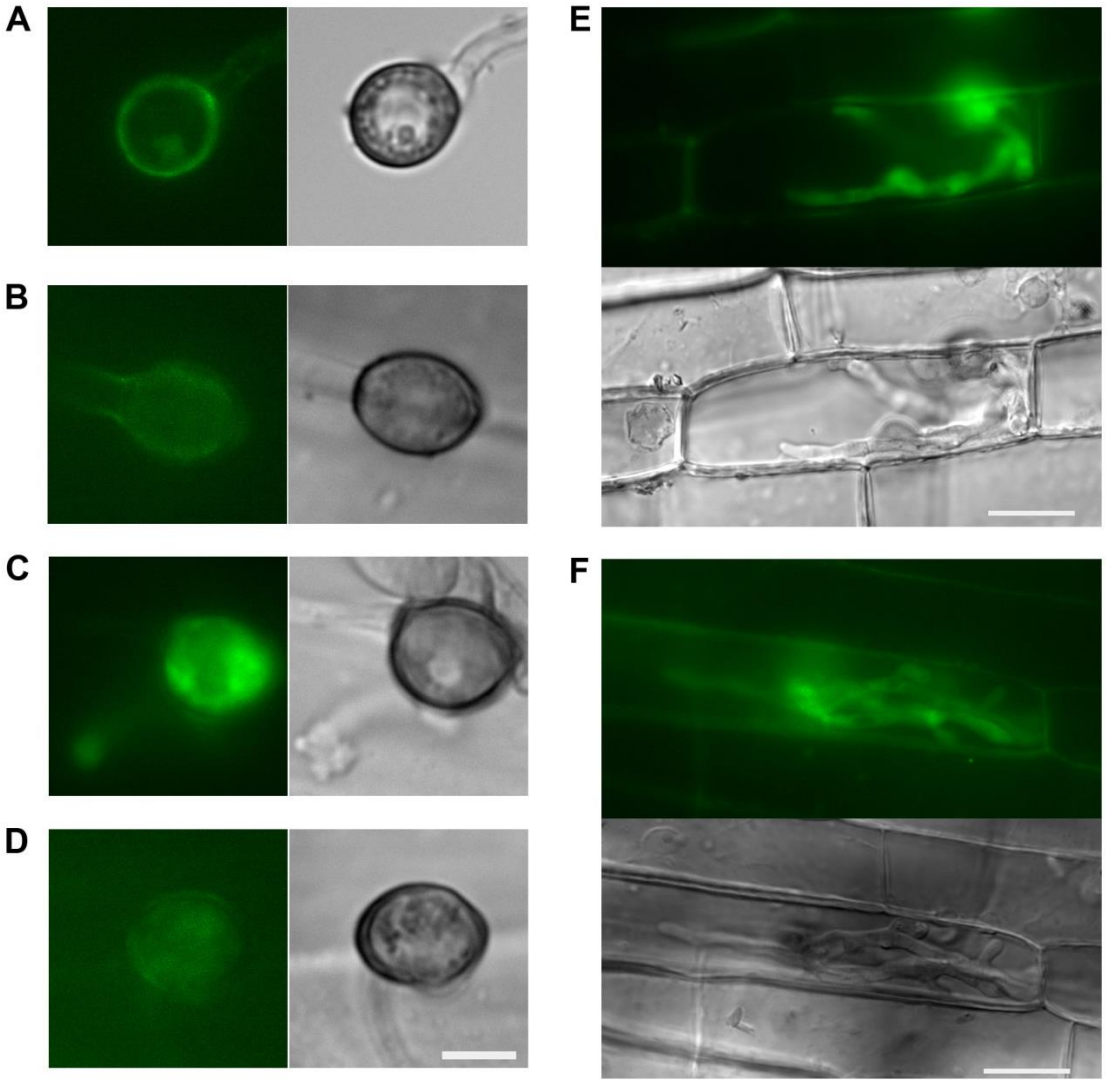

Figure 5.14 *BAS3* promoter activity is regulated by the Pmk1 MAPK. Cytosolic GFP was expressed under control of the *BAS3* promoter in the *pmk1*^{AS} mutant. **(A)** Appressoria developed on glass cover slips did not show significant cytosolic signal of GFP. **(B)** to **(D)** Expression of cytosolic GFP in appressoria formed on rice surface recorded at 24 h**.** Scale bar represents 10 µm. **(B)** Appressoria that had not produced penetration hyphae did not show significant GFP signal. **(C)** Appressoria that had produced a short penetration hypha, showed GFP signal in the cytosol. **(D)** Addition of 1NA-PP1 at 8 hpi prevented production of GFP. **(E)** to **(F)** Expression of GFP in invasive hyphae at 32 hpi. Scale bars indicate 20 µm. **(E)** In the absence of 1NA-PP1, GFP was observed in cytosol of IH. **(F)** Slightly reduced GFP signal observed in the *pmk1*^{AS} mutant treated with 1NA-PP1 at 26 hpi.

5.2.7 Intervention of ROS accumulation did not restore cell-to-cell movement to the *pmk1*^{AS} mutant in the presence of 1NA-PP1

Previous studies showed that virulence of some *M. oryzae* and *U. maydis* mutants that failed to suppress the defence-associated ROS burst can be restored by chemical inhibition of host derived-ROS (Hemetsberger *et al.*, 2012, Fernandez *et al.*, 2014). In plants, NADPH oxidases are important sources of ROS in respond to stress (Baxter *et al.,* 2013). I applied an NADPH oxidase inhibitor, diphenylene iodonium chloride (DPI), and the ROS scavengers, ascorbic acid and MnTMPyP, a cell-permeable superoxide dismutase mimetic, to rice leaf sheaths infected with the *pmk1*^{AS} mutant. These inhibitors had been used at higher concentrations than those in previous studies where suppression was successful (Fernandez *et al*., 2014a; Doehlemann *et al*., 2009). These chemical treatments did not rescue the cell-to-cell movement defect observed in the *pmk1*^{AS} mutant in the presence of 1NA-PP1 in more than 200 sites observed each experiment (Fig 5.15). However, it is important to note that the addition of ROS inhibitors without 1NA-PP1 did not affect cell wall crossing but instead enhanced fungal growth in rice tissues treated with DPI or MnTMPyP, likely due to suppression of ROS-dependent immune signalling of the host cells. Taken together, these results indicate that chemical inhibition of the ROS burst by inhibitors tested here cannot restore the defect in cell wall crossing caused by Pmk1 inhibition.

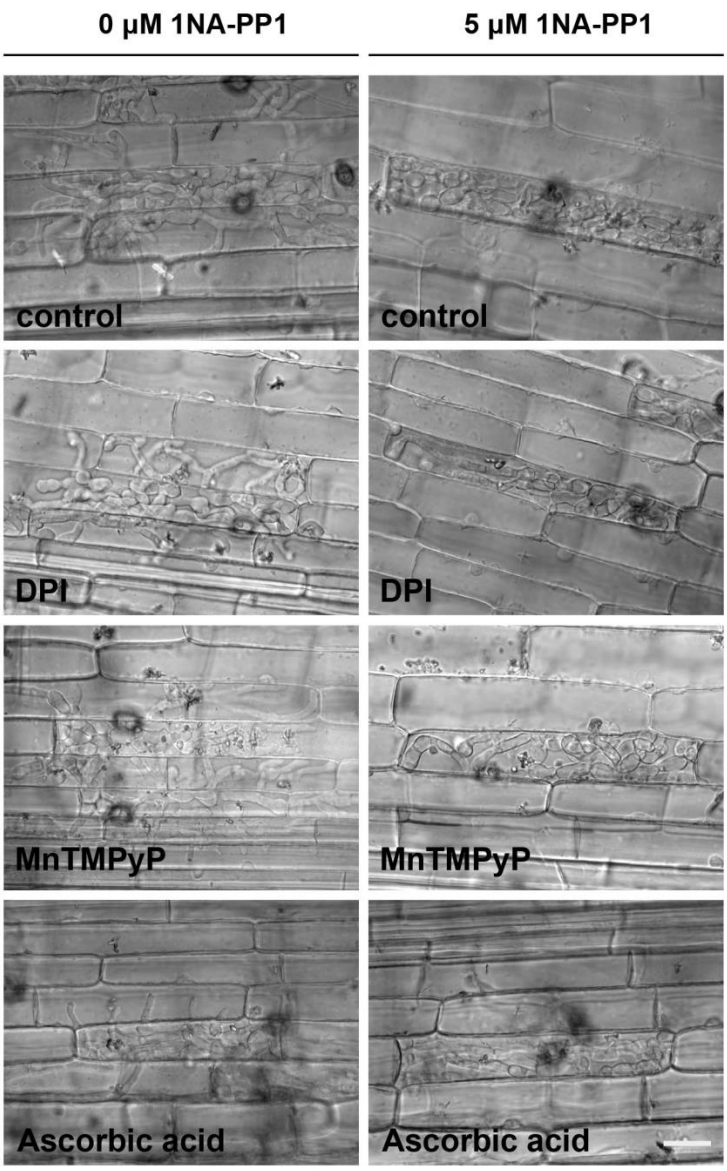

Figure 5.15 Perturbation of ROS accumulation did not restore the defects in cell-to-cell movement caused by Pmk1 inhibition. Representative micrographs showing the effect of ROS inhibition in cell-to-cell movement of the *pmk*^{AS} mutant. Infected rice sheaths were added with 10 µM DPI, 100 µM MnTMPyP, and 10 mM ascorbic acid, with or without 5 µM 1NA-PP1 at 26 hpi and observed at 48 hpi. No any combinations of chemical treatment can restore the defect of cell-to-cell movement during 1NA-PP1 treatment in more than 200 infection sites assessed each. Scale bar represents 20 µm.

5.2.8 Defect in cell-to-cell movement of *pmk1^{AS}* is not obviated by SA depletion

Chemical intervention of ROS burst did not restore the defect in cell-to-cell movement of the *pmk1^{AS}* mutant, so I next sought out to test whether SA signalling might be involved in the intercellular passage by the fungus. The SA pathway regulates PD permeability during pathogen defence response (Wang *et al*, 2013). In *Arabidopsis*, SA signalling induces transcription of a regulator of PD gating, PDLP5, which operates upstream of callose synthases responsible for callose deposition at PD. In rice, SA is also required for resistance against *M. oryzae* (Yang *et al.*, 2004). Here, a susceptible rice line expressing bacterial SA hydrolase *NahG* that cannot accumulate high levels of SA (Yang *et al*., 2004) was infected with the *pmk1^{AS}* mutant. In the presence of 1NA-PP1, invasive hyphae of *pmk1^{AS}* mutant were blocked in the first cell either in un-transformed or in *NahG* rice lines (Fig 5.16). These results indicate that depletion of SA by expression of SA-degrading enzymes did not rescue the phenotype of the *pmk1^{AS}* mutant in cell wall crossing.

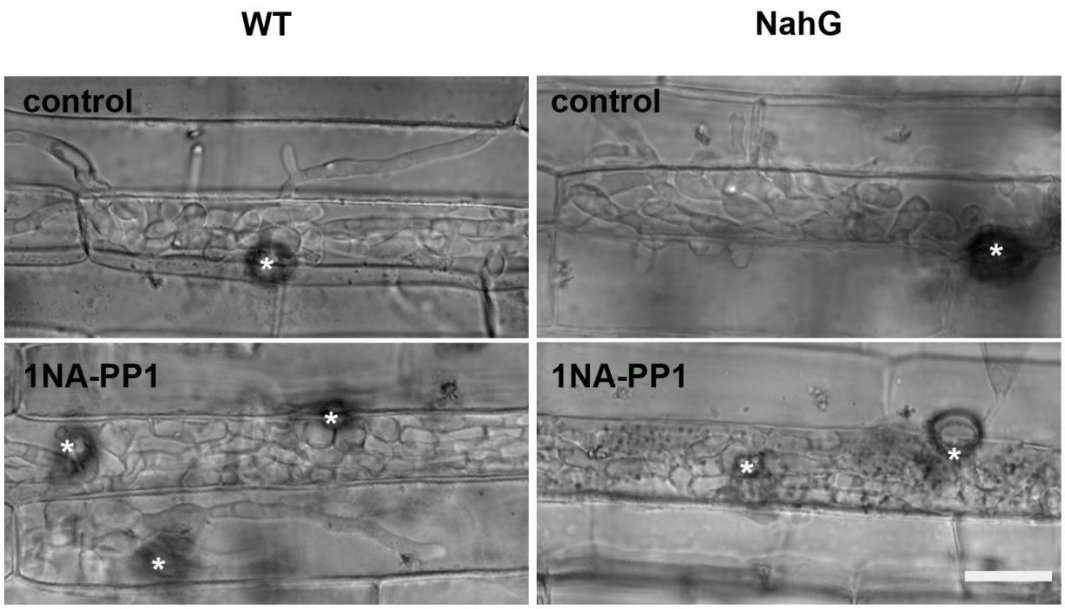

Figure 5.16 Depletion of SA level did not restore the ability of the *pmk1*^{AS} mutant to cross rice cell wall. Representative micrographs to show the effect of 1NA-PP1 treatment in un-transformed wild-type Nipponbare cultivar (WT, right panel) and NahG rice lines (left panel). 1NA-PP1 (5 µM) was added to infected rice leaf sheaths at 26 hpi and infection progress was assessed at 48 hpi. None of the invasive hyphae were able to cross rice cell wall in both WT and NahG rice lines in more than 100 infection sites assessed with two biological replicates. Scale bar indicates 20 µm. The Nipponbare rice cultivar and NahG rice lines (Yang *et al*., 2004) were provided as a kind gift from Dr. Satoko Yoshida (RIKEN Centre for Sustainable Resource Science, Japan).

5.2.9 Pmk1 activity is essential for cell-to-cell movement even when the entire host response is disabled

Previous observations clearly showed that Pmk1 inactivation resulted in intracellular entrapment of invasive hyphae of *M. oryzae* that exhibited unsuccessful attempts to penetrate rice cell walls and induction of host defence responses. However, it was unclear whether such defects were due to solely host defence responses or morphogenetic defects of invasive hyphae that failed to elaborate narrow invasive hyphae. Inhibition of the defence-related ROS burst and SA signalling, important host defence mechanisms and implicated in plasmodesmatal regulation, did not restore the defect in cell-to-cell movement in the *pmk1*^{AS} mutant 1NA-PP1. Also, I have showed that obvious PD callose deposition was not detected in uninfected rice epidermal cells, suggesting that PD were initially open allowing flow of molecules between cells that had not yet experienced fungal invasion (Fig. 5.3). To rapidly inactivate the entire host defence response, rice leaf sheaths were killed before being inoculated with conidia of the *pmk1*^{AS} strain. Dead rice leaf sheaths were prepared by fixing in absolute ethanol overnight, and then rehydrated before spore inoculation. Appressorium differentiation occurred in dead plant tissues, and plant penetration was initiated as early as 14 hpi. Treatment of 1NA-PP1 post-penetration did cause entrapment of invasive hyphae in first invaded cells (Fig. 5.17). Other killing methods were found not suitable for observation of leaf sheath epidermal cells. Killing rice sheathes by UV exposure caused severe stress to plant cells leading to cell death, and affected fungal growth. Heat-killed leaf sheaths were too soft to be hand-trimmed into thin sections. These results suggest that Pmk1 activity is also required for cell-to-cell

movement of invasive hyphae independently of the suppression of host defences, so Pmk1 must therefore regulate morphogenesis of invasive hyphae during cell wall crossing.

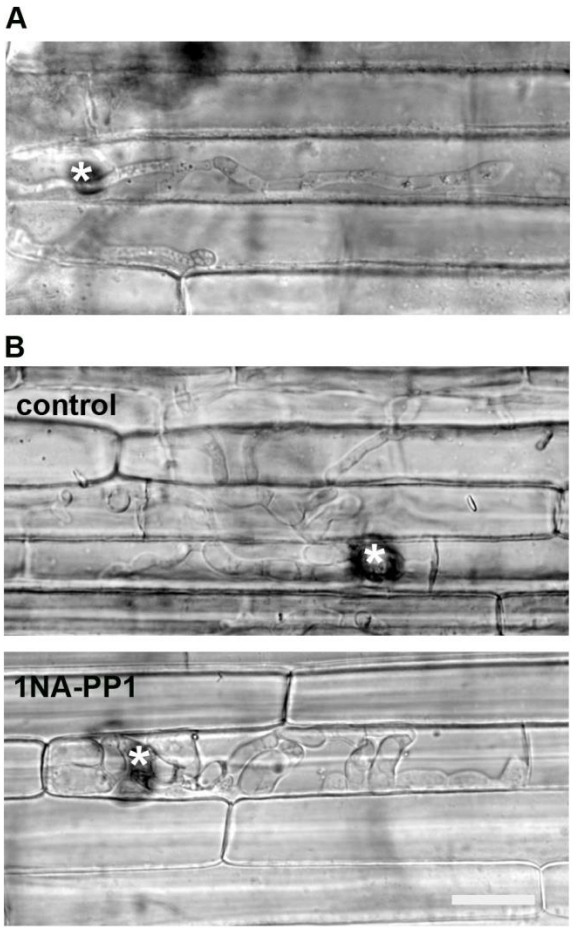

Figure 5.17 The *pmk1*^{AS} mutant failed to move from cell-to-cell in dead rice tissue in the presence of 1NA-PP1. Representative micrographs of dead tissue colonisation by the *pmk1*^{AS} mutant. Detached rice sheaths were fixed in 70% for 2 h, and in 100% ethanol overnight, followed by rehydrating with distilled water in room temperature for 6 h. Scale bar represents 20 µm. **(A)** The *pmk1*^{AS} mutant entered dead rice cells around 14 hpi. **(B)** 1NA-PP1 was added to infection sites at 14 hpi and infection process was monitored at 48 hpi. Untreated *pmk1*^{AS} mutant invaded neighbouring cells, while the 1NA-PP1-treated *pmk1*^{AS} mutant was completely unable to cross rice cell walls. Two biological replicates were carried out with more than 100 infection sites evaluated in each experiment. Bar = 20 µm.

5.2.10 Regulation of fungal cell morphogenesis during tissue colonisation

I next sought to define which fungal morphogenetic determinants are controlled by the Pmk1 MAPK, and required for cell-to-cell movement. Internal cell wall crossing by invasive hyphae of *M. oryzae* shares some cellular aspects with appressorial penetration: (1) growth of narrow hyphae traverse the cell wall and gain entry into new plant cells, followed by nuclear division and migration (Kankanala *et al*, 2007; Jones *et al*., 2016); (2) septin ring assembly occupies the base of cell constriction sites and fungal hyphae traverse host cell walls (Dagdas *et al*, 2012). I hypothesised that certain morphogenetic determinants promoting appressorial penetration and internal cell wall penetration might be regulated by the Pmk1 MAPK. Septins are conserved GTPases involved in many biological processes, including cytokinesis and cell polarisation. In filamentous fungi, septins form a variety of higher-order structures, such as filaments, gauzes, and rings, at growing hyphal tips, hyphal branch sites, the base of cellular protrusions and future sites of septum formation (Gladfelter, 2006; Gladfelter and Berman, 2009). Septin assembly at the appressorium pore is important in emergence of the penetration peg (Dagdas *et al.,* 2012). In chapter 3, I showed that Pmk1 activity is required for septin ring assembly at the base of the appressorium and for appressorial penetration.

In this chapter, I examined whether septin assembly is involved in cell-to-cell movement by *M. oryzae*, and whether this process is regulated by the Pmk1 MAPK pathway. To do this, I observed septin ring assembly at cell wall contact points in the *pmk1*^{AS} strain. In the absence of 1NA-PP1, Sep5-GFP formed an hourglass structure at cell wall crossing sites, in addition to its accumulation at septa (Fig

5.18). However in 1NA-PP1-treated infections, Sep5 was also detected at hyphal cells that were pressed against plant wall, but these diffuse septin patches did not form a ring or hourglass shape at cell wall contact points (Fig 5.18 B). Therefore, Pmk1 activity is necessary for septin re-organisation leading to re-polarisation of hyphal growth at cell wall crossing points.

To test whether these morphogenetic determinants are necessary for internal wall penetration by the IH, septin deletion mutants, Δ*sep3,* Δ*sep4,* Δ*sep5* and Δ*sep6,* and a mutant of the polarity regulator, Δ*cdc42,* were inoculated onto rice leaf sheaths and infection-related development monitored over 48 hpi. The septin mutants and Δ*cdc42* mutants penetrated plant cuticles and invaded neighbouring rice cells but at highly reduced frequency (Fig 5.19). Although these mutants were able to escape first invaded cells, they colonised significantly fewer surrounding rice cells, suggesting that septins may be involve in cell-to-cell movement by *M. oryzae*.

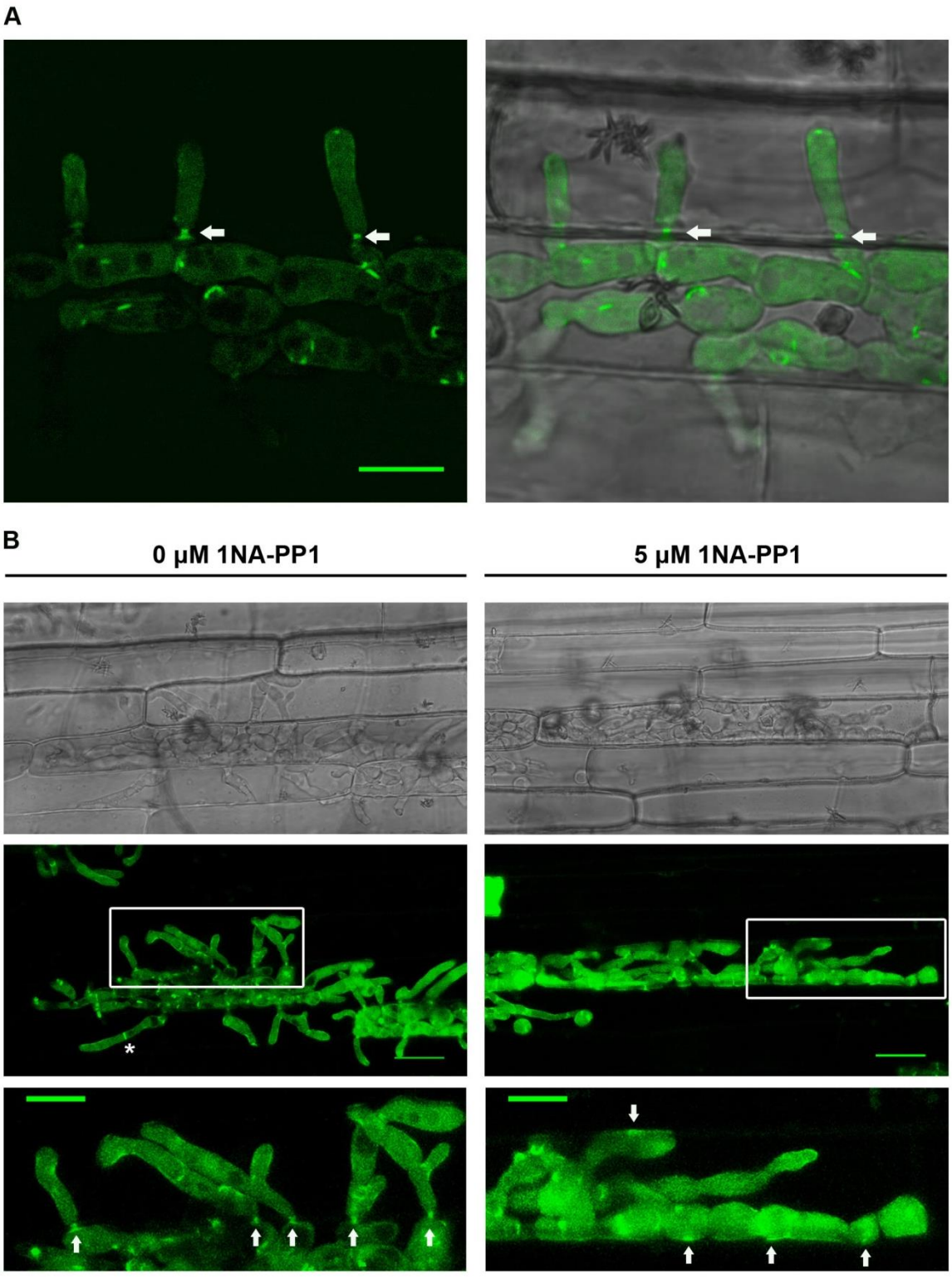

Figure 5.18 Visualisation of septin GTPase at cell wall crossing points of *M. oryzae*. The *pmk1*^{AS} strain expressing Sep5-GFP was used to infect a susceptible CO-39 rice cultivar. Infection development was imaged at 42 hpi using a laser confocal microscope. **(A)** Single-plane confocal image showing Sep5-GFP

localisation at cell wall crossing points (arrows) in this. GFP fluorescence (right panel) and merge (left panel). Scale bar represent 10 µm. **(B)** Localisation of Sep5-GFP is shown as Z-projections of confocal optical sections. DIC images (top) and GFP fluorescence (middle) with scale bars representing 20 µm; high magnification images (bottom) of areas in rectangular with scale bars indicating 10 µm. In the absence of 1NA-PP1, Sep5-GFP accumulated at crossing points (arrows) and septum (asterisk) at 42 hpi. In the presence of 1NA-PP1, the mutant was unable to cross host cell wall, but Sep5-GFP was recruited to cell wall-contact points (arrows). These patterns of septin localisation are based on observation of >20 independent infection sites in each treatment.

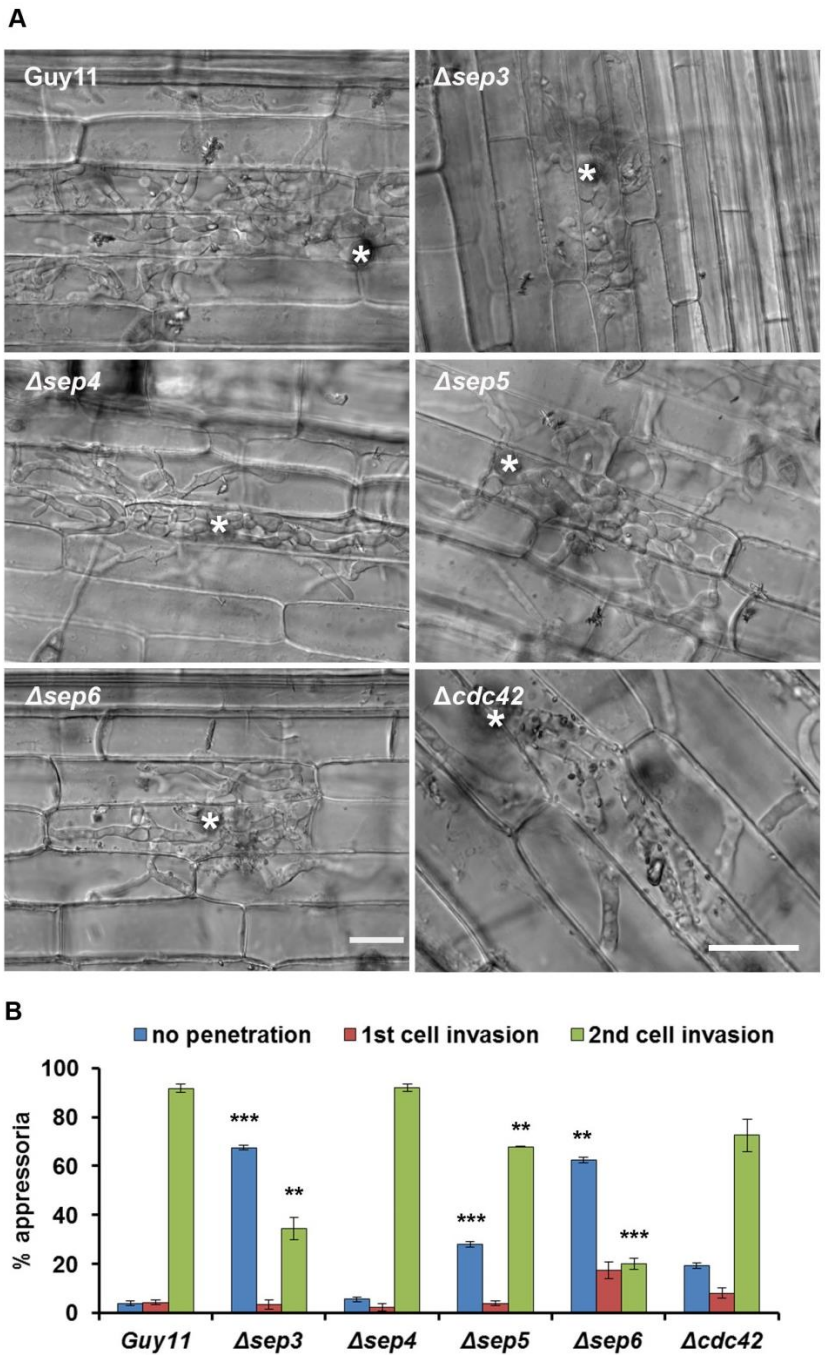

Figure 5.19 Septin GTPases are involved in cell-to-cell spread of blast invasive hyphae. (A) Secondary cell invasion by Guy11 wild type strain, Δ*cdc42*, and septin mutants at 48 hpi. Asterisks indicate appressorial penetration sites. Scale bar indicates 20 µm. Note that the infection by Δ*cdc42* mutant is imaged at a slightly higher magnification than others. **(B)** Bar chart to show frequency of different stages of infection-related development (appressorium without penetration hyphae, first cell invasion and second cell invasion) at 48 hpi.

5.11 Ultrastructure analysis of pathogen-rice interactions during cell-to-cell movement by the rice blast fungus

The rice blast fungus appears to spread from cell-to-cell through plasmodesmata during growth within plant tissue (Kankanala *et al.,* 2007). Around the time that invasive hyphae start to invade adjacent cells, the first-invaded host cells seem to undergo cell death in which the rice cells loss plasmolysis ability and their organelles collapse or disintegrated (Kankanala *et al.,* 2007; Mochizuki *et al.,* 2015). To understand the nature of Pmk1-regulated intracellular movement of blast IH, ultrastructure analysis on infected rice sheath cells were performed using conventional TEM. Rice leaf sheaths were inoculated with Guy11 strain, and harvested at 42 hpi when invasive hyphae already invaded the next cells, and ultrathin (80 nm) tissue sections were produced for TEM analysis. The overall quality of specimens obtained in these conventionally fixed samples was adequate for a general morphological description of invasive hyphae and host cell responses.

As shown in Fig 5.20 A, an invasive hyphal cell exhibits extreme constriction (~0.5 µm) at the internal cell wall penetration site, consistent with a previous study (Kankanala *et al.*, 2007). Rice plasma membrane in second invaded cell remained visible as electron-dense lining near rice cell wall, and was continuous with the EIHM surrounding the fungus in the second rice cell (Fig 5.20 B). In contrast, rice plasma membrane in the first invaded cell was not well-defined, suggesting that it might lose integrity (Fig. 5.20 A and B). Interestingly, constricted invasive hyphae at crossing site appeared lack surrounding plant membrane, so that the fungal cell wall may directly contact with rice cell wall (Fig. 5.20 B). Figure 5.20 C shows that

cytoplasmic area of the first infected cell lacked much of typical cellular components, while these remained in second cell, and invasive hyphae also invaginated vacuolar membrane. The change in plant plasma membrane integrity was also observed in rice cells infected with the *pmk1*^{AS} mutant with 1NA-PP1 treatment (Fig. 5.22 B). These TEM data are consistent with previous studies showing that: (1) *M. oryzae* invasive hyphae do not breach but instead invaginate rice plasma membrane at each new cell entry (Mochizuki *et al.,* 2015); (2) first infected rice cells undergo cell death, as indicated by the loss of plasmolysis capacity (Kankanala *et al.,* 2007), and disintegration of endomembrane system and plasma membrane when *M. orzae* had moved into the next cell (Mochizuki *et al.,* 2015); (3) invagination of vacuolar membrane by invasive hyphae occurs in both first- and second-invaded cells (Mochizuki *et al.,* 2015). An obvious collar of host cell wall material around the neck region or proximal end of the invasive hyphae newly penetrated rice cell wall (Fig 5.20 A), consistent with confocal images of aniline blue staining to show callose collars encircled the invasive hyphae that entered new rice cells (Fig. 5.3 B) (Mims *et al*., 2004). Immunogold labelling of callosic polymer using a monoclonal antibody recognising (1,3)-β-glucan epitopes is needed to confirm the presence of callose collar around invasive hyphae.

TEM images showed that invasive hyphae of the *pmk1*^{AS} mutant had traversed a pit field (Fig. 5.21). This pit field lacked obvious deposition of host cell wall materials (Fig. 5.21). In contrast, another pit field that had not been contacted with invasive hyphae did show certain callose deposition (Fig. 5.22). These events are consistent with the visualisation of callose deposition using aniline blue staining descripted in a previous section in this chapter that plasmodesmatal callose

occurred in rice cells infected with wild type or *pmk1*^{AS} strains (Fig. 5.3 and Fig. 5.4). These TEM images suggest that *M. oryzae* may clear out callose at individual pit fields before crossing.

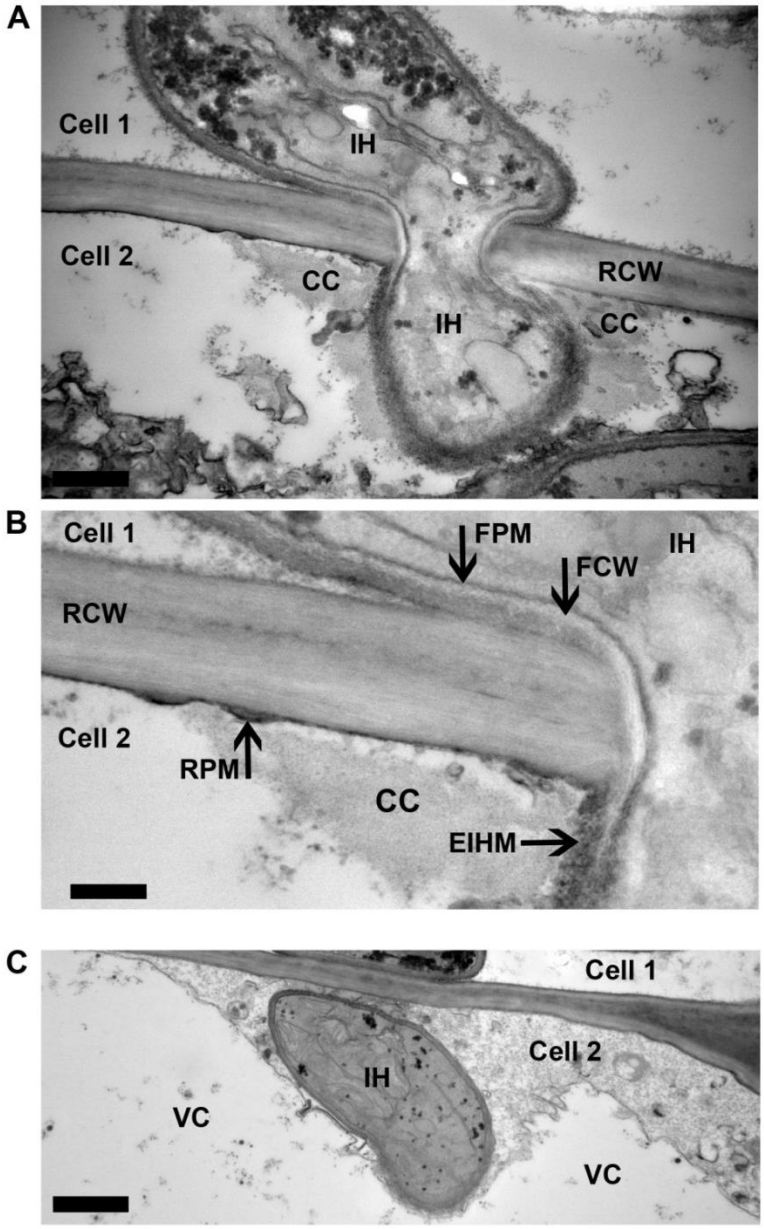

Figure 5.20 Cell wall crossing site by Guy11 invasive hyphae and cytological difference between first- and second-infected host cells. (A) TEM image to show invasive hyphae that had traversed rice cell wall (RCW) with callose collar (CC) around IH. Bar indicates 0.5 µm. **(B)** High magnification view showing the rice plasma membrane (RPM) in cell 2. FPM, fungal plasma membrane; FCW, fungal cell wall; EIHM, extra-invasive hyphal membrane. Bar indicates 20 nm. **(C)** TEM image showing invasive hyphae newly invaded cell 2. Cytoplasmic contents of cell 2 are well-preserved, whereas the cell 1 seems to disintegrate. Invasive hyphae in cell 2 completed cellular space with host vacuole (VC). Bar represents 1 µm.

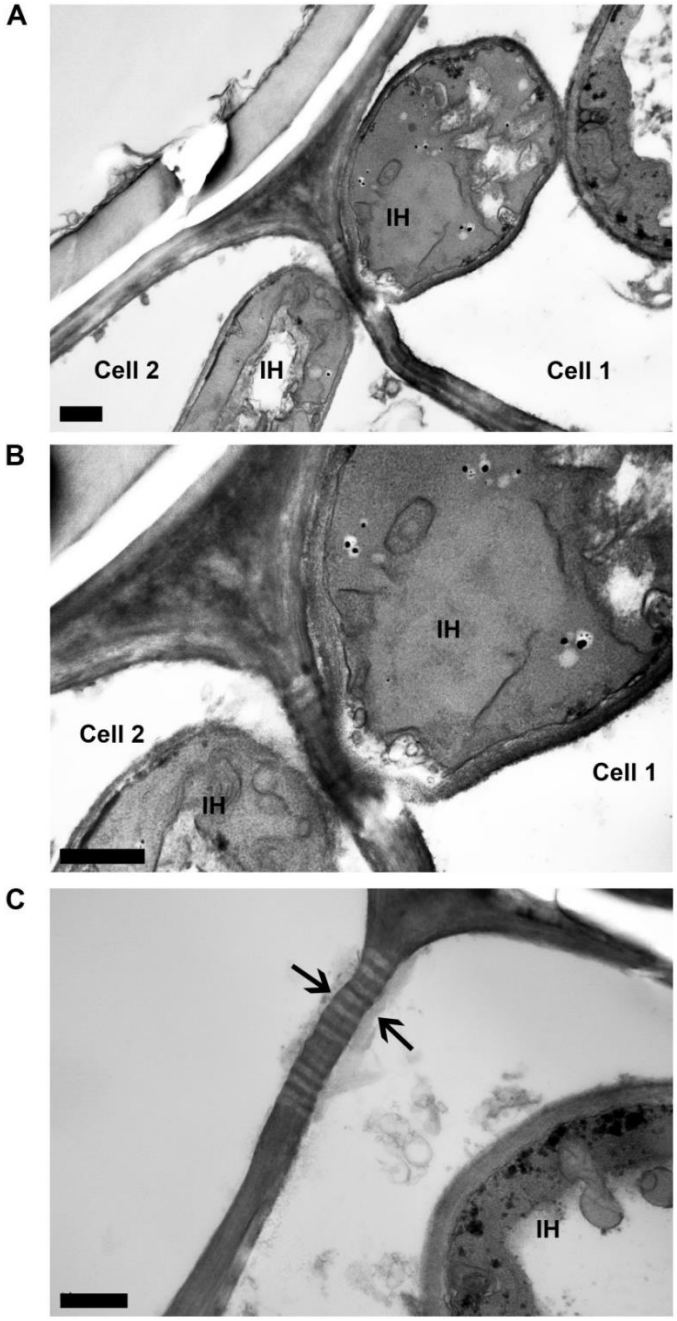

Figure 5.21 TEM images to show rice cells harbouring invasive hyphae of *pmk1*^{AS} strain without 1NA-PP1 treatment associated with pit field. (A) and **(B)** TEM section just grazed near a crossing site at a pit field. **(B)** High magnification view of the crossing site. The pit field that an invasive hypha had traversed did not show signs of cell wall material deposition or extensive damage and significant dilation of PD channels beside the crossing point. **(C)** A pit field that had not been contacted with invasive hyphae showed the accumulation of cell wall material (arrows). All bars represent 500 nm.

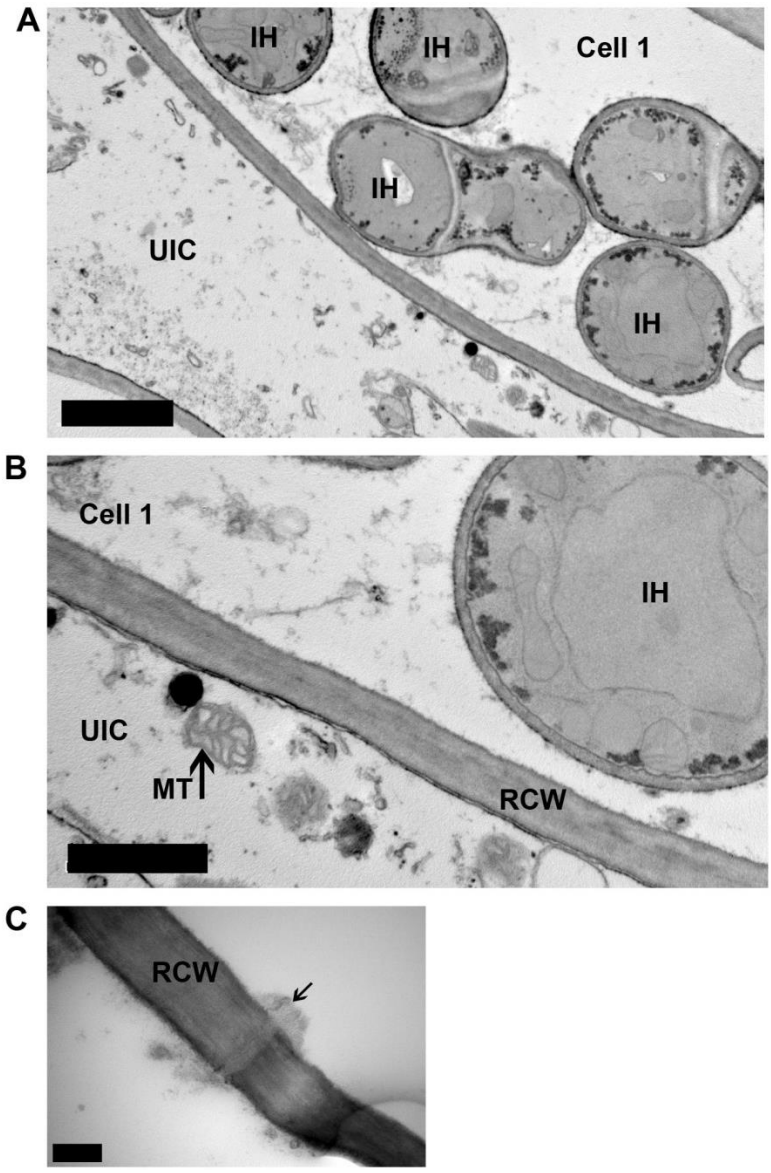

Figure 5.22 TEM images to show rice cells harbouring invasive hyphae of *pmk1*^{AS} strain treated with 1NA-PP1. (A) The *pmk1*^{AS} mutant was confined in the first invaded cell. UIC, un-infected cell. Bar indicates 2 µm. **(B)** High magnification view to show the differences between rice plasma membrane and cytoplasmic contents of infected and uninfected rice cells. MT, mitochondrion. Bar indicates 1 µm. **(C)** Plasmodesmatal channel exhibiting accumulation of cell wall material (arrow). Bar represents 200 nm.

5.3 Discussion

To colonise plant tissues, *M. oryzae* secretes effector molecules to suppress host immunity and traverse pit fields to spread into neighbouring host cells (Kankanala *et al.*, 2007; Mosquera *et al.*, 2009). However, it is not clear how such events are co-ordinately regulated leading to successful establishment of rice blast disease. The Pmk1 MAPK pathway plays crucial roles in the regulation of appressorium development and plant penetration (Xu and Hamer, 1996; Park *et al*., 2002; Zhao *et al*., 2005). Importantly, the Δ*pmk1* mutant is unable to infect rice plants through wounds, suggesting that this pathway may also have roles during *in planta* growth. In this chapter, I set out to explore the biological functions of the Pmk1 MAPK pathway during invasive growth using a chemical genetic approach, combined with live-cell imaging and transcriptomic analyses.

The current study provides cellular and molecular evidence that the Pmk1 MAPK pathway controls both effector-driven defence suppression and fungal development during cell-to-cell movement by *M. oryzae*. Classical host defence responses were de-repressed upon Pmk1 inhibition, partly due to the inability of invasive hyphae to produce sufficient effector proteins. The consequences of this were strong accumulation of hydrogen peroxide, an important ROS involved in plant immune signalling, and hyper-accumulation of callose deposition at the plant cell walls. However, callose deposition also occurs in compatible interactions. These observations suggest that *M. oryzae* can overcome callose-mediated plasmodesmatal closure, thereby using polarised cell growth to mechanically force narrow hyphae through pit fields, leading extensive modification of plasmodesmatal channels, or a combination of these factors. Despite strong elicitation of plant

immune responses in term of a ROS burst and callose production, very few rice genes showed differential expression during Pmk1 inactivation according to RNA-seq analysis. Because RNA samples were obtained from plant tissue containing infected cells, un-infected rice cells, and healthy rice cells, a very high degree of heterogeneity of plant gene expression across tissues might however hinder the identification of defence responsive-rice genes. ROS production and callose deposition might be however largely regulated at the post-transcriptional levels (Couto and Zipfel, 2016).

The RNA-seq analysis reported here revealed that the Pmk1 MAPK pathway regulates production of a large set of putative fungal effectors. These include those with known roles in evasion or suppression of host defences, such as Slp1 and Mep1, and others with unknown functions, such as AVR-Pita and AVR-Pik (Jia *et al.*, 2000; Yoshida *et al*., 2009; Mentlak *et al.,* 2012; Xia Yan, unpublished data). Interestingly, two *M. oryzae* effectors, Bas2 and Bas3, which accumulate at BICs, at appressorium penetration sites and at cell wall crossing points, appear to be controlled by the Pmk1 MAPK pathway. However, single gene deletion of *BAS2* and *BAS3* did not show any discernable phenotype, possibly due to extensive functional redundancy of the effector repertoire in *M. oryzae* (Mosquera *et al.*, 2009). *M. oryzae* secreted effectors that are targeted to crossing points, such as Bas2 and Bas3, may have roles in suppression of the recognition of damage-associated molecular patterns (DAMPs), for example sequestering cell wall fragments released from appressorial or internal cell wall penetration sites which potentially trigger host immune responses (Boller & Felix, 2009). Further biochemical characterisation of crossing point-associated effectors will provide

insight into the mechanism by which *M. oryzae* facilitates invasive cell-to-cell movement.

Little is known about how production of fungal effectors is fine-tuned during the infection process. Recently, the MoGTI1 transcription factor has been shown to be involved in penetration peg formation as well as regulation of a sub-set of effectors (Chen *et al.,* 2014; Li *et al.*, 2016). In *U. maydis,* a WOPR transcriptional regulator Ros1 triggers a dramatic switch in the expression of a large set of effector genes (Tollot *et al.*, 2016). Early endosome-mediated signalling is also necessary for expression of several key effectors during host cell invasion by *U. maydis* (Bielska *et al.*, 2014). Identification of fungal transcription factors operating downstream of the Pmk1 cascade will provide insights into a hierarchical regulation of cell signalling and effector gene expression during plant infection by *M. oryzae.*

Inactivation of Pmk1 activity resulted in misregulation of genes encoding proteins involved in metabolism, nutrient acquisition and cell wall degradation, such as sugar transporters and extracellular glycosyl hydrolases. Studies on the sugar sensing Tps1-dependent pathway demonstrate the importance of this pathway in integration of carbon, nitrogen metabolism and fine-tuning expression of genes encoding cell wall-degrading enzymes during biotrophic growth of *M. oryzae* (Fernadez *et al.,* 2012). Therefore, the failure in modulating these classes of genes found in the Δ*tps1* mutants and during the Pmk1 inactivation may also be associated with the elicitation of host defence.

The second major finding in this study is that the Pmk1 MAPK also regulates cellular morphogenesis during internal cell wall penetration. A previous study demonstrated that *M. oryzae* co-opts plasmodesmata for cell-to-cell spread

in host tissue (Kankanala *et al.,* 2007). Time-lapse imaging showed that invasive hyphae of *M. oryzae* select for particular sites to traverse with highly constricted hyphae to cross the cell wall, consistent with TEM analysis that showed how hyphae preferentially contact plant cell wall at pit fields (Kankanala *et al.,* 2007). Importantly, *M. oryzae* cannot move into or escape from guard cells, suggesting that functional plasmodesmata are required for fungal cell-to-cell passage, because plasmodesmata degenerate as guard cells mature (Kankanala *et al*., 2007, Oparka & Roberts, 2001). Passage through PD or pit fields is also found in another fungal pathogen. *F. graminearum,* a major causal agent of *Fusarium* ear blight on wheat, colonises the entire ear using both intercellular and intracellular hyphae. When the fungus grows from node to rachis, intracellular hyphae become extremely constricted where they traverse host cell wall via pit fields and then return to the original hyphal diameter (Brown *et al*., 2010). By contrast with previously described *M. oryzae* metabolic mutants that reduced in growth of invasive hyphae (Fernandez *et al*., 2013; Fernandez *et al*., 2014a,b), this study demonstrates that targeted inactivation of Pmk1 function at post-penetration stages severely blocked cell-to-cell movement, and this is independent of cell growth or inability to dampen host defence. These resulted in the initially invaded cells being densely packed with fungal hyphae. A significant consequence of Pmk1 inhibition was still however observed in rice tissues that different aspects of plant immune mechanisms were inhibited by chemical treatment or by depletion of SA, a key phytohormone in host defence signalling or by killing host tissues. These independent lines of evidence support a hypothesis that the Pmk1 MAPK regulates morphogenesis of hyphal constriction at cell wall crossing points.

The morphogenetic events during cell wall crossing by invasive hyphae are analogous to those observed during appressorium penetration, which also require the activation of the Pmk1 MAPK pathway. For each new host cell invasion, both appressoria or invasive hyphal cells undergo asymmetric cell division, sending out an initially anucleate daughter cell that breaches rice cell wall, followed by nuclear division and migration into the daughter cell (Kankanala *et al.,* 2007; Jones *et al.,* 2016). These processes involve re-organisation of septins into higher-order structures to stablise cellular constriction: the toroidal shape at appressorium pore and hourglass shape at cell wall crossing sites (Dagdas *et al.,* 2012). The Mst12 transcription factor operates downstream of the Pmk1 cascade, and is required for cytoskeleton remodelling appressorium pore, suggesting a role of Pmk1 pathway in morphogenetic regulation. Using live-cell imaging, I confirmed that septin assembly at cell wall crossing points depends on Pmk1 kinase activity. Consistent with a role of septins in the cellular morphogenesis, *M. oryzae* mutants lacking individual septins displayed a highly reduced ability to colonise the host epidermis. The Cdc42 GTPase however appears to be dispensable for cell wall crossing, and other septin regulators must therefore control cell-to-cell movement. It will be necessary to investigate additional morphogenetic determinants involved in the morphogenesis of invasive hyphal cells. Interestingly, RNA-seq analysis indicates that the Pmk1 MAPK induces expression of the PAK kinase gene, *CHM1,* which is essential for appressorial penetration and plant infection. Deletion mutants of *CHM1* are unable to re-organise septins and F-actin around the appressorium pore, leading to failure in a penetration peg development (Li *et al*., 2004; Dagdas *et al.*, 2012). These results suggest a potential link between the Pmk1 MAPK

pathway and fungal cell morphogenesis. We are currently generating analogue-sensitive mutants of *CHM1 (chm1^{AS})* to test whether Chm1 is required for septin assembly and cell-to-cell movement by *M. oryzae.*

Around the time that the fungus invades neighbouring cells, the EIHM appears to lose integrity, showing release of Bas4-GFP into cytosol (Mochizuki *et al.*, 2015). Interestingly, Bas4-GFP did not diffuse into neighbouring rice cell, suggesting that PD of the initial invaded cells were then closed (Mochizuki *et al.*, 2015; Chang Hyun Khang, personal communication; George Littlejohn, unpublished data). Here, I have reported that callose deposition at plant cell walls gradually increased over time that *M. oryzae* developed in the first rice cells and reached a maximum when cross the cell wall, consistent with previous observations, suggesting that the fungus can overcome callose-mediated plasmodesmatal closure to spread into adjacent rice cells. Attempts to measure conductivity of infected rice cells have proven challenging. I performed dye-loading experiment using small fluorescent tracer to rice leaf sheath infection (Lee *et al.*, 2011), but this was not successful. Further assays to assess dynamics of PD permeability, for example biolistic transient expression assays, will help or refute the hypothesis of manipulation of plasmodesmata during blast infection. What I cannot address at this time is whether the rice blast fungus secretes callose-degrading enzymes to open plasmodesmatal channels for cell-to-cell movement. Transcriptional profiling of blast biotrophic invasion, however, showed previously that cell wall-degrading enzymes were not significantly induced during infection (Mosquera *et al*., 2009). Upon cell wall crossing, an invasive hyphal cell that reaches a pit field sends out a narrow invasive hyphae toward PD, and the PD then

simply be spread out due to a physical force generated by hyphal growth. This force may be the primary mechanism to allow internal wall penetration by *M. oryzae*. Taken together, the present results show that the Pmk1 MAPK regulates septin-mediated morphogenesis of invasive hyphal cells necessary for cell-to-cell movement of *M. oryzae* biotrophic hyphae.

The evolutionarily conserved MAPK signalling cascade, homologous to the yeast pheromone response and filamentous growth pathway, is important for virulence in various plant pathogenic fungi (Li and Xu, 2012; Hamel *et al*., 2012; Turra *et al.*, 2014). A *Fusarium oxysporum* orthologue of yeast Fus3/Kss1, Fmk1, is essential for infection of tomato plants. The Fmk1 MAPK regulates surface penetration required for invasive hyphal growth, as experimentally shown by penetration through cellophane membranes (Prados Rosales & Di Pietro, 2008). Nonetheless, understanding of how intracellular signalling is associated with sensing plant factors during blast invasive growth is in its infancy. A G-protein, Mgb1, and two mucin proteins, MoMsb2 and MoCbp1, participate in recognition of environmental signals (Nishimura *et al.,* 2003; Wang *et al.*, 2015). Mutants lacking these proteins failed to form appressoria on inductive surfaces or grow invasively in rice tissues (Nishimura *et al.,* 2003; Wang *et al.*, 2015). Observations of morphological changes of invasive hyphae touching internal cell wall before crossing imply that the pathogen may sense particular features of plant cell walls and undergo cellular differentiation (Kankanala *et al.*, 2007). I hypothesise that thigmotropism is one possible mechanism by which *M. oryzae* senses unique properties of the pit field site. Although it is more tractable to define physical and chemical stimuli that activate signalling cascades necessary for appressorium development, because

such events occur *ex planta*, the mechanisms regulating signalling pathways during biotrophic growth remain largely unknown. Additional study will be needed to explore how the Pmk1 MAPK signalling is activated upon cell wall contact to initiate emergence of narrow invasive hyphae during cell wall crossing.

In summary, the Pmk1 MAPK regulates cell fate determination during invasive growth, thereby inducing differentiation of narrow invasive hyphae crossing internal cell wall in a septin-dependent manner. The Pmk1 MAPK also modulates production of a set of putative effectors required for host immune suppression as well as fine-tuned expression of many cell wall degrading enzymes.

Chapter 6 General Discussion and Future Perspectives

In this thesis, I set out to explore molecular mechanisms regulating the invasion and colonisation of host tissue by the fungal pathogen. I focused on two major regulators of fungal morphogenesis, the regulation of cell cycle control and the Pmk1 MAPK pathway, which are known to play pivotal roles in early pathogenic development by *M. oryzae.* The study sought to address two principle questions:

1. How does cell cycle progression regulate appressorium development and plant penetration?
2. How does the Pmk1 MAPK pathway regulate the post-penetration stages of plant infection?

This study provided a complementary genetic analysis which showed that the canonical cell cycle machinery drives S-phase progression, which is essential for initiation of plant infection. This finding is based on the generation of thermosensitive *M. oryzae* mutants of the B-type cyclin gene, *cyc1*^{nimE10} and *cyc1*^{nimE6}*,* which conditionally arrest at S and G2 phases, respectively. During appressorium formation, the *cyc1*^{nimE10} mutant was unable to produce terminal swelling of germ tube tips, whereas the *cyc1*^{nimE6} mutant displayed swollen germ tube tips but failed to expand isotropically. These results suggest that hooking depends on S-phase progression, while formation of a dome-shaped appressorium requires G2 progression. The *cyc1*^{nimE10} mutants were both unable to initiate emergence of penetration hyphae at the restrictive temperature, similar to the *nim1*^{I327E} mutant defective in S-phase progression and activation of the DNA

replication checkpoint (Saunders *et al*., 2010a). Therefore, I propose that the rice blast fungus also employs the conserved cell cycle machinery to drive cellular morphogenesis, in which the polarised growth relies on G1-S phase activity of CDK and isotropic growth depends on the G2-M transition, similar to the functions of CDK-cyclin complex in budding yeast (Lew & Reed, 1993).

Recently, elements of the classical DNA damage checkpoint have been showed to monitor completion of DNA replication during appressorium morphogenesis of *M. oryzae*. By contrast, a distinct, novel S-phase checkpoint instead operates during plant penetration stage (Miriam Oses-Ruiz, PhD thesis, Biosciences, University of Exeter; Appendix 2). Application of a chromosomal tagging system using LacO/LacI to visualise replicated DNA, revealed that cell cycle progression into the S-phase of the appressorial nucleus is likely to be induced by increased levels of turgor pressure within the melanised appressorium (Miriam Oses-Ruiz, unpublished data; Appendix 2). I speculate that the differentiation of appressorium may lead to cell cycle exit. To re-enter the cell cycle and to produce penetration peg, distinct signals, possibly associated with the turgor pressure, are needed to trigger the cell cycle control system. In *U. maydis*, appressorium formation is incompatible with an active cell cycle, so multiple signalling cascades are involved in cell cycle arrest at G2, in order to achieve successful plant penetration (Castanheira *et al*., 2014). By contrast, our study suggests that *M. oryzae* appressorium appears to arrest in G1 of the cell cycle prior to plant penetration until certain threshold level of turgor is reached. This finding is based observations that appressoria of melanin mutants of *M. oryzae* are unable to progress into S-G2 phase, and there by fail to penetrate rice cuticle

(Miriam Oses-Ruiz, unpublished data; Appendix 2). We found that the Pmk1 MAPK and Nox-derived ROS signalling pathways appear to operate in parallel with the cell cycle control to initiate penetration peg emergence, because appressoria of Δ*mst12* and Δ*noxR* mutants of *M. oryzae* can progress through S-phase but fail to penetrate host surface (Miriam Oses-Ruiz, unpublished data; Appendix 2). It is possible that other pathways, such as the cAMP-PKA and cell wall integrity Mps1 MAPK signalling, may participate in sensing sufficient levels of turgor and thereby induce re-entry to the cell cycle of the appressorium prior to plant penetration. This might, for example, involve up-regulation of G1 cyclin in the appressorium that drives entry into S-phase.

Characterisation of cell cycle regulators in *M. oryzae* has proven challenging. My initial attempts to characterise cyclin genes, including a G1 cyclin encoding gene, *CLN1,* were for example unsuccessful. I failed to isolate any deletion mutants, suggesting that these genes might serve a crucial function in cellular viability of the fungus. To the best of my knowledge, temperature-sensitive mutants of G1 cyclins have not been isolated in any genetic models, hindering the generation of a conditional allele of *CLN1* by reverse genetics. Expression of a Cln1 protein fused with GFP at, either N- or C-termini, also did not obtain reproducible results. I also attempted to generate analogue-sensitive (AS) mutants of the Cdc28 CDK in *M. oryzae*, based on a successful strategy reported in *S. cerevisiae* and *S. pombe* (Bishop *et al.,* 2000; Aoi *et al.*, 2014). Unfortunately, the *cdc28-as1* allele harbouring a point mutation at gatekeeper residue was likely to be non-functional, because we failed to isolate any gene replacement mutants. Introduction of an additional point mutation, reported to help stabilising the

conformation of an engineered Cdc28 (Aoi *et al.*, 2014), resulted in a functional Cdc28-as2 protein but this prone to be insensitive to any ATP-analogues tested. Development of controllable promoters will therefore help with characterisation of the Cdc28 and G1 cyclins in *M. oryzae*.

The concept of virulence specific-cell cycle regulation has become more evidence. Upon recognition of appropriate environmental signals, intracellular signalling pathways influence the modification of cell cycle control which then translates into morphogenesis of plant infection structures (Perez-Martin *et al*., 2016, Sudbery & Gladfelter, 2008). Future studies will focus on finding links between among these processes, and understanding the nature of cell cycle regulation during formation of plant infection structures. There are some outstanding questions in cell cycle-regulated host cell invasion yet to be elucidated:

- How does integration of different intracellular and extracellular signals culminate in S-phase entry leading to initiation of plant penetration?
- Does the cAMP response pathway influence cell cycle progression during appressorium development and plant penetration?
- Does the emergence of narrow invasive hyphae that traverse internal cell walls also depend on S-phase progression similar to appressorium penetration?

Although cellular controls exerted on morphogenesis of infection structure, such as cell cycle progression, melanisation and autophagic cell death are differentially regulated and needed, even in closely-related fungal pathogens (Perez-Martin *et al*., 2016), the evolutionarily conserved Pmk1-type MAPK

pathways are important for surprisingly diverse infection strategies, in not only plant pathogenic fungi but also in animal-infecting fungi (Zhao *et al*., 2007).

The Pmk1 MAPK pathway plays a pivotal role in the regulation of appressorium development and plant penetration by *M. oryzae* (Xu and Hamer, 1996; Park *et al*., 2002; Zhao *et al*., 2005). However, *Δpmk1* mutants are unable to infect rice plants through wounds, suggesting that the MAPK pathway also play a role during *in planta* growth (Xu and Hamer, 1996). Although genetic determinants regulating formation and function of the appressorium have been described, very little is known regarding how *M. oryzae* completes late stages of its life cycle in plant tissues. Invasive hyphae of *M. oryzae* switch from bulbous pseudohyphae to filamentous tubular hyphae for each cell wall crossing points which occur through primary pit fields where plasmodesmata are located in order to invade neighbouring rice cells (Kankanala *et al.,* 2007). To this end, a chemical genetic approach was applied to characterise the biological functions of the Pmk1 MAPK at various stages of plant infection. Generation of an analogue-sensitive *PMK1* (*pmk1*^{AS}) mutant allowed rapid and highly selective inhibition of the modified Pmk1 protein by simply adding an ATP analogue, 1NA-PP1. Addition of 1NA-PP1 during early conidial germination of the *pmk1*^{AS} mutant blocked appressorium formation, reminiscent of the phenotype of the Δ*pmk1* mutants and a kinase-inactive *PMK1* mutation. By contrast, addition of 1NA-PP1 at later time points instead prevented re-organisation of the septin cytoskeleton and subsequent plant infection resembling the Δ*mst12* mutants. These results confirmed the feasibility of using a chemical genetic technique for targeted inhibition of protein kinases in *M. oryzae*. Chemical inactivation of the Pmk1 MAPK after host cell penetration did not affect

growth and differentiation of bulbous invasive hyphae nor the development of the biotrophic interfacial complexes (BICs), but instead severely prevented cell-to-cell movement by the fungus. ROS burst and callose deposition at host cell wall, were also strongly induced, suggesting that general host defences were de-repressed as a result of Pmk1 inhibition. Comparative transcriptomic analysis using RNA-seq then revealed that a large set of putative secreted effectors and cell wall degrading enzymes appear to be under the control of the Pmk1 MAPK pathway. Many of these genes have roles in host defence suppression as well as the evasion of host detection (Mentlak *et al*., 2012, Mogga *et al.*, 2016, Sharpee *et al*., 2016), consistent with the roles of Pmk1 MAPK in regulating the ability of invasive hyphae in suppression of host defences. The Pmk1 MAPK was also found to control gene expression of several sugar transporter and carbohydrate-active enzyme-encoding genes, suggesting that this pathway is required for fungal adaptation to nutrient availability during biotrophic colonisation.

The elicitation of host defence responses caused by Pmk1 inhibition does not solely explain the function of Pmk1 MAPK in regulating cell-to-cell movement during invasive growth. Inhibition of host immune responses by addition of an NADPH oxidase inhibitor, ROS scavenger, depletion of salicylic acid, or even killing plant cells before infection, did not restore the severe defect in cell-to-cell invasion by the *pmk1*^{AS} mutant. These results suggest that the Pmk1 MAPK also control invasive hyphal morphogenesis independent of host defence suppression. Live-cell imaging showed that Pmk1-inactivated invasive hyphae were unable to organise the septin cytoskeleton into an hourglass shape at cell wall contact points. Mutants lacking individual septin genes were, furthermore, unable to colonise rice

tissue, consistent with a role for septins in cellular morphogenesis during cell wall penetration. During appressorium-mediated plant infection, septins maintain cortical rigidity and mediate membrane curvature, important for protrusion of a rigid penetration peg to rupture the rice surface (Dagdas *et al.,* 2012). The present results indicate that Pmk1 activation regulates re-organisation of the septin cytoskeleton into higher order structures required for generating cellular protrusion, both at the base of appressorium and at cell wall crossing sites. RNA-seq analysis, moreover, showed that expression of the Chm1 PAK, a regulator of septin assembly and morphogenesis, appears to be activated by the Pmk1 MAPK. Although cell-to-cell movement does not require melanin-mediated high turgor pressure as found in appressorium penetration (Kankanala *et al.,* 2007), this study provides lines of evidence to support a hypothesis that several mechanisms are shared with appressorial penetration. These involve septin-dependent constriction of fungal cells, asymmetric cell division accompanied with long distance nuclear migration, and, importantly, activation of the Pmk1 MAPK pathway. However, this study cannot rule out the possibility that invasive hyphae of *M. oryzae* secrete call wall or callose-degrading enzymes, or carry out additional manipulation of plasmodesmatal channels to facilitate intercellular passage. This process might also be controlled independently of the Pmk1 pathway.

Cellular and molecular mechanisms participating in cell-to-cell movement by invasive hyphae of *M. oryzae* are fascinating biological processes to be further explored in detail. Super-resolution microscopy is urgently needed to visualise the delicate dynamics of plant and fungal subcellular components during cell wall crossing. Kankanala *et al.* (2007) showed that transient expression of GFP-tagged

tobacco virus movement protein (TMP-GFP) was possible to visualise rice plasmodesmata. However, co-localisation of rice plasmodesmata with cell wall crossing sites using stable expression of TMP-GFP in rice cells proven difficult, because the fluorescence signal were very low and easily lost in subsequent rice generations (George Littlejohn, personal communication). To target the TMP into host cells and visualise accumulations at rice plasmodesmata, I have attempted to express TMP-mCherry fused with a cytoplasmic effector Pwl2 that is known to be translocated into host cytoplasm. The Pwl2-TMP-mCherry fusion protein was found to accumulate at BICs and in host cytoplasm, but unfortunately no punctate signals was observed at rice cell walls, possibly due to insufficient amounts of fusion proteins delivered into host cells. However, TMPs potentially interfere with gating regulation of rice plasmodesmata and make interpretation complicated (Oparka *et al*., 1997). Plasmodesmata-located proteins (PDLPs) will be good candidates for the visualisation of rice plasmodesmata (den Hollander *et al.*, 2016). Transient expression using particle bombardment with additional optimisation for leaf sheath assays may, for example, help to localise native rice components during *M. oryzae* infections (Wang *et al.*, 2013b). Phosphoproteomic analysis combined with chemical genetic approach established in this study may allow the identification of direct and indirect targets of the Pmk1 MAPK cascade, such as transcription factors, in order to understand the complex regulatory network necessary to initiate virulence program and cellular proliferation by *M. oryzae*. In addition, it is largely unknown which *in planta* signals trigger activation of the Pmk1 MAPK pathway and translate into the regulation of effector production as well as hyphal morphogenesis during tissue colonisation by the rice blast fungus. There are several specific

questions regarding the regulation of cell-to-cell movement by *M. oryzae* during host tissue colonisation that remain to be addressed:

- What is the nature of the fungal and plant interface during cell wall crossing?
- How does the fungus sense *in planta* cues/signals that activate the Pmk1 MAPK cascade?
- What are these cues/signals?
- What is the nature of spatio-temporal dynamics of Pmk1 MAPK activation during *in planta* growth?
- What are the downstream targets of the Pmk1 MAPK pathway that facilitate adaptation of the fungus to biotrophic growth, especially the regulation of effector production?
- Does the rice blast fungus modify individual plasmodesmata channels and suppress plasmodesmatal-related immunity in order to move from cell-to-cell?
- Does this process involve actions of secreted effectors?

I propose here a model depicting the coordination between signalling pathways and cell cycle control during plant infection by *M. oryzae*. Upon conidial germination, surface sensors comprised of G-protein coupled receptors and surface proteins, Sho1 and Msb2, the cAMP-PKA and Pmk1 MAPK pathways detect extracellular signals derived from host plants and activate downstream signalling pathways. The cAMP-PKA and Pmk1 MAPK pathways appear to induce cell cycle progression of the conidial nucleus to initiate appressorium morphogenesis. S-phase in turn induces deformation of germ tube tips, whereas

G2 progression promotes isotropic growth of the tips. This round of the cell cycle leads to the formation of a dome-shaped appressorium. One daughter nucleus migrates into the differentiating appressorium and remains in G1 phase. The cAMP-PKA and Pmk1 MAPK pathway also control the generation of glycerol-mediated turgor pressure in the appressorium. Once a critical turgor level has reached, S-phase progression of the appressorial nucleus is triggered by unknown signalling pathways. This round of the cell cycle triggers rearrangement of septin and actin cytoskeletons into a large ring around the appressorium pore, necessary for polarised secretion and cell growth. However, cell cycle progression and the Pmk1 activation during appressorium penetration are likely to operate in parallel to initiate the formation of penetration peg. The completion of S phase in turn sends off an inhibitory signal to turgor generation machinery, possibly via the Sln1 two-component signalling pathway (Zhang *et al.,* 2010), in order to modulate the turgor level during plant penetration. A penetration peg emerges from the base of the appressorium and ruptures host surface. The peg differentiates into a filamentous primary hypha which begins to secrete effector proteins into a host cell. A BIC is established at the tip of the primary hypha, before being relocated to subapical position when a bulbous invasive hyphal cell develops. The differentiation of bulbous invasive hyphal cell is likely to depend on the arrival of a daughter nucleus after a successful nuclear division in the appressorium. Multiple rounds of mitosis occur when the fungus proliferates in the first-invaded host cells. *M. oryzae* starts to invade neighbouring plant cells by sending off narrow invasive hyphae through pit fields. The formation of narrow filamentous invasive hyphal cells traversing host internal walls shares several cytological aspects with the appressorial penetration,

and may be regulated by S-phase of the cell cycle. Obviously, second cell invasion by *M. oryzae* depends on the Pmk1 activation during invasive growth. The Pmk1 MAPK pathway also control the production of a subset of secreted effectors required for suppression of host immunity, ultimately important for the establishment of biotrophic interaction between rice and *M. oryzae* (Fig. 6.1).

In conclusion, this study provides a fascinating insight into the molecular and cellular mechanisms by which a phytopathogenic fungus colonises host tissue, which are critical for establishment of plant infection. I have provided direct genetic evidence that conserved cell cycle machinery drives S-phase progression to initiate plant penetration by the appressorium of the rice blast fungus. I have also demonstrated that the Pmk1 MAPK cascade, a canonical fungal MAPK pathway, regulates multiple stages of plant infection by *M. oryzae*. During tissue colonisation, the Pmk1 MAPK pathway controls production of several secreted effectors involving in host immune suppression and also cellular morphogenesis of penetration hyphae crossing internal cell wall. Understanding of infection-related morphogenesis, effector functions and virulence-associated cell signalling holds promise for developing novel strategies for intervention of fungal diseases in food crops and ultimately helping to ensure global food security.

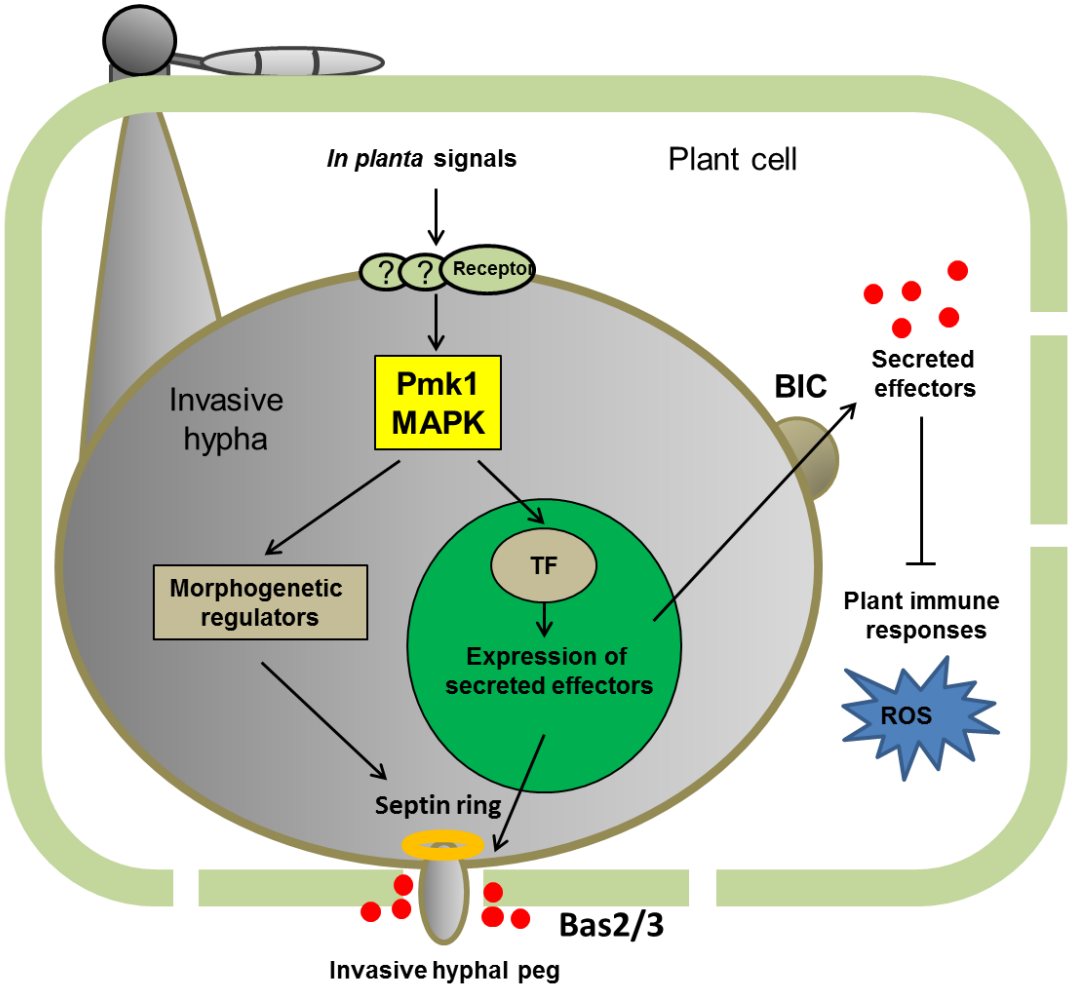

Figure 6.1 Model illustrating the Pmk1-regulated invasive growth by the rice blast fungus.

Bibliography

Adachi, K. and Hamer, J. E. (1998) Divergent cAMP signaling pathways regulate growth and pathogenesis in the rice blast fungus *Magnaporthe grisea*. *Plant Cell,* **10,** 1361-1374.

Akamatsu, A., Wong, Hann L., Fujiwara, M., Okuda, J., Nishide, K., Uno, K.*, et al.* (2013) An OsCEBiP/OsCERK1-OsRacGEF1-OsRac1 module is an essential early component of chitin-induced rice immunity. *Cell Host & Microbe,* **13,** 465-476.

Anders, S. and Huber, W. (2010) Differential expression analysis for sequence count data. *Genome biology,* **11,** 1.

Anders, S., Pyl, P. T. and Huber, W. (2014) HTSeq–a Python framework to work with high-throughput sequencing data. *Bioinformatics***,** btu638.

Arazoe, T., Miyoshi, K., Yamato, T., Ogawa, T., Ohsato, S., Arie, T.*, et al.* (2015) Tailor-made CRISPR/Cas system for highly efficient targeted gene replacement in the rice blast fungus. *Biotechnology and bioengineering,* **112,** 2543-2549.

Balhadère, P. V. and Talbot, N. J. (2001) PDE1 encodes a P-type ATPase involved in appressorium-mediated plant infection by the rice blast fungus *Magnaporthe grisea*. *The Plant Cell,* **13,** 1987-2004.

Banuett, F. and Herskowitz, I. (1994) Identification of fuz7, a *Ustilago maydis* MEK/MAPKK homolog required for a-locus-dependent and -independent steps in the fungal life cycle. *Genes Dev,* **8,** 1367-1378.

Baxter, A., Mittler, R. and Suzuki, N. (2013) ROS as key players in plant stress signalling. *Journal of Experimental Botany*.

Bergen, L., Upshall, A. and Morris, N. (1984a) S-phase, G2, and nuclear division mutants of *Aspergillus nidulans*. *Journal of Bacteriology,* **159,** 114-119.

Bergen, L. G., Upshall, A. and Morris, N. R. (1984b) S-phase, G2, and nuclear division mutants of *Aspergillus nidulans*. *Journal of Bacteriology,* **159,** 114-119.

Berman, J. (2006) Morphogenesis and cell cycle progression in *Candida albicans*. *Current opinion in microbiology,* **9,** 595-601.

Bielska, E., Higuchi, Y., Schuster, M., Steinberg, N., Kilaru, S., Talbot, N. J.*, et al.* (2014) Long-distance endosome trafficking drives fungal effector production during plant infection. *Nature communications,* **5**.

Bishop, A. C., Ubersax, J. A., Petsch, D. T., Matheos, D. P., Gray, N. S., Blethrow, J.*, et al.* (2000a) A chemical switch for inhibitor-sensitive alleles of any protein kinase. *Nature,* **407,** 395-401.

Bishop, A. C., Ubersax, J. A., Petsch, D. T., Matheos, D. P., Gray, N. S., Blethrow, J.*, et al.* (2000b) A chemical switch for inhibitor-sensitive alleles of any protein kinase. *Nature,* **407,** 395-401.

Bloom, J. and Cross, F. R. (2007) Multiple levels of cyclin specificity in cell-cycle control. *Nature Reviews Molecular Cell Biology,* **8,** 149-160.

Blümke, A., Falter, C., Herrfurth, C., Sode, B., Bode, R., Schäfer, W.*, et al.* (2014) Secreted fungal effector lipase releases free fatty acids to inhibit innate immunity-related callose formation during wheat head infection. *Plant Physiology,* **165,** 346-358.

Boller, T. and Felix, G. (2009) A renaissance of elicitors: perception of microbe-associated molecular patterns and danger signals by pattern-recognition receptors. *Annual review of plant biology,* **60,** 379-406.

Bougourd, S., Marrison, J. and Haseloff, J. (2000) Technical advance: an aniline blue staining procedure for confocal microscopy and 3D imaging of normal and perturbed cellular phenotypes in mature Arabidopsis embryos. *Plant J,* **24,** 543-550.

Bourett, T. M. and Howard, R. J. (1990) *In vitro* development of penetration structures in the rice blast fungus *Magnaporthe grisea*. *Canadian Journal of botany,* **68,** 329-342.

Brachmann, A., Schirawski, J., Muller, P. and Kahmann, R. (2003) An unusual MAP kinase is required for efficient penetration of the plant surface by *Ustilago maydis*. *Embo j,* **22,** 2199-2210.

Bradley, D. J., Kjellbom, P. and Lamb, C. J. (1992) Elicitor- and wound-induced oxidative cross-linking of a proline-rich plant cell wall protein: a novel, rapid defense response. *Cell,* **70,** 21-30.

Brefort, T., Doehlemann, G., Mendoza-Mendoza, A., Reissmann, S., Djamei, A. and Kahmann, R. (2009) *Ustilago maydis* as a pathogen. *Annu Rev Phytopathol,* **47,** 423-445.

Brown, N. A., Urban, M., van de Meene, A. M. and Hammond-Kosack, K. E. (2010) The infection biology of *Fusarium graminearum*: defining the pathways of spikelet to spikelet colonisation in wheat ears. *Fungal biology,* **114,** 555-571.

Bruno, K. S., Tenjo, F., Li, L., Hamer, J. E. and Xu, J.-R. (2004) Cellular localization and role of kinase activity of PMK1 in *Magnaporthe grisea*. *Eukaryotic Cell,* **3,** 1525-1532.

Burch-Smith, T. M. and Zambryski, P. C. (2012) Plasmodesmata paradigm shift: regulation from without versus within. *Annual review of plant biology,* **63,** 239-260.

Cain, C. W., Lohse, M. B., Homann, O. R., Sil, A. and Johnson, A. D. (2012) A conserved transcriptional regulator governs fungal morphology in widely diverged species. *Genetics,* **190,** 511-521.

Carella, P., Isaacs, M. and Cameron, R. K. (2015) Plasmodesmata-located protein overexpression negatively impacts the manifestation of systemic acquired resistance and the long-distance movement of Defective in Induced Resistance1 in Arabidopsis. *Plant Biology,* **17,** 395-401.

Castanheira, S., Mielnichuk, N. and Perez-Martin, J. (2014) Programmed cell cycle arrest is required for infection of corn plants by the fungus *Ustilago maydis*. *Development (Cambridge, England),* **141,** 4817-4826.

Cesari, S., Thilliez, G., Ribot, C., Chalvon, V., Michel, C., Jauneau, A.*, et al.* (2013) The rice resistance protein pair RGA4/RGA5 recognizes the *Magnaporthe oryzae* effectors AVR-Pia and AVR1-CO39 by direct binding. *The Plant Cell Online*.

Chambard, J.-C., Lefloch, R., Pouysségur, J. and Lenormand, P. (2007) ERK implication in cell cycle regulation. *Biochimica et Biophysica Acta (BBA)-Molecular Cell Research,* **1773,** 1299-1310.

Chanclud, E., Kisiala, A., Emery, N. R. J., Chalvon, V., Ducasse, A., Romiti-Michel, C.*, et al.* (2016) Cytokinin production by the rice blast fungus is a pivotal requirement for full virulence. *PLoS Pathog,* **12,** e1005457.

Chen, J., Zheng, W., Zheng, S., Zhang, D., Sang, W., Chen, X.*, et al.* (2008) Rac1 is required for pathogenicity and Chm1-dependent conidiogenesis in rice fungal pathogen *Magnaporthe grisea*. *PLoS Pathog,* **4,** e1000202.

Chen, R. E. and Thorner, J. (2007) Function and regulation in MAPK signaling pathways: lessons learned from the yeast *Saccharomyces cerevisiae*. *Biochimica et Biophysica Acta (BBA)-Molecular Cell Research,* **1773,** 1311-1340.

Chen, X. and Ronald, P. C. (2011) Innate immunity in rice. *Trends in plant science,* **16,** 451-459.

Chen, Y., Zhai, S., Zhang, H., Zuo, R., Wang, J., Guo, M.*, et al.* (2014) Shared and distinct functions of two Gti1/Pac2 family proteins in growth, morphogenesis and pathogenicity of *Magnaporthe oryzae*. *Environmental microbiology,* **16,** 788-801.

Chi, M.-H., Park, S.-Y., Kim, S. and Lee, Y.-H. (2009) A novel pathogenicity gene is required in the rice blast fungus to suppress the basal defenses of the host. *PLoS Pathog,* **5,** e1000401.

Choi, W. and Dean, R. A. (1997) The adenylate cyclase gene MAC1 of *Magnaporthe grisea* controls appressorium formation and other aspects of growth and development. *The Plant Cell,* **9,** 1973-1983.

Chumley, F. G. and Valent, B. (1990) Genetic analysis of melanin-deficient, nonpathogenic mutants of *Magnaporthe grisea*. *Mol. Plant-Microbe Interact,* **3,** 135-143.

Cid, V. J., Adamikova, L., Sanchez, M., Molina, M. and Nombela, C. (2001) Cell cycle control of septin ring dynamics in the budding yeast. *Microbiology (Reading, England),* **147,** 1437-1450.

Conesa, A. and Götz, S. (2008) Blast2GO: a comprehensive suite for functional analysis in plant genomics. *International Journal of Plant Genomics,* **2008,** 619832.

Couch, B. C. and Kohn, L. M. (2002) A multilocus gene genealogy concordant with host preference indicates segregation of a new species, *Magnaporthe oryzae*, from *M. grisea*. *Mycologia,* **94,** 683-693.

Coudreuse, D. and Nurse, P. (2010) Driving the cell cycle with a minimal CDK control network. *Nature,* **468,** 1074-1079.

Cousin, A., Mehrabi, R., Guilleroux, M., Dufresne, M., T, V. D. L., Waalwijk, C.*, et al.* (2006) The MAP kinase-encoding gene MgFus3 of the non-appressorium phytopathogen *Mycosphaerella graminicola* is required for penetration and in vitro pycnidia formation. *Mol Plant Pathol,* **7,** 269-278.

Couto, D. and Zipfel, C. (2016) Regulation of pattern recognition receptor signalling in plants. *Nat Rev Immunol,* **16,** 537-552.

Cui, H., Tsuda, K. and Parker, J. E. (2015) Effector-triggered immunity: from pathogen perception to robust defense. *Annual review of plant biology,* **66,** 487-511.

Cui, W. and Lee, J. Y. (2016) Arabidopsis callose synthases CalS1/8 regulate plasmodesmal permeability during stress. *Nature plants,* **2,** 16034.

Cullen, P. J. and Sprague, G. F. (2012) The regulation of filamentous growth in yeast. *Genetics,* **190,** 23-49.

Dagdas, Y. F., Yoshino, K., Dagdas, G., Ryder, L. S., Bielska, E., Steinberg, G.*, et al.* (2012) Septin-mediated plant cell invasion by the rice blast fungus, *Magnaporthe oryzae*. *Science,* **336,** 1590-1595.

Dangl, J. L. and Jones, J. D. G. (2001) Plant pathogens and integrated defence responses to infection. *Nature,* **411,** 826-833.

de Guillen, K., Ortiz-Vallejo, D., Gracy, J., Fournier, E., Kroj, T. and Padilla, A. (2015) Structure analysis uncovers a highly diverse but structurally conserved effector family in phytopathogenic fungi. *PLoS Pathog,* **11,** e1005228.

de Jong, J. C., McCormack, B. J., Smirnoff, N. and Talbot, N. J. (1997) Glycerol generates turgor in rice blast. *Nature,* **389,** 244-244.

de Jonge, R., van Esse, H. P., Kombrink, A., Shinya, T., Desaki, Y., Bours, R.*, et al.* (2010) Conserved fungal LysM effector Ecp6 prevents chitin-triggered immunity in plants. *Science,* **329,** 953-955.

De Storme, N. and Geelen, D. (2014) Callose homeostasis at plasmodesmata: molecular regulators and developmental relevance. *Front Plant Sci,* **5,** 138.

Dean, R. A., Talbot, N. J., Ebbole, D. J., Farman, M. L., Mitchell, T. K., Orbach, M. J.*, et al.* (2005) The genome sequence of the rice blast fungus *Magnaporthe grisea*. *Nature,* **434,** 980-986.

den Hollander, P. W., Kieper, S. N., Borst, J. W. and van Lent, J. W. (2016) The role of plasmodesma-located proteins in tubule-guided virus transport is limited to the plasmodesmata. *Archives of virology,* **161,** 2431-2440.

DeZwaan, T. M., Carroll, A. M., Valent, B. and Sweigard, J. A. (1999) *Magnaporthe grisea* pth11p is a novel plasma membrane protein that mediates appressorium differentiation in response to inductive substrate cues. *Plant Cell,* **11,** 2013-2030.

Dhillon, A. S., Hagan, S., Rath, O. and Kolch, W. (2007) MAP kinase signalling pathways in cancer. *Oncogene,* **26,** 3279-3290.

Di Pietro, A., Garcia-MacEira, F. I., Meglecz, E. and Roncero, M. I. (2001) A MAP kinase of the vascular wilt fungus *Fusarium oxysporum* is essential for root penetration and pathogenesis. *Mol Microbiol,* **39,** 1140-1152.

Dietz, K.-J., Mittler, R. and Noctor, G. (2016) Recent progress in understanding the role of reactive oxygen species in plant cell signaling. *Plant Physiology,* **171,** 1535-1539.

Dixon, K. P., Xu, J.-R., Smirnoff, N. and Talbot, N. J. (1999) Independent signaling pathways regulate cellular turgor during hyperosmotic stress and appressorium-mediated plant infection by *Magnaporthe grisea*. *The Plant Cell,* **11,** 2045-2058.

Dodds, P. N. and Rathjen, J. P. (2010) Plant immunity: towards an integrated view of plant–pathogen interactions. *Nat Rev Genet,* **11,** 539-548.

Ebbole, D. J. (2007) Magnaporthe as a model for understanding host-pathogen interactions. *Annu. Rev. Phytopathol.,* **45,** 437-456.

Egan, M. J., Wang, Z.-Y., Jones, M. A., Smirnoff, N. and Talbot, N. J. (2007) Generation of reactive oxygen species by fungal NADPH oxidases is required for rice blast disease. *Proceedings of the National Academy of Sciences,* **104,** 11772-11777.

Faulkner, C., Petutschnig, E., Benitez-Alfonso, Y., Beck, M., Robatzek, S., Lipka, V.*, et al.* (2013) LYM2-dependent chitin perception limits molecular flux via

plasmodesmata. *Proceedings of the National Academy of Sciences,* **110,** 9166-9170.

Feldbrügge, M., Kämper, J., Steinberg, G. and Kahmann, R. (2004) Regulation of mating and pathogenic development in *Ustilago maydis*. *Current opinion in microbiology,* **7,** 666-672.

Fernandez-Calvino, L., Faulkner, C., Walshaw, J., Saalbach, G., Bayer, E., Benitez-Alfonso, Y.*, et al.* (2011) Arabidopsis plasmodesmal proteome. *PLoS ONE,* **6,** e18880.

Fernandez, J., Marroquin-Guzman, M., Nandakumar, R., Shijo, S., Cornwell, K. M., Li, G.*, et al.* (2014) Plant defence suppression is mediated by a fungal sirtuin during rice infection by *Magnaporthe oryzae*. *Mol Microbiol,* **94,** 70-88.

Fernandez, J. and Wilson, R. A. (2011) The sugar sensor, trehalose-6-phosphate synthase (Tps1), regulates primary and secondary metabolism during infection by the rice blast fungus: Will *Magnaporthe oryzae*'s "sweet tooth" become its "Achilles' heel"? *Mycology,* **2,** 46-53.

Fernandez, J. and Wilson, R. A. (2014) Cells in cells: morphogenetic and metabolic strategies conditioning rice infection by the blast fungus *Magnaporthe oryzae*. *Protoplasma,* **251,** 37-47.

Fernandez, J., Wright, J. D., Hartline, D., Quispe, C. F., Madayiputhiya, N. and Wilson, R. A. (2012) Principles of carbon catabolite repression in the rice blast fungus: Tps1, Nmr1-3, and a MATE-family pump regulate glucose metabolism during infection. *PLoS genetics,* **8,** e1002673.

Fisher, M. C., Henk, D. A., Briggs, C. J., Brownstein, J. S., Madoff, L. C., McCraw, S. L.*, et al.* (2012) Emerging fungal threats to animal, plant and ecosystem health. *Nature,* **484,** 186-194.

Fleißner, A. (2013) Turning the switch: using chemical genetics to elucidate protein kinase functions in filamentous fungi. *Fungal Biology Reviews,* **27,** 25-31.

Fleissner, A., Leeder, A. C., Roca, M. G., Read, N. D. and Glass, N. L. (2009) Oscillatory recruitment of signaling proteins to cell tips promotes coordinated behavior during cell fusion. *Proceedings of the National Academy of Sciences,* **106,** 19387-19392.

Foster, A. J., Jenkinson, J. M. and Talbot, N. J. (2003) Trehalose synthesis and metabolism are required at different stages of plant infection by *Magnaporthe grisea*. *The EMBO journal,* **22,** 225-235.

Fu, J., Liu, H., Li, Y., Yu, H., Li, X., Xiao, J.*, et al.* (2011) Manipulating broad-spectrum disease resistance by suppressing pathogen-induced auxin accumulation in rice. *Plant physiology,* **155,** 589-602.

Fujisaki, K., Abe, Y., Ito, A., Saitoh, H., Yoshida, K., Kanzaki, H.*, et al.* (2015) Rice Exo70 interacts with a fungal effector, AVR-Pii, and is required for AVR-Pii-triggered immunity. *The Plant Journal,* **83,** 875-887.

Fukada, F. and Kubo, Y. (2015) Colletotrichum orbiculare regulates cell cycle G1/S progression via a two-component GAP and a GTPase to establish plant infection. *The Plant Cell,* **27,** 2530-2544.

Furnari, B., Blasina, A., Boddy, M. N., McGowan, C. H. and Russell, P. (1999) Cdc25 inhibited in vivo and in vitro by checkpoint kinases Cds1 and Chk1. *Molecular biology of the cell,* **10,** 833-845.

Gartner, A., Jovanović, A., Jeoung, D.-I., Bourlat, S., Cross, F. R. and Ammerer, G. (1998) Pheromone-dependent G1 cell cycle arrest requires Far1 phosphorylation, but may not involve inhibition of Cdc28-Cln2 kinase, in vivo. *Molecular and Cellular Biology,* **18,** 3681-3691.

Gilbert, M. J., Thornton, C. R., Wakley, G. E. and Talbot, N. J. (2006) A P-type ATPase required for rice blast disease and induction of host resistance. *Nature,* **440,** 535-539.

Giraldo, M. C., Dagdas, Y. F., Gupta, Y. K., Mentlak, T. A., Yi, M., Martinez-Rocha, A. L.*, et al.* (2013) Two distinct secretion systems facilitate tissue invasion by the rice blast fungus *Magnaporthe oryzae*. *Nat Commun,* **4,** 1996.

Giraldo, M. C. and Valent, B. (2013) Filamentous plant pathogen effectors in action. *Nat Rev Micro,* **11,** 800-814.

Gosling, P., Jones, J. and Bending, G. D. (2016) Evidence for functional redundancy in arbuscular mycorrhizal fungi and implications for agroecosystem management. *Mycorrhiza,* **26,** 77-83.

Gupta, Y. K., Dagdas, Y. F., Martinez-Rocha, A.-L., Kershaw, M. J., Littlejohn, G. R., Ryder, L. S.*, et al.* (2015) Septin-dependent assembly of the exocyst is essential for plant infection by *Magnaporthe oryzae*. *The Plant Cell,* **27,** 3277-3289.

Hacker, C., Howell, M., Bhella, D. and Lucocq, J. (2014) Strategies for maximizing ATP supply in the microsporidian *Encephalitozoon cuniculi*: direct binding of mitochondria to the parasitophorous vacuole and clustering of the mitochondrial porin VDAC. *Cellular microbiology,* **16,** 565-579.

Hamel, L.-P., Nicole, M.-C., Duplessis, S. and Ellis, B. E. (2012) Mitogen-activated protein kinase signaling in plant-interacting fungi: distinct messages from conserved messengers. *The Plant Cell,* **24,** 1327-1351.

Hamer, J. E., Howard, R. J., Chumley, F. G. and Valent, B. (1988) A mechanism for surface attachment in spores of a plant pathogenic fungus. *Science,* **239,** 288-290.

Haueisen, J. and Stukenbrock, E. H. (2016) Life cycle specialization of filamentous pathogens - colonization and reproduction in plant tissues. *Curr Opin Microbiol,* **32,** 31-37.

Hemetsberger, C., Herrberger, C., Zechmann, B., Hillmer, M. and Doehlemann, G. (2012) The *Ustilago maydis* effector Pep1 suppresses plant immunity by inhibition of host peroxidase activity. *PLoS Pathog,* **8,** e1002684.

Herskowitz, I. (1995) MAP kinase pathways in yeast: for mating and more. *Cell,* **80,** 187-197.

Howard, R. J., Ferrari, M. A., Roach, D. H. and Money, N. P. (1991) Penetration of hard substrates by a fungus employing enormous turgor pressures. *Proceedings of the National Academy of Sciences of the United States of America,* **88,** 11281-11284.

Howard, R. J. and Valent, B. (1996) Breaking and entering: host penetration by the fungal rice blast pathogen *Magnaporthe grisea*. *Annual Reviews in Microbiology,* **50,** 491-512.

Howell, A. S. and Lew, D. J. (2012) Morphogenesis and the cell cycle. *Genetics,* **190,** 51-77.

Igarashi, S., Utiamada, C. M., Igarashi, L. C., Kazuma, A. H. and Lopes, R. S. (1986) Pyricularia em trigo. 1. Ocorrência de Pyricularia sp. no estado do Paraná. *Fitopatologia Brasileira,* **11,** 351-352.

Islam, T., Croll, D., Gladieux, P., Soanes, D., Persoons, A., Bhattacharjee, P.*, et al.* (2016) Emergence of wheat blast in Bangladesh was caused by a South American lineage of *Magnaporthe oryzae*. *bioRxiv*.

Jacob, S., Foster, A. J., Yemelin, A. and Thines, E. (2014) Histidine kinases mediate differentiation, stress response, and pathogenicity in *Magnaporthe oryzae*. *MicrobiologyOpen,* **3,** 668-687.

James, S. W., Banta, T., Barra, J., Ciraku, L., Coile, C., Cuda, Z.*, et al.* (2014) Restraint of the G2/M transition by the SR/RRM family mRNA shuttling binding protein SNXAHRB1 in *Aspergillus nidulans*. *Genetics,* **198,** 617-633.

Jenczmionka, N. J. and Schäfer, W. (2005) The Gpmk1 MAP kinase of *Fusarium graminearum* regulates the induction of specific secreted enzymes. *Current genetics,* **47,** 29-36.

Jeon, J., Park, S. Y., Chi, M. H., Choi, J., Park, J., Rho, H. S.*, et al.* (2007) Genome-wide functional analysis of pathogenicity genes in the rice blast fungus. *Nature genetics,* **39,** 561-565.

Jia, Y., McAdams, S. A., Bryan, G. T., Hershey, H. P. and Valent, B. (2000) Direct interaction of resistance gene and avirulence gene products confers rice blast resistance. *The EMBO Journal,* **19,** 4004-4014.

Jones, J. D. G. and Dangl, J. L. (2006) The plant immune system. *Nature,* **444,** 323-329.

Jones, K., Jenkinson, C. B., Borges Araujo, M., Zhu, J., Kim, R. Y., Kim, D. W.*, et al.* (2016a) Mitotic stopwatch for the blast fungus *Magnaporthe oryzae* during invasion of rice cells. *Fungal genetics and biology : FG & B,* **93,** 46-49.

Jones, K., Kim, D. W., Park, J. S. and Khang, C. H. (2016b) Live-cell fluorescence imaging to investigate the dynamics of plant cell death during infection by the rice blast fungus *Magnaporthe oryzae*. *BMC Plant Biology,* **16,** 1-8.

Kahmann, R. and Kämper, J. (2004) *Ustilago maydis*: how its biology relates to pathogenic development. *New Phytologist,* **164,** 31-42.

Kamper, J., Kahmann, R., Bolker, M., Ma, L.J., Brefort, T., Saville, B. J.*, et al.* (2006) Insights from the genome of the biotrophic fungal plant pathogen *Ustilago maydis*. *Nature,* **444,** 97-101.

Kankanala, P., Czymmek, K. and Valent, B. (2007) Roles for rice membrane dynamics and plasmodesmata during biotrophic invasion by the blast fungus. *The Plant Cell,* **19,** 706-724.

Kershaw, M. J. and Talbot, N. J. (2009) Genome-wide functional analysis reveals that infection-associated fungal autophagy is necessary for rice blast disease. *Proceedings of the National Academy of Sciences of the United States of America,* **106,** 15967-15972.

Khang, C. H., Berruyer, R., Giraldo, M. C., Kankanala, P., Park, S.Y., Czymmek, K.*, et al.* (2010) Translocation of *Magnaporthe oryzae* effectors into rice cells and their subsequent cell-to-cell movement. *Plant Cell,* **22**.

Kihoro, J., Bosco, N. J., Murage, H., Ateka, E. and Makihara, D. (2013) Investigating the impact of rice blast disease on the livelihood of the local farmers in greater Mwea region of Kenya. *SpringerPlus,* **2,** 308.

Kim, D., Pertea, G., Trapnell, C., Pimentel, H., Kelley, R. and Salzberg, S. L. (2013) TopHat2: accurate alignment of transcriptomes in the presence of insertions, deletions and gene fusions. *Genome biology,* **14,** 1.

Kim, S., Park, S. Y., Kim, K. S., Rho, H. S., Chi, M. H., Choi, J.*, et al.* (2009) Homeobox transcription factors are required for conidiation and appressorium development in the rice blast fungus *Magnaporthe oryzae*. *PLoS genetics,* **5,** e1000757.

Kim, Y.-K., Kawano, T., Li, D. and Kolattukudy, P. E. (2000) A mitogen-activated protein kinase kinase required for induction of cytokinesis and appressorium formation by host signals in the conidia of *Colletotrichum gloeosporioides*. *The Plant Cell,* **12,** 1331-1344.

Kleemann, J., Rincon-Rivera, L. J., Takahara, H., Neumann, U., van Themaat, E. V. L., van der Does, H. C.*, et al.* (2012) Sequential delivery of host-induced virulence effectors by appressoria and intracellular hyphae of the phytopathogen *Colletotrichum higginsianum*. *PLoS Pathog,* **8,** e1002643.

Knox, J. P. and Benitez-Alfonso, Y. (2014) Roles and regulation of plant cell walls surrounding plasmodesmata. *Curr Opin Plant Biol,* **22,** 93-100.

Kouzai, Y., Mochizuki, S., Nakajima, K., Desaki, Y., Hayafune, M., Miyazaki, H.*, et al.* (2014a) Targeted gene disruption of OsCERK1 reveals its indispensable role in chitin perception and involvement in the peptidoglycan response and immunity in rice. *Molecular Plant-Microbe Interactions,* **27,** 975-982.

Kouzai, Y., Nakajima, K., Hayafune, M., Ozawa, K., Kaku, H., Shibuya, N.*, et al.* (2014b) CEBiP is the major chitin oligomer-binding protein in rice and plays a main role in the perception of chitin oligomers. *Plant molecular biology,* **84,** 519-528.

Kroj, T., Chanclud, E., Michel-Romiti, C., Grand, X. and Morel, J. B. (2016) Integration of decoy domains derived from protein targets of pathogen effectors into plant immune receptors is widespread. *The New phytologist,* **210,** 618-626.

Lee, J.-Y., Wang, X., Cui, W., Sager, R., Modla, S., Czymmek, K.*, et al.* (2011) A plasmodesmata-localized protein mediates crosstalk between cell-to-cell communication and innate immunity in Arabidopsis. *The Plant Cell,* **23,** 3353-3373.

Lee, J. Y. (2015) Plasmodesmata: a signaling hub at the cellular boundary. *Curr Opin Plant Biol,* **27,** 133-140.

Lee, Y. H. and Dean, R. A. (1993) cAMP Regulates Infection Structure Formation in the Plant Pathogenic Fungus *Magnaporthe grisea*. *The Plant Cell,* **5,** 693-700.

Lev, S., Sharon, A., Hadar, R., Ma, H. and Horwitz, B. A. (1999) A mitogen-activated protein kinase of the corn leaf pathogen *Cochliobolus heterostrophus* is involved in conidiation, appressorium formation, and pathogenicity: diverse roles for mitogen-activated protein kinase homologs in foliar pathogens. *Proceedings of the National Academy of Sciences,* **96,** 13542-13547.

Lew, D. J. and Reed, S. I. (1993) Morphogenesis in the yeast cell cycle: regulation by Cdc28 and cyclins. *The Journal of cell biology,* **120,** 1305-1320.

Li, G., Zhou, X., Kong, L., Wang, Y., Zhang, H., Zhu, H.*, et al.* (2011) MoSfl1 is important for virulence and heat tolerance in *Magnaporthe oryzae*. *PLoS One,* **6,** e19951.

Li, G., Zhou, X. and Xu, J.R. (2012) Genetic control of infection-related development in *Magnaporthe oryzae*. *Current opinion in microbiology,* **15,** 678-684.

Li, L., Xue, C., Bruno, K., Nishimura, M. and Xu, J.-R. (2004) Two PAK kinase genes, CHM1 and MST20, have distinct functions in *Magnaporthe grisea*. *Molecular plant-microbe interactions,* **17,** 547-556.

Li, W., Wang, B., Wu, J., Lu, G., Hu, Y., Zhang, X.*, et al.* (2009) The *Magnaporthe oryzae* avirulence gene AvrPiz-t encodes a predicted secreted protein that triggers the immunity in rice mediated by the blast resistance gene Piz-t. *Molecular Plant-Microbe Interactions,* **22,** 411-420.

Li, Y., Wang, G., Xu, J.-R. and Jiang, C. (2015) Penetration peg formation and invasive hyphae development require stage-specific activation of MoGTI1 in *Magnaporthe oryzae*. *Molecular Plant-Microbe Interactions,* **29,** 36-45.

Liu, B., Li, J. F., Ao, Y., Qu, J., Li, Z., Su, J.*, et al.* (2012) Lysin motif-containing proteins LYP4 and LYP6 play dual roles in peptidoglycan and chitin perception in rice innate immunity. *Plant Cell,* **24,** 3406-3419.

Liu, H., Suresh, A., Willard, F. S., Siderovski, D. P., Lu, S. and Naqvi, N. I. (2007) Rgs1 regulates multiple Gα subunits in Magnaporthe pathogenesis, asexual growth and thigmotropism. *The EMBO Journal,* **26,** 690-700.

Liu, S. and Dean, R. A. (1997) G protein α subunit genes control growth, development, and pathogenicity of *Magnaporthe grisea*. *Molecular Plant-Microbe Interactions,* **10,** 1075-1086.

Liu, W., Liu, J., Ning, Y., Ding, B., Wang, X., Wang, Z.*, et al.* (2013) Recent progress in understanding PAMP- and effector-triggered immunity against the rice blast fungus *Magnaporthe oryzae*. *Molecular Plant,* **6,** 605-620.

Liu, W., Liu, J., Triplett, L., Leach, J. E. and Wang, G.-L. (2014) Novel insights into rice innate immunity against bacterial and fungal pathogens. *Annual Review of Phytopathology,* **52,** 213-241.

Liu, W., Zhou, X., Li, G., Li, L., Kong, L., Wang, C.*, et al.* (2011) Multiple plant surface signals are sensed by different mechanisms in the rice blast fungus for appressorium formation. *PLoS Pathog,* **7,** e1001261.

Lo Iacono, G., van den Bosch, F. and Gilligan, C. A. (2013) Durable resistance to crop pathogens: an epidemiological framework to predict risk under uncertainty. *PLoS Computational Biology,* **9,** e1002870.

Lo Presti, L., Lanver, D., Schweizer, G., Tanaka, S., Liang, L., Tollot, M.*, et al.* (2015) Fungal effectors and plant susceptibility. *Annual review of plant biology,* **66,** 513-545.

Lucas, W. J. (2006) Plant viral movement proteins: agents for cell-to-cell trafficking of viral genomes. *Virology,* **344,** 169-184.

Malaker, P. K., Barma, N. C. D., Tiwari, T. P., Collis, W. J., Duveiller, E., Singh, P. K.*, et al.* (2016) First report of wheat blast caused by *Magnaporthe oryzae* pathotype triticum in Bangladesh. *Plant Disease***,** PDIS-05-16-0666-PDN.

Malinovsky, F. G., Fangel, J. U. and Willats, W. G. T. (2014) The role of the cell wall in plant immunity. *Frontiers in Plant Science,* **5**.

Maqbool, A., Saitoh, H., Franceschetti, M., Stevenson, C. E. M., Uemura, A., Kanzaki, H.*, et al.* (2015) Structural basis of pathogen recognition by an integrated HMA domain in a plant NLR immune receptor. *eLife,* **4,** e08709.

Mathioni, S. M., Patel, N., Riddick, B., Sweigard, J. A., Czymmek, K. J., Caplan, J. L.*, et al.* (2013) Transcriptomics of the rice blast fungus *Magnaporthe oryzae* in response to the bacterial antagonist Lysobacter enzymogenes reveals candidate fungal defense response genes. *PloS one,* **8,** e76487.

Mayer, F. L., Wilson, D. and Hube, B. (2013) *Candida albicans* pathogenicity mechanisms. *Virulence,* **4,** 119-128.

Mayorga, M. E. and Gold, S. E. (1999) A MAP kinase encoded by the ubc3 gene of *Ustilago maydis* is required for filamentous growth and full virulence. *Mol Microbiol,* **34,** 485-497.

McCusker, D., Denison, C., Anderson, S., Egelhofer, T. A., Yates, J. R., Gygi, S. P.*, et al.* (2007) Cdk1 coordinates cell-surface growth with the cell cycle. *Nat Cell Biol,* **9,** 506-515.

Mentlak, T. A., Kombrink, A., Shinya, T., Ryder, L. S., Otomo, I., Saitoh, H.*, et al.* (2012) Effector-mediated suppression of chitin-triggered immunity by *Magnaporthe oryzae* is necessary for rice blast disease. *Plant Cell,* **24,** 322-335.

Mims, C. W., Richardson, E. A., Holt Iii, B. F. and Dangl, J. L. (2004) Ultrastructure of the host–pathogen interface in *Arabidopsis thaliana* leaves infected by the downy mildew *Hyaloperonospora parasitica*. *Canadian Journal of Botany,* **82,** 1001-1008.

Mitchell, T. K. and Dean, R. A. (1995) The cAMP-dependent protein kinase catalytic subunit is required for appressorium formation and pathogenesis by the rice blast pathogen *Magnaporthe grisea*. *The Plant Cell,* **7,** 1869-1878.

Mizunuma, M., Tsubakiyama, R., Ogawa, T., Shitamukai, A., Kobayashi, Y., Inai, T.*, et al.* (2013) Ras/cAMP-dependent protein kinase (PKA) regulates multiple aspects of cellular events by phosphorylating the Whi3 cell cycle regulator in budding yeast. *Journal of Biological Chemistry,* **288,** 10558-10566.

Mochizuki, S., Minami, E. and Nishizawa, Y. (2015) Live-cell imaging of rice cytological changes reveals the importance of host vacuole maintenance for biotrophic invasion by blast fungus, *Magnaporthe oryzae*. *MicrobiologyOpen,* **4,** 952-966.

Mogga, V., Delventhal, R., Weidenbach, D., Langer, S., Bertram, P. M., Andresen, K.*, et al.* (2016) *Magnaporthe oryzae* effectors MoHEG13 and MoHEG16 interfere with host infection and MoHEG13 counteracts cell death caused by Magnaporthe-NLPs in tobacco. *Plant cell reports,* **35,** 1169-1185.

Mosquera, G., Giraldo, M. C., Khang, C. H., Coughlan, S. and Valent, B. (2009) Interaction transcriptome analysis identifies *Magnaporthe oryzae* BAS1-4 as biotrophy-associated secreted proteins in rice blast disease. *The Plant Cell,* **21,** 1273-1290.

Nguyen, L. N., Dao, T. T., Živković, T., Fehrholz, M., Schäfer, W. and Salomon, S. (2010) Enzymatic properties and expression patterns of five extracellular lipases of *Fusarium graminearum in vitro*. *Enzyme and microbial technology,* **46,** 479-486.

Nishimura, M., Park, G. and Xu, J.-R. (2003) The G-beta subunit MGB1 is involved in regulating multiple steps of infection-related morphogenesis in *Magnaporthe grisea*. *Molecular Microbiology,* **50,** 231-243.

Nishizawa, Y., Mochizuki, S., Yokotani, N., Nishimura, T. and Minami, E. (2016) Molecular and cellular analysis of the biotrophic interaction between rice and *Magnaporthe oryzae*–Exploring situations in which the blast fungus controls the infection. *Physiological and Molecular Plant Pathology,* **95,** 70-76.

O'Connell, M., Osmani, A., Morris, N. and Osmani, S. (1992) An extra copy of nimEcyclinB elevates pre-MPF levels and partially suppresses mutation of nimTcdc25 in *Aspergillus nidulans*. *The EMBO Journal,* **11,** 2139.

O'Connell, M. J., Walworth, N. C. and Carr, A. M. (2000) The G2-phase DNA-damage checkpoint. *Trends in cell biology,* **10,** 296-303.

Oliveira-Garcia, E. and Valent, B. (2015) How eukaryotic filamentous pathogens evade plant recognition. *Current Opinion in Microbiology,* **26,** 92-101.

Oparka, K. J., Prior, D. A., Santa Cruz, S., Padgett, H. S. and Beachy, R. N. (1997) Gating of epidermal plasmodesmata is restricted to the leading edge of expanding infection sites of tobacco mosaic virus (TMV). *Plant J,* **12,** 781-789.

Oparka, K. J. and Roberts, A. G. (2001) Plasmodesmata. A not so open-and-shut case. *Plant Physiology,* **125,** 123-126.

Orbach, M. J., Farrall, L., Sweigard, J. A., Chumley, F. G. and Valent, B. (2000) A telomeric avirulence gene determines efficacy for the rice blast resistance gene Pi-ta. *The Plant Cell,* **12,** 2019-2032.

Osés-Ruiz, M., Sakulkoo, W. and Talbot, N. J. (2016) 4 Septation and cytokinesis in pathogenic fungi. In: *Growth, Differentiation and Sexuality.* (Wendland, J., ed.). Cham: Springer International Publishing, pp. 67-79.

Park, C.-H., Chen, S., Shirsekar, G., Zhou, B., Khang, C. H., Songkumarn, P.*, et al.* (2012) The *Magnaporthe oryzae* effector AvrPiz-t targets the RING E3 Ubiquitin Ligase APIP6 to suppress pathogen-associated molecular pattern–triggered immunity in rice. *The Plant Cell,* **24,** 4748-4762.

Park, C. H., Shirsekar, G., Bellizzi, M., Chen, S., Songkumarn, P., Xie, X.*, et al.* (2016) The E3 ligase APIP10 connects the effector AvrPiz-t to the NLR receptor Piz-t in rice. *PLoS Pathog,* **12,** e1005529.

Park, G., Bruno, K. S., Staiger, C. J., Talbot, N. J. and Xu, J. R. (2004) Independent genetic mechanisms mediate turgor generation and penetration peg formation during plant infection in the rice blast fungus. *Molecular microbiology,* **53,** 1695-1707.

Park, G., Xue, C., Zhao, X., Kim, Y., Orbach, M. and Xu, J.-R. (2006) Multiple upstream signals converge on the adaptor protein Mst50 in *Magnaporthe grisea*. *The Plant Cell,* **18,** 2822-2835.

Park, G., Xue, C., Zheng, L., Lam, S. and Xu, J.-R. (2002) MST12 regulates infectious growth but not appressorium formation in the rice blast fungus *Magnaporthe grisea*. *Molecular plant-microbe interactions,* **15,** 183-192.

Parker, D., Beckmann, M., Zubair, H., Enot, D. P., Caracuel-Rios, Z., Overy, D. P.*, et al.* (2009) Metabolomic analysis reveals a common pattern of metabolic re-programming during invasion of three host plant species by *Magnaporthe grisea*. *The Plant Journal,* **59,** 723-737.

Patkar, R. N., Benke, P. I., Qu, Z., Chen, Y. Y. C., Yang, F., Swarup, S.*, et al.* (2015) A fungal monooxygenase-derived jasmonate attenuates host innate immunity. *Nature chemical biology,* **11,** 733-740.

Patkar, R. N., Ramos-Pamplona, M., Gupta, A. P., Fan, Y. and Naqvi, N. I. (2012) Mitochondrial β-oxidation regulates organellar integrity and is necessary for conidial germination and invasive growth in *Magnaporthe oryzae*. *Molecular microbiology,* **86,** 1345-1363.

Penn, T. J., Wood, M. E., Soanes, D. M., Csukai, M., Corran, A. J. and Talbot, N. J. (2015) Protein kinase C is essential for viability of the rice blast fungus *Magnaporthe oryzae*. *Molecular microbiology,* **98,** 403-419.

Perez-Martin, J., Bardetti, P., Castanheira, S., de la Torre, A. and Tenorio-Gomez, M. (2016) Virulence-specific cell cycle and morphogenesis connections in pathogenic fungi. *Seminars in cell & developmental biology,* **57,** 93-99.

Pérez-Martín, J., Castillo-Lluva, S., Sgarlata, C., Flor-Parra, I., Mielnichuk, N., Torreblanca, J.*, et al.* (2006) Pathocycles: *Ustilago maydis* as a model to study the relationships between cell cycle and virulence in pathogenic fungi. *Molecular Genetics and Genomics,* **276,** 211-229.

Perez-Nadales, E., Almeida Nogueira, M. F., Baldin, C., Castanheira, S., El Ghalid, M., Grund, E.*, et al.* (2014) Fungal model systems and the elucidation of pathogenicity determinants. *Fungal Genetics and Biology,* **70,** 42-67.

Pham, C. L. L., Rey, A., Lo, V., Soulès, M., Ren, Q., Meisl, G.*, et al.* (2016) Self-assembly of MPG1, a hydrophobin protein from the rice blast fungus that forms functional amyloid coatings, occurs by a surface-driven mechanism. *Scientific Reports,* **6,** 25288.

Prados Rosales, R. C. and Di Pietro, A. (2008) Vegetative hyphal fusion is not essential for plant infection by *Fusarium oxysporum*. *Eukaryot Cell,* **7,** 162-171.

Qi, L., Kim, Y., Jiang, C., Li, Y., Peng, Y. and Xu, J. R. (2015) Activation of Mst11 and feedback inhibition of germ tube growth in *Magnaporthe oryzae*. *Molecular plant-microbe interactions : MPMI,* **28,** 881-891.

Ramanujam, R., Yishi, X., Liu, H. and Naqvi, N. I. (2012) Structure-function analysis of Rgs1 in *Magnaporthe oryzae*: role of DEP domains in subcellular targeting. *PLoS One,* **7,** e41084.

Rauyaree, P., Ospina-Giraldo, M. D., Kang, S., Bhat, R. G., Subbarao, K. V., Grant, S. J.*, et al.* (2005) Mutations in VMK1, a mitogen-activated protein kinase gene, affect microsclerotia formation and pathogenicity in *Verticillium dahliae*. *Current genetics,* **48,** 109-116.

Reynolds, E. S. (1963) The use of lead citrate at high pH as an electron-opaque stain in electron microscopy. *J Cell Biol,* **17,** 208-212.

Rhind, N., Furnari, B. and Russell, P. (1997) Cdc2 tyrosine phosphorylation is required for the DNA damage checkpoint in fission yeast. *Genes & Development,* **11,** 504-511.

Rhind, N. and Russell, P. (2000) Chk1 and Cds1: linchpins of the DNA damage and replication checkpoint pathways. *Journal of Cell Science,* **113,** 3889-3896.

Rispail, N. and Di Pietro, A. (2009) *Fusarium oxysporum* Ste12 controls invasive growth and virulence downstream of the Fmk1 MAPK cascade. *Molecular plant-microbe interactions : MPMI,* **22,** 830-839.

Rispail, N., Soanes, D. M., Ant, C., Czajkowski, R., Grünler, A., Huguet, R.*, et al.* (2009) Comparative genomics of MAP kinase and calcium-calcineurin signalling components in plant and human pathogenic fungi. *Fungal Genetics and Biology,* **46,** 287-298.

Ruiz-Roldan, M. C., Maier, F. J. and Schafer, W. (2001) PTK1, a mitogen-activated-protein kinase gene, is required for conidiation, appressorium formation, and pathogenicity of *Pyrenophora teres* on barley. *Molecular plant-microbe interactions : MPMI,* **14,** 116-125.

Ryder, L. S., Dagdas, Y. F., Mentlak, T. A., Kershaw, M. J., Thornton, C. R., Schuster, M.*, et al.* (2013) NADPH oxidases regulate septin-mediated cytoskeletal remodeling during plant infection by the rice blast fungus. *Proceedings of the National Academy of Sciences,* **110,** 3179-3184.

Ryder, L. S. and Talbot, N. J. (2015) Regulation of appressorium development in pathogenic fungi. *Curr Opin Plant Biol,* **26**.

Salomon, S., Gácser, A., Frerichmann, S., Kröger, C., Schäfer, W. and Voigt, C. A. (2012) The secreted lipase FGL1 is sufficient to restore the initial infection step to the apathogenic *Fusarium graminearum* MAP kinase disruption mutant Δ*gpmk1*. *European journal of plant pathology,* **134,** 23-37.

Sanchez-Vallet, A., Saleem-Batcha, R., Kombrink, A., Hansen, G., Valkenburg, D. J., Thomma, B. P.*, et al.* (2013) Fungal effector Ecp6 outcompetes host immune receptor for chitin binding through intrachain LysM dimerization. *Elife,* **2,** e00790.

Sanchez, Y., Bachant, J., Wang, H., Hu, F., Liu, D., Tetzlaff, M.*, et al.* (1999) Control of the DNA damage checkpoint by chk1 and rad53 protein kinases through distinct mechanisms. *Science,* **286,** 1166-1171.

Sarris, P. F., Duxbury, Z., Huh, S. U., Ma, Y., Segonzac, C., Sklenar, J.*, et al.* (2015) A plant immune receptor detects pathogen effectors that target WRKY transcription factors. *Cell,* **161,** 1089-1100.

Sasaki, T. and Burr, B. (2000) International Rice Genome Sequencing Project: the effort to completely sequence the rice genome. *Curr Opin Plant Biol,* **3,** 138-141.

Saunders, D. G., Aves, S. J. and Talbot, N. J. (2010a) Cell Cycle–Mediated Regulation of Plant Infection by the Rice Blast Fungus. *The Plant Cell Online,* **22,** 497-507.

Saunders, D. G., Dagdas, Y. F. and Talbot, N. J. (2010b) Spatial uncoupling of mitosis and cytokinesis during appressorium-mediated plant infection by the rice blast fungus *Magnaporthe oryzae*. *The Plant Cell,* **22,** 2417-2428.

Sequencing ProjectInternational Rice, G. (2005) The map-based sequence of the rice genome. *Nature,* **436,** 793-800.

Sharpee, W., Oh, Y., Yi, M., Franck, W., Eyre, A., Okagaki, L.*, et al.* (2016) Identification and Characterization of Suppressors of Plant Cell Death (SPD) Genes from *Magnaporthe oryzae*. *Mol Plant Pathol*.

Shi, Z., Christian, D. and Leung, H. (1998) Interactions between spore morphogenetic mutations affect cell types, sporulation, and pathogenesis in *Magnaporthe grisea*. *Molecular Plant-Microbe Interactions,* **11,** 199-207.

Shimizu, T., Nakano, T., Takamizawa, D., Desaki, Y., Ishii-Minami, N., Nishizawa, Y.*, et al.* (2010) Two LysM receptor molecules, CEBiP and OsCERK1, cooperatively regulate chitin elicitor signaling in rice. *Plant J,* **64,** 204-214.

Shinya, T., Nakagawa, T., Kaku, H. and Shibuya, N. (2015) Chitin-mediated plant–fungal interactions: catching, hiding and handshaking. *Current Opinion in Plant Biology,* **26,** 64-71.

Singh, R., Dangol, S., Chen, Y., Choi, J., Cho, Y.-S., Lee, J.-E.*, et al.* (2016) *Magnaporthe oryzae* effector AVR-Pii helps to establish compatibility by inhibition of the rice NADP-Malic enzyme resulting in disruption of oxidative burst and host innate immunity. *Molecules and cells,* **39,** 426.

Skamnioti, P. and Gurr, S. J. (2009) Against the grain: safeguarding rice from rice blast disease. *Trends in biotechnology,* **27,** 141-150.

Soanes, D. M., Chakrabarti, A., Paszkiewicz, K. H., Dawe, A. L. and Talbot, N. J. (2012) Genome-wide transcriptional profiling of appressorium development by the rice blast fungus *Magnaporthe oryzae*. *PLoS Pathog,* **8,** e1002514.

Solomon, P. S., Waters, O. D., Simmonds, J., Cooper, R. M. and Oliver, R. P. (2005) The Mak2 MAP kinase signal transduction pathway is required for pathogenicity in *Stagonospora nodorum*. *Current genetics,* **48,** 60-68.

Sudbery, P. E. (2011) Growth of *Candida albicans* hyphae. *Nature reviews. Microbiology,* **9,** 737-748.

Sudbery, P. E. and Gladfelter, A. S. (2008) Pathocycles. *Fungal genetics and biology : FG & B,* **45,** 1-5.

Takano, Y., Kikuchi, T., Kubo, Y., Hamer, J. E., Mise, K. and Furusawa, I. (2000) The *Colletotrichum lagenarium* MAP kinase gene CMK1 regulates diverse aspects of fungal pathogenesis. *Molecular Plant-Microbe Interactions,* **13,** 374-383.

Talbot, N. J. (2003) On the trail of a cereal killer: exploring the biology of *Magnaporthe grisea*. *Annual Reviews in Microbiology,* **57,** 177-202.

Talbot, N. J., Ebbole, D. J. and Hamer, J. E. (1993) Identification and characterization of MPG1, a gene involved in pathogenicity from the rice blast fungus *Magnaporthe grisea*. *The Plant Cell,* **5,** 1575-1590.

Tanaka, E., Koga, H., Mori, M. and Mori, M. (2011) Auxin production by the rice blast fungus and its localization in host tissue. *Journal of Phytopathology,* **159,** 522-530.

Thines, E., Weber, R. W. and Talbot, N. J. (2000) MAP kinase and protein kinase A–dependent mobilization of triacylglycerol and glycogen during appressorium turgor generation by *Magnaporthe grisea*. *The Plant Cell,* **12,** 1703-1718.

Thomson, D. D., Berman, J. and Brand, A. C. (2016) High frame-rate resolution of cell division during *Candida albicans* filamentation. *Fungal Genetics and Biology,* **88,** 54-58.

Tilsner, J., Nicolas, W., Rosado, A. and Bayer, E. M. (2016) Staying Tight: Plasmodesmal Membrane Contact Sites and the Control of Cell-to-Cell Connectivity in Plants. *Annual review of plant biology,* **67,** 337-364.

Tollot, M., Assmann, D., Becker, C., Altmüller, J., Dutheil, J. Y., Wegner, C.-E.*, et al.* (2016) The WOPR protein Ros1 is a master regulator of sporogenesis and late effector gene expression in the maize pathogen *Ustilago maydis*. *PLoS Pathog,* **12,** e1005697.

Torres, M. A., Jones, J. D. G. and Dangl, J. L. (2006) Reactive oxygen species signaling in response to pathogens. *Plant Physiology,* **141,** 373-378.

Trapnell, C., Roberts, A., Goff, L., Pertea, G., Kim, D., Kelley, D. R.*, et al.* (2012) Differential gene and transcript expression analysis of RNA-seq experiments with TopHat and Cufflinks. *Nature protocols,* **7,** 562-578.

Turra, D., Segorbe, D. and Di Pietro, A. (2014) Protein kinases in plant-pathogenic fungi: conserved regulators of infection. *Annu Rev Phytopathol,* **52,** 267-288.

Urban, M., Mott, E., Farley, T. and Hammond-Kosack, K. (2003) The *Fusarium graminearum* MAP1 gene is essential for pathogenicity and development of perithecia. *Mol Plant Pathol,* **4,** 347-359.

Valent, B., Farrall, L. and Chumley, F. G. (1991) *Magnaporthe grisea* genes for pathogenicity and virulence identified through a series of backcrosses. *Genetics,* **127,** 87-101.

Veneault-Fourrey, C., Barooah, M., Egan, M., Wakley, G. and Talbot, N. J. (2006) Autophagic fungal cell death is necessary for infection by the rice blast fungus. *Science,* **312,** 580-583.

Versele, M. and Thorner, J. (2004) Septin collar formation in budding yeast requires GTP binding and direct phosphorylation by the PAK, Cla4. *J Cell Biol,* **164,** 701-715.

Villalba, F., Collemare, J., Landraud, P., Lambou, K., Brozek, V., Cirer, B.*, et al.* (2008) Improved gene targeting in *Magnaporthe grisea* by inactivation of MgKU80 required for non-homologous end joining. *Fungal genetics and biology : FG & B,* **45,** 68-75.

Voigt, C. A., Schäfer, W. and Salomon, S. (2005) A secreted lipase of *Fusarium graminearum* is a virulence factor required for infection of cereals. *The Plant Journal,* **42,** 364-375.

Wang, G., Li, G., Zhang, S., Jiang, C., Qin, J. and Xu, J. R. (2015) Activation of the signalling mucin MoMsb2 and its functional relationship with Cbp1 in *Magnaporthe oryzae*. *Environ Microbiol,* **17,** 2969-2981.

Wang, X., Sager, R., Cui, W., Zhang, C., Lu, H. and Lee, J.-Y. (2013a) Salicylic acid regulates plasmodesmata closure during innate immune responses in Arabidopsis. *The Plant Cell,* **25,** 2315-2329.

Wang, Y., Wu, J., Kim, S. G., Kim, S. T. and Kang, K. Y. (2013b) A Transient Gene Expression Protocol for Subcellular Protein Localization and Protein Secretion Analyses in Rice.

Wang, Z., Gerstein, M. and Snyder, M. (2009) RNA-Seq: a revolutionary tool for transcriptomics. *Nature reviews genetics,* **10,** 57-63.

Wang, Z. Y., Thornton, C. R., Kershaw, M. J., Debao, L. and Talbot, N. J. (2003) The glyoxylate cycle is required for temporal regulation of virulence by the plant pathogenic fungus *Magnaporthe grisea*. *Molecular microbiology,* **47,** 1601-1612.

Weber, R. W. S., Wakley, G. E., Thines, E. and Talbot, N. J. (2001) The vacuole as central element of the lytic system and sink for lipid droplets in maturing appressoria of*Magnaporthe grisea*. *Protoplasma,* **216,** 101-112.

Weiss, E. L., Bishop, A. C., Shokat, K. M. and Drubin, D. G. (2000) Chemical genetic analysis of the budding-yeast p21-activated kinase Cla4p. *Nat Cell Biol,* **2,** 677-685.

Whisson, S. C., Boevink, P. C., Moleleki, L., Avrova, A. O., Morales, J. G., Gilroy, E. M.*, et al.* (2007) A translocation signal for delivery of oomycete effector proteins into host plant cells. *Nature,* **450,** 115-118.

Widmann, C., Gibson, S., Jarpe, M. B. and Johnson, G. L. (1999) Mitogen-activated protein kinase: conservation of a three-kinase module from yeast to human. *Physiological reviews,* **79,** 143-180.

Wilson, R. A., Gibson, R. P., Quispe, C. F., Littlechild, J. A. and Talbot, N. J. (2010) An NADPH-dependent genetic switch regulates plant infection by the rice blast fungus. *Proceedings of the National Academy of Sciences,* **107,** 21902-21907.

Wilson, R. A., Jenkinson, J. M., Gibson, R. P., Littlechild, J. A., Wang, Z. Y. and Talbot, N. J. (2007) Tps1 regulates the pentose phosphate pathway, nitrogen metabolism and fungal virulence. *The EMBO journal,* **26,** 3673-3685.

Wilson, R. A. and Talbot, N. J. (2009) Under pressure: investigating the biology of plant infection by *Magnaporthe oryzae*. *Nature Reviews Microbiology,* **7,** 185-195.

Wu, C.-H., Krasileva, K., Banfield, M., Terauchi, R. and Kamoun, S. (2015) The "sensor domains" of plant NLR proteins: more than decoys? *Frontiers in Plant Science,* **6,** 134.

Xu, J.-R. and Hamer, J. E. (1996) MAP kinase and cAMP signaling regulate infection structure formation and pathogenic growth in the rice blast fungus *Magnaporthe grisea*. *Genes & development,* **10,** 2696-2706.

Xu, J.-R., Staiger, C. J. and Hamer, J. E. (1998) Inactivation of the mitogen-activated protein kinase Mps1 from the rice blast fungus prevents penetration of host cells but allows activation of plant defense responses. *Proceedings of the National Academy of Sciences,* **95,** 12713-12718.

Yan, X., Li, Y., Yue, X., Wang, C., Que, Y., Kong, D.*, et al.* (2011) Two novel transcriptional regulators are essential for infection-related morphogenesis and pathogenicity of the rice blast fungus *Magnaporthe oryzae*. *PLoS Pathog,* **7,** e1002385.

Yang, D.-L., Yang, Y. and He, Z. (2013) Roles of Plant Hormones and Their Interplay in Rice Immunity. *Molecular Plant,* **6,** 675-685.

Yang, Y., Qi, M. and Mei, C. (2004) Endogenous salicylic acid protects rice plants from oxidative damage caused by aging as well as biotic and abiotic stress. *The Plant Journal,* **40,** 909-919.

Yi, M., Chi, M.-H., Khang, C. H., Park, S.-Y., Kang, S., Valent, B.*, et al.* (2009) The ER chaperone LHS1 is involved in asexual development and rice infection by the blast fungus *Magnaporthe oryzae*. *The Plant Cell,* **21,** 681-695.

Yi, M. and Valent, B. (2013) Communication between filamentous pathogens and plants at the biotrophic interface. *Annu Rev Phytopathol,* **51,** 587-611.

Yoshida, K., Saitoh, H., Fujisawa, S., Kanzaki, H., Matsumura, H., Yoshida, K.*, et al.* (2009) Association genetics reveals three novel avirulence genes from the rice blast fungal pathogen *Magnaporthe oryzae*. *The Plant Cell,* **21,** 1573-1591.

Yu, J., Hu, S., Wang, J., Wong, G. K.-S., Li, S., Liu, B.*, et al.* (2002) A draft sequence of the rice genome (*Oryza sativa* L. ssp. indica). *science,* **296,** 79-92.

Yue, X., Que, Y., Xu, L., Deng, S., Peng, Y., Talbot, N. J., *et al.* (2016) ZNF1 encodes a putative C2H2 zinc-finger protein essential for appressorium differentiation by the rice blast fungus *Magnaporthe oryzae*. *Molecular plant-microbe interactions : MPMI,* **29,** 22-35.

Zeng, Y., Forbes, K. C., Wu, Z., Moreno, S., Piwnica-Worms, H. and Enoch, T. (1998) Replication checkpoint requires phosphorylation of the phosphatase Cdc25 by Cds1 or Chk1. *Nature,* **395,** 507-510.

Zhang, H., Liu, K., Zhang, X., Song, W., Zhao, Q., Dong, Y., *et al.* (2010) A two-component histidine kinase, MoSLN1, is required for cell wall integrity and pathogenicity of the rice blast fungus, *Magnaporthe oryzae*. *Current genetics,* **56,** 517-528.

Zhang, H., Xue, C., Kong, L., Li, G. and Xu, J. R. (2011) A Pmk1-interacting gene is involved in appressorium differentiation and plant infection in *Magnaporthe oryzae*. *Eukaryot Cell,* **10,** 1062-1070.

Zhang, N., Luo, J., Rossman, A. Y., Aoki, T., Chuma, I., Crous, P. W., *et al.* (2016a) Generic names in Magnaporthales. *IMA Fungus,* **7,** 155-159.

Zhang, S., Jiang, C., Zhang, Q., Qi, L., Li, C. and Xu, J.-R. (2016b) Thioredoxins are involved in the activation of the PMK1 MAP kinase pathway during appressorium penetration and invasive growth in *Magnaporthe oryzae*. *Environmental Microbiology***,** n/a-n/a.

Zhao, X., Kim, Y., Park, G. and Xu, J.-R. (2005) A mitogen-activated protein kinase cascade regulating infection-related morphogenesis in *Magnaporthe grisea*. *The Plant Cell,* **17,** 1317-1329.

Zhao, X., Mehrabi, R. and Xu, J.-R. (2007) Mitogen-activated protein kinase pathways and fungal pathogenesis. *Eukaryotic cell,* **6,** 1701-1714.

Zhao, X. and Xu, J. R. (2007) A highly conserved MAPK-docking site in Mst7 is essential for Pmk1 activation in *Magnaporthe grisea*. *Molecular microbiology,* **63,** 881-894.

Zhou, B., Qu, S., Liu, G., Dolan, M., Sakai, H., Lu, G., *et al.* (2006) The eight amino-acid differences within three leucine-rich repeats between Pi2 and Piz-t resistance proteins determine the resistance specificity to *Magnaporthe grisea*. *Molecular plant-microbe interactions,* **19,** 1216-1228.

Zhou, X., Zhang, H., Li, G., Shaw, B. and Xu, J. R. (2012) The Cyclase-associated protein Cap1 is important for proper regulation of infection-related morphogenesis in *Magnaporthe oryzae*. *PLoS Pathog,* **8,** e1002911.

Zhou, X., Zhao, X., Xue, C., Dai, Y. and Xu, J. R. (2014) Bypassing both surface attachment and surface recognition requirements for appressorium formation by overactive ras signaling in *Magnaporthe oryzae*. *Molecular plant-microbe interactions : MPMI,* **27,** 996-1004.

Appendix 1

Metadata of the chapter that will be visualized online

Chapter Title	4 Septation and Cytokinesis in Pathogenic Fungi	
Copyright Year	2016	
Copyright Holder	Springer International Publishing Switzerland	
Author	Family Name	**Osés-Ruiz**
	Particle	
	Given Name	**Míriam**
	Suffix	
	Division	Biosciences
	Organization	College of Life and Environmental Sciences, University of Exeter
	Address	Geoffrey Pope Building, Stocker Road, Exeter EX4 4QD, UK
Author	Family Name	**Sakulkoo**
	Particle	
	Given Name	**Wasin**
	Suffix	
	Division	Biosciences
	Organization	College of Life and Environmental Sciences, University of Exeter
	Address	Geoffrey Pope Building, Stocker Road, Exeter EX4 4QD, UK
Corresponding Author	Family Name	**Talbot**
	Particle	
	Given Name	**Nicholas J.**
	Suffix	
	Division	Biosciences
	Organization	College of Life and Environmental Sciences, University of Exeter
	Address	Geoffrey Pope Building, Stocker Road, Exeter EX4 4QD, UK
	Email	N.J.Talbot@exeter.ac.uk

Abstract

The control of cytokinesis and septation by pathogenic fungi is critical to the developmental changes associated with host invasion and fungal pathogenesis. Pathogenic processes, such as growth within host tissue, often require changes between yeast-like, determinate, isotropic growth and hyphal, polarised, anisotropic growth, which must be appropriately regulated in concert with nuclear division. In plant pathogenic fungi, a body of evidence, primarily generated from studies of the rice blast fungus *M. oryzae*, shows that septin-mediated remodelling of the actin cytoskeleton is fundamental to the action of its specialised infection cells,

called appressoria, during plant infection. Future studies will need to ask several questions which logically follow these recent discoveries. First of all, is the role of septin GTPases in appressorium repolarisation regulated distinctly from their role in each round of septation within vegetative and invasive hyphae? For example, is there a turgor-sensing mechanism that regulates septin ring formation only once the required turgor has been generated in the infection structure to breach the plant cuticle? Is the regulated synthesis of reactive oxygen species, which is essential for septin assembly in *M. oryzae* appressoria, a common mechanism by which septin-dependent processes are regulated in fungi? Can this explain why regulated bursts of ROS are often associated with cellular differentiation in fungi, such as fruit body formation and sporulation? Are the processes identified in *M. oryzae* appressorium development highly conserved among appressorium-forming fungi, such as the rusts, anthracnose-causing fungi and the powdery mildews? If so, can we find evidence for common mechanisms that regulate appressorium-mediated plant infection, such as the conserved MAP kinase cascades (Perez-Nadales et al. 2014), that might be targeted to develop broad spectrum anti-penetrant fungicides? Finally, it is clear that there are important parallels between the way in which yeast budding operates and the operation of fungal appressoria, particularly in the processes leading up to penetration peg formation and repolarisation. Some of the most conserved components probably play similar roles. Clearly, there are important differences as well, not least of all in the enormous invasive forces deployed by appressoria, but the conserved components involved in some of these processes can provide an important roadmap to test hypotheses and define the fundamental mechanisms by which infection structures work in plant pathogenic fungi.

4 Septation and Cytokinesis in Pathogenic Fungi

Míriam Osés-Ruiz[1], Wasin Sakulkoo[1], Nicholas J. Talbot[1]

CONTENTS

I. Introduction to Septation and Cytokinesis

Cell division in all organisms requires the coordination of all cellular processes to allow the formation of two new individual cells. During the eukaryotic cell cycle, correct duplication of genetic material and its subsequent even division, together with the contents of the cytoplasm, are necessary for successful generation of daughter cells. In order to ensure this outcome, the cell possesses cell cycle checkpoints at crucial stages to ensure fidelity and temporal coordination of cell division. In eukaryotes the mechanism that allows final coordination of cell division and compartmentalisation of new cellular components is called cytokinesis. In fungi, cytokinesis adopts different forms. In *Saccharomyces cerevisiae* the process of cytokinesis is called budding, resulting in a new daughter cell from a bud formed by the mother, while in the other major model yeast species *Schizosaccharomyces pombe*, it is called fission and results in two daughter cells of equal size. In filamentous fungi, cytokinesis within a hypha is known as septation and results in discrete hyphal compartments within the multicellular fungal hyphal filament. The processes of budding and fission lead to separation of a daughter cell from its mother cell, allowing formation of new individuals. However, the equivalent process in filamentous fungi, septation, results in new hyphal compartments in which daughter cells remain attached to form a continuous, multicellular organism. This important principle means there are major mechanistic differences in cytokinesis among fungi. In both budding and fission yeast, for example, when a septum is being formed, septum-related proteins are recruited to the site creating a septum and establishing the plane of cell division. It is only after cytokinesis that the septum is degraded and cell separation begins. However, in filamentous fungi, cell separation does not occur, and the septum remains intact, and instead, cell wall material is deposited to the site to contribute to compartmentalisation of the organism (Fig. 4.1), although in the majority of cases, septa remain open, to allow movement of organelles and cytoplasm between fungal cells, which is important for long-distance trafficking and communication, both of which are pivotal to growth and development of filamentous fungi.

The life cycles of pathogenic fungal species are often characterised by morphogenetic

[1]Biosciences, College of Life and Environmental Sciences, University of Exeter, Geoffrey Pope Building, Stocker Road, Exeter EX4 4QD, UK; e-mail: N.J.Talbot@exeter.ac.uk

Growth, Differentiation and Sexuality, 3rd Edition
The Mycota I
J. Wendland (Ed.)

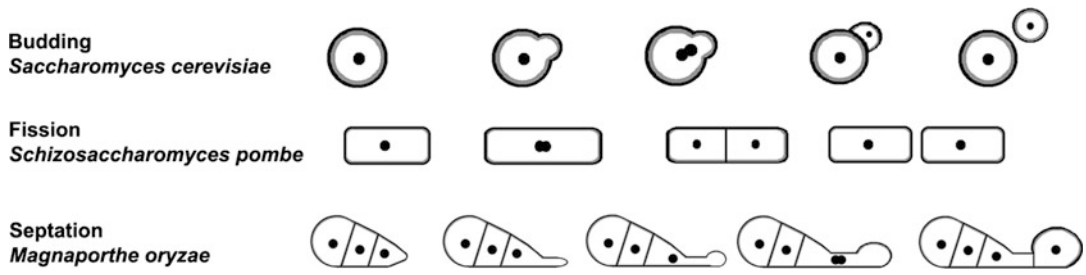

Fig. 4.1 Septation and cytokinesis in filamentous fungi and yeast model organisms. Diagram to show the patterns of nuclear division and septum formation that occur in the budding yeast *S. cerevisiae,* the fission yeast *Sch. pombe* and the filamentous, ascomycete, rice blast fungus *M. oryzae* during infection-associated development

changes, with different fungal growth forms being associated with primary host infection, invasive growth, propagation and dispersal. Many of these developmental transitions have been shown to be essential for the ability to cause disease. For example, the opportunistic pathogen of humans, *Candida albicans*, the cotton pathogen *Ashbya gossypii* and the corn smut fungus *Ustilago maydis* all display pleomorphism with yeast-hyphal transitions and formation of other differentiated cellular forms such as resting spores. These are essential to their ability to cause disease. On many instances, a discrete septation event is necessary for developmental transitions required to cause disease. For example in *Candida albicans*, the core septin GTPase, Cdc12, is associated with cytokinesis and required for virulence (Li et al. 2012). This is part of an emerging body of evidence which suggests that septation and cytokinesis are often key processes in conditioning fungal pathogenicity, due to their important role in infection-related morphogenesis and the changes in cellular form that accompany host invasion (Bridges and Gladfelter 2014). In this chapter, we evaluate emerging evidence that points to a vital role for septation in plant pathogenic fungi, which undergo appressorium development to facilitate entry into their plant hosts. We specifically focus on the filamentous ascomycete fungus *Magnaporthe oryzae*, which is the causal agent of rice blast disease. We have focused on rice blast because of rapid progress in this appressorium-forming fungus compared to other species, which has largely resulted from the size of its research community, driven by the economic importance of the disease. We draw conclusions, however, which we believe may be of more general significance in plant pathogens and, indeed, in other pathogenic fungal species. We also describe parallel studies in other experimental systems that point to more general principles. Finally, we look ahead to the research that will be needed to translate recent advances in understanding the cell biology of infection into a set of more general concepts about fungal biology.

II. The Rice Blast Fungus *Magnaporthe oryzae*

Rice blast disease represents a worldwide threat to food security, causing severe crop losses every year (Talbot 2003). In order to feed the growing world population, which is estimated to reach 9 billion by 2050, global food production will need to increase by at least threefold over the next three decades (Godfray et al. 2010). It is estimated that at least 800 million of the world's population currently live with insufficient nutrition and at least 10 % of the world's food crop production is lost due to plant diseases and infection (Strange and Scott 2005). One of the world's most important crops is rice (*Oryza sativa*), upon which half of the world's population relies (Strange and Scott 2005) and which supplies 23 % of the total calorific intake of humankind. Global rice production is 874 million tonnes per annum (FAO Figures 2012–2013), but as the world population grows, it is predicted that rice yields will

have to double by 2050 to meet increasing demand and projected population growth (Godfray et al. 2010).

Rice blast disease is caused by the heterothallic ascomycete fungus *Magnaporthe oryzae* and is responsible for up to 30 % annual losses to the rice harvest (Talbot 2003; Thinlay et al. 2000) (Talbot 2003; Thinlay et al. 2000). The name 'rice blast' is due to rapid development of the disease in the field, causing 'blasting' of entire crops (Ou 1985). *M. oryzae* can, however, also infect other important grass crops, such as barley (*Hordeum vulgare*), finger millet (*Eleusine coracana*) and wheat (*Triticum aestivum*) (Talbot 2003). Furthermore, blast disease of wheat, known as 'brusone' disease, which was first reported in 1985, is an emerging problem across South America, and, due to the lack of effective disease control by either resistant cultivars or fungicide treatment, serious outbreaks of brusone have occurred since 2009, especially across Brazil, Paraguay and Bolivia (Maciel et al. 2014).

Rice blast disease is currently controlled by fungicide treatment or disease resistant cultivars, developed by plant breeding. These methods have had limited success, however, because of the rapid emergence of new pathotypes, fungicide-resistant strains and the high genetic variability of *M. oryzae* in the field (Latterell and Rossi 1986). As a consequence of its importance and difficulty to control, *M. oryzae* has emerged as a model pathogenic fungus over the last 30 years for understanding fungal-pathogen interactions (Dean et al. 2005; Perez-Nadales et al. 2014).

III. Septation and Cytokinesis in *Magnaporthe oryzae*

In filamentous fungi, septation is required for fungal growth, differentiation and cell division and thereby guarantees correct compartmentalisation and development. Septation can be divided into four main steps. These are (1) selection of a future division plane, (2) assembly at this site of a contractile actomyosin ring (CAR), (3) constriction of the CAR coupled with plasma membrane invagination and (4) formation and deposition of cross-wall materials (Harris et al. 1994).

The septation site selection systems used in the model yeasts, *S. cerevisiae* and *Sch. pombe*, are fundamentally different. In *S. cerevisiae*, for instance, the site of a future bud is determined by a cortical cue generated by the previous cell division and cell-end-dependent spatial signals (Wu et al. 2013). After the site is selected, the mitotic nucleus is positioned in the selected site, and a nuclear division across the cell division plane occurs (Wu et al. 2013). By contrast, in *Sch. pombe*, the future site of cytokinesis is specified by the pre-mitotic nucleus itself with negative signals originating from both cell ends (Chang and Peter 2003). Interestingly, septation in filamentous fungi is a variable process that has fundamental similarities and differences from that of the model yeast organisms. For example, selection of the future septation site in the two filamentous *Pezizomycotina* species, *Aspergillus nidulans* and *Neurospora crassa*, employs a closely related programme to the one of fission yeast (reviewed by Seiler and Justa-Schuch (2010). In other filamentous fungi, however, septation is only loosely coordinated with nuclear division, resulting in multinuclear hyphal compartments with daughter cells remaining attached to one another (Gladfelter 2006). During conidial germination in *A. nidulans*, the conidium undergoes a short period of isotropic growth before the emergence of a germ tube. Only once the germ tube has reached a certain size and after the third round of mitosis has occurred is the first septum formed between two nuclei near the base of the germ tube (Harris et al. 1994). Using conditional mutants defective in cell cycle control and nuclear migration, Wolkow et al. (1996) demonstrated that formation of the first septum is triggered by nuclear division, after the cell reaches a certain threshold size. Therefore, in a similar manner to fission yeast, the position of the *A. nidulans* mitotic nucleus specifies the future site of septation (Wolkow et al. 1996). One hypothesis that may explain the multinucleate nature of *A. nidulans* hyphae is that a gradient of an inhibitory factor is formed, which originates at the hyphal tip, that restricts

septum formation until each cell achieves a certain size. However, the exact nature of such an inhibitory gradient controlling septation of *A. nidulans* germling remains unknown.

The septation initiation network (SIN) was first described in *Sch. pombe* and consists of a signal transduction cascade which ensures temporal coordination between nuclear division and cytokinesis. Septation initiation has also been extensively studied in filamentous fungi, and it has been shown to have a number of functions, one of which is to act as a checkpoint to ensure coordination of the cell cycle when there are defects in CAR assembly or integrity. Activation of SIN depends on cyclin-dependent kinase (Cdk) activity and has been shown to activate a guanine nucleotide exchange factor-GTPase-activating protein (GEF-GTPase) module, composed of Bud3 and Rho4, which triggers recruitment of formins, which nucleate actin filaments to initiate CAR assembly (Si et al. 2010). In *A. nidulans*, a homologue of the SIN protein kinase Cdc7 from fission yeast, SepH, for example, is required for formation of contractile actin ring during cytokinesis. When SepH activity is disrupted, it prevents AnBud3 from localising as a ring at the incipient septation site, thereby preventing septum formation. At the same time, *A. nidulans* mutants lacking AnBud3 also fail to produce septate hyphae (Bruno et al. 2001; Si et al. 2010). In the filamentous ascomycete *Neurospora crassa*, the Rho-type GTPase Rho4, along with its GEFs BudS and Rgf3, activates septation. Rho4 is dependent on an anilin-like landmark protein Bud4 which accumulates as punctate structures at the plasma membrane at the future site of septation, which coalesce into a ring during septation (Justa-Schuch et al. 2010). Rho4 and Bud3 are proposed to recruit and trigger the formin Bni1, which regulates the position and formation of the CAR. Formins are conserved nucleators of actin filaments and contain a formin homology 1 domain (FH1), which serves as a binding site for the profilin-actin complex, and a formin homology 2 domain (FH2), which regulates actin nucleation and cable assembly. Upon binding with activated Rho GTPases, formins become activated and able to catalyse actin nucleation (Evangelista et al. 2002). *A. nidulans* and *N. crassa* possess a single formin, namely SepA and Bni1, respectively, which are essential for viability. A *sepA* conditional mutant causes dramatic defects in hyphal development, and hyphae are morphologically abnormal and aseptate. In both *A. nidulans* and *N. crassa*, the formins localise as a crescent at hyphal tips or at the extreme apex of a hypha and as dot-like structures which colocalise with the lipophilic styryl dye, FM4-64, in the Spitzenkörper and to the septum where they promote CAR formation. Recruitment of SepA and Bni1 to the site of incipient CAR formation can be prevented in *A. nidulans* and *N. crassa* in mutants lacking Bud3 or Bud4 homologues. Therefore, in *A. nidulans* and probably *N. crassa* too, the SIN is likely to operate upstream of the Bud3-Rho4 module controlling selection of future septation sites by recruiting formins to the incipient septum (Si et al. 2010). How the precise position of the CAR is determined in filamentous fungi and how CAR formation is controlled are not well understood and require further investigation.

In vegetative hyphae of *M. oryzae,* the site of septation is consistently associated with the medial position of the spindle during the preceding nuclear division. This pattern also occurs during hyphal branching, defining the position of the subsequent septum, and cellular compartments are, as a consequence, evenly distributed along hyphae with a relatively uniform intercalary length and a single nucleus typically maintained in each hyphal cell. Therefore, mitosis and cytokinesis are spatially coupled during hyphal growth of *M. oryzae.* However, strikingly it has been shown that cytokinesis is regulated asymmetrically from the position of nuclear division during the formation of appressoria for plant infection (Saunders et al. 2010b).

M. oryzae undergoes several morphogenetic transitions before successful formation of the appressorium, which leads to cuticle rupture and entry of the fungus into rice tissue. The infection cycle of *M. oryzae* starts when a three-celled conidium lands on a rice leaf, to which it attaches by secreting spore tip mucilage from an apical compartment at the apex of the

pyriform conidium (Hamer et al. 1988). From the apical cell, a polarised germ tube elongates and, after 4–6 h, changes direction to form a flattened hook at the leaf surface and, ultimately, to form a unicellular dome-shaped appressorium. The appressorium generates a melanin layer in the inner part of the chitin-rich cell wall, which prevents efflux of osmotically active solutes in the appressorium. As a consequence, the appressorium takes up external water against the high osmotic gradient generated inside the cell by accumulation of polyols, such as glycerol (de Jong et al. 1997; Talbot 2003). High turgor inside the appressorium is focused as mechanical force at the appressorium pore to pierce the tough cuticle of the leaf (Howard et al. 1991; Howard and Valent 1996; de Jong et al. 1997; Talbot 2003). At the same time, generation of turgor is achieved by relocation of storage products from the conidium to the incipient appressorium, followed by autophagic cell death of the conidium (Kershaw and Talbot 2009; Thines et al. 2000). To pierce the cuticle of the leaf, the fungus develops a penetration peg, which is a specialised narrow hypha that emerges from the appressorium pore (Bourett 1990). After breaching the cuticle, the peg develops into a primary invasive hypha which at its tip forms a biotrophic interfacial complex (BIC). The BIC is a membrane-rich plant-derived structure, which may be associated with fungal effector delivery into the plant or be a focal immune response by the host plant. The primary invasive hypha develops into bulbous invasive hyphae to invade and colonise the initial epidermal cell and adjacent tissues (Zhang and Xu 2014), and the BIC becomes associated with a subapical invasive cell during further fungal proliferation and appears to be the site of active fungal secretion (Giraldo et al. 2013). After 3 days, small oval lesions appear on the leaf and become necrotic, and after 5 days they develop aerial conidiophores which sporulate profusely and are splash dispersed to adjacent plants (Talbot 2003).

The infection cycle is tightly dependent on cell cycle regulation (Saunders et al. 2010a; Talbot 2003). The switch from anisotropic growth at the germ tube tip to isotropic growth, which leads to formation of the incipient appressorium, depends on successful DNA replication (S phase entry) in *M. oryzae* (Saunders et al. 2010a). After hooking, a single round of mitosis must occur prior to development of a mature appressorium and subsequent infection. Temperature-sensitive mutants in either the mitosis-promoting kinase, NimA, which is associated with regulation of the G2 to M transition, prevented maturation of appressoria (Saunders et al. 2010a). By contrast, appressoria still form in a conditional mutant, bimE, which is blocked within mitosis and when a stabilised version of the B cyclin, Cyc1, is expressed preventing mitotic exit. When considered together, these experiments suggest that entry into S phase controls initiation of appressorium development, its maturation requires entry into mitosis and completion of mitosis is a prerequisite for the appressorium to be functional (Saunders et al. 2010a).

A single septation event occurs during appressorium development at the neck of the appressorium, where it is joined to the germ tube tip (Fig. 4.2). The position of this septum is first defined by a hetero-oligomeric septin complex which occurs prior to mitosis. The contractile actomyosin ring (CAR) then forms at the neck of the appressorium after mitosis allowing nuclear migration into the developing appressorium. After this single round of mitosis, one of the daughter nuclei migrates back into the conidial cell from which its mother nucleus originated. This leads to degeneration of the conidium in an autophagy-dependent process leaving a single nucleus in the appressorium at the time of plant penetration (Kershaw and Talbot 2009; Veneault-Fourrey et al. 2006). Penetration of the fungus into plant tissue occurs by formation of a peg emerging from the appressorial pore, which develops into the primary invasive hypha. Therefore, the appressorium pore marks the point of the direct contact between the host and the fungus and is marked by a very thin pore wall overlay at the contact point with the rice leaf (de Jong et al. 1997; Howard et al. 1991; Howard and Valent 1996; Talbot 2003). At the

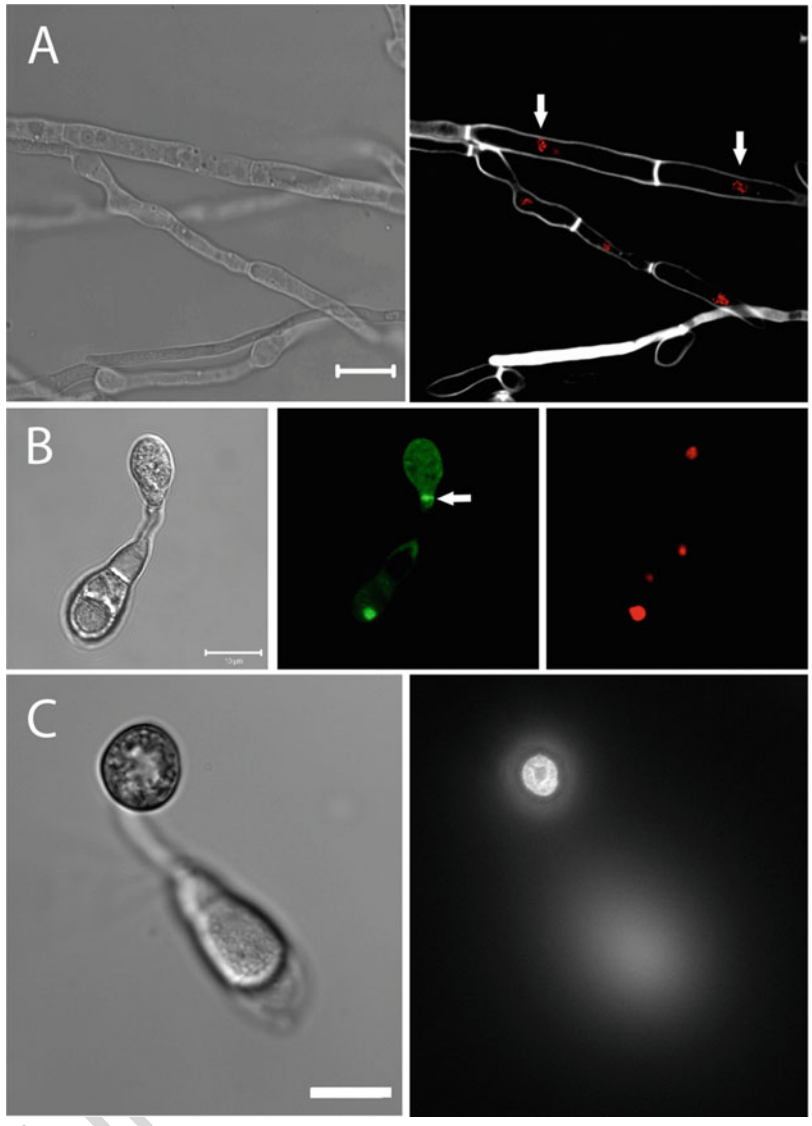

Fig. 4.2 Septation during different developmental stages of the plant pathogenic fungus *M. oryzae*. (**a**) Micrographs showing vegetative hyphae of *M. oryzae* strain expressing nuclear marker, fluorescently labelled histone H1, with cell wall staining by calcofluor white. *White arrows* indicate fungal nuclei. (**b**) Micrographs showing contractile actomyosin ring at the neck of developing appressorium marked by the accumulation of fluorescently tagged tropomyosin (*white arrow*). (**c**) Septin ring formation around appressorium pore in mature appressorium of *M. oryzae* strain expressing Sep4-GFP fusion (Dagdas et al. 2012) (Images (**a**) and (**b**) were taken from Diane G.O. Saunders' PhD thesis. Scale bar = 10 μm)

appressorium pore, the core septin GTPases, Sep3, Sep4, Sep5 and Sep6 (which are homologues of Cdc3, Cdc10, Cdc11 and Cdc12 from *S. cerevisiae*), form a toroidal ring structure at the base of the appressorium. This structure is required for appressorium-mediated plant penetration (Dagdas et al. 2012).

IV. Septin Ring Formation at the Base of the Appressorium

During cytokinesis, the coordinated interaction of cytoskeletal components is required for assembly and progressive constriction of the

Table 4.1 Septin homologues and their biological functions in selected model fungi

Species	Septin homologues	Biological functions	References
Saccharomyces cerevisiae	Cdc3, Cdc10, Cdc11, Cdc12 and Shs1	Scaffold or diffusion barrier during cytokinesis and cell polarity	Oh and Bi (2011)
Ashbya gossypii	Cdc3, Cdc10, Cdc11, Cdc12 and Shs1	Sporulation, limiting hyphal diameter and polarity and branch pattern	Schmitz et al. (2006)
Aspergillus nidulans	AspA, AspB, AspC, AspD and AspE	Chitin deposition, branching pattern and conidiophore development	Momany et al. (2001)
Candida albicans	Cdc3, Cdc10, Cdc11, Cdc12 and Sep7	Scaffold, cell division, cell polarity, chitin deposition, virulence	Warenda and Konopka (2002)
Magnaporthe oryzae	Sep3, Sep4, Sep5, Sep6 and a putative AspE homologue	Plant penetration and morphogenesis of infection structure	Dagdas et al. (2012), Saunders et al. (2010b)
Ustilago maydis	Sep1, Sep2, Sep3 and Sep4	Cellular morphology, cell division of budding haploid cells, minor role in virulence	Alvarez-Tabares and Perez-Martin (2010)

actomyosin ring at the cell cortex, as well as for scaffolding the cross-wall-synthesising machinery during cytokinesis and septation. The CAR consists of actin, myosin II and other actin-binding proteins and is assembled at the septation site followed by actomyosin-mediated constriction, which ultimately leads to membrane invagination and deposition of cell wall components (Wu et al. 2013).

The role of actin during septation in filamentous fungi was first investigated in *A. nidulans* by using the actin-depolymerising agent cytochalasin A and its effect on septum formation and cytokinesis (Harris et al. 1994). The CAR marks the future site of septation and forms a cortical ring which constricts leading to invagination of the plasma membrane. The CAR later broadens, invaginates and forms an hourglass structure at the site of septation (Momany and Hamer 1997). In *N. crassa*, by using live-cell imaging of fluorescently tagged proteins, the accumulation of actin cables was shown as a mass of thick filaments associated with tropomyosin and class II myosin. This 'septal associated tangle' (SAT) was identified as the earliest marker of septum development (Delgado-Alvarez et al. 2014). The SAT then condenses into the F-actin ring of the CAR. After that, the actin ring splits into two rings, and cross-wall materials are deposited (Berepiki et al. 2010; Delgado-Alvarez et al. 2014).

Septins are morphogenetic GTPases that act as cytoskeletal components by forming hetero-oligomers and various higher-order structures, including filaments, rings and gauzes, and serving as platforms for recruitment and organisation of proteins at sites of polarised growth and cytokinesis (Oh and Bi 2011). They were first identified in *S. cerevisiae* through analysis of mutants unable to complete cytokinesis and which produced elongated buds that do not separate from the mother cell (Hartwell 1971). Later studies defined four important groups of septins from metazoans and an extra group, specific to filamentous fungi (Pan et al. 2007), as shown in Table 4.1. *S. cerevisiae* possesses five septins, Cdc3, Cdc10, Cdc11, Cdc12 and Shs1, of which the first four are considered core septins. During budding, the initial septin ring then forms an hourglass structure, called the septin collar, linked with the plasma membrane at the bud neck. The septin collar scaffolds proteins associated with cell division and septation, but also acts as a lateral diffusion barrier to spatially regulate morphogenetic factors to the site of cytokinesis (Oh and Bi 2011). Recently, septins have been demonstrated to serve roles in cell signalling, membrane remodelling, cellular morphology and, most importantly, pathogenesis in filamentous fungi (Bridges and Gladfelter 2014). Septins in filamentous fungi appear to be able to form more diverse higher-order structures than those of unicellular yeasts (Hernandez-Rodriguez et al. 2012). For example, the filamentous fungus *A. nidulans* pos-

sesses four core septins, AspA, AspB, AspC and AspD, that form hetero-polymeric complexes, while the additional septin, AspE, plays a minor role in stabilising other core septins (Hernandez-Rodriguez et al. 2014). At the septation site, AspB forms a postmitotic single ring which then splits into two rings at the division plane across the main hypha. After completion of septation, the ring of AspB located at the basal side of the septum is lost, while the one at the apical side persists. AspB also localises into a ring on the side of hypha just before branch emergence, therefore suggesting that the AspB septin is an early marker for hyphal branch formation (Hernandez-Rodriguez et al. 2012; Westfall and Momany 2002).

In *M. oryzae*, four core septins have been identified, Sep3, Sep4, Sep5, Sep6, as well as fungal-specific septin Sep7 (Dagdas et al. 2012; Saunders et al. 2010b). The core septins showed 47 % amino acid identity to Cdc3, 55 % to Cdc10, 45 % to Cdc11 and 57 % to Cdc12 of *S. cerevisiae,* respectively. Sep7 shows 55 % identity to AspE from *Aspergillus nidulans*. During early appressorium formation, the core septins localise to the germ tube tip during its initial apical polarised growth. At 4 h, an incipient appressorium is formed, and core septins localise at the appressorial neck, prior to mitosis, at the site of the septation event that delimits the appressorium from the other pre-penetration structures. From 8 h onwards, until the primary invasive hypha is formed and the cuticle of the rice leaf has been breached, the core septins form a ring at the base of the appressorium (Dagdas et al. 2012). The septins are required for the remodelling of actin to form a toroidal F-actin network at the base of the appressorium. Null mutants in any of the core septins result in a dramatic disorganisation of the F-actin structure leading to impairment of penetration peg formation and failure to cause tissue invasion (Dagdas et al. 2012). The septin structure not only provides rigidity to the cortex around the appressorium pore but also appears to act as a diffusion barrier to restrict proteins to the pore region that are required for generating curvature of the plasma membrane and F-actin polymerisation during polarity re-establishment and penetration peg development. In budding yeast, activation of the master polarity regulator, Cdc42, must occur, to generate apical polarised growth and bud formation (Howell and Lew 2012). Null mutants of *CDC42* in *M. oryzae* are able to form appressoria that have a disrupted cytoskeleton and are therefore unable to cause infection (Zheng et al. 2009). Cdc42 acts through two PAK kinases, Ste20 and Cla4, and two formins, Bni and Bnr, to activate formation of F-actin and septin toroidal ring structures (Howell and Lew 2012). The PAK kinase Cla4 homologue, Chm1, is required for septin ring formation at the base of the appressorium and is therefore necessary for infection (Dagdas et al. 2012; Kadota et al. 2004). Surprisingly, these null mutants are able to form appressoria, suggesting that the activity of septins during earlier stages of development is regulated distinctly than during appressorium function. Moreover, the mechanism involved in the formation and recruitment of the septin ring at the base of the appressorium is still not known. Other cytoskeleton components that are also localised to the appressorium pore include a homologue of the ezrin/radixin/moesin protein Tea1, which in yeast binds at its N-terminal domain to the plasma membrane to connect to F-actin (Turunen et al. 1994). Tea1 has also been reported to be required for septin-mediated scaffolding. At least one of the Bin-amphiphysin-Rvs (BAR) domain proteins in *M. oryzae* also localises to the appressorium pore in a septin-dependent manner. BAR proteins have been extensively studied in budding yeast and are involved in generation of cellular invaginations (F-BAR proteins) or protrusions (inverse or I-BAR proteins) (Dawson et al. 2006). Bar proteins bind to actin and to phosphatidylinositol (4, 5)-bisphosphate (PtdIns(4, 5)P2) (Bompard et al. 2005; Miki et al. 2009). Localisation of the BAR protein, Rvs167, in *M. oryzae* to the appressorium pore has been shown, suggesting localising of endocytic and perhaps exocytic machinery to the appressorium pore (Dagdas et al. 2012). Las17 is part of the actin-related protein 2/3 complex (Arp2/3) involved in F-actin polymerisation (Urbanek et al. 2013). The Arp2/3 complex is necessary for F-actin polymerisation, organisation and recycling (Goley and Welch 2006). In

M. oryzae Las17-GFP was shown to be localised to the appressorial pore, in a septin-dependent manner (Dagdas et al. 2012).

The septin ring in the appressorium pore therefore acts as a means of coordinating processes associated with polarity re-establishment and the rapid F-actin polymerisation and membrane curvature necessary for development and protrusion of a penetration peg at the base of the infection cell. It appears to fulfil this role by acting as a means of scaffolding these proteins at the appropriate point in the cell and spatially focusing proteins involved in polarity to the correct domain, probably by preventing their diffusion from the region. In this way, the penetration peg resembles a bud site in *S. cerevisiae*, where similar concentration of polarity determinants is required to complete budding. The key difference, however, is the generation of enormous invasive forces at the appressorium pore that are sufficient to rupture the cuticle and allow the fungus entry into epidermal cells. This implies a level of controlled application of force generated by the repolarisation process itself and the focusing of the enormous turgor of the cell at this point of contact with the underlying leaf surface. The septin complex itself appears to require regulated synthesis of reactive oxygen species (ROS) by means of the Nox2 NADPH oxidase complex in order to form (Ryder et al. 2013). Deletion of the *NOX2* gene or its cognate regulator *NOXR* prevents penetration peg formation (Egan et al. 2007) and rice blast disease because the septin ring cannot be formed, and, as a consequence, Las17, Tea1, Rvs167, cdc42 and other components are not localised correctly to the appressorium pore (Ryder et al. 2013). It seems likely that a turgor-sensing mechanism exists in the appressorium which, upon reaching a threshold level of turgor, triggers the Nox2 complex to release ROS which acts directly on actin cytoskeletal components and, through redox signalling, affects a complex of proteins, including Bem1 and Cdc24, that leads to the activation of Chm1 and assembly of the septin complex. Understanding the details of this process and the precise function of Nox2 remains a high priority.

A. Dynamics of Septin Ring Formation in *M. oryzae*

Septin ring assembly at the base of the appressorium also requires activation of the Pmk1 and Mps1 MAPK signalling pathways (Dagdas et al. 2012). The Pmk1 MAPK signalling, homologous to the Fus3 MAP kinase signalling pathway involved in the yeast mating response and invasive growth in yeast, regulates infection-related development in *M. oryzae*. Deletion of *PMK1* results in mutants that are unable to form appressoria and fail to infect rice plant through wounds (Talbot 2003; Xu and Hamer 1996). The Δ*pmk1* phenotype suggests that Pmk1 is required for appressorium morphogenesis, but also for invasive growth in *M. oryzae* (Xu and Hamer 1996). In addition, the Mst12 transcription factor, a homologue of *S. cerevisiae* Ste12, was identified to operate downstream of the Pmk1 MAP kinase cascade and is essential for appressorium-mediated plant penetration. Δ*mst12* null mutants are able to form melanised, pressurised appressoria but cannot develop penetration pegs and, therefore, fail to grow invasively in plant tissue (Park et al. 2002, 2004). Formation of the penetration peg at the base of the appressorium also requires the Mps1 MAPK signalling pathway, homologous to the Slt2 MAP kinase-dependent cell integrity pathway in *S. cerevisiae* (Xu et al. 1998). The role of these pathways in the control of septin ring formation in the appressorium is important. Deletion of genes, encoding either the Mst12 transcription factor or the Mps1 MAP kinase, not only prevents plant penetration but also prevents assembly of the septin and actin network at the base of the appressorium (Dagdas et al. 2012). During initiation of appressorium formation, loss of apical polarised growth occurs leading to isotropic expansion of the germ tube tip and formation of the dome-shaped appressorium. Conversely penetration peg development requires correct assembly and maintenance of the septin and F-actin rings (Dagdas et al. 2012; Ryder et al. 2013). Both the Pmk1 and Mps1 MAP kinase signalling pathways are necessary for repolarisation of the appressorium. Involvement of

these signalling pathways is consistent with the functional similarities between penetration peg formation in *M. oryzae* and budding in *S. cerevisiae* in which a future bud site is specified by septin collar assembly early in the cell cycle, followed by polarised bud growth. In *M. oryzae*, emergence of the penetration peg during plant penetration involves repolarisation and maintenance of polarised cell growth at the base of the appressorium. This leads to further questions such as how appressorium-mediated plant penetration is regulated with the cell division cycle.

B. Cell Cycle Regulation of Septin Ring Formation

Recent evidence in *M. oryzae* suggests that appressorium morphogenesis is tightly linked to cell cycle control (Saunders et al. 2010a), as described above. Correct progression through DNA replication is known, for example, to be required for appressorium formation (Saunders et al. 2010a). An open question is whether the nucleus within the developing appressorium, from which all subsequent genetic information during plant infection is derived, has to be arrested in the cell cycle in order for turgor to be generated correctly prior to repolarisation of the appressorium. Recent evidence suggests that DNA replication is necessary for stabilisation of the appressorium septin ring, as HU treatment leads to breakdown of the septin ring and lack of sustained organisation of F-actin at the appressorium pore (M. Oses-Ruiz, W. Sakulkoo, and N.J.Talbot, unpublished). Furthermore, arresting the cell cycle in G1 phase appears to prevent plant infection by mature appressoria (S. Sakulkoo and N.J. Talbot, unpublished). When considered together, this suggests that progression of the appressorium nucleus into G2 may also be necessary for repolarisation of the appressorium to occur. In such a model, septin ring formation would occur in G1 as soon as a threshold level of appressorium turgor is generated, leading to cell cycle progression into S phase and subsequent extension of the penetration peg. Therefore, coordination of cell cycle regulation with septin-mediated remodelling of the F-actin cytoskeleton in the appressorium is likely to be critical for plant infection.

V. Conclusions

The control of cytokinesis and septation by pathogenic fungi is critical to the developmental changes associated with host invasion and fungal pathogenesis. Pathogenic processes, such as growth within host tissue, often require changes between yeast-like, determinate, isotropic growth and hyphal, polarised, anisotropic growth, which must be appropriately regulated in concert with nuclear division. In plant pathogenic fungi, a body of evidence, primarily generated from studies of the rice blast fungus *M. oryzae*, shows that septin-mediated remodelling of the actin cytoskeleton is fundamental to the action of its specialised infection cells, called appressoria, during plant infection. Future studies will need to ask several questions which logically follow these recent discoveries. First of all, is the role of septin GTPases in appressorium repolarisation regulated distinctly from their role in each round of septation within vegetative and invasive hyphae? For example, is there a turgor-sensing mechanism that regulates septin ring formation only once the required turgor has been generated in the infection structure to breach the plant cuticle? Is the regulated synthesis of reactive oxygen species, which is essential for septin assembly in *M. oryzae* appressoria, a common mechanism by which septin-dependent processes are regulated in fungi? Can this explain why regulated bursts of ROS are often associated with cellular differentiation in fungi, such as fruit body formation and sporulation? Are the processes identified in *M. oryzae* appressorium development highly conserved among appressorium-forming fungi, such as the rusts, anthracnose-causing fungi and the powdery mildews? If so, can we find evidence for common mechanisms that regulate appressorium-mediated plant infection, such as the conserved MAP kinase cascades (Perez-Nadales et al. 2014), that might be targeted to

develop broad spectrum anti-penetrant fungicides? Finally, it is clear that there are important parallels between the way in which yeast budding operates and the operation of fungal appressoria, particularly in the processes leading up to penetration peg formation and repolarisation. Some of the most conserved components probably play similar roles. Clearly, there are important differences as well, not least of all in the enormous invasive forces deployed by appressoria, but the conserved components involved in some of these processes can provide an important roadmap to test hypotheses and define the fundamental mechanisms by which infection structures work in plant pathogenic fungi.

References

Alvarez-Tabares I, Perez-Martin J (2010) Septins from the phytopathogenic fungus Ustilago maydis are required for proper morphogenesis but dispensable for virulence. PLoS ONE 5, e12933

Berepiki A, Lichius A, Shoji J-Y, Tilsner J, Read ND (2010) F-actin dynamics in *Neurospora crassa*. Eukaryot Cell 9:547–557

Bompard G, Sharp SJ, Freiss G, Machesky LM (2005) Involvement of Rac in actin cytoskeleton rearrangements induced by MIM-B. J Cell Sci 118:5393–5403

Bourett TMH (1990) In vitro development of penetration structures in the rice blast fungus *Magnaporthe grisea*. Can J Bot Rev Can Bot 68:329–342

Bridges AA, Gladfelter AS (2014) Fungal pathogens are platforms for discovering novel and conserved septin properties. Curr Opin Microbiol 20:42–48

Bruno KS, Morrell JL, Hamer JE, Staiger CJ (2001) SEPH, a Cdc7p orthologue from *Aspergillus nidulans*, functions upstream of actin ring formation during cytokinesis. Mol Microbiol 42:3–12

Chang F, Peter M (2003) Yeasts make their mark. Nat Cell Biol 5:294–299

Dagdas YF, Yoshino K, Dagdas G, Ryder LS, Bielska E, Steinberg G, Talbot NJ (2012) Septin-mediated plant cell invasion by the rice blast fungus, *Magnaporthe oryzae*. Science 336:1590–1595

Dawson JC, Legg JA, Machesky LM (2006) Bar domain proteins: a role in tubulation, scission and actin assembly in clathrin-mediated endocytosis. Trends Cell Biol 16:493–498

de Jong JC, McCormack BJ, Smirnoff N, Talbot NJ (1997) Glycerol generates turgor in rice blast. Nature 389:244–244

Dean RA, Talbot NJ, Ebbole DJ, Farman ML, Mitchell TK, Orbach MJ, Thon M, Kulkarni R, Xu JR, Pan H et al (2005) The genome sequence of the rice blast fungus *Magnaporthe grisea*. Nature 434:980–986

Delgado-Alvarez DL, Bartnicki-Garcia S, Seiler S, Mourino-Perez RR (2014) Septum development in *Neurospora crassa*: the septal actomyosin tangle. PLoS ONE 9, e96744

Egan MJ, Wang ZY, Jones MA, Smirnoff N, Talbot NJ (2007) Generation of reactive oxygen species by fungal NADPH oxidases is required for rice blast disease. Proc Natl Acad Sci USA 104:11772–11777

Evangelista M, Pruyne D, Amberg DC, Boone C, Bretscher A (2002) Formins direct Arp2/3-independent actin filament assembly to polarize cell growth in yeast. Nat Cell Biol 4:260–269

Giraldo MC, Dagdas YF, Gupta YK, Mentlak TA, Yi M, Martinez-Rocha AL, Saitoh H, Terauchi R, Talbot NJ, Valent B (2013) Two distinct secretion systems facilitate tissue invasion by the rice blast fungus *Magnaporthe oryzae*. Nat Commun 4:1996

Gladfelter AS (2006) Control of filamentous fungal cell shape by septins and formins. Nat Rev Microbiol 4:223–229

Godfray HCJ, Beddington JR, Crute IR, Haddad L, Lawrence D, Muir JF, Pretty J, Robinson S, Thomas SM, Toulmin C (2010) Food security: the challenge of feeding 9 billion people. Science 327:812–818

Goley ED, Welch MD (2006) The ARP2/3 complex: an actin nucleator comes of age. Nat Rev Mol Cell Biol 7:713–726

Hamer JE, Howard RJ, Chumley FG, Valent B (1988) A mechanism for surface attachment in spores of a plant pathogenic fungus. Science 239:288–290

Harris SD, Morrell JL, Hamer JE (1994) Identification and characterization of *Aspergillus nidulans* mutants defective in cytokinesis. Genetics 136:517–532

Hartwell LH (1971) Genetic control of the cell division cycle in yeast. IV. Genes controlling bud emergence and cytokinesis. Exp Cell Res 69:265–276

Hernandez-Rodriguez Y, Hastings S, Momany M (2012) The septin AspB in *Aspergillus nidulans* forms bars and filaments and plays roles in growth emergence and conidiation. Eukaryot Cell 11:311–323

Hernandez-Rodriguez Y, Masuo S, Johnson D, Orlando R, Smith A, Couto-Rodriguez M, Momany M (2014) Distinct septin heteropolymers co-exist during multicellular development in the filamentous fungus *Aspergillus nidulans*. PLoS ONE 9, e92819

Howard RJ, Valent B (1996) Breaking and entering: host penetration by the fungal rice blast pathogen *Magnaporthe grisea*. Annu Rev Microbiol 50:491–512

Howard RJ, Ferrari MA, Roach DH, Money NP (1991) Penetration of hard substrates by a fungus employing enormous turgor pressures. Proc Natl Acad Sci USA 88:11281–11284

Howell AS, Lew DJ (2012) Morphogenesis and the cell cycle. Genetics 190:51–77

Kadota J, Yamamoto T, Yoshiuchi S, Bi E, Tanaka K (2004) Septin ring assembly requires concerted action of polarisome components, a PAK kinase Cla4p, and the actin cytoskeleton in *Saccharomyces cerevisiae*. Mol Biol Cell 15:5329–5345

Kershaw MJ, Talbot NJ (2009) Genome-wide functional analysis reveals that infection-associated fungal autophagy is necessary for rice blast disease. Proc Natl Acad Sci USA 106:15967–15972

Latterell FMR, Rossi AE (1986) Longevity and pathogenic stability of *Pyricularia oryzae*. Phytopathology 76:231–235

Li L, Zhang C, Konopka JB (2012) A Candida albicans temperature-sensitive cdc12-6 mutant identifies roles for septins in selection of sites of germ tube formation and hyphal morphogenesis. Eukaryot Cell 11:1210–1218

Maciel JL, Ceresini PC, Castroagudin VL, Zala M, Kema GH, McDonald BA (2014) Population structure and pathotype diversity of the wheat blast pathogen *Magnaporthe oryzae* 25 years after its emergence in Brazil. Phytopathology 104:95–107

Miki S, Matsui K, Kito H, Otsuka K, Ashizawa T, Yasuda N, Fukiya S, Sato J, Hirayae K, Fujita Y et al (2009) Molecular cloning and characterization of the AVR-Pia locus from a Japanese field isolate of *Magnaporthe oryzae*. Mol Plant Pathol 10:361–374

Momany M, Hamer JE (1997) Relationship of actin, microtubules, and crosswall synthesis during septation in *Aspergillus nidulans*. Cell Motil Cytoskeleton 38:373–384

Momany M, Zhao J, Lindsey R, Westfall PJ (2001) Characterization of the *Aspergillus nidulans* septin (asp) gene family. Genetics 157:969–977

Oh Y, Bi E (2011) Septin structure and function in yeast and beyond. Trends Cell Biol 21:141–148

Ou SH (1985) Rice disease. Commonwealth Mycological Institute, Surrey

Pan F, Malmberg RL, Momany M (2007) Analysis of septins across kingdoms reveals orthology and new motifs. BMC Evol Biol 7:103

Park G, Xue C, Zheng L, Lam S, Xu JR (2002) MST12 regulates infectious growth but not appressorium formation in the rice blast fungus *Magnaporthe grisea*. Mol Plant Microbe Interact 15:183–192

Park G, Bruno KS, Staiger CJ, Talbot NJ, Xu JR (2004) Independent genetic mechanisms mediate turgor generation and penetration peg formation during plant infection in the rice blast fungus. Mol Microbiol 53:1695–1707

Perez-Nadales E, Almeida Nogueira MF, Baldin C, Castanheira S, El Ghalid M, Grund E, Lengeler K, Marchegiani E, Mehrotra PV, Moretti M et al (2014) Fungal model systems and the elucidation of pathogenicity determinants. Fungal Genet Biol 70:42–67

Ryder LS, Dagdas YF, Mentlak TA, Kershaw MJ, Thornton CR, Schuster M, Chen J, Wang Z, Talbot NJ (2013) NADPH oxidases regulate septin-mediated cytoskeletal remodeling during plant infection by the rice blast fungus. Proc Natl Acad Sci USA 110:3179–3184

Saunders DG, Aves SJ, Talbot NJ (2010a) Cell cycle-mediated regulation of plant infection by the rice blast fungus. Plant Cell 22:497–507

Saunders DG, Dagdas YF, Talbot NJ (2010b) Spatial uncoupling of mitosis and cytokinesis during appressorium-mediated plant infection by the rice blast fungus *Magnaporthe oryzae*. Plant Cell 22:2417–2428

Schmitz HP, Kaufmann A, Kohli M, Laissue PP, Philippsen P (2006) From function to shape: a novel role of a formin in morphogenesis of the fungus *Ashbya gossypii*. Mol Biol Cell 17: 130–145

Seiler S, Justa-Schuch D (2010) Conserved components, but distinct mechanisms for the placement and assembly of the cell division machinery in unicellular and filamentous ascomycetes. Mol Microbiol 78:1058–1076

Si H, Justa-Schuch D, Seiler S, Harris SD (2010) Regulation of septum formation by the Bud3-Rho4 GTPase module in *Aspergillus nidulans*. Genetics 185:165–176

Strange RN, Scott PR (2005) Plant disease: a threat to global food security. Annu Rev Phytopathol 43: 83–116

Talbot NJ (2003) On the trail of a cereal killer: exploring the biology of *Magnaporthe grisea*. Annu Rev Microbiol 57:177–202

Thines E, Weber RW, Talbot NJ (2000) MAP kinase and protein kinase A-dependent mobilization of triacylglycerol and glycogen during appressorium turgor generation by *Magnaporthe grisea*. Plant Cell 12:1703–1718

Thinlay X, Finckh MR, Bordeos AC, Zeigler RS (2000) Effects and possible causes of an unprecedented rice blast epidemic on the traditional farming system of Bhutan. Agric Ecosyst Environ 78: 237–248

Turunen O, Wahlstrom T, Vaheri A (1994) Ezrin has a COOH-terminal actin-binding site that is conserved in the ezrin protein family. J Cell Biol 126:1445–1453

Urbanek AN, Smith AP, Allwood EG, Booth WI, Ayscough KR (2013) A novel actin-binding motif in Las17/WASP nucleates actin filaments independently of Arp2/3. Curr Biol 23:196–203

Veneault-Fourrey C, Barooah M, Egan M, Wakley G, Talbot NJ (2006) Autophagic fungal cell death is necessary for infection by the rice blast fungus. Science 312:580–583

Warenda AJ, Konopka JB (2002) Septin function in *Candida albicans* morphogenesis. Mol Biol Cell 13:2732–2746

Westfall PJ, Momany M (2002) *Aspergillus nidulans* septin AspB plays pre- and postmitotic roles in septum, branch, and conidiophore development. Mol Biol Cell 13:110–118

Wolkow TD, Harris SD, Hamer JE (1996) Cytokinesis in *Aspergillus nidulans* is controlled by cell size, nuclear positioning and mitosis. J Cell Sci 109:2179–2188

Wu CF, Savage NS, Lew DJ (2013) Interaction between bud-site selection and polarity-establishment machineries in budding yeast. Philos Trans R Soc Lond Ser B Biol Sci 368:20130006

Xu JR, Hamer JE (1996) MAP kinase and cAMP signaling regulate infection structure formation and pathogenic growth in the rice blast fungus *Magnaporthe grisea*. Genes Dev 10:2696–2706

Xu J-R, Staiger CJ, Hamer JE (1998) Inactivation of the mitogen-activated protein kinase Mps1 from the rice blast fungus prevents penetration of host cells but allows activation of plant defense responses. Proc Natl Acad Sci 95:12713–12718

Zhang S, Xu JR (2014) Effectors and effector delivery in *Magnaporthe oryzae*. PLoS Pathog 10, e1003826

Zheng W, Zhao Z, Chen J, Liu W, Ke H, Zhou J, Lu G, Darvill AG, Albersheim P, Wu S et al (2009) A Cdc42 ortholog is required for penetration and virulence of *Magnaporthe grisea*. Fungal Genet Biol 46:450–460

Author Queries

Chapter No.: 4 28652_3_En

Query Refs.	Details Required	Author's response
AU1	Latterell, 1986 has been changed to Latterell and Rossi 1986 as per the reference list. Please check if okay.	
AU2	"Justa-Schuch et al. 2010" is cited in text but not given in the reference list. Please provide details in the list or delete the citation from the text.	
AU3	Please check if "sepA" should be changed to "SepA" for consistency.	
AU4	Hamer, 1988 has been changed to Hamer et al. 1988 as per the reference list. Please check if okay.	
AU5	Please check "in either the mitosis-promoting kinase, NimA" for correctness.	
AU6	Please check if "septal associated tangle" should be changed to "septal actomyosin tangle".	
AU7	Please check if edit to table entry starting "Plant penetration and. . ." is okay.	

Appendix 2

Two independent S-phase checkpoints regulate appressorium-mediated plant infection by the rice blast fungus *Magnaporthe oryzae*

Míriam Osés-Ruiz, Wasin Sakulkoo, George R. Littlejohn, Magdalena Martin-Urdiroz and Nicholas J. Talbot

School of Biosciences, University of Exeter, Exeter, EX4 4QD, United Kingdom

Corresponding author: Nicholas J. Talbot

School of Biosciences, University of Exeter, Geoffrey Pope Building, Stocker Road, Exeter, EX4 4QD, United Kingdom

N.J.Talbot@exeter.ac.uk

Keywords: plant pathogen, S-phase, cell cycle, GTPase, *Magnaporthe oryzae*

Abstract

To cause rice blast disease, the fungal pathogen *Magnaporthe oryzae* develops a specialised infection structure called an appressorium. This dome-shaped, melanin-pigmented cell generates enormous turgor and applies physical force to rupture the rice leaf cuticle using a rigid penetration peg. Appressorium-mediated infection requires septin-dependent re-orientation of the F-actin cytoskeleton at the base of the infection cell, which organises polarity determinants necessary for plant cell invasion. Here, we show that plant infection by *M. oryzae* requires two independent S-phase cell cycle checkpoints. Initial formation of appressoria on the rice leaf surface requires an S-phase checkpoint that acts through the DNA damage response (DDR) pathway, involving the Cds1 kinase. By contrast, appressorium repolarization involves a novel, DDR-independent S-phase checkpoint, triggered by appressorium turgor generation and melanisation. This second checkpoint specifically regulates septin-dependent, NADPH oxidase-regulated F-actin dynamics to organise the appressorium pore and facilitate entry of the fungus into host tissue.

Significance Statement

Rice blast disease is the most important disease of cultivated rice and a significant threat to global rice production. The rice blast fungus develops a special cell, the appressorium, to breach the tough outer cuticle of a rice leaf and gain entry to rice tissue. We have defined two control points for appressorium development, linked to regulation of the cell cycle. Initial formation of the appressorium is controlled at S-phase which precedes a single round of mitosis. In the appressorium a second cell cycle checkpoint occurs, in which S-phase entry is controlled by build-up of cellular pressure in the appressorium and is necessary for septin-dependent, actin-driven re-polarisation of the infection cell that leads to plant infection.

\body

Introduction

To cause disease, many plant pathogenic fungi elaborate specialized infection structures called appressoria. These are swollen, dome-shaped cells that adhere tightly to the plant cell surface, where they develop turgor and bring about rupture of the host cell using mechanical force, or focused secretion of lytic enzymes. The rice blast fungus, *Magnaporthe oryzae*, has emerged as a valuable experimental model for understanding the biology of appressorium formation (1-3). Rice blast disease claims up to 30% of the annual rice harvest (4) and is therefore a significant global problem. Understanding appressorium development in this organism has the potential to lead to better rice blast disease control, by being able to target the earliest stages of plant infection.

In this study, we set out to investigate the control of appressorium development by means of cell cycle regulation. Rice blast infections start when a three-celled conidium of *M. oryzae* lands on the rice leaf surface and germinates to form a highly polarized germ tube. The germ tube elongates and becomes flattened against the plant surface, before forming a hooked tip (5). A single round of mitosis then occurs and one daughter nucleus migrates into the swollen germ tube tip (6). Growth at the germ tube tip then ceases and the tip swells isotropically, resulting in formation of a dome-shaped appressorium. A thick layer of melanin is synthesized in the appressorium cell wall and glycerol rapidly accumulates inside the cell. At the same time, the spore collapses and its nuclei are degraded by autophagy, with the entire spore contents being trafficked to the appressorium (6). These coupled

processes generate enormous hydrostatic turgor in the appressorium, measured at up to 8.0MPa (7, 8). When maximum turgor is achieved, the appressorium undergoes dynamic re-modeling of its actin cytoskeleton to form a toroidal F-actin network at the base of the cell. Septin GTPases scaffold cortical F-actin to the appressorium pore, from which a rigid penetration peg emerges to rupture the leaf cuticle (5, 9). This requires the Nox2 NADPH oxidase complex, which regulates septin assembly and F-actin re-modelling to the point of plant infection (10).

Previous work demonstrated that appressorium formation in *M. oryzae* is linked to a single round of mitosis that is always observed before cellular differentiation (11). Early appressorium development requires the nucleus in the germinating conidial cell to undergo DNA replication. Exposure to a DNA replication inhibitor, hydroxyurea, for example, or generation of a temperature-dependent mutant in the regulatory subunit of the Dbf4-Cdc7 kinase complex, $\Delta nim1^{ts}$, completely arrests development of an appressorium (11). How this cell cycle control point operates, however, is not understood. Subsequent entry into mitosis is also clearly necessary for appressorium maturation; a temperature sensitive $\Delta nimA^{ts}$ mutant blocked at the G2-M boundary develops non-melanised appressoria that cannot cause disease (6). Blocking the cell cycle by impairment of the anaphase-promoting complex, using a $\Delta bimE^{ts}$ mutant, or preventing mitotic exit by generating mutants expressing stabilized B-type cyclins, also prevents appressorium maturation and plant infection, highlighting the need for fungal mitosis to precede plant infection (11).

In this study we set out to investigate precisely how cell cycle control is exerted during appressorium morphogenesis by the rice blast fungus. We show here that initiation of appressorium development requires an S-phase checkpoint that operates through the DNA damage response pathway, requiring the Cds1 kinase. By contrast during the next cell cycle, a second S-phase checkpoint is triggered in the appressorium and is required for the cell to re-polarise. This novel checkpoint is activated by turgor sensing and is linked to melanin biosynthesis. The appressorium S-phase checkpoint controls NADPH oxidase-activated, septin-dependent F-actin re-modeling at the base of the appressorium. This regulates penetration peg emergence and allows plant infection to occur.

Manuscript text

Results

Appressorium morphogenesis is S-phase regulated and requires activation of CDK1 by the Cyc1 B-type cyclin

In *M. oryzae*, appressorium morphogenesis is always preceded by a single round of mitosis, resulting in one daughter nucleus moving to the incipient appressorium and autophagic degradation of the remaining three conidial nuclei (see Movie 1). To investigate the nature of the cell cycle checkpoint governing initial appressorium morphogenesis (11), we germinated conidia in the presence of the DNA replication inhibitor hydroxyurea (HU). Exposure to HU led to development of undifferentiated germ tubes, while untreated conidia developed normal melanised appressoria (Fig. 1A and 1B), consistent with previous observations (6, 11), and suggesting that DNA replication must occur before initiation of appressorium development. To study the temporal dynamics of cell cycle progression during plant infection by *M. oryzae*, we expressed a Lac repressor fused with GFP that is targeted to the fungal nucleus (GFP-LacI-NLS). This was expressed in a construct that also contained an array of 256 Lac operator repeats inserted into a single chromosomal locus in the genome (Fig. 1C). In this way, it is possible to observe whether cells are in the pre-replicative stage (G1), in which only a single GFP punctum is observed in the nucleus, or in the post-replicative (S/G2), in which two closely spaced puncta are observed, one on each sister chromatid (12). We generated a *M. oryzae* strain expressing a single integration of the GFP-LacI-NLS – $lacO^{X256}$ and found that S-phase entry occurs in the apical conidial cell between 2 and 3 h after germination (Fig S1).

In eukaryotic cells, progression from S-phase to mitosis is driven by the activity of B-type cyclins and associated cyclin-dependent kinases (CDKs) (13). To test whether progression of S-phase is mediated through activity of the B-type cyclin-CDK complex, we generated mutations in the *M. oryzae* B-type cyclin gene, *CYC1*, which is functionally equivalent to the *Aspergillus nidulans NIME* gene (11). In *A. nidulans*, two distinct point mutations in *NIME*, the *nimE*10 (originally identified as *nimG*10) and *nimE*6 alleles confer temperature sensitivity and distinct cell cycle arrest in either the S or G2 phase, respectively (14-17). To test whether appressorium morphogenesis is directly dependent on activity of the CDK-cyclin B complex, we carried out targeted allelic replacements to generate $cyc1^{nimE10}$ and $cyc1^{nimE6}$ mutants, carrying S389R and F465P mutations respectively, which are equivalent to the mutations found in the corresponding *nimE*10 and *nimE*6 of *A. nidulans* (17) (Fig. S2). These mutants carried a single targeted allelic replacement of the $cyc1^{nimE10}$ and $cyc1^{nimE6}$ alleles, confirmed by DNA sequencing, and showed severe growth defects at the semi-restrictive temperature of 30°C (Fig. S3). We evaluated the ability of these mutants to make appressoria at a semi-restrictive temperature (29°C). Conidia of the $cyc1^{nimE10}$ strain produced hyperpolarized germ tubes that failed to develop appressoria, whereas the $cyc1^{nimE6}$ mutant produced relatively thicker germ tubes that underwent flattening and hooking of the germ tube tip, consistent with incipient appressorium formation (Fig. 1D). We also analysed a $nim1^{I327E}$ mutant, which fails to initiate DNA synthesis and instead undergoes mitotic catastrophe (11). The $nim1^{I327E}$ mutant was also unable to develop appressoria. By contrast, a $bim1^{F1763*}$ mutant, which arrests during mitosis,

161 prior to anaphase, developed appressoria normally (Fig. 1D) (6, 11). We
162 conclude that appressorium morphogenesis in *M. oryzae* requires an S-phase
163 checkpoint which operates via activation of the B-type cyclin-CDK1 complex.
164
165 **The appressorium development S-phase checkpoint operates through**
166 **the DNA damage response pathway**
167 During DNA damage, or in the presence of un-replicated chromatin, cells are
168 able to arrest the cell cycle by inhibitory phosphorylation of the B-cyclin-CDK1
169 complex. This allows DNA repair to occur and ensure successful segregation
170 of genetic material (18). Inhibitory phosphorylation of B-type cyclin-CDK1
171 complex is mediated by two serine threonine protein kinases of the DNA
172 damage response (DDR) pathway (19). We identified a serine threonine
173 protein kinase, Chk1, and a fork-head associated (FHA) domain-containing
174 protein kinase, Cds1, which show 35% and 30% amino acid sequence
175 similarity to *Saccharomyces cerevisiae* Chk1 and Rad53, respectively. To
176 determine whether the DDR monitors DNA replication during appressorium
177 morphogenesis, we generated targeted gene replacement mutants, *Δchk1*,
178 *Δcds1*, and a double *Δchk1Δcds1* mutant (Fig. S4 and S5) and then
179 investigated the ability of these mutants to restore appressorium formation in
180 the presence of the DNA replication inhibitor HU. We inoculated conidia of the
181 wild type strain Guy11, and the isogenic *Δchk1*, *Δcds1*, *Δchk1Δcds1* mutants
182 onto hydrophobic plastic surfaces and monitored appressorium formation at
183 24 h in the presence or absence of HU. In the presence of HU, both Guy11
184 (2.13% ± 0.63) and the *Δchk1* null mutant (3.34% ± 2.01) produced
185 undifferentiated germlings and were unable to developed appressoria. By

186 contrast, appressorium formation was restored in *Δcds1* (79.3% ± 6.73) and
187 *Δchk1Δcds1* (52.74% ± 7.46%) mutants (Fig. 2A and 2B). This result
188 indicates that *Δcds1* and *Δchk1Δcds1* mutants were able to bypass the S
189 phase arrest triggered by HU, suggesting that Chk1 and Cds1 act co-
190 operatively to inhibit activity of the B-type cyclin-CDK and ensure successful
191 S-phase transition during appressorium morphogenesis.
192
193 **A novel S-phase checkpoint regulates plant infection**
194 To study mitosis during plant infection we used live cell imaging of a Guy11
195 strain expressing H1-RFP (tdTomato) (11) to monitor cell cycle progression
196 during rice infection. We observed that following penetration peg formation, a
197 single round of mitosis always occurs from the single nucleus inside the
198 appressorium (Fig. 3A and 3B; Movie 2). This suggests that DNA replication
199 must occur in the appressorium before emergence of the penetration peg. To
200 test this idea, we incubated spores of GFP-LacI-NLS strain onto hydrophobic
201 surfaces, and monitored the proportion of appressoria in G1 (one punctum)
202 and S/G2 (two puncta). We found that after 6 h inoculation, nearly 70% of
203 cells were in G1, whereas by 24 h after inoculation, more than 50% of cells
204 had progressed to S/G2, indicating that DNA replication precedes
205 appressorium-mediated plant infection (Fig 3C; Fig S3). We reasoned that re-
206 polarization of the appressorium leading to the formation of the penetration
207 hypha, might therefore require S-phase progression. To test this idea, we first
208 constructed a Guy11 strain expressing H1-RFP and inoculated rice leaf
209 sheath for 10 h, after which we added HU to inhibit DNA replication. When we
210 examined rice leaf sheath infections 30 h after inoculation, we observed that

in non-HU treated infection more than 80% of appressoria had successfully penetrated rice tissue and developed primary invasive hyphae. By contrast, when HU was applied, no plant infection occurred and a single nucleus remained in the appressorium dome (Fig. 3D and 3E; Fig. S6). To investigate whether the cell cycle control point was at the G2/M boundary, we treated a Guy11 strain expressing H1-RFP with the microtubule inhibitor benomyl (50 μg ml^{-1}) and found that the frequency primary invasive hypha formation was the same as in untreated samples, suggesting that simply exerting a mitotic block does not prevent plant infection. (Fig 3F and 3G). We then examined conditional *nim1*^{I327E}, *cyc1*^{nimE10}, *cyc1*^{nimE6} and *bim1*^{F1763*} mutants, impaired at different cell cycle stages. We inoculated rice leaf sheath at the permissive temperature (24^{o}C) and allowed them to develop for 10 h to allow completion of the first round of mitosis in the germ tube and to develop an appressorium. We then incubated them at the semi-restrictive temperature (29^{o}C) for 30 h in total. We found that *nim1*^{I327E} and *cyc1*^{nimE10} mutants, which are defective in S-phase progression, were unable to infect rice tissue and form primary invasive hyphae at 29^{o}C (Fig. 3H and 3I). However *cyc1*^{nimE6} and *bim1*^{F1763*} mutants, which are arrested at G2 and pre-anaphase respectively, were able to infect rice tissue and generate invasive hyphae at 29^{o}C (Fig. 3H and 3I). Rice infection is therefore dependent on S-phase progression in the appressorium.

Turgor-dependent S-phase progression regulates appressorium re-polarisation

We next explored the nature of the S-phase checkpoint that operates during appressorium-mediated plant penetration. As the initial S-phase checkpoint that controls appressorium morphogenesis depends on the DDR and, more specifically, the serine threonine protein kinase Cds1, we investigated whether this was the case for control of appressorium maturation. We inoculated Δ*cds1*, Δ*chk1*Δ*cds1* null mutants and Guy11, on rice leaf sheath and exposed appressoria to HU, 10 h after inoculation. Strikingly, none of the checkpoint kinase mutants were able to penetrate rice tissue in the presence of HU (Fig. 4A). We conclude that the DDR is therefore not involved in S-phase control during appressorium maturation.

We reasoned that appressorium maturation and the control of penetration peg development therefore requires an S-phase checkpoint, regulated by a distinct DDR-independent mechanism. Appressorium maturation is associated with rapid generation of enormous turgor pressure, so we decided to test whether mutants impaired in turgor generation were affected in cell cycle control. Appressorium turgor is generated by glycerol accumulation (7) and development of a thick melanin layer in the appressorium dome. Melanin-deficient mutants, such as *rsy1*$^{-}$ and *buf1*$^{-}$ lack key enzymes for synthesis of di-hydroxynaphthalene (DHN) melanin, and consequently are non-pathogenic and do not generate appressorium turgor (8). We expressed GFP-LacI-NLS in *rsy1*$^{-}$ and *buf1*$^{-}$ mutants containing the LacO^{x256} construct integrated into their genomes at a single locus. We then monitored the DNA replication status of the appressorium nucleus and found that *rsy1*$^{-}$ and *buf1*$^{-}$ mutants are arrested in G1 with a single GFP-LacI-NLS punctum in the appressorium. By contrast, the wild type progressed through S-phase normally. To test whether this effect

was associated with turgor control we then tested S-phase progression in penetration-deficient mutants that were not affected in turgor control. To do this we expressed GFP-LacI-NLS in *ΔnoxR,* null mutants. NoxR is the $p67^{phox}$ –like regulator of the NADPH oxidase complex that regulates septin-mediated F-actin re-modeling and plant infection (10), Strikingly, *ΔnoxR* penetration-deficient mutants displayed two separate puncta, like the wild type Guy11, indicating that S-phase was able to proceed normally (Fig. 4B and 4C). Our results therefore suggest that appressorium turgor generation, which requires melanin synthesis, is necessary for progression from G1 to S-phase.

To investigate the interdependency of turgor control and S-phase progression, we decided to carry out an incipient cytorrhysis experiment to measure cellular turgor in the presence of the DNA-replication inhibitor HU. Cytorrhysis provides a measure of internal cellular turgor, based on the external solute concentration necessary to collapse the appressorium (7, 8). We observed that 24% (± 15.6 SE) of appressoria remained intact when 1 M of glycerol was applied to non-treated appressoria, whereas 71% (± 7.06 SE) of intact appressoria were still observed when 5 M glycerol was applied to appressoria that had been exposed to HU. This observation indicates that impairment of S-phase progression leads to excess turgor generation in the appressorium, which further suggests that S-phase control is necessary for turgor modulation in mature appressoria. To test this hypothesis, we investigated the effect of S-phase progression on cytoskeleton remodeling, which is necessary for appressorium re-polarisation (9, 10). Appressorium function requires assembly of a hetero-oligomeric septin ring composed of four septin GTPases (Sep3, Sep4, Sep5 and Sep6) that scaffolds F-actin to generate a penetration

peg that ruptures the plant cuticle (9, 10). We expressed Sep3-GFP, LifeAct-RFP and Gelsolin-GFP in Guy11 and germinated conidia on hydrophobic plastic surfaces to monitor the frequency of septin and F-actin ring formation at the appressorium pore in the presence or absence of HU. In the absence of HU, a Sep3-GFP ring was always present at the base of the appressorium pore (Fig. 3D). In the presence of HU, however, Sep3-GFP was severely disrupted and the septin ring no longer maintained. Disruption of appressorium pore organization was also observed in LifeAct-RFP and Gelsolin-GFP expressing strains of *M. oryzae* after exposure to HU (Fig. 3D). Moreover when septin-dependent components of the appressorium pore (9), such as the PAK kinase Chm1, the ERM (Ezrin/ Radiixin/ Moesin domain) protein Tea1, the Bim1, Amphiphysin, and Rvs167 BAR domain protein, or the actin nucleation protein, Las17, were localised in the presence of HU, they all showed abnormal localization patterns (Fig. S7). We conclude that septin-dependent F-actin re-modeling at the base of the appressorium requires S-phase progression to have taken place.

Discussion

In this study we have shown that rice infection by the rice blast fungus is controlled by two discrete S-phase checkpoints that operate over two successive cell cycles in the fungus. One of these checkpoints operates at the initial stages of appressorium formation and is connected to the DNA damage response pathway, while the second checkpoint is controlled in a completely novel manner by the prevailing turgor pressure within the appressorium.

309 Appressorium morphogenesis by *M. oryzae* is induced when a spore
310 lands on a hard, hydrophobic surface and by perception of wax monomers
311 released from the rice cuticle. Arresting the cell cycle at S-phase, either
312 through application of hydroxyurea, or generation of conditional *nim1* and
313 *cyc1* ^{nimE10} mutants affected in DNA replication, prevented formation of the
314 hooked, terminal swelling of the germ tube from which the appressorium
315 forms. Live cell imaging confirmed that formation of this terminal swelling is
316 significant, because it provides the destination for the daughter nucleus,
317 following the single round of mitosis that precedes appressorium
318 differentiation. The S-phase is therefore critical in controlling initiation of
319 appressorium development (11).
320 Operation of the initial S-phase checkpoint involves the DNA damage
321 response (DDR), because deletion of the Cds1 kinase-encoding gene allows
322 appressorium morphogenesis to proceed even in the presence of HU. It is
323 increasingly apparent that the DDR interacts with the morphogenesis
324 checkpoint and nutrient sensing pathways (21). In *S. cerevisiae*, for example,
325 the Cds1 homologue, Rad53, interacts with septins and Swe1, linking
326 cytokinesis with control of DNA replication (22, 23). The Cyclic AMP-
327 dependent protein kinase A pathway (PKA) may also interact with the DDR,
328 because in *S. cerevisiae* PKA regulates cell cycle progression and cell size
329 through the RNA-binding protein Whi3 (24). In *M. oryzae*, cAMP-dependent
330 PKA is necessary for differentiation and cell size control of appressoria (25).
331 We observed in this study that, in contrast to early appressorium
332 development, maturation of the infection cell and, in particular, its ability to re-
333 polarise and form a penetration hypha, is regulated by a separate S-phase

checkpoint. Following autophagic cell death of the conidium and nuclear degeneration (6), the single nucleus in the nascent appressorium appears to be arrested at G1, based on our observations using the LacO/LacI biomarker. However, it is also clear that plant infection cannot proceed until this nucleus has passed into S-phase and without this cell cycle progression the appressorium does not initiate polarised growth to infect plant cells.

Generation of a minimum turgor threshold therefore appears to be necessary for progression into S-phase, because melanin-deficient mutants, that are well known to be impaired in turgor generation, form appressoria that stay arrested in G1. Preventing S-phase progression, in *cyc1*^{nimE10} mutants, or by exposure to HU, furthermore prevents septin-mediated remodelling of the F-actin cytoskeleton to the appressorium pore and organisation of the nascent penetration peg. Control of septin organisation and F-actin dynamics at the point of plant infection are therefore dependent on S-phase progression. These observations lead us to propose a model (Fig. 4G) in which a minimum turgor threshold must be achieved in the appressorium, dependent on osmolyte accumulation and melanin deposition. Achievement of this turgor threshold in the appressorium therefore regulates entry intro S-phase. The threshold of turgor also facilitates remodelling of the cytoskeleton, controlled by regulated synthesis of reactive oxygen species by the Nox2 complex (10), which acts upon septin GTPases (9) to organise the appressorium pore, regulating membrane curvature generation, polarised exocytosis and exocyst organisation (26), followed by rapid actin polymerisation to drive polarised growth of the penetration hypha into the rice cuticle.

How might such cell cycle control operate in the appressorium? Perhaps the most useful analogy for penetration peg emergence is the control of budding in *S. cerevisiae* in which cells are initially arrested in G1 (27, 28) and the tyrosine kinase Swe1 plays an important role in monitoring cytoskeletal organization, leading ultimately to Cdc28 activation, which triggers polarized growth through activation of the guanine nucleotide exchange factor (GEF) of the Cdc42 GTPase, Cdc24 (29). Components of this GTPase signalling module are direct targets of Cdc28 and control subsequent bud emergence (28). In *M. oryzae*, CDK1/cyclin complexes may also control the GTPase signalling module to direct growth towards the base of the appressorium, controlling septin and F-actin organisation. The Cdc42 GTPase and its effector Chm1 (a Cla4 homologue) have, for instance, been shown to be required for cytoskeletal reorganisation at the appressorium pore and for plant penetration (9, 30, 31). Cdc42 may therefore activate septin ring assembly through action of the PAK kinases Chm1 and activate F-actin remodelling through the Nox2/NoxR complex and its interaction with Rac (10, 32).

It is also apparent that S-phase progression is contingent on turgor control rather than being explicitly linked to DDR control, because deletion of Cds1 does not restore plant infection to *M. oryzae* appressoria that have been exposed to HU. Consistent with such a model, HU treatment leads to runaway turgor generation and an inability to re-polarise, suggesting that integrated control of DNA replication and turgor modulation is necessary for operation of the infection cell.

When considered together, our results suggest that infection of rice tissue by *M. oryzae* requires discrete cell cycle morphogenetic transitions to enable appressorium formation, appresorium re-polarisation and cuticle rupture, thereby enabling host cell invasion. This temporal sequence of shape transitions by the fungus is tightly co-ordinated with nuclear division, and critical to the establishment of rice blast disease.

Material and Methods

Fungal Strains, Growth Conditions and DNA Analysis

Storage, maintenance and growth of *M. oryzae* strains, media composition, nucleic acid extraction and fungal transformation were all as previously described (33). Generation of DNA fragments, gel electrophoresis, restriction enzyme digestion, gel blots and sequencing were performed using standard procedures (34).

Generation of *cyc1^{nimE10}*, *cyc1^{nimE6}*, Δ*chk1*, Δ*cds1* and Δ*chk1*Δ*cds1* Mutants and Strains Expressing GFP Fusions

Details of construction for allelic replacement vectors for generating *cyc1^{nimE10}*, *cyc1^{nimE6}* mutants are given in Supplemental Methods. DNA sequences were retrieved from the *M. oryzae* genome database of the Broad Institute at the Massachusetts Institute of Technology, Cambridge, MA (www.broad.mit.edu/annotation/fungi/magnaporthe) and used to design primers. Targeted gene replacement of *CHK1* and *CDS1* was performed using hygromycin B (*hph*), and bialaphos (*bar*) selectable markers, respectively, by the split marker technique described previously (35). The *chk1:hph* construct

407 was introduced into Guy11 and transformants selected on hygromycin B (200
408 µg mL^{-1}). Both Guy11 and Δ*chk1* mutants were transformed with *cds1:bar* and
409 transformants selected on glufosinate (30 µg mL^{-1}). Transformants were
410 assessed by Southern Blot. Plasmids expressing GFP and RFP fusions were
411 transformed into Δ*chk1*, Δ*cds1* and Δ*chk1*Δ*cds1* mutants and single-insertion
412 transformants selected by Southern blot. For chromosome tagging, a plasmid
413 containing the GFP-lac repressor fusion containing a nuclear localization
414 signal (GFL-LacI-NLS) and a plasmid containing an array of 256 lac operator
415 repeats were co-transformed into each fungal strain and selected in the
416 presence of glufosinate (30 µg ml^{-1}) and secondly in the presence of
417 chlorimuron ethyl (50 µg ml^{-1}).
418
419 **Infection Structure Development Assays, Plant Infection Assays and**
420 **Live-Cell Imaging of Nuclei and Cytoskeletal Components of *M. oryzae***
421 Appressorium development was induced *in vitro* on borosilicate 18 x 18 mm
422 glass coverslips (Fisher Scientific UK Ltd), adapted from (36). Fifty microliters
423 of conidial suspension (5 $x10^4$ mL^{-1}) was placed on a coverslip and incubated
424 at 24°C. Rice leaf sheath inoculations, adapted from (37), were performed to
425 observe development of invasive hyphae. At desired time points, the DNA
426 replication inhibitor hydroxyurea (HU) was added to germinating spores (200
427 mM) or appressoria on leaf sheaths (1 M) after removing pre-existing water.
428 Benomyl was used at a final condcentration of 50 µg mL^{-1} (6) and samples
429 incubated at 24°C. Development of appressoria was observed using a IX81
430 motorized inverted microscope (Olympus, Hamburg, Germany) and images
431 captured using a Photometrics CoolSNAP HQ2 camera (Roper Scientific,

Germany), under control of MetaMorph software package (MDS Analytical Technologies, Winnersh, UK). Onion epidermis assays and leaf drop experiments were performed, as described previously (38, 39).

Laser Scanning Confocal Microscopy of Infected Plant Tissue

A Leica SP8 Laser Scanning Confocal Microscope equipped with an HC PC APO CS2 63 x/1.40 oil immersion lens was used to collect signal from Guy11 H1-RFP cells during infection of rice leaf sheath. RFP was excited using a DPSS 561 nm laser at 0.1 % transmission and emitted signal collected from 590-632 nm using the SP8 HyD detector, with gain set to 77. DIC images were collected using the same laser settings, and PMT gain of 254. Movies were generated from x,y,z,t series (x,y 512 x 512 pixels; z step was 0.34 µm with a pinhole set to 1 A.U. and taken at a frame rate of one frame every 10 minutes) from infected tissue samples. Data used to generate Supplemental movies 1 and 2 represents an x,y,z,t cropped selection from the original data file.

Accession Numbers Sequence data from this article can be found in the GenBank/EMBL databases under the following accession numbers: *M. oryzae* NIM1 (MGG_00597), *M. oryzae* BIM1 (MGG_03314), *M. oryzae* CYC1 (MGG_05646), *M. oryzae* CHK1 (MGG_03729), *M. oryzae* CDS1 (MGG_04790), and *A. nidulans* NimE (X64602).

Acknowledgements

This work was supported by EU-Initial Training Network Marie Curie (PITN-GA-2009-237936) (to M.O.R.), a Halpin Scholarship (to W.S.), and a

European Research Council Advanced Investigator award (to N.J.T.) under the European Union's Seventh Framework Programme (FP7/2007-2013)/ERC grant agreement 294702 GENBLAST. We gratefully acknowledge Stephen A. Osmani (The Ohio State University) and Steven W. James (Gettysburg College) for providing unpublished data regarding the specific DNA sequence changes present in the *Aspergillus nidulans nimE*10 and *nimE*6, as well as for providing these fungal strains. We also thank Yasuyuki Kubo and Fumi Fukada (Kyoto Prefectural University) for providing the LacO/LacI biomarker.

References

1. Martin-Urdiroz M, Oses-Ruiz M, Ryder LS, & Talbot NJ (2016) Investigating the biology of plant infection by the rice blast fungus *Magnaporthe oryzae*. *Fungal Genet Biol* 90:61-68.
2. Talbot NJ (2003) On the trail of a cereal killer: Exploring the biology of *Magnaporthe grisea*. *Annu Rev Microbiol* 57:177-202.
3. Wilson RA & Talbot NJ (2009) Under pressure: investigating the biology of plant infection by *Magnaporthe oryzae*. *Nat Rev Micro* 7:185-195.
4. Fisher MC*, et al.* (2012) Emerging fungal threats to animal, plant and ecosystem health. *Nature* 484:186-194.
5. Bourett TMH, R. J. (1990) Invitro development of penetration structures in the rice blast fungus *Magnaporthe grisea*. *Can. J. Bot.* 68:329-342.
6. Veneault-Fourrey C, Barooah M, Egan M, Wakley G, & Talbot NJ (2006) Autophagic fungal cell death is necessary for infection by the rice blast fungus. *Science* 312:580-583.

481 7. de Jong JC, McCormack BJ, Smirnoff N, & Talbot NJ (1997) Glycerol
482 generates turgor in rice blast. *Nature* 389:244-244.
483 8. Howard RJ & Valent B (1996) Breaking and entering: host penetration
484 by the fungal rice blast pathogen *Magnaporthe grisea*. *Annual Rev*
485 *Microbiol* 50:491-512.
486 9. Dagdas YF*, et al.* (2012) Septin-mediated plant cell invasion by the rice
487 blast fungus, *Magnaporthe oryzae*. *Science* 336:1590-1595.
488 10. Ryder LS*, et al.* (2013) NADPH oxidases regulate septin-mediated
489 cytoskeletal remodeling during plant infection by the rice blast fungus.
490 *Proc. Natl Acad Sci USA* 110:3179-3184.
491 11. Saunders DG, Aves SJ, & Talbot NJ (2010) Cell cycle-mediated
492 regulation of plant infection by the rice blast fungus. *The Plant Cell*
493 22:497-507.
494 12. Straight AF, Belmont AS, Robinett CC, & Murray AW (1996) GFP
495 tagging of budding yeast chromosomes reveals that protein–protein
496 interactions can mediate sister chromatid cohesion. *Current Biol.*
497 6(12):1599-1608.
498 13. Coudreuse D & Nurse P (2010) Driving the cell cycle with a minimal
499 CDK control network. *Nature* 468:1074-1079.
500 14. Morris NR (1976) Nucleosome structure in *Aspergillus nidulans*. *Cell*
501 8(3):357-363.
502 15. Bergen LG, Upshall A, & Morris NR (1984) S-phase, G2, and nuclear
503 division mutants of *Aspergillus nidulans*. *J Bacteriol* 159:114-119.

16. O'Connell MJ, Osmani AH, Morris NR, & Osmani SA (1992) An extra copy of nimEcyclinB elevates pre-MPF levels and partially suppresses mutation of nimTcdc25 in Aspergillus nidulans. *EMBO J.* 11:2139-49.
17. James SW*, et al.* (2014) Restraint of the G2/M transition by the SR/RRM family mRNA shuttling binding protein SNXAHRB1 in *Aspergillus nidulans*. *Genetics* 198:617-633.
18. Rhind N & Russell P (1998) Mitotic DNA damage and replication checkpoints in yeast. *Curr Opin Cell Biol* 10:749-758.
19. Sanchez Y*, et al.* (1999) Control of the DNA damage checkpoint by Chk1 and Rad53 protein kinases through distinct mechanisms. *Science* 286:1166-1171.
20. Park G, Xue C, Zheng L, Lam S, & Xu JR (2002) MST12 regulates infectious growth but not appressorium formation in the rice blast fungus *Magnaporthe grisea*. *Molecular plant-microbe interactions : MPMI* 15:183-192.
21. de Sena-Tomas C, Fernandez-Alvarez A, Holloman WK, & Perez-Martin J (2011) The DNA damage response signaling cascade regulates proliferation of the phytopathogenic fungus *Ustilago maydis* in planta. *The Plant Cell* 23:1654-1665.
22. Enserink JM, Smolka MB, Zhou H, & Kolodner RD (2006) Checkpoint proteins control morphogenetic events during DNA replication stress in *Saccharomyces cerevisiae*. *J Cell Biol* 175:729-741.
23. Smolka MB*, et al.* (2006) An FHA domain-mediated protein interaction network of Rad53 reveals its role in polarized cell growth. *J Cell Biol* 175:743-753.

529 24. Wang H, Gari E, Verges E, Gallego C, & Aldea M (2004) Recruitment
530 of Cdc28 by Whi3 restricts nuclear accumulation of the G1 cyclin-Cdk
531 complex to late G1. *EMBO J.* 23:180-190.
532 25. Xu JR & Hamer JE (1996) MAP kinase and cAMP signaling regulate
533 infection structure formation and pathogenic growth in the rice blast
534 fungus *Magnaporthe grisea*. *Genes Dev* 10:2696-2706.
535 26. Gupta YK*, et al.* (2015) Septin-Dependent Assembly of the Exocyst Is
536 Essential for Plant Infection by *Magnaporthe oryzae*. *The Plant cell*
537 27:3277-3289.
538 27. Bishop AC*, et al.* (2000) A chemical switch for inhibitor-sensitive alleles
539 of any protein kinase. *Nature* 407:395-401.
540 28. McCusker D*, et al.* (2007) Cdk1 coordinates cell-surface growth with
541 the cell cycle. *Nature Cell Biol.* 9:506-515.
542 29. Howell AS*, et al.* (2012) Negative feedback enhances robustness in the
543 yeast polarity establishment circuit. *Cell* 149:322-333.
544 30. Li L, Xue C, Bruno K, Nishimura M, & Xu JR (2004) Two PAK kinase
545 genes, CHM1 and MST20, have distinct functions in *Magnaporthe*
546 *grisea*. *Molecular Plant-Microbe interact.* 17:547-556.
547 31. Zheng W*, et al.* (2009) A Cdc42 ortholog is required for penetration and
548 virulence of *Magnaporthe grisea*. *Fungal Genetics Biol.* 46:450-460.
549 32. Chen J*, et al.* (2008) Rac1 Is Required for Pathogenicity and Chm1-
550 Dependent Conidiogenesis in Rice Fungal Pathogen *Magnaporthe*
551 *grisea*. *PLoS Pathogens* 4:e1000202.

552 33. Talbot NJ, Ebbole DJ, & Hamer JE (1993) Identification and
553 characterization of MPG1, a gene involved in pathogenicity from the
554 rice blast fungus *Magnaporthe grisea*. *The Plant Cell* 5:1575-1590.
555 34. Sambrook J, Fritsch, E.F., and Maniatis, T (1989) *Molecular Cloning - a*
556 *laboratory manual, second edition.* (Cold Spring Harbour Laboratory
557 press.).
558 35. Sweigard JA, Carroll AM, Farrall L, Chumley FG, & Valent B (1998)
559 *Magnaporthe grisea* pathogenicity genes obtained through insertional
560 mutagenesis. *Molec. Plant-Microbe Interact.* 11:404-412.
561 36. Hamer JE, Howard, R.J., Chumley, F.G., and Valent, B. (1988) A
562 mechanism for surface attachment in spores of a plant pathogenic
563 fungus. *Science* 239:288-190.
564 37. Kankanala P, Czymmek K, & Valent B (2007) Roles for rice membrane
565 dynamics and plasmodesmata during biotrophic invasion by the blast
566 fungus. *The Plant Cell* 19:706-724.
567 38. Chida T & Sisler HD (1987) Restoration of appressorial penetration
568 ability by melanin precursors in Pyricularia oryzae treated with
569 antipenetrants and in melanin-deficient mutants. *J. Pestic. Sci.* 12(49-
570 55).
571 39. Jia Y, Valent B, & Lee FN (2003) Determination of host responsesto
572 Magnaporthe grisea on detached rice leaves using a spot inoculation
573 method. *Plant Disease* 87:129-133.
574
575
576

577

578

579

580

581

582

583 **Figure Legends**

584 **Figure 1. Appressorium morphogenesis is an S-phase regulated**
585 **developmental process in *M. oryzae*. (A)** Micrographs to show effect of
586 inhibition of DNA replication by 200 mM Hydroxyurea (HU) on appressorium
587 formation in *M. oryzae,* added at 2 hpi and observed at 24 h (Scale bar, 20
588 µm.) **(B)** Bar chart to show frequency of appressorium formation after
589 exposure to HU. (****= P< 0.0001; unpaired Student's *t*-test; n= 3
590 experiments, spores= 300) **(C)** Diagram of LacO/LacI operator system. A
591 construct containing 256 LacO repeats was integrated at a random locus in
592 the genome. Fluorescence visualized by expressing GFP-LacI-NLS which
593 binds to LacO repeats. In a pre-replicative cell (G1) in which a single locus is
594 present, a single punctum is observed, whereas in a post-replicative (S/G2)
595 nucleus, two puncta appear. (Scale bar, 10 µm.) **(D)** Micrographs to show
596 appressorium formation of Guy11, *nim1*^{I327E}, *cyc1*^{nimE10}, *cyc1*^{nimE6} and
597 *bim1*^{F1673*} mutants at 24°C and 30°C. (Scale bar, 20 µm) **(E)** Bar chart to
598 show frequency of appressorium formation by Guy11, *nim1*^{I327E}, *cyc1*^{nimE10},
599 *cyc1*^{nimE6} and *bim1*^{F1673*} mutants at 24°C and 30°C. (**= P< 0.01; ***= P<
600 0.001; ****= P< 0.0001; unpaired Student's *t*-test; n= 3 experiments, spores
601 observed per experiment = 300).
602
603 **Figure 2. An S-phase checkpoint for appressorium morphogenesis**
604 **requires the DNA damage response in *M. oryzae*. (A)** Micrographs
605 showing appressorium formation by Guy11, *Δchk1*, *Δcds1* and *Δchk1Δcds1*
606 mutants following exposure to 200 mM HU, added at 1 hpi and observed at
607 24h (Scale bar, 10 µm.) **(B)** Bar chart to show frequency of germling (blue)

608 and appressoria (red) formation by Guy11, *Δchk1*, *Δcds1* and *Δchk1Δcds1*
609 mutants (****= P< 0.0001; unpaired Student's *t*-test; n= 3 experiments, spores
610 observed per experiment= 136-601).
611
612 **Figure 3. Inhibition of DNA replication impairs plant infection by**
613 ***M.oryzae*. (A)** Micrographs of rice leaf sheath infection by *M. oryzae* Guy11
614 expressing H1-RFP. Appressoria contain a single nucleus at time of
615 development of a penetration primary invasive hypha (PH) while invasive
616 hyphae (IH) contain two nuclei. **(B)** Bar chart to show number of nuclei in
617 appressoria and primary invasive hyphae during time course of plant infection
618 at 20, 22, 24 and 26 h. **(C)** Micrographs to show appressorium development
619 of Guy11 expressing GFP-LacI-NLS and LacO repeats at 6 h and 24 h,
620 showing progression from G1 to G2. **(D)** Rice leaf sheath observed 30 h after
621 inoculation with Guy11 H1-RFP following exposure to HU at 10 h. **(E)** Bar
622 chart to show frequency of appressoria that had formed a primary invasive
623 hypha in the presence or absence of 1 M HU. (**= P< 0.01; unpaired
624 Student's *t*-test; n = 3 experiments, appressoria observed= 557-582). **(F)**
625 Micrographs of rice leaf sheath infections of Guy11 expressing H1-RFP to
626 show effect of a G2-arrest by exposure to benomyl (50 μg mL^{-1}). **(G)** Bar chart
627 to show frequency of appressoria forming a penetration peg in the presence
628 or absence of benomyl (50 μg mL^{-1}). (ns= P> 0.05; unpaired Student's *t*-test;
629 n= 5 experiments, appressoria= 479-475) **(H)** Micrographs of rice leaf sheath
630 inoculated with Guy11, *nim1*^{I327E}, *cyc1*^{nimE10}, *cyc1*^{nimE6} and *bim1*^{F1673*} mutants
631 at 48 h to show effect of cell cycle arrest points on frequency of plant
632 infection. (Scale bar, 10 μm.) **(I)** Bar chart to show the frequency of invasion

633 of rice leaf sheath by Guy11, *nim1*^{I327E}, *cyc1*^{nimE10}, *cyc1*^{nimE6} and *bim1*^{F1673*}
634 mutants at permissive (24°C) and non-permissive (30°C) temperatures. (*=
635 P< 0.05; ***= P< 0.001; unpaired Student's *t*-test; n= 3 experiments;
636 appressoria= 138-371).
637
638 **Figure 4. S-phase regulation during plant infection is coordinated with**
639 **turgor generation. (A)** Micrograph to show rice leaf sheath inoculated with
640 Guy11, *Δcds1* and *Δchk1Δcds1* mutants ±HU, added at 10 h, observed at 30
641 h (Scale bar, 10 µm). **(B)** Micrographs of Guy11, Δ*mst12*, *rsy*$^{-}$ and *buf*$^{-}$
642 mutants expressing GFP-LacI-NLS and LacO repeat construct to show effect
643 on G1 to G2 progression. **(C)** Bar chart to show frequency of progression to
644 G2 in appressoria of Guy11, Δ*mst12*, *rsy*$^{-}$ and *buf*$^{-}$ expressing GFP-LacI-NLS
645 and LacO repeat construct. **(D)** Micrographs of Guy11 expressing Sep3-GFP,
646 LifeAct-RFP, and Gelsolin-GFP ±HU, added at 10 h observed at 30 h. (Scale
647 bar, 10 µm.). **(E)** Incipient cytorrhysis assay to measure appressorium turgor
648 generation ±HU. Appressoria were allowed to form on hydrophobic plastic
649 coverslips for 10 h, when 200 mM HU was added. At 24 h, appressoria were
650 exposed to increasing concentrations of glycerol, and the percentage of intact
651 appressoria recorded (*= P< 0.05; **= P<0.01; ****= P< 0.0001; unpaired
652 Student's *t*-test; n= 3 experiments; appressoria observed= 90- 126). **(F)** Model
653 depicting cell cycle transitions necessary for appressorium-mediated plant
654 infection by *M. oryzae.* An S-phase checkpoint operates during initial
655 appressorium morphogenesis and depends on the DNA damage repair
656 response (DDR). A second S-phase checkpoint operates during appressorium
657 maturation and depends on cellular turgor. **(G)** Model to show cell cycle

658 control of rice cell entry by *M. oryzae*. A newly formed appressorium is initially
659 arrested in G1 with a minimum turgor pressure level (Tmin). Turgor
660 accumulates due to glycerol synthesis and melanisation of the appressorium
661 cell wall. A threshold of turgor is generated (Tmax) in the appressorium in
662 order for S-phase entry, which is necessary for septin-dependent F-actin
663 remodeling at the base of the appressorium. This leads to formation of a
664 penetration peg to rupture the plant cuticle.
665
666

667 **Fig 1.**

668

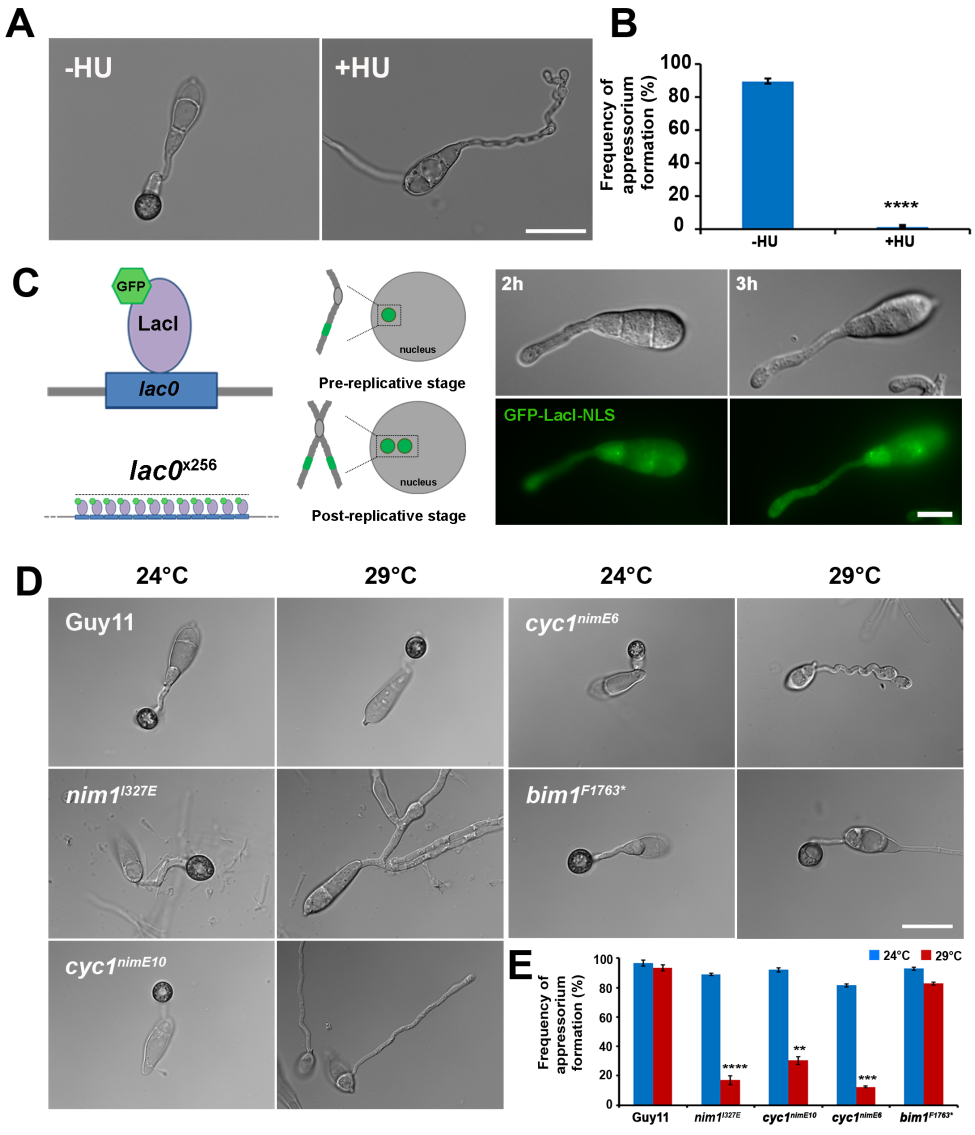
A
-HU
+HU
B
Frequency of appressorium formation (%)
100
80
60
40
20
0
****
-HU
+HU
C
GFP
LacI
lac0
lac0x256
nucleus
Pre-replicative stage
nucleus
Post-replicative stage
2h
3h
GFP-LacI-NLS
D
24°C
29°C
24°C
29°C
Guy11
cyc1nimE6
nim1I327E
bim1F1763*
cyc1nimE10
E
Frequency of appressorium formation (%)
24°C
29°C
****
**
***
Guy11
nim1I327E
cyc1nimE10
cyc1nimE6
bim1F1763*

Fig 2.

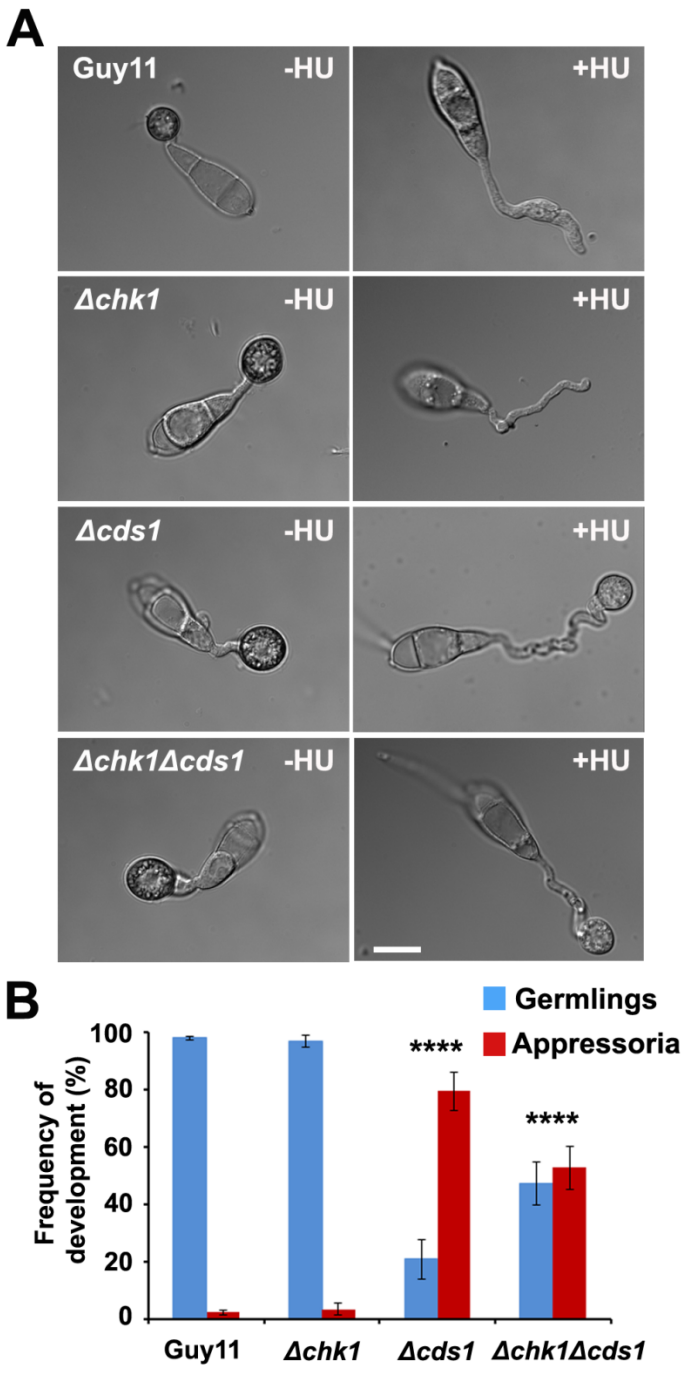
A
Guy11
-HU
+HU
Δchk1
-HU
+HU
Δcds1
-HU
+HU
Δchk1Δcds1
-HU
+HU
B
Germlings
Appressoria
Frequency of development (%)
100
80
60
40
20
0
****
****
Guy11
Δchk1
Δcds1
Δchk1Δcds1

Fig 3.

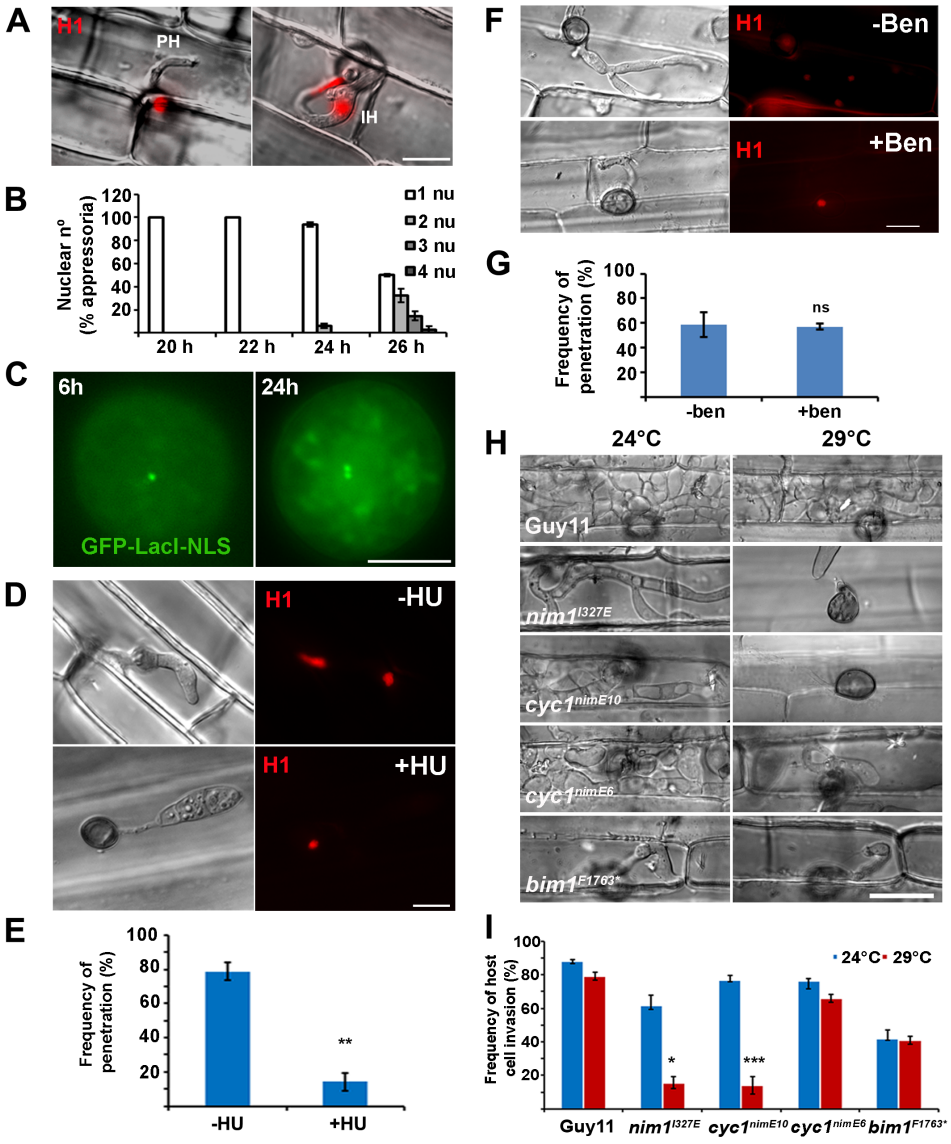
A
H1
PH
IH
B
Nuclear n° (% appressoria)
120
100
80
60
40
20
1 nu
2 nu
3 nu
4 nu
20 h
22 h
24 h
26 h
C
6h
24h
GFP-LacI-NLS
D
H1
-HU
H1
+HU
E
Frequency of penetration (%)
100
80
60
40
20
**
-HU
+HU
F
H1
-Ben
H1
+Ben
G
Frequency of penetration (%)
100
80
60
40
20
ns
-ben
+ben
H
24°C
29°C
Guy11
nim1I327E
cyc1nimE10
cyc1nimE6
bim1F1763*
I
Frequency of host cell invasion (%)
100
80
60
40
20
24°C
29°C
*
***
Guy11
nim1I327E
cyc1nimE10
cyc1nimE6
bim1F1763*

Fig 4.

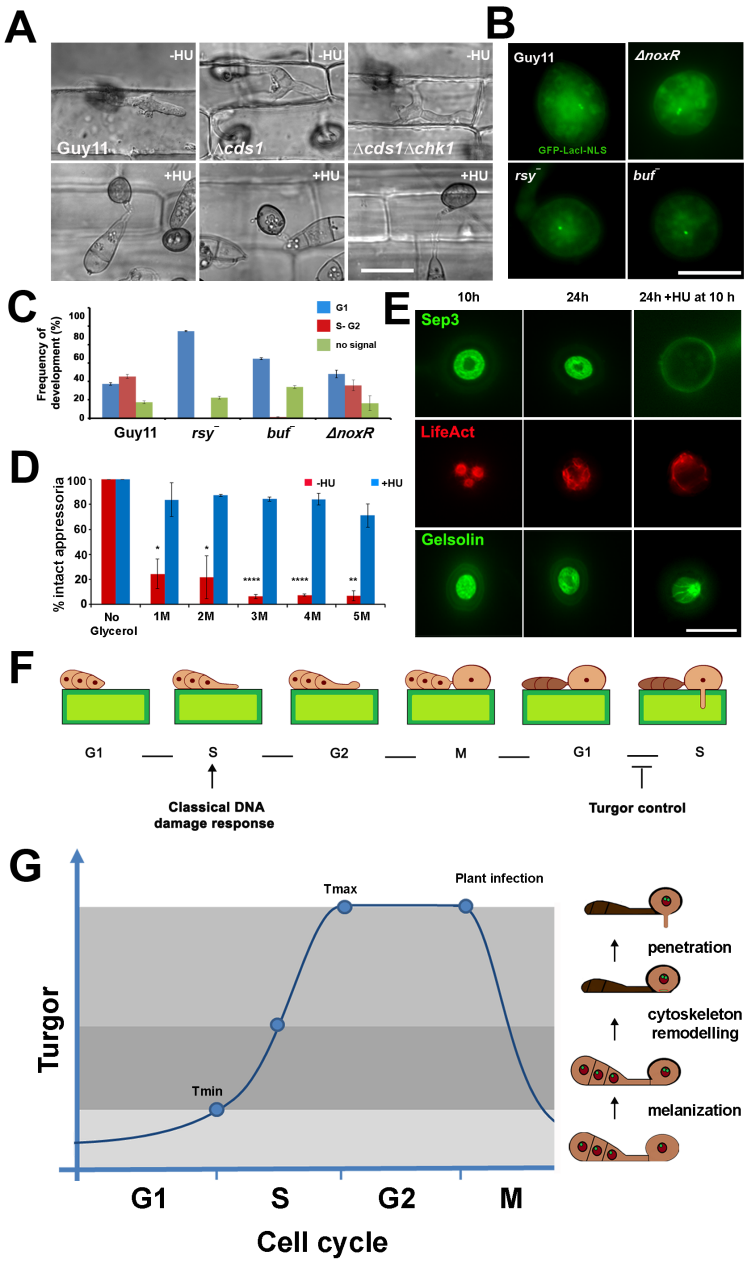
A
-HU
+HU
Guy11
Δcds1
Δcds1Δchk1
B
Guy11
ΔnoxR
GFP-LacI-NLS
rsy⁻
buf⁻
C
Frequency of development (%)
G1
S- G2
no signal
Guy11
rsy⁻
buf⁻
ΔnoxR
D
% intact appressoria
-HU
+HU
No Glycerol
1M
2M
3M
4M
5M
E
10h
24h
24h +HU at 10 h
Sep3
LifeAct
Gelsolin
F
G1
S
G2
M
G1
S
Classical DNA damage response
Turgor control
G
Turgor
Tmax
Plant infection
Tmin
G1
S
G2
M
Cell cycle
penetration
cytoskeleton remodelling
melanization

Supplementary information

Figure S1. Cell cycle progression during appressorium development shown by GFP-LacI-NLS co-expressed with 256 repeats of LacO. (A) Diagram to show the stages of development during appressorium formation. Green dot depicts the fluorescence dot resulting from GFP-LacI-NLS co-expressed with 256 repeats of LacO. One dot indicates a pre-replicative stage (G1) and two dots indicate a post-replicative stage (S/G2). **(B)** Bar chart to show the frequency of developmental stages for every time point. Error bars represented the standard deviation from three independent replicates.

Figure S2. Amino acid sequence alignment of the predicted *M. oryzae* Cyc1 and targeted gene replacement of *M. oryzae CYC1*. (A) *NIME* locus of wild type, *nimE*10 and *nimE*6 *A. nidulans* strains was sequenced to show point mutations associated with temperature sensitivity. Amino acid alignment was generated using ClustalW2 and shaded using Boxshade version 3.21. Numbers on the right indicate positions of amino acid residue. Amino acid shaded with black background are identical among two fungi, dark grey shaded residues are similar in two out of three, and those in white background do not show any similarity. Black arrow indicates position of amino acid substitution of $cyc1^{nimE10}$ (S389R), while white arrow indicates that of $cyc1^{nimE6}$ (F465P), consistent with Steve Osmani's personal communication. **(B)** Schematic diagram indicates gene replacement strategy of $cyc1^{nimE10}$ and $cyc1^{nimE6}$ alleles. **(C)** Southern blot analysis to show the successful replacement of temperature sensitive alleles of $cyc1^{nimE10}$ (upper panel) and $cyc1^{nimE6}$ alleles (lower panel). The size difference in each blot is consistent with successful replacement of the gene construct containing the resistance cassette *HPH*. Genomic DNA of putative transformants and the wild type Guy11 were digested with *Sal*I enzyme.

After fractionation by gel electrophoresis, blots were probed with a restriction fragment comprising the 3' UTR of *CYC1.*

Figure S3. Vegetative growth of Guy11, *cyc1*^{nimE10} and *cyc1*^{nimE6} mutants at 24°C and 30°C.

Figure S4. Targeted gene replacement of *M. oryzae CHK1* into Guy11 background, *M. oryzae CDS1* into Guy11 background and *M. oryzae CDS1* into Δ*chk1* background and pathogenicity assay in a rice spray experiment. A) Southern blot analysis carried out to identify *CHK1* targeted gene replacement showing PvuI restriction digestions followed by probing with the 1 Kb upstream region of CHK1 (Chk1.LF). The result showed a 4.4 Kb band when no gene replacement had occurred and a 2.6 Kb band when the corresponding resistance cassette was integrated at the *CHK1* locus. The Southern confirmed the positive result for T44. **B)** Southern blot analysis result showing a PstI enzyme restriction digestion followed by probing with the 1 Kb upstream region of *CDS1* (Cds1.LF) that generated a 5.5 Kb band when no gene replacement had occurred and a 2.5 Kb band when the corresponding resistance cassette was integrated at the *CDS1* locus. Numbers 2 and 7 correspond to Δ*chk1* background, number 15 corresponded to an unrelated background to this research, and number 19 and 20 corresponded to Guy11 background. **(C)** Pathogenicity assay of CO-39 rice leaves inoculated with Guy11, *Δchk1*, *Δcds1* and *Δchk1Δcds1* mutants after 5 dpi.

Figure S5. Vegetative growth and colony morphology of DNA replication checkpoint mutants. A) A mycelial plug of Guy11, Δ*chk1*, Δ*cds1* and Δ*chk1*Δ*cds1*, were inoculated onto 0.001% alkylating agent methyl methanesulfonate (MMS) and in CM plates and incubated during 12 days at 26 °C. Images were taken by using an

Epson Expression 1680 Pro scanner after 10 days post inoculation. **B)** Colony growth of Guy11, Δ*chk1*, Δ*cds1* and Δ*chk1*Δ*cds1* over the period of 12 days. Error bars represented the standard error from three independent replicates.

Figure S6. HU blocks *M. oryzae* plant penetration in a dose dependent manner. **A)** Bar chart to show the effect of 200 mM, 500 mM, 800 mM and 1M HU concentrations on rice leaf sheath into 28 day-old CO-39 rice plants. HU was added at 10 hpi and results were scored at 30 h (n=3 experiments; appressoria= 50). **B)** Effect of 200 mM, 500 mM, 800 mM and 1 M HU concentrations on a leaf spot assay of wild-type Guy11 into 28 day-old CO-39 rice plants. HU was added at 10 h.

Figure S7. S-phase regulation is independent of DDR (A) Involvement of DNA checkpoint kinases in appressorium-mediated plant penetration. Bar chart showing the percentage penetration of CO-39 rice leaf sheath at 30 h inoculated with wild-type Guy11, *Δcds1* and *Δchk1Δcds1* at 30 h without HU and with addition of 1M HU at 10 h (n=3 experiments; appressoria= 50). **(B)** HU affects localization of F-actin cytoskeleton-associated proteins during appressorium formation on glass coverslips. Micrographs to show localization Chm1-GFP, Tea1-GFP, Rvs167-GFP and Las17-GFP during appressorium development at 10 h, 24 h and 24 h when HU was added at 10 h. (Scale bar, 10 µm).

Table S1. Reciprocal shift experiment. Reciprocal shift method was used to establish the arrest points of the cell cycle mutants (15). Conidia of the indicated strains were induced for appressorium development on cover slips and percentages of conidia in which appressorium maturation had occurred indicating completion of mitosis. At least 200 conidia were counted for each determination. **Control**, 24 hours at 24°C; **A** 24 hours at 29°C; **B,** 8 hours at 29°C then 16 hours at 24°C; **C**, 8 hours at

29°C then 16 hours at 24°C with HU; **D**, 24 hours at 24°C with HU; **E,** 8 hours at 24°C with HU then 16 hours without HU; **F**, 8 hours at 24°C, then 16 hours at 29°C without HU.

Table S2. Primers used in this study.

Supplemental Movie S1. Live- cell imaging of cell cycle progression during appressorium development in *M. oryzae*. Movie of Guy11 strain expressing H1-RFP during appressorium development germinated in hydrophobic coverslips during 24 h.

Supplemental Movie S2. Live- cell imaging of cell cycle progression during appressorium mediated plant penetration in M. oryzae. Movie of Guy11 strain expressing H1-RFP during rice cuticle rupture and entry into the cell.

Supplemental methods

Construction of the *M. oryzae cyc1*^{niEG10} and *cyc1*^{nimE6} gene replacement vectors

The partial length of *A. nidulans nimE* gene was amplified from *A. nidulans nimE10 (*previously named *nimG10)* and *nimE6* and an isogenic wild type strain (kindly provided by Steve W. James, Gettysburg College, Gettysburg, PA). The *A. nidulans nimE10* and *nimE6* alleles were amplified (primers NIME-P1 and NIME-P2) and sequenced to reveal point mutations. The *A. nidulans nimE10* allele contains a serine residue altered to arginine at position 369. The *nimE6* allele has a leucine residue mutated to proline at position 445.

In-Fusion Cloning based on *in vitro* homologous recombination was performed to generate temperature-sensitive alleles of *M. oryzae,* using a commercial kit (In-Fusion Cloning Kit, Clontech Laboratories, Inc.). The *cyc1*^{nimE10} and *cyc1*^{nimE6} alleles carry S389R and F465P mutations, respectively, equivalent the corresponding *A. nidulans* mutants. For generating *cyc1*^{nimE10} allele, the *CYC1* gene (genomic locus MGG_05646) was amplified in two fragments. A 1.3 kb *CYC1* fragment (primers V-BamHI-nimG11_P1, Mut-nimG11_P2) and a 0.5 kb *CYC1* fragment (primers Mut-nimG11_P3, Hyg-nimG11_P4) were amplified with either side of the region requiring nucleotide substitution, and have 15 base pair overhangs complementary to the adjacent fragment. Substitution of codon 389 from serine (AGC) to arginine (CGC) was introduced to the 0.5 kb *CYC1* fragment by primers Mut-nimG11_P3. A 1.4 kb hygromycin resistance cassette *HPH* was amplified from pCB1004 using primers M13F and M13R. A 1.0 kb 3' untranslated region (3' UTR) downstream of the *CYC1* locus was amplified (primers Hyg-nimG11-3UTR_P5, V-BamHI-nimG11-3UTR_P6) to provide a region homology 3' to the *HPH* cassette in the gene replacement vector. Four inserts including the 1.3 kb and 0.5 kb fragments of *CYC1* gene, the *HPH* cassette and the 3' UTR were cloned into a *Hin*dIII-cut *1284 pNEB-Nat-Yeast* cloning vector.

For the *cyc1*^{nimE6} allele, A 1.6 kb *CYC1* fragment (primers V-BamHI-nimG11_P1, Mut-nimE6_P2), and a 178 bp *CYC1* fragment (primers Mut-nimE6_P3, Hyg-nimG11_P4) were amplified. Substitution of codon 465 from phenylalanine (TTC) to proline (CCT) was introduced to the 178 bp *CYC1* fragment by primer Mut-nimE6_P3. Four inserts including the 1.6 kb and 178 bp fragments of *CYC1* gene, the *HPH* cassette and the 3' UTR were cloned into a *Hin*dIII-cut *1284 pNEB-Nat-Yeast* cloning vector. The *cyc1*^{nimE10} and *cyc1*^{nimE6} constructs were excised by *Bam*HI

to generate the full length 4.2 kb gene replacement constructs and transformed into the Guy11 wild type strain.

Table S1. Reciprocal shift experiment

Strains	Control	A	B	C	D	E	F	Cell phase
Guy11	98.2	95.1	95	91	0	94	93.2	no arrest
cyc1^{nimE10}	90	10	50	0	0	87	10.3	S
cyc1^{nimE6}	82	28.3	40.38	43.8	0	78	6	G2
nimA^{E37G}	88	40	80	29.4	0	81	0	G2

Reciprocal shift method was used to establish the arrest points of the cell cycle mutants (15). Conidia of the indicated strains were induced for appressorium development on cover slips and percentages of conidia in which appressorium maturation had occurred indicating completion of mitosis. At least 200 conidia were counted for each determination. **Control**, 24 hours at 24°C; **A** 24 hours at 29°C; **B,** 8 hours at 29°C then 16 hours at 24°C; **C**, 8 hours at 29°C then 16 hours at 24°C with HU; **D**, 24 hours at 24°C with HU; **E,** 8 hours at 24°C with HU then 16 hours without HU; **F**, 8 hours at 24°C, then 16 hours at 29°C without HU.

Table S2. Primers used in this study

Name	Sequence
NIME-P1	TTGGTGTTGCTGCCATGTTT
NIME-P2	AGGCAAAGTATCCCGGAGAC
V-BamHI-nimG11_P1	GCAGGCATGCAAGCTGGATCCCACAGACTTGTACACCGGACAAGA
Mut-nimG10_P2	GCGGATTTCCATGAGATACTTGCC
Mut-nimG10_P3	TATCTCATGGAAATCCGCCTTCTCGATCATCGCTTCT
Hyg-nimG10_P4	GGGAAAACCCTGGCGTCTCCTACAGCTGGTCGATAGC
Hyg-nimG10-3UTR_P5	AAATTGTTATCCGCTTTTGGATGGGAAGTTTTGGACC
V-BamHI-nimG10-3UTR_P6	TGATTACGCCAAGCTGGATCCGGACGATCACGACAAGCATAT
Mut-nimE6_P2	AGGGAATTTCTTGCTGGCATATTTCTT
Mut-nimE6_P3	AGCAAGAATTCCCTAAGGGTATGTTATCCGTCTCGT
M13F	CGCCAGGGTTTTCCCAGTCACGAC
M13R	AGCGGATAACAATTTCACACAGGA
CYC1-int-P1	CTACCCCAACCCCATGAACT
CYC1-int-P2	ACGTCTGTTTGGTCAATGCC
Chk1_50.1	GGGATGGTATATGGGCGTCTTG
Chk1_M13F	GTCGTGACTGGGAAAACCCTGGCGATTGCTGTACTTCGTAGGTCCGTT
Chk1_M13R	TCCTGTGTGAAATTGTTATCCGCTTCCCATTTCCAGGTCTGTAATAGT
Chk1_30.1	TTCCTCTTCCTCCTTATTTTTGCT
Cds1_50.1	TCAGCAGCCAACACATCTTTTTAC
Cds1_M13F	GTCGTGACTGGGAAAACCCTGGCGTCGTCACCATCCAGTCTAGCCT
Cds1_M13R	TCCTGTGTGAAATTGTTATCCGCTACATCTAAGCCGCGCATTGGAG
Cds1_30.1	TGGTTGCGGCTTATCTGGAGGC
HY split	GGATGCCTCCGCTCGAAGTA
YG split	CGTTGCAAGACCTGCCTGAA

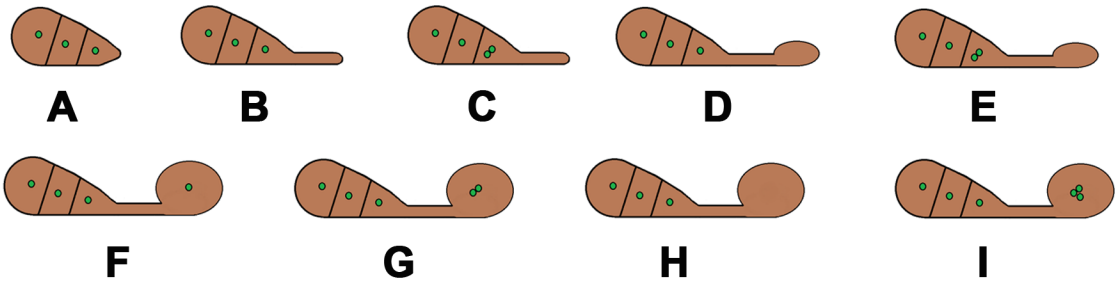
A
B
C
D
E
F
G
H
I

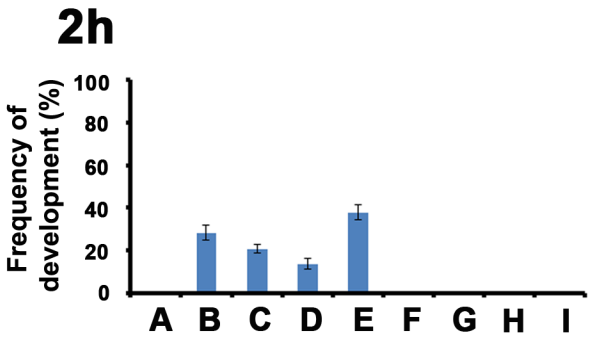
2h
Frequency of development (%)
100
80
60
40
20
0
A B C D E F G H I

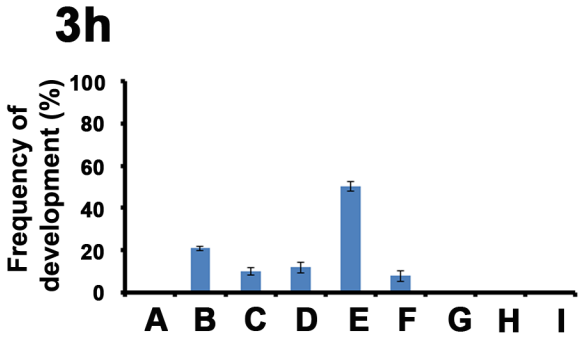
3h
Frequency of development (%)
100
80
60
40
20
0
A B C D E F G H I

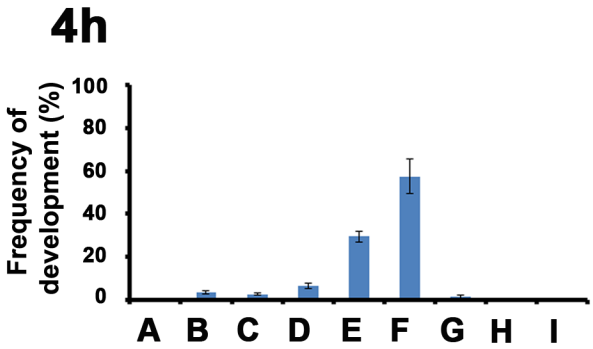
4h
Frequency of development (%)
100
80
60
40
20
0
A B C D E F G H I

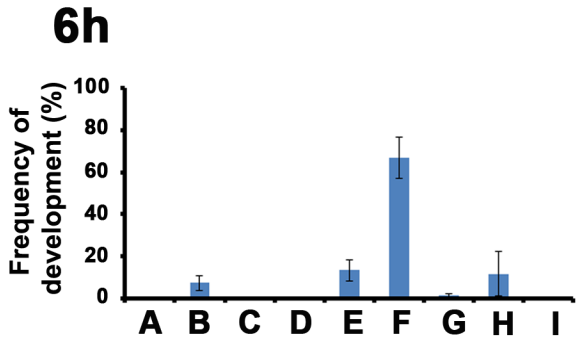
6h
Frequency of development (%)
100
80
60
40
20
0
A B C D E F G H I

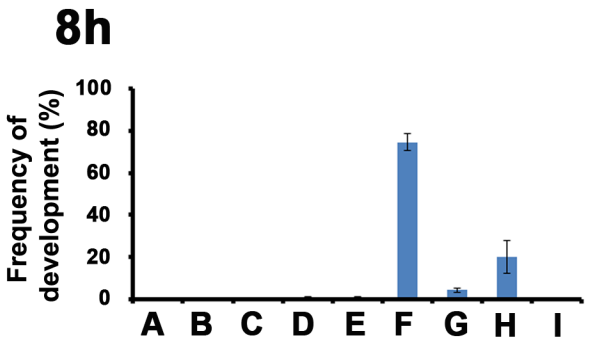
8h
Frequency of development (%)
100
80
60
40
20
0
A B C D E F G H I

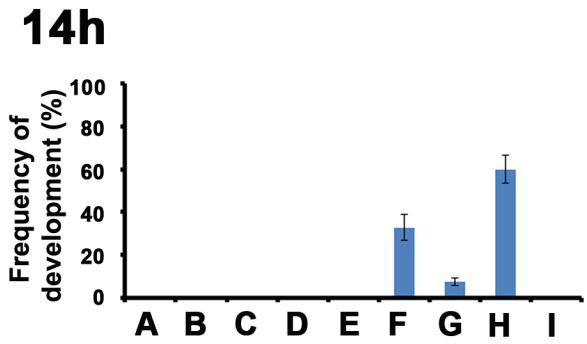
14h
Frequency of development (%)
100
80
60
40
20
0
A B C D E F G H I

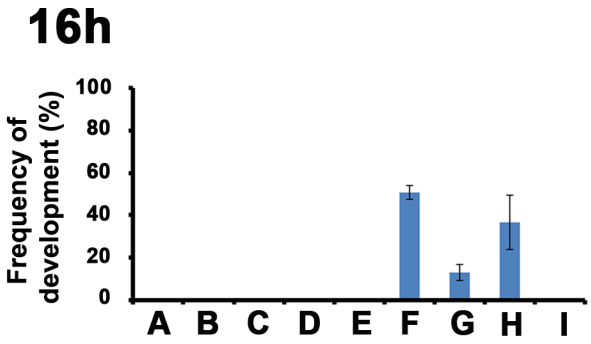
16h
Frequency of development (%)
100
80
60
40
20
0
A B C D E F G H I

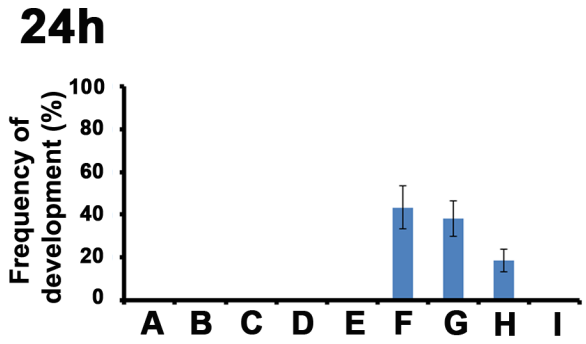
24h
Frequency of development (%)
100
80
60
40
20
0
A B C D E F G H I

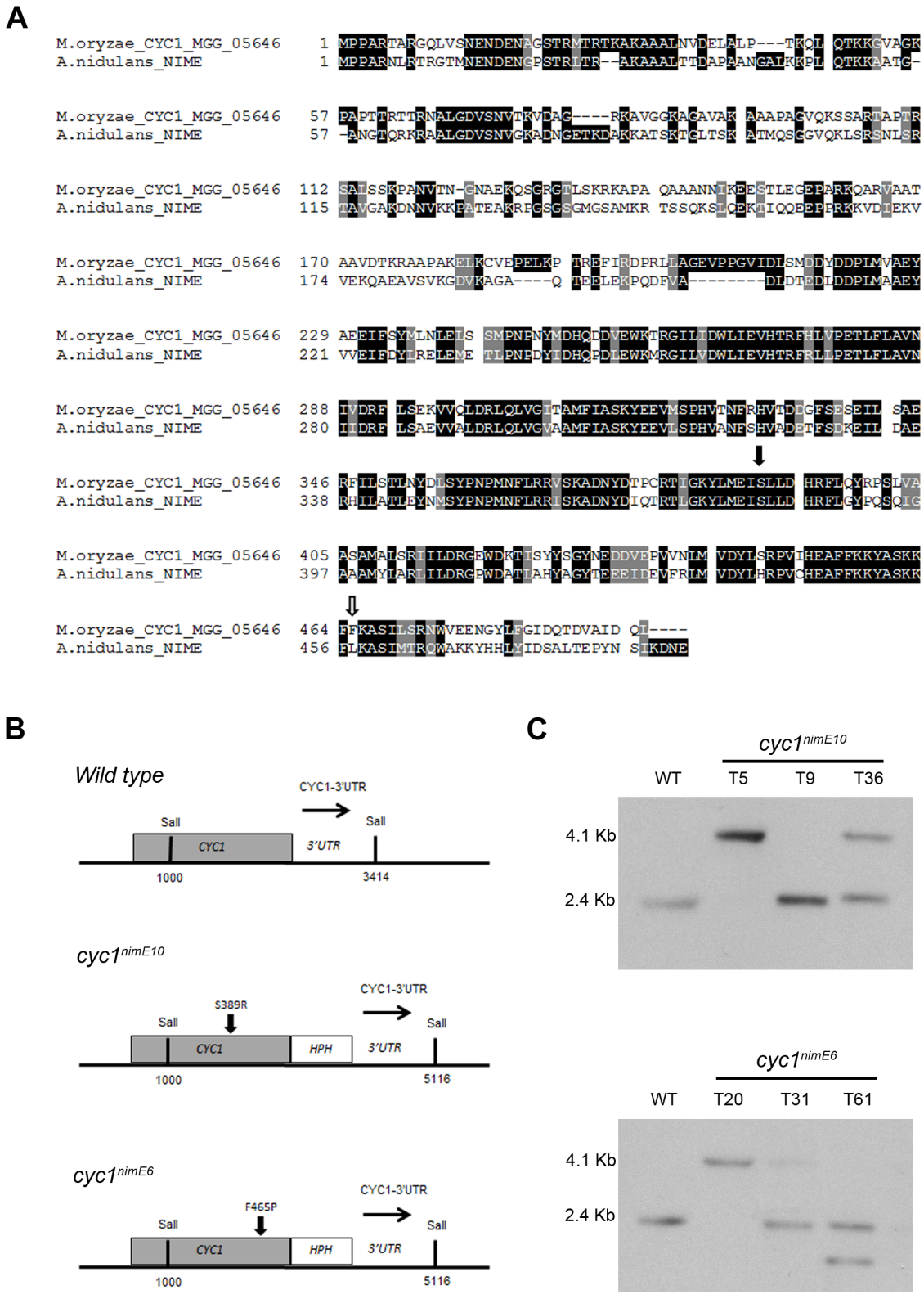
A
M.oryzae_CYC1_MGG_05646
A.nidulans_NIME
B
Wild type
CYC1-3'UTR
SalI
SalI
CYC1
3'UTR
1000
3414
cyc1nimE10
S389R
HPH
5116
cyc1nimE6
F465P
C
cyc1nimE10
WT
T5
T9
T36
4.1 Kb
2.4 Kb
cyc1nimE6
T20
T31
T61

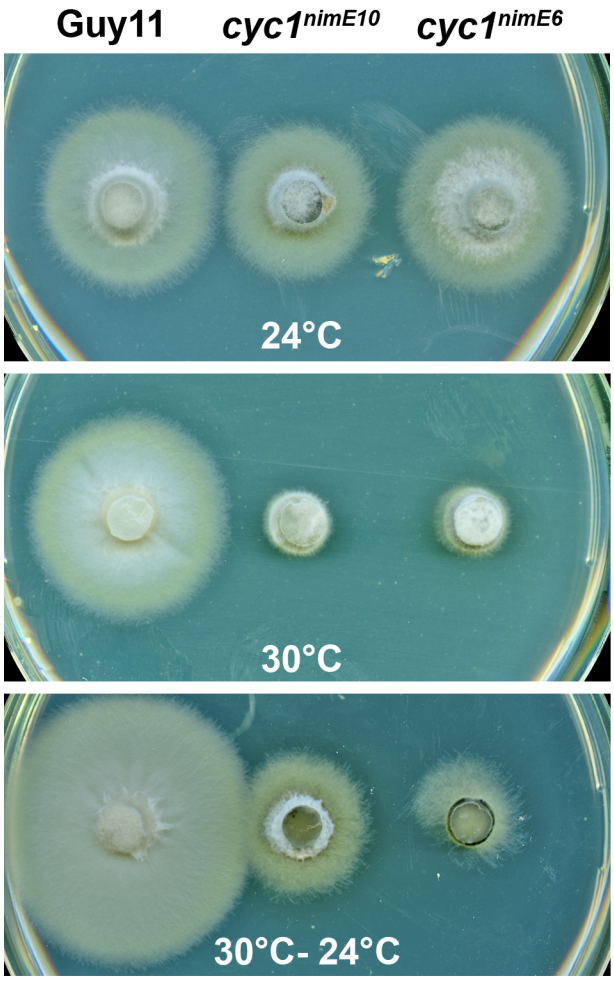
Guy11
cyc1nimE10
cyc1nimE6
24°C
30°C
30°C- 24°C

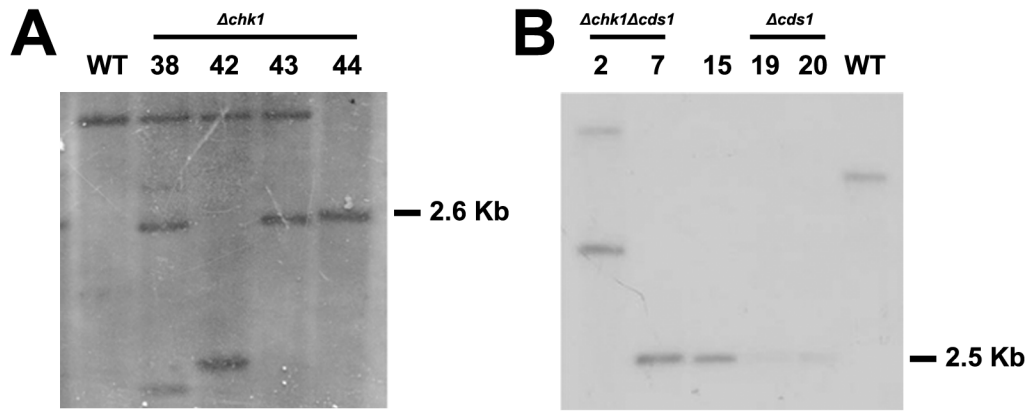
A
Δchk1
WT
38
42
43
44
2.6 Kb
B
Δchk1Δcds1
Δcds1
2
7
15
19
20
WT
2.5 Kb


C
Guy11
Δchk1
Δcds1
Δchk1Δcds1

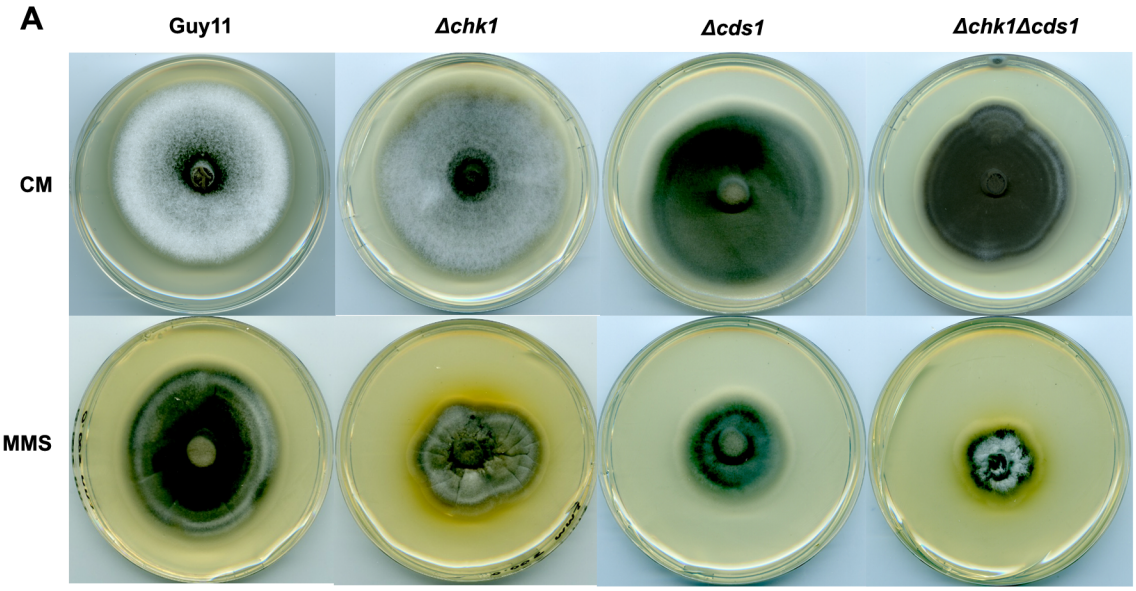
A
Guy11
Δchk1
Δcds1
Δchk1Δcds1
CM
MMS

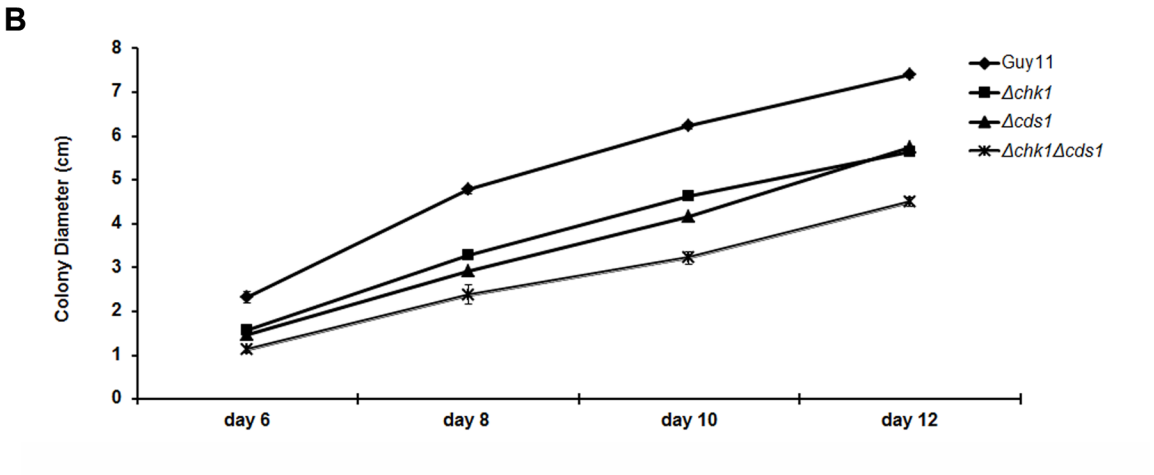
B
Colony Diameter (cm)
0
1
2
3
4
5
6
7
8
day 6
day 8
day 10
day 12
Guy11
Δchk1
Δcds1
Δchk1Δcds1

A

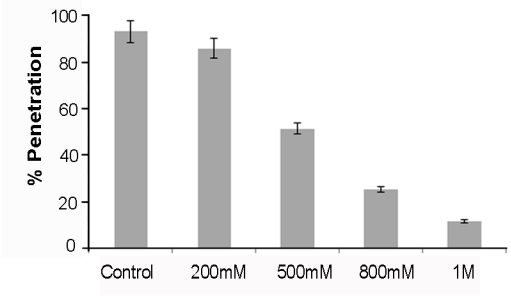

B

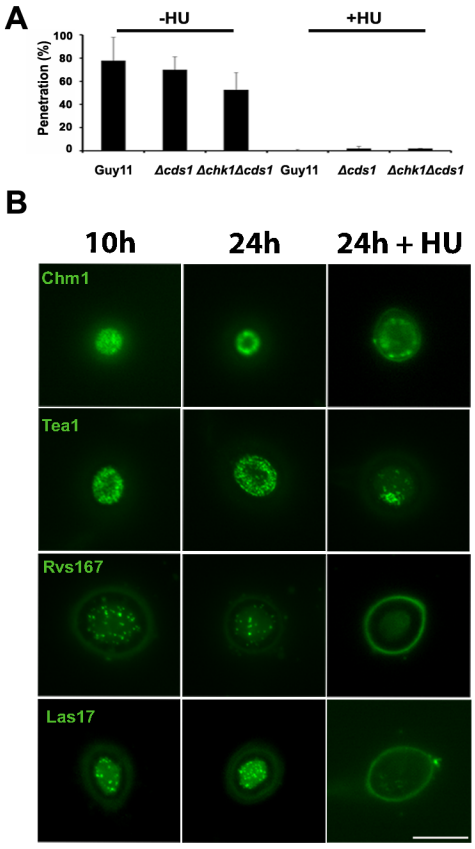
A
-HU
+HU
Penetration (%)
100
80
60
40
20
0
Guy11
Δcds1
Δchk1Δcds1
Guy11
Δcds1
Δchk1Δcds1
B
10h
24h
24h + HU
Chm1
Tea1
Rvs167
Las17